Systematics and morphology of Ischyrosonychini, with an investigation of color change in the Geiger tortoise beetle (Coleoptera: Chrysomelidae)

By

Chulwoo Shin

Submitted to the graduate degree program in Ecology and Evolutionary Biology and the Graduate Faculty of the University of Kansas in partial fulfillment of the requirements for the degree of Doctor of Philosophy.

_____

Chairperson Kirsten Jensen

_____

Michael S. Engel

_____

Mark T. Holder

_____

Bruce S. Lieberman

_____

Paulyn Cartwright

_____

James A. Orr

Date Defended: 15 July 2015

The Dissertation Committee for Chulwoo Shin

certifies that this is the approved version of the following dissertation:

Systematics and morphology of Ischyrosonychini, with an investigation of color change in the Geiger tortoise beetle (Coleoptera: Chrysomelidae)

_____

Chairperson Kirsten Jensen

Date approved: 15 July 2015

ABSTRACT

The New World tribe Ischyrosonychini consists of 66 described species in seven genera. Seven genera in the tribe were traditionally recognized in three distinct tribes (Asterizini, Ischyrosonychini and Physonotini). However, the monophyly of Ischyrosonychini including three traditional tribes has been weakly supported.

The monophyly of the tribe Ischyrosonychini and its phylogenetic relationship to other tortoise beetle tribes were tested by analysis of morphological characters. As a first step, two genera (*Asteriza* Chevrolat and *Eurypedus* Gistel) were revised. In the revision of the genus *Asteriza* (Chapter 1), the morphology of *Asteriza* was explored, two new species (*A. blakeae* Shin et al. and *A. tainosa* Shin et al.) were described, and the monophyly of *Asteriza* with four species was confirmed by a phylogenetic analysis based on morphological characters. In the revision of the genus *Eurypedus* (Chapter 2), *E. thoni* Barber was synonymized with *E. peltoides* (Boheman) because both species were described based on different colorations while other differences were demonstrated to merely represent intraspecific morphological variation. New diagnostic characters such as antennal notches on the ventral surface of the pronotum, the presence of head stridulatory file, and a projection of each antero-lateral region of the prosternum on the ventral surface of the pronotum were documented and illustrated. In addition, new host plants were reported for *E. nigrosignatus* (Boheman) and a distribution map was provided for two remaining species of *Eurypedus* (*E. nigrosignatus* and *E. peltoides*). Most locality data from the examined specimens and previously known distributions suggest that the distributions of the two species of *Eurypedus* are likely separated by the Amazon Basin.

In Chapter 3, a phylogenetic analysis of tortoise beetles was conducted based on 155 morphological characters with 84 species representing 35 genera in 10 tribes. As a preceding

step to the phylogenetic analysis, morphological terminology of tortoise beetles was reviewed using *Physonota alutacea* Boheman as an exemplar. Taxon sampling was focused on the historically recognized tribe Ischyrosonychini to test its monophyly and the validity of each genus within the group. The results indicate that the current tribe Ischyrosonychini should include only species of *Cistudinella* and *Eurypedus*, and the tribe Asterizini was resurrected to include *Asteriza*, *Enagria*, *Eurypepla*, *Physonota*, and *Platycycla*. In Asterizini, *Enagria* and *Physonota* were synonymized with *Asteriza*. With regard to tribal-level relationships, Asterizini and Ischyrosonychini formed a clade with Eugenysini, Goniocheniini, Mesomphaliini, and Omocerini. At the generic level, the monophyly of both *Cistudinella* and *Eurypedus* was confirmed. As new morphological characters, characters of the gastral spiculum on the aedeagus and of the head stridulatory file were introduced and used in the phylogenetic analysis. The distribution of terminal taxa of the Asterizini and Ischyrosonychini were mapped onto the resulting phylogeny.

In Chapters 4 and 5, the biology of the Geiger Tortoise beetle (*Eurypepla calochroma* Blake) is documented with images from live specimens in South Florida. In Chapter 4, the whole life cycle (egg to adult) of *E. calochroma* is documented and illustrated. Two color morphotypes (green and brown) were observed in adults. The detailed morphology of elytral cuticular layers for the two morphotypes and differences between them were documented and illustrated by histology and scanning electron microscopy (SEM). The green individual possessed a thicker endocuticle with several layers and an endocuticular multi-layer reflector (EMLR), while these were lacking in brown individuals. It is suggested that the green coloration required the presence of an EMLR with hemolymph filling the spaces between its thin layers.

In Chapter 5, the dorsal color change in green individuals of *E. calochroma* (green to blue) was observed as the response of visual and physical disturbances. The pattern of color change was documented and illustrated with images from live specimens. The internal staining of the elytra demonstrated that the EMLR was in contact with hemolymph. The EMLR was composed of over 40 thin layers and each layer nearly subequal in thickness; the dorsal layers were slightly thicker than the ventral ones, and the distance between the layers also appeared greater between the dorsal layers than between the ventral layers. The previously known causes of color change in tortoise beetles (freezing, pH, and physiology) were tested with *E. calochroma*. The mechanism of color change in *E. calochroma* is hypothesized as a structural change caused by a reduction in the amount of hemolymph within the elytra: when the hemolymph volume is reduced it decreases the distance between the thin layers in the EMLR and consequently causes reflection of shorter wavelength light. The hypothesized mechanism of the dorsal color change in *E. calochroma* was compared to the color change of another tortoise beetle species, *Charidotella egregia* (Boheman). Unlike the red dorsal color in *C. egregia*, which originates from red pigments in the epidermis, the blue coloration of *E. calochroma* originates from the EMLR. Thin-film theory (= hydraulic theory) was invoked to explain the proposed hypothesis.

AUTHOR'S DISCLAIMER

All taxonomic actions in this work are hereby disclaimed for nomenclatural purposes, as recommended in Article 8 of the International Code of Zoological Nomenclature.

ACKNOWLEDGMENTS

First of all, I am deeply grateful for the mentorship of Dr. Kirsten Jensen and Dr. Michael S. Engel. It would not have been possible for me to reach this stage of my academic life without their support and guidance. They have inspired and encouraged me in my study, and assisted me in all aspects of my research such as in the philosophy of systematics, writing manuscripts, preparing presentations and histological techniques. The most important lesson I have learned from them is that a scientist should always diligently be working and humbly studying with a passion for discovery. I would also like to express my profound thanks to the other members of my doctoral committee: Drs. Mark Holder, Bruce Lieberman, Paulyn Cartwright and James Orr, who always kindly encouraged me, showed interest in my research, and provided instructive insights. I deeply appreciate their contributions to my research and development as a scientist.

It would have been impossible for me to conduct my research without the generous funding provided by the Entomology program in the Department of Ecology and Evolutionary Biology (EEB), the Biodiversity Institution (BI), the Kansas Biological Survey (KBS), the Graduate Program, all at the University of Kansas (KU). I am aware of how fortunate I have been during my doctoral program at KU. The funding allowed me to develop my research skills, attend professional meetings, and visit collections for my research.

None of my research would have been possible without the generous help and loan of specimen from the following institutions and their collection managers, curators, and professors:

Lee Herman and Sarfraz Lodhi (American Museum of Natural History, New York, NY, USA); Sang-Mi Lee (University of Arizona, Frank M. Hasbrouck Insect Collection, Tempe, AZ, USA); Max Barclay, Michael Geiser and Mike Fitton (Museum of Natural History, London, UK); Shawn M. Clark (Monte L. Bean Life Science Museum, Brigham Young University. Provo, UT,

USA); John Rawlins and Robert Davidson (Carnegie Museum of Natural History, Pittsburgh, PA, USA); Jim Liebherr and Richard Hoebeke (Cornell University, Ithaca, NY, USA); Lucia M. Almeida (Museum of Entomology, Federal University of Paraná, Curitiba Paraná, Brazil); Brian Brown and Weiping Xie (Los Angeles County Museum of Natural History, Los Angeles, CA, USA); Miguel Monné (National Museum, University of Rio Janeiro, Rio de Janeiro, Brazil); Gerardo Lamas (San Marcos University Natural History Museum, Lima, Peru); Johannes Bergsten and Bert Viklund (Museum of Natural History, Stockholm, Sweden); Edward G. Riley (Texas A & M University, College Station, TX, USA); Alexander Konstantinov, David Furth and Steven Lingafelter (National Museum of Natural History, Washington D.C., USA); Michael C. Thomas and Paul Skelley (Florida State Collection of Arthropods, Gainesville, FL, USA); Carmelo Nuñez (National Museum of Natural History, Santo Domingo, Dominican Republic); Michael A. Ivie (The West Indian Beetle Fauna Project collection, Montana State University, MT, USA); and Ottö Merkl (Hungarian Natural History Museum, Budapest, Hungary), Santiago Zaragoza-Caballero (National Collection of Insects, Institute of Biology, National University of México, México D.F., México); Graham E. Rotheray and Richard Lyszkowski (National Museums of Scotland, Edinburgh, UK); and Phil Perkins (Museum of Comparative Zoology, Harvard University, Cambridge, MA, USA).

During the past six years of my doctoral program in EEB, I was fortunate to have my graduate student colleagues and dear friends who have generously helped me, inspired and encouraged me: Ismael A. Hinojosa, Daniel J. Bennett, Steven Davis, Joanna Cielocha, Taro Eldredge, Cyrstal Maier, Mabel Alvarado, Sofia Muñoz, Marianna Simões, Laura Breitkreuz, Stephen Baca, Rachel Guyer and Kaylee Herzog.

I also deeply appreciate my M.A. degree mentor, Dr. Ahn, Kee-Jeong (Chungnam National University, South Korea). It was Dr. Ahn who guided my first studies in Entomology and provided me with the opportunity to learn so much about insects and enjoy field work while I was his student; Dr. Cho, Young-Bok (Hannam University, South Korea), who assisted my research and helped me develop my knowledge in Entomology; and Dr. Earl Jackson, Jr. (National Chiao Tung University, Taiwan) for his personal assistance and encouragement over the years in many ways.

Finally, I would like to express my utmost gratitude to family: my husband, Cal Gordon Melick for his endless support and those wonderful days together; Richard Alexander for his commitment and for providing me support during the most difficult moments; and my mother (Sundeok Baek) and brother (Changhwan Shin) for their generous support. My research would not have been possible without such strong support from them.

TABLE OF CONTENTS

TITLE PAGE……..……..... i

APPROVAL PAGE……... ii

ABSTRACT……. iii

AUTHOR'S DISCLAIMER…….. vi

ACKNOWLEDGMENTS..…….……..… vii

INTRODUCTION ……...……... 1

CHAPTER 1. Revision of the endemic Hispaniolan genus *Asteriza* Chevrolat, 1836, with descriptions of two new species (Coleoptera: Chrysomelidae: Cassidinae)……...…… 7

CHAPTER 2. A revision of the Neotropical tortoise beetle genus *Eurypedus* (Coleoptera: Chrysomelidae)…… 28

CHAPTER 3. Phylogeny of the tortoise beetle tribe Ischyrosonychini based on morphological data (Coleoptera: Chrysomelidae)…….……...… 64

Appendix 1. Specimens Examined...…….. 145

Appendix 2. Characters and Associated States Used in Phylogenetic Analysis…...….. 158

Appendix 3. Data Matrix for Cladistic Analysis...…….. 201

CHAPTER 4. A histological comparison of the two color morphotypes of the Geiger tortoise beetle with a brief natural history (Coleoptera: Chrysomelidae)…….……. 207

CHAPTER 5. Observation and histological study on color change in the Geiger tortoise beetle (Coleoptera: Chrysomelidae) ……..… 225

DISCUSSION AND FUTURE DIRECTIONS ……..… 255

INTRODUCTION

The subfamily Cassidinae is the second most speciose subfamily with over 6,000 described species (Borowiec & Świętojańska 2014, Staines 2014). The members of Cassidinae are generally divided into two groups, the tortoise beetles and the leaf-mining beetles (Borowiec 1995, Hsiao & Windsor 1999, Chaboo 2007, Borowiec & Świętojańska 2014, Staines 2014). The tortoise beetles are readily observed on the surface of leaves on their host plants and generally exhibit a distinct morphology which is a round body often with broad lamellae on the pronotum and elytra (Chaboo 2007, Borowiec & Świętojańska 2014). The oldest record of tortoise beetles was by Linnaeus (1758). Linnaeus described 18 species of *Cassida* Linnaeus. Although the taxonomic history of the tortoise beetles is fairly long, the phylogenetic relationship to leaf-mining beetles, and among the tribes of the tortoise beetles are still far from well-established (Chaboo 2007, Borowiec & Świętojańska 2014, Staines 2014). Currently, the leaf-mining beetles are accepted as a basal grade to the more derived cassidoid beetles (Hsiao & Windsor 1999, Chaboo 2007, Borowiec & Świętojańska 2014, Staines 2014).

The New World tribe Ischyrosonychini is a little known group with 66 described species in seven genera (Borowiec & Świętojańska 2014). The genera of Ischyrosonychini used to be recognized as three distinct lineages in Hincks (1952) (Asterizini, Ischyrosonychini, and Physonotini). Ischyrosonychini was first proposed in Chapuis (1875) only for *Ischyrosonyx* Sturm (= *Eurypedus* Gistel). Later, *Cistudinella* Champion (1894) was included in Ischyrosonychini. When Ischyrosonychini was erected, the members of Asterizini Hincks (*Asteriza* Chevrolat) and Physonotini Hincks (*Enagria* Spaeth, *Eurypepla* Boheman, *Physonota* Boheman, and *Platycycla* Boheman) were included in Cassidini Gyllenhal until Hincks (1952) proposed these two tribes. In Hincks (1952), Physonotini was diagnosed by the broad elytral

lamellae; yellow antennae with black distal antennomeres; and yellow and opalescent body color, and Asterizini was diagnosed by narrow elytral lamellae with thickened lateral margin; broad, flat and arrow-shaped prosternal process; and opalescent dorsal coloration and yellow antennae with three reddish proximal antennomeres. The classification by Hincks (1952) as three separate tribes was used until the first phylogenetic study of Cassidinae at the tribal level by Borowiec (1995). Borowiec (1995) created a data matrix of 21 tribes including two leaf-mining beetle tribes (Callispini and Cephaloleiini) with 20 morphological characteristics from the identification couplets by Spaeth in Hincks (1952), and arbitrarily synonymized Asterizini and Physonotini with Ischyrosonychini without providing evidence. Hsiao & Windsor (1999) performed a molecular phylogenetic analysis using 12s mtDNA sequence data of 47 species (mainly from Panama) representing both leaf-mining beetles and tortoise beetles including a species each of *Eurypedus* and *Physonota*. Hsiao & Windsor (1999) recovered a sister taxa relationship of *Eurypedus* + *Physonota*. Chaboo (2007) performed a phylogenetic analysis for the full diversity of Cassidinae. Her study was based on 210 morphological characters with 98 species in 94 genera of Cassidinae including six species from six subfamilies of leaf beetles (Chrysomelidae) as outgroups. Chaboo included four species from four genera of Ischyrosonychini (*Asteriza*, *Eurypedus*, *Eurypepla*, and *Physonota*) and the four species of Ischyrosonychini was placed separately in the terminal polytomy. After Chaboo's phylogenetic study (2007), no other study concerning the phylogenetic relationship of the tortoise beetles was conducted. The tribal classification in general has remained at a stand-still since Borowiec (1995).

The biology of the tortoise beetles has been studied in various aspects (see Chaboo 2007). However, the biology of Ischyrosonychini is also little known. *Eurypepla* consists of four species, and they are distributed in Yucatan Mexico, Jamaica, Cuba and southern Florida, USA. During

field observation in southern Florida, the whole life cycle, two color morphotypes of adult (brown and green), and color change (green to blue) were observed in Geiger tortoise beetle (*Eurypepla calochroma* (Blake)).

This study focused on the morphology and systematics of Ischyrosonychini, and the biology of the Geiger tortoise beetle, especially focusing on the coloration and dorsal color change. A revision or morphological review was conducted for each subgroup (Asterizini, Ischyrosonychini and Physonotini) as a preceding step to the phylogenetic analysis.

In Chapter 1, the endemic Hispaniolan genus *Asteriza* was revised. In this study, the name bearing type specimens of *A. flavicornis* (Olivier) and *A. darlingtoni* Blake were examined and illustrated. Morphology was described in detail including mouthparts and genitalia and illustrated for each species. In addition, two new species were described. The monophyly and previously known diagnostic characters of *Asteriza* were tested by a morphological phylogenetic analysis.

In Chapter 2, a little known New World genus *Eurypedus* was revised. The current morphological circumscription of *Eurypedus* follows: tarsomere IV without basal tooth, pronotal base emarginate with well-defined postero-lateral angles, oblong and laterally parallel-sided body, elytral lamella narrower than elytral inner marginal line, and prosternal process between procoxae narrower than trochanter (Borowiec and Świętojańska 2014). Six name-bearing type specimens were examined and illustrated. For the first time, a detailed description of *Eurypedus* was provided with illustrations including mouthparts and genitalia for each species. Based on morphological examination, the species membership of *Eurypedus* was revised. Records of new host plants were reported and discussed from the label data of the examined specimens. Stridulatory file on head, and antennal notches on the ventral surface of the antennae were

described as new diagnostic characters, and illustrated with images by scanning electron microscopy (SEM). The distributions of the valid species, based on the collecting locality from the examined specimens and previously known data, are mapped. Distribution of each species was discussed along with geography and the distributions of the host plants.

In Chapter 3, morphology and terminology of the tortoise beetles were reviewed and illustrated with *Physonota alutacea* Boheman as an exemplar, and a phylogenetic analysis was performed with tortoise beetles. The phylogenetic analysis was performed based on 155 morphological characters with 84 species representing 35 genera in 10 tribes of tortoise beetles. The taxa sampling was focused on the tribe Ischyrosonychini to test its monophyly and the validity of each genus in Ischyrosonychini. As a secondary goal, the phylogenetic relationship to other tortoise beetles tribes and monophyly of other tortoise beetle tribes were tested. The morphology of stridulatory file on head and gastral spiculum in male genitalia was introduced and used in the phylogenetic analysis for the first time. The phylogeny and morphological characters in Borowiec (1995) were reviewed and compared to those in this study. The distributions of the species in Ischyrosonychini were illustrated in a phylogenetic context.

In Chapter 4, the brief life history of the Geiger tortoise beetle (*E. calochroma*) was reviewed with images of all stage of life cycle from live specimens on the Geiger tree in southern Florida. The whole life cycle of the Geiger tortoise beetle occurs on the host plant (Geiger tree, *Cordia sebestena*), and consists of an egg, four instar stages, a pupal stage, and an adult stage. Eggs and two color morphotypes (brown and green) of adults are introduced for the first time. The two different color morphotypes were observed together on the host plant. The general external morphology and body coloration of the two color morphotypes were identical except for the elytral and pronotal discs. The internal structure of the elytra was compared and illustrated

for both morphotypes with images by histology and SEM. The conditions of presence of green coloration in live specimens were suggested.

In Chapter 5, a reversible dorsal color change of *E. calochroma* was investigated.

In contrast to the passive color change in the Hercules beetle (*Dynastes Hercules* Linnaeus), which changed the elytral color from yellow to black when the air contains more moisture (Hinton 1973), green individuals of the Geiger tortoise beetle actively changed the dorsal coloration (pronotal disc and elytral disc) to blue in response to external disturbances. The pattern of color change in the Geiger tortoise beetle was consistent among individuals. The duration of the color change varied individually between 2–20 minutes after physical or subsequent visual disturbances. In this chapter, the pattern of color change was documented with illustrations from live specimens. Internal staining with toluidine blue was performed to confirm the hydration of the endocuticular multilayer reflector (EMLR) by hemolymph. Scanning transmission electron microscopic (STEM) images were taken of the elytron to observe the detailed structure of EMLR. Sagittal semi-thin sections were provided to explain the limitation in color change to only the anterior and posterior regions of the pronotum. Based on the observed structures and performed experiments, the mechanism of the color change in the Geiger tortoise beetle was hypothesized. The color change in *E. calochroma* was illustrated and documented, and comparison was made to the color change in *Charidotella egregia* (gold to red, Vigneron et al. 2007). The function of color change in tortoise beetles was reviewed and further discussed.

CITATIONS

Borowiec, L. 1995. Tribal classification of the cassidoid Hispinae (Coleoptera: Chrysomelidae). In: Biology, Phylogeny, and Classification of Coleoptera. (eds.) Pakaluk, J. & Ślipiński, S.A., Warszawa, 541–558.

Borowiec, L. & Świętojańska, J. 2014. Cassidinae of the World – an interactive manual (Coleoptera: Chrysomelidae). Available from http://www.biol.uni.wroc.pl/cassidae/katalog%20internetowy/index.htm (Accessed: July 1 2015).

Chaboo, C.S. 2007. Biology and phylogeny of Cassidinae Gyllenhal (tortoise and leaf-mining beetles) (Coleoptera: Chrysomelidae). Bulletin of the American Museum of Natural History, 305: 1–250.

Hincks, W.D. 1952. The genera of the Cassidinae (Coleoptera: Chrysomelidae). Transactions of the Royal Entomological Society of London, 103: 327–358.

Hinton, H. E. 1973. Natural deception [pp. 97–159]. *In*: Illusion in nature and art (Gregory, R. L. and E. H. Gombrich, editors). Duckworth, London, U.K..

Hsiao, T.H. & Windsor, D.M. 1999. Historical and biological relationships among Hispinae inferred from 12S mtDNA sequence data. In: Advances in Chrysomelidae Biology 1. (ed.) Cox, M.L., Backhuys Publishers, Leiden, 39–50.

Staines, C.L. 2014. Hispines of the world. Available from http://idtools.org/id/beetles/hispines/index.php. (Accessed: July 1 2015).

Vigneron, J. P., J. M. Pasteels, D. M. Windsor, Z. Vértesy, M. Rassart, T. Seldrum, J. Dumont, O. Deparis, V. Lousse, L. P. Biró, D. Ertz and V. Welch. 2007. Switchable reflector in the Panamanian tortoise beetle *Charidotella egregia* (Chrysomelidae: Cassidinae), Physical Review 76(31907): 1–10.

CHAPTER 1

Revision of the endemic Hispaniolan genus *Asteriza* Chevrolat, 1836, with description of two new species (Coleoptera: Chrysomelidae: Cassidinae: Ischyrosonychini)

*Previously published in *Zootaxa* (2012) 32247:34–53 with co-author C. S. Chaboo and S. M. Clark. Reproduced with permission by Chief Editor & Founder (Z.-Q. Zhang).

Zootaxa 3227: 34–53 (2012)
www.mapress.com/zootaxa/

Article

ISSN 1175-5326 (print edition)
ZOOTAXA
ISSN 1175-5334 (online edition)

Revision of the endemic Hispaniolan genus *Asteriza* Chevrolat, 1836, with description of two new species (Coleoptera: Chrysomelidae: Cassidinae: Ischyrosonychini)

CHULWOO SHIN[1,3], CAROLINE S. CHABOO[1] & SHAWN M. CLARK[2]

[1]*Department of Ecology and Evolutionary Biology, Museum of Natural History and Biodiversity Research Institute, 1501 Crestline Drive, Suite #140, Lawrence, Kansas 66049, U. S. A.*
[2]*Monte L. Bean Life Science Museum, Brigham Young University, Provo, Utah 84602, U. S. A.*
[3]*Corresponding author. E-mail: shinio@ku.edu*

Abstract

The cassidine genus *Asteriza* Chevrolat, 1836 is redescribed and two new species, *Asteriza blakeae* Shin, Chaboo & Clark and *Asteriza tainosa* Shin, Chaboo & Clark, are described from the Dominican Republic. A phylogenetic analysis and an illustrated key to the four *Asteriza* species are provided. *Asteriza blakeae* is diagnosed by the reddish lateral margin of the pronotum and more swollen brownish elytral margins. *Asteriza tainosa* is diagnosed by the relatively swollen maxillary and labial palpi and dominant yellow coloration of the elytra and pronotum.

Introduction

Chevrolat (1836) erected the genus name *Asteriza* for the Hispaniolan species, *Cassida flavicornis* Olivier, 1790. He listed two other names, *Asteriza punctatissima* Klug and *Asteriza flavicornis* var. *retigera* Mannerheim, whose origins are unclear since Klug (1829) and Mannerheim (1825) did not include any *Asteriza* species. Both these two names lack valid records (ICZN 1999, Article 12), and are therefore *nomina nuda*. Dugès (1901: 111) listed the name *Asteriza mexicana* Dugès from Mexico; we obtained photographs of Dugès's specimens and determined this to be *Physonota disjuncta* (Chevrolat, 1834), so the name *A. mexicana* is a junior synonym of *P. disjuncta*. The genus name is often cited as *Asteriza* Chevrolat, 1837 but Madge (1988) determined the date of publication to be 1836. A second species, *Asteriza darlingtoni* Blake, 1939 from the Dominican Republic, was diagnosed on the basis of elytral color, puncture pattern, and aedeagal form. Blake (1939) commented that specimens of *A. darlingtoni* recovered an opalescent color when they were soaked, consistent with Hincks's (1952) distinction that Physonotini Spaeth, 1942 are opalescent. Blackwelder (1946) included *Asteriza* in the tribe Cassidini Gyllenhal, 1813 and treated other genera of Ischyrosonychini Chapuis, 1875 (*Cistudinella* Champion, 1894; *Enagria* Spaeth, 1913; *Eurypedus* Gistel, 1834; *Eurypepla* Boheman, 1854; *Physonota* Boheman, 1854; and *Platycycla* Boheman, 1854) in the tribe Mesomphaliini Hope, 1840. Hincks (1952) erected the tribe Asterizini for *Asteriza* alone; he distinguished three tribes, Asterizini, Ischyrosonychini, and Physonotini on the basis of differences in the elytral margin, pronotal form, prosternal process form, color and opalescence. In couplet 29 (28), he mentioned another taxon, "Eurypedini. However, no morphological features or taxon names were associated and Eurypedini is not used in modern cassidine studies.

Seeno & Wilcox (1982) recognized three distinct tribes—Asterizini Hincks, 1952, Ischyrosonychini Hincks, 1952, and Physonotini Hincks, 1952. The author of Asterizini is indeed Hincks; however, the author of Ischyrosonychini and Physonotini is not Hincks because both tribes were validated previously by Chapuis (1875) and Spaeth (1942). Hincks (1952) only Latinized the family group names (ICZN [1999] article 11.7.2). Borowiec (1995) synonymised Asterizini with Ischyrosonychini and Physonotini under the oldest name Ischyrosonychini, because he considered the tribal boundaries ambiguous. However, Borowiec (1999) used the tribal name Physonotini because *Ischyrosonyx* Sturm, 1843 was already recognized as a junior synonym of *Eurypedus* by Barber (1946). In contrast,

 Accepted by M.L. Chamorro: 20 Jan. 2012; published: 8 Mar 2012

Riley *et al.* (2002) used the oldest name Ischyrosonychini from Ischyrosonychites Chapuis, 1875. We follow this latter usage, which concurs with the arguments and conclusions of Bouchard *et al.* (2011)

Asteriza specimens are poorly represented in museum collections and their biology is virtually unknown. Until this paper, *Asteriza* was comprised of two species from Hispaniola. The genus can be identified using online keys of Borowiec and Świętojańska (2011). Chaboo (2007) found the four sampled ischyrosonychine genera (*Asteriza*, *Eurypepla, Eurypedus*, and *Physonota*) to not be closely related, but within a large polytomy of derived cassidines. *Asteriza*'s diagnostic elytral margin (narrowed and thickened) is homoplasious in Cassidinae.

A host plant, *Cordia* Linnaeus (Boraginaceae), and mature larvae and pupae are documented for *A. flavicornis* (Świętojańska & Windsor 2008). *Cordia* is a common host of ischyrosonychine species (Borowiec & Świętojańska 2011).

An inventory of the entomofauna of the Dominican Republic by the Carnegie Museum of Natural History (CMNH), Pittsburgh, USA and Museo Nacional de Historia Natural (MHND), Santo Domingo, Dominican Republic has assembled the largest specimen series that we are aware of. In sorting these specimens, we discovered two new species which stimulated this study.

Material and methods

Descriptions are based on pinned specimens from the Carnegie Museum of Natural History. Specimens were dissected in 100% alcohol or glycerin. For description of internal morphology and sexual organs, the specimens were treated in 5% KOH overnight at room temperature. Hydrogen peroxide was used for bleaching legs. For the observations of the tarsal formula and genitalia, specimens were stained in chlorozol black. All dissections are preserved in glycerin.

The two syntypes of *A. flavicornis* (Figs. 1–2) deposited in the National Museums of Scotland (RSME) and Edinburgh, UK, were examined and the lectotype (Fig. 1) and paralectotype are hereby designated from these syntypes. According to Blake (1939), the holotype and two paratypes of *A. darlingtoni* are deposited in the Museum of Comparative Zoology (MCZ), Harvard University, Cambridge, MA and two paratypes are in the U.S. National Museum of Natural History (USNM), Washington, D.C. However the online cassidine catalog of Borowiec & Świętojańska (2011) currently indicates that the types of *A. darlingtoni* are deposited in the USNM. During a collections study visit by CWS, we discovered that these USNM specimens are actually two paratypes, and the holotype (Fig. 3) is housed in the MCZ as in the original description (Blake 1939). The holotype was borrowed and examined for the present study.

Specimens were examined with an Olympus SZX7 microscope and an Olympus BX51 compound microscope. Measurements were made with an ocular micrometer. Photographs were taken with the Microptics camera system. Illustrations were made with a camera lucida attached to the microscope. Terminology follows Lawrence & Britton (1991) and Chaboo (2007). Label data are transcribed exactly from specimen labels. Museum acronyms (Table. 1) follow Evenhuis (2011).

Cladistic analysis. A character matrix was scored for six taxa: the four species of *Asteriza* (Tables 2, 3) and two outgroups, a species of *Spaethiella* Barber & Bridwell 1940 (tribe Hemisphaerotini Monrós & Viana, 1951) and *Physonota attenuata* Boheman (tribe Ischyrosonychini). Chaboo's (2007) phylogenetic analyses found 10 tribes of derived cassidines collapsed as a polytomy; our two outgroup selections for the present study samples one close relative in Ischyrosonychini and one Hemisphaerotini species, which is outside the Chaboo polytomy. We scored 17 characters (Tables 2, 3) derived from Chaboo (2007), Borowiec & Świętojańska (2011), and seven new characters developed here. The relationship of *Asteriza* with other genera in the tribe Ischyrosonychini has been noted in other studies (Borowiec 1995, Chaboo 2007, Borowiec & Świętojańska 2011). The phylogenetic analysis was performed using WinClada (Nixon 2002), which incorporates Nona (Goloboff 1998). All characters were equally weighted and unordered (Fitch optimization).

Although we found coloration of dried specimens useful for diagnosing each species, we did not use color as a phylogenetic character since the diagnostic colors are autapomorphies, which do not help resolve evolutionary relationships.

TABLE 1. Museum acronyms used in this study (by Neal L. Evenhuis, 2011)**.**

AMNH	American Museum of Natural History, New York, USA
BYU	Brigham Young University, Monte L. Bean Life Science Museum Provo, Utah, USA
CCC	Caroline Chaboo Collection, University of Kansas, Lawrence, USA
CMNH	Carnegie Museum of Natural History, Pittsburgh, Pennsylvania, USA
CUIC	Cornell University, Ithaca, New York, USA
FSCA	Florida State Collection of Arthropods, Gainesville, Florida, USA
HNHM	Hungarian Natural History Museum, Budapest, Hungary
MCZ	Museum of Comparative Zoology, Harvard University, Cambridge, MA, USA
MHND	Museo Nacional de Historia Natural, Santo Domingo, Dominican Republic
RSME	National Museums of Scotland, Edinburgh, United Kingdom
USNM	National Museum of Natural History, Washington D.C., USA
WIBF	The West Indian Beetle Fauna Project collection, Montana State University, Montana, USA
ZMHB	Museum für Naturkunde der Humboldt-Universität, Berlin, Germany

Results

Asteriza Chevrolat, 1836

Asteriza Chevrolat 1836: 372 [type species: *Cassida flavicornis* Olivier, 1790 by monotypy]; Chapuis 1875: 387 [description]; Spaeth 1914: 122 [catalog]; Barber & Bridwell 1940: 10 [nomenclature]; Blackwelder 1946: 748; Hincks 1952: 336 [key to genera]; Wilcox 1975: 154 [catalog]; Seeno & Wilcox 1982: 175 [checklist]; Borowiec 1999: 169 [checklist]; Perez-Gelabert 2008: 125 [checklist]; Takizawa 2003: 97 [checklist]; Borowiec & Świętojańska 2011 [catalog].

Diagnosis of *Asteriza*. Adults of *Asteriza* have an oval body shape in dorsal aspect (Figs. 4–5, 7–8, 10–11, 13–14) and a hemispherical shape without angles in lateral aspect (Figs. 16–23). In dorsal view, the pronotum and elytra are continuous to slightly discontinuous in females (Figs. 5, 8, 11, 14) and slightly to moderately discontinuous in males (Figs. 4, 7, 10, 13). The antennae are pale with scape, pedicel and often antennomere III shiny red to reddish brown and the apical half of the last antennomere tanned. The lateral margins of the pronotum and elytra are moderately explanate, the explanate portion being less than half the width of discal area. The dorsal color (4–5, 7–8, 10–11, 13–14) is mottled or speckled yellow to tan and black. The pronotum (Fig. 42) is smooth. The pronotal anterior margin is semicircular, completely covering the head. The prosternal process (Fig. 43) separates the procoxae by a distance approximately equal to the width of each procoxa. The elytral explanate portion (Figs. 47–54) is interrupted medially by a discal sublateral "bulge and is narrowed posteriad. The elytral edge is moderately thickened. The elytral disc is moderately punctate, with the punctures scattered. Each terminal tarsomere is unmodified.

Redescription of *Asteriza* Chevrolat. *Body* oval in dorsal view (Figs. 4–5, 7–8, 10–11, 13–14); head entirely concealed; pronotum and elytra continuous to slightly discontinuous in females (Figs. 5, 8, 11, 14) and slightly to moderately discontinuous in males (Figs. 4, 7, 10, 13). In lateral view (Figs. 16–23), body hemispherical, highest at middle of elytra. Pronotal and elytral disc moderately to well defined. Pronotal and elytral lateral margins (Figs. 4–5, 7–8, 10–11, 13–14) moderately explanate, explanate portion less than half width of discal area.

Head (Figs. 24–26) withdrawn into pronotum approximately halfway, completely covered dorsally by pronotal margin and partially concealed ventrally by prosternal margin; prosternal margin covering base of maxillary palpi. In dorsal view of dissected specimens (Fig. 25), shape subquadrate, widest medially, moderately rounded on sides, 1.25 times as broad as long; surface finely and sparsely pubescent. *Eyes* (Fig. 24) large, nearly flush with head, not protruding; egg-shaped, with dorsal width narrower than ventral width. Interocular distance 1.5 times as broad as widest part of eye. *Vertex* very finely striate, striations slightly elevated; in dissected specimens, stridulatory file distinct, elongate and slightly convex (Figs. 24–25). *Frontal tubercles* (= antennal calli, Chaboo 2007) similar in size to antennal socket, elevated and flattened. *Coronal suture* in two sections, with mid-cranial suture posteriad

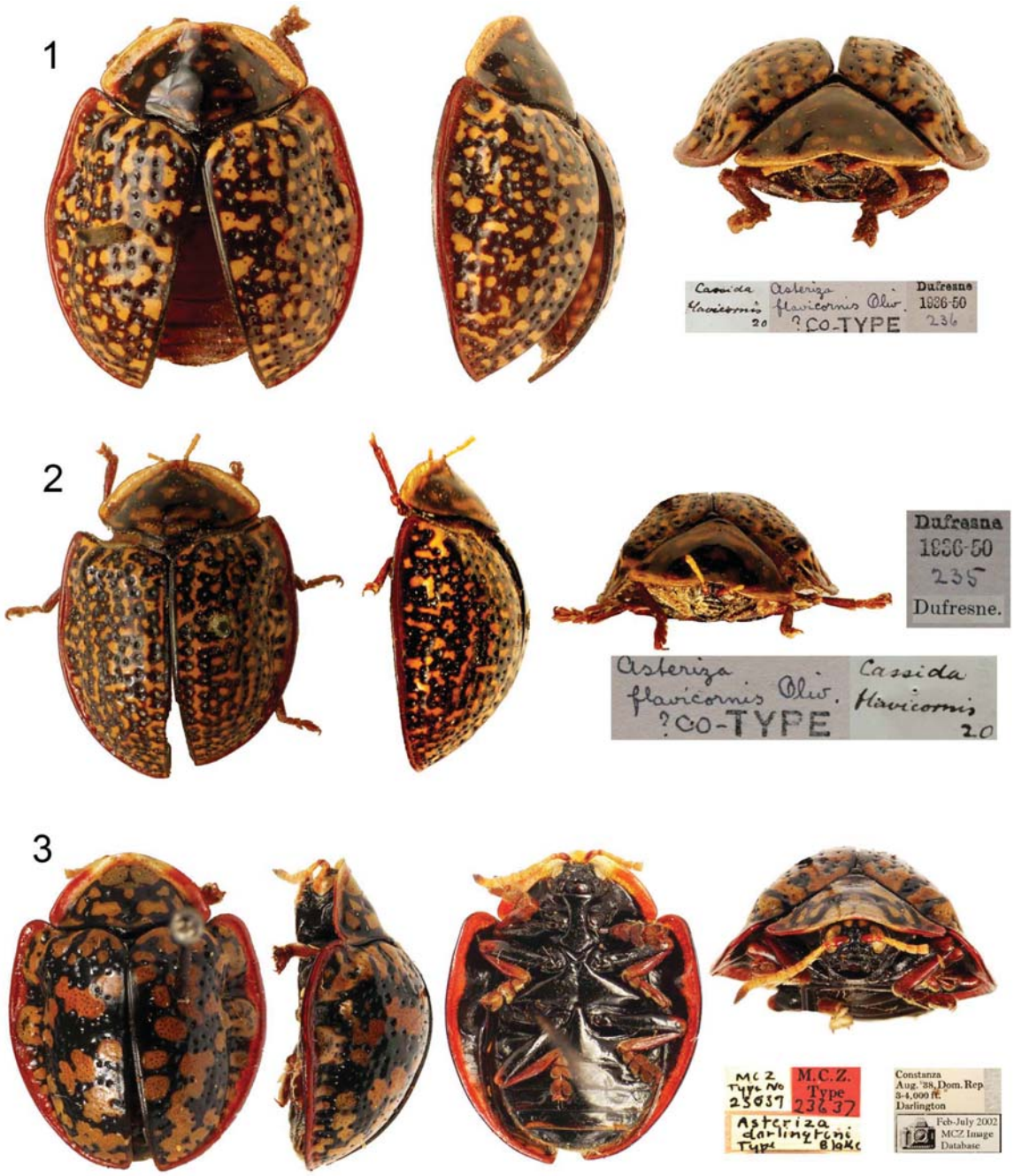

FIGURES 1–3. Type specimens: 1, *Asteriza flavicornis*, lectotype (RSME); 2, *Asteriza flavicornis*, paralectotype (RSME); 3, *Asteriza darlintoni*, holotype (MCZ).

(hidden by pronotum in intact specimens) extending to anterior margin of stridulatory file; mid-frontal sulcus extending to or bisecting anterior frontoclypeal margin (Figs. 24, 30–33). *Gena* slightly protuberant in mandibular region; prosternum abutting behind protuberance. *Frontoclypeus* (Figs. 30–33) triangular, slightly protuberant anteriorly; epistomal suture barely discernible in dissected specimens; anterior margin of frontoclypeus either uninterrupted or bisected by mid-frontal sulcus; surface flattened or slight swollen, finely to coarsely punctate, with punctures unevenly distributed and finely setose. *Antenna* (Fig. 27) with 11-antennomeres, reaching basal margin

of pronotum. Distance between antennal sockets as broad as socket; distance between antennal socket and eye margin less than half width of socket (Fig. 24). Scape longer than wide; II (pedicel) shortest and rounded; III 1.5 times as long as broad; I–III with relative length ratio 2/1/1.5; IV–X as long as broad; IV as long as III; V–X similar in shape and length; XI longest, 2 times as long as broad. Antennomeres I–III with surface shiny, tanned, and reddish brown, finely and sparsely setose; I finely wrinkled; IV–X pale and densely setose, with fine, long setae at apex; XI longest densely setose with longer fine setae on apical half, with apical half tanned black.

Mouth fossa (Fig. 26) large, irregularly pentagonal, broadest at mandibular articulating region, angled laterad, narrower ventrad. *Labrum* (Fig. 28) well sclerotized; basal half trapezoidal, roughly punctate, longitudinal midline with sparse long setae; anterior half shifted ventrad, narrower anteriad, with apical margin sinuate and narrowly emarginate. *Mandible* (Fig. 29) well sclerotized, fist-shaped; middle-part projected, with some setae; apical half finely wrinkled, with 5 teeth. *Maxilla* (Figs. 34–37) long and slender; cardo long, medially narrower, sclerotized, with three tendons on basal margin; stipes weakly sclerotized and membranous, irregularly triangular, finely punctate and setose; lacinia broad, weakly sclerotized basally, flattened, membranous apically, with fine setation; galea broadly connected to stipes, with basal half weakly sclerotized and setose, with apical half more sclerotized and densely setose, with medial surface finely and coarsely setose; maxillary palpus with 5-palpomeres, palpifer laterally connected to stipes, weakly sclerotized; palpomere I as long as palpifer, more sclerotized, with setae; palpomere II setose, longer than I and III, broader anteriad; III setose, as long as I; IV as long as II, with sensilla on apex. *Labium* (Fig. 38–41) with mentum subrectangular, 1.5 times as broad as long, finely punctate medially, sparsely setose; prementum subquadrate, apicomedially broadly emarginate; ligula oval with long and narrowly extended tendon, with anterior half more setose than posterior half; labial palpus with three-palpomeres and setose; palpomere I shorter than II and III, weakly sclerotized; palpomere II setose, broader anteriad; palpomere III as long as II, setose, with sensilla on apex and subapical region.

Pronotum (Fig. 42) with anterior margin semicircular; posterolateral and posteromedial angles well developed; maximum width across posteromedial angles. Dorsum smooth, without punctation or setation. Anterior and lateral margins explanate; explanate portion broader posteriad; width less than half width of disc. Posterior margin smooth, shallowly sinuate, angled from lateral corners toward scutellum. Disc slightly convex in profile; anterior margin flattened or slightly convex; lateral margins reflexed, forming shallow groove that may be absent anteriorly. Posteromedial angle overlapping scutellum. *Prosternum* (Fig. 43) with hypomeron angled medially, surface with weak microsculpture, with some shallow ridges and microelevations; hypomeral process narrow, meeting apex of prosternal process. Anterior prosternal margin smooth, curving around head laterally, expanded, covering mouth parts up to basal part of maxillary palpi, with edge slightly concave laterally. Prosternal process shiny, flat, smooth, overlapping mesosternal margin, with scattered fine punctation posteriorly; tip articulating with recess in mesosternal process; apex medially angled or rounded, broadly expanded behind procoxae, meeting hypomeron. Cervical cavity oval; posterior prothoracic foramen setose internally on ventral half, setose externally in dorsolateral region.

Mesonotum (Fig. 44) obtusely pentagonal, finely setose, 0.5 times as large as pronotum in width and length; anterior margin continuous medially with longitudinal mesothoracic suture; axillary cord finely wrinkled, marginate. *Scutellum* with exposed portion triangular, convex posteriad; frontal margin covered by pronotum; apical margin acute. *Mesosternum* (Fig. 46) deeply notched, receiving procoxal process; exposed portion generally U-shaped; mesosternal process thickened, well sclerotized. *Mesepisternum* pale to dark colored, somewhat triangular, with narrow side towards mesocoxa; mesepisternal ridge well defined, with transverse groove on posterior side. *Mesepimeron* with exposed portion trapezoidal; anterolateral corner triangularly expanded, anterolaterally forming tubercle, with tubercle hidden by elytra in intact specimens (in ventral aspect); ventral surface microreticulate.

Metasternum (Fig. 46) dark, smooth, shiny, medially flat; anterolateral area declivous; posterolateral portion projected, with projection sharply angular; median longitudinal groove faint. Anterior margin in intact specimens deeply fused with mesosternum. Anterior metacoxal process deeply grooved and bilobed. Metepisternum densely punctate.

Elytra (Figs. 47–56), together with pronotum, oval in dorsal view, widest near mid-length, explanate laterad and posteriad; surface shining and punctate; punctures only on black colored surface, deep and coarse, especially at junction of disc and lateral margin area basal margin black, sinuate, weakly denticulate from scutellar angle to area in front of humeral callus; disc swollen at humeral region and mediolateral region; explanate margin distinct from disc, tanned to reddish brown, narrower posteriad, translucent with internal netted pattern in some specimens. In

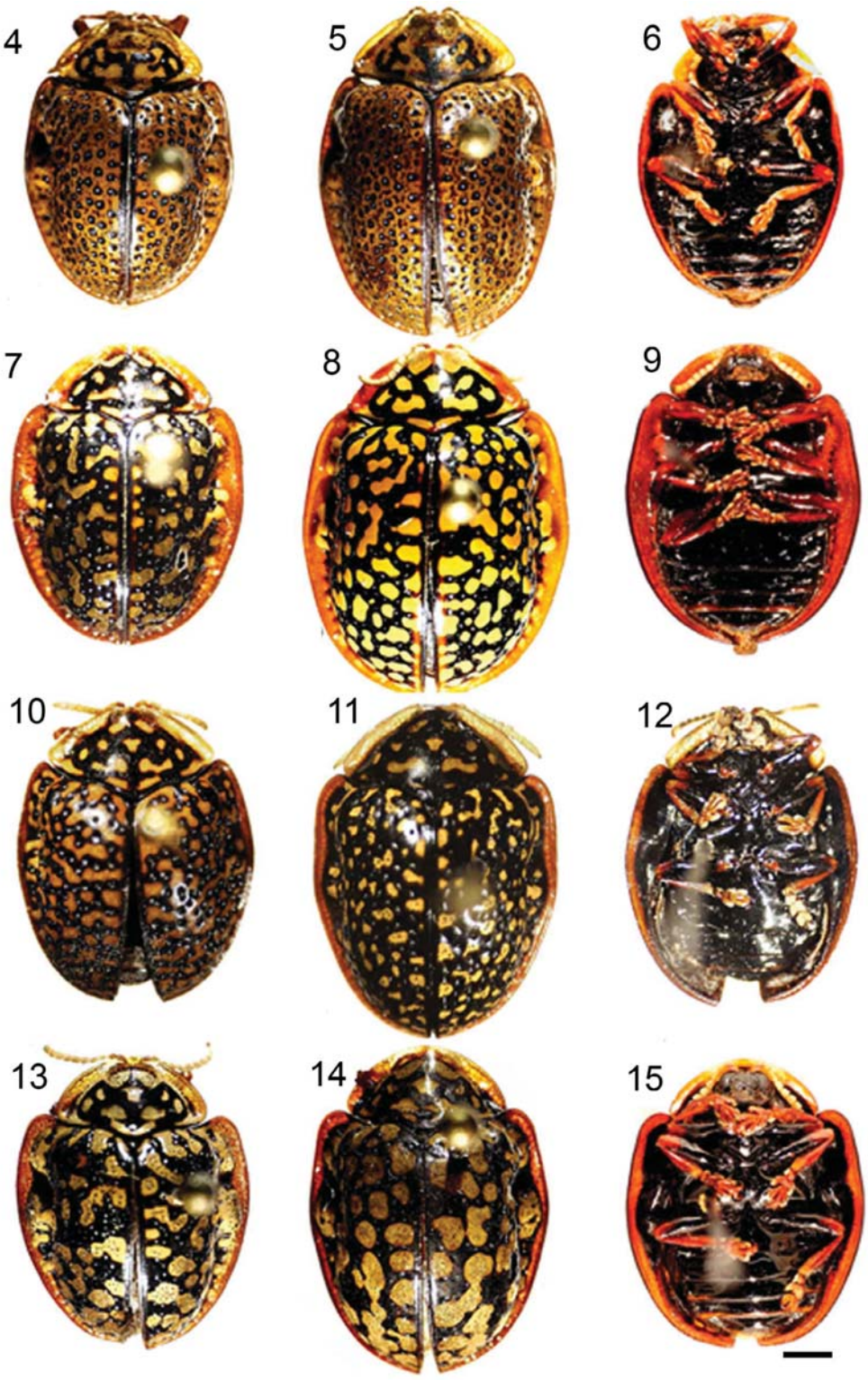

FIGURES 4–6. *Asteriza tainosa*, new species: 4, male, dorsal view; 5, female, dorsal view; 6, male, ventral view. Figs. 7–9. *Asteriza blakeae*, new species: 7, male, dorsal view; 8, female, dorsal view; 9, male, ventral view. Figs. 10–12. *Asteriza flavicornis*: 10, male, dorsal view; 11, female, dorsal view; 12, male, ventral view. Figs. 13–15. *Asteriza darlingtoni*: 13, male, dorsal view; 14, female, dorsal view; 15, male, ventral view. Scale bar = 1.0 mm.

FIGURES 16–23. Lateral view: *Asteriza tainosa*, new species, 16, male; 17, female; *Asteriza blakeae*, new species, 18, male; 19, female; *Asteriza flavicornis*, 20, male; 21, female; *Asteriza darlingtoni*, 22, male; 23, female. Scale bar = 1.0 mm.

ventral view of disarticulated specimens, anterior margin of elytra finely setose; sutural margin slightly explanate in scutellar area; brace forming distinct swelling at posterior humeral region; longitudinal carina present laterome-dially, partly connected to brace; humeral and external brace-longitudinal carina region with patches of very short setae; dorsal black punctures indicated ventrally by minute denticles set in annulate depressions; posterolateral por-tion of epipleuron setose along internal margin.

Hind wing (Figs. 57–58) well developed; coloration varying across wing; radial cell small, irregularly triangular.

Legs slender, long, shiny, sparsely and finely setose except densely setose at tibial apex and ventral portion of tarsi; apex of mid- and hind femora fitting into epipleural concavities when at rest. Visible portion of procoxae and especially metacoxae transverse, mesocoxae less so, all laterally angulate. Trochanters triangular in ventral view, with posterior surface convexly rounded. Each femur 6 times as long as each trochanter, with external surface slightly curved. Each tibia long and slender, 5 times as long as each trochanter, broader distally, with apical third

densely setose and with dorsodistal surface broadly notched to receive tarsus. Tarsi 4-4-4; tarsomeres I, II, III, and IV (= tarsomere V of most Chrysomelidae) dorsally convex with sparse, long setae, with ventral surfaces densely setose; tarsomere I small, as long as broad; tarsomere II shallowly bilobed, base as long as tarsomere I, lobes as long as base, distal half finely setose; tarsomere III deeply bilobed, 3 times as long as tarsomere I; tarsomere IV 4 times as long as tarsomere I, distally setose and covering base of claws; claws evenly curved, tapered, with inner face smooth.

Abdomen completely covered by elytra, broadly rounded; ventrite I dark brown to black, shiny, with well sclerotized hind coxal process; ventrite II as long as I (except for hind coxal process length), longer than III, IV or V; ventrites I–IV with medial regions slightly convex, with oval depression laterally; ventrites II–V sparsely and finely setose laterally; posterior 1/3 of ventrite V sparsely punctate, with setae; spiracles on dorsolateral margins; spiracle openings oval, internal surface smooth; peritremes well sclerotized. Pygidium semicircular, densely punctate, densely and finely setose.

Male genitalia (Figs. 59–63): Testes located near each side of aedeagal base; vasa deferentia loosely coiled, confluent and connected to seminal vesicle; aedeagus long with apex acute, normally laying on side within abdomen, curved from left to right in dorsal view; spicules (Fig. 64) sclerotized, slightly broader distally, 0.5 times as long as basal part of aedeagus; ejaculatory duct long, loosely coiled, weakly sclerotized, connected to aedeagus internally, more sclerotized in opening of seminal vesicle.

Female genitalia (Figs. 62–67): Spermatheca well sclerotized, falcate, with two openings and muscles on inner margin; spermathecal duct sclerotized, coiled and entwined on common oviduct, connected to common oviduct; paired accessory glands laid side by side; accessory gland duct extended posteriad and connected to paired reservoir organs.

Sexual dimorphism. Male (Figs 4, 7, 10, 13) often smaller in overall size and slightly rounded relative to more oval shaped female (Figs. 5, 8, 11, 14). Often, male elytral explanate margin broader; elytral anterolateral region slightly more explanate and angled; profile continuous between pronotum and elytra at scutellum (Figs. 16, 18, 20, 22).

Remarks. The male genitalia are positioned on its side in the abdomen, such that the morphological dorsal and ventral surfaces are oriented laterally. Because of this positioning, the genitalia are rotated in a counterclockwise direction for copulation, which is described by the term deversement (Jeannel 1955; Verma 2009). The apical part of the aedeagus is surrounded by membrane and the pair of spicules are attached to the membrane.

In some specimens, the thickening on the inner surface of the cervical cavity (anterior prothoracic cavity) is developed into an articulating ridge, which is probably the scraper with the stridulatory file as in *Physonota* species (CWS, personal observation).

Key to species

1. Pronotum moderately narrower than elytral base (Figs. 13, 14), in dorsal view not forming nearly regular oval together with elytra; elytral punctures more sparsely, irregularly arranged; discal pale markings of elytra in form of numerous, irregularly shaped blotches, in most specimens much larger than those of pronotal disc; each femur black, with apex pale (Fig. 15) . . . . . *Asteriza darlingtoni* Blake
- Pronotum nearly as wide as elytral base (Figs. 4–12), in dorsal view forming nearly regular oval together with elytra; elytral punctures more closely and regularly arranged; elytral disc either pale with black speckles, or black with pale markings subequal in size to those of pronotal disc; femora variable in color. 2
2. Elytral explanate area (Figs. 7–8) broadly impunctate, translucent without black coloration; pronotal lateral edges reddish, same coloration as on elytral lateral edge; femora unicolorous, reddish brown . . . . . *Asteriza blakeae*, **n. sp.**
- Elytral explanate area (Figs. 4–5, 10–11) closely punctate, with black coloration; pronotal lateral edges pale; each femora black, with apex pale (Figs. 6, 12) 3
3. Elytra pale, with black speckles largely confined to punctures and immediately surrounding areas (Figs. 4–5); frontoclypeus (Fig. 30) brown, finely or shallowly punctuate, maxillary palpomeres III–IV (Fig. 34) and labial palpomere III (Figs. 38) swollen . . . . . *Asteriza tainosa*, **n. sp.**
- Elytral disc black, with numerous small, irregularly shaped pale blotches (Figs. 10–11); frontoclypeus (Fig. 32) black, distinctly to moderately punctuate; maxillary palpomeres III–IV (Fig. 36) and labial palpomere III (Fig. 40) not swollen . . . . . *Asteriza flavicornis* (Olivier)

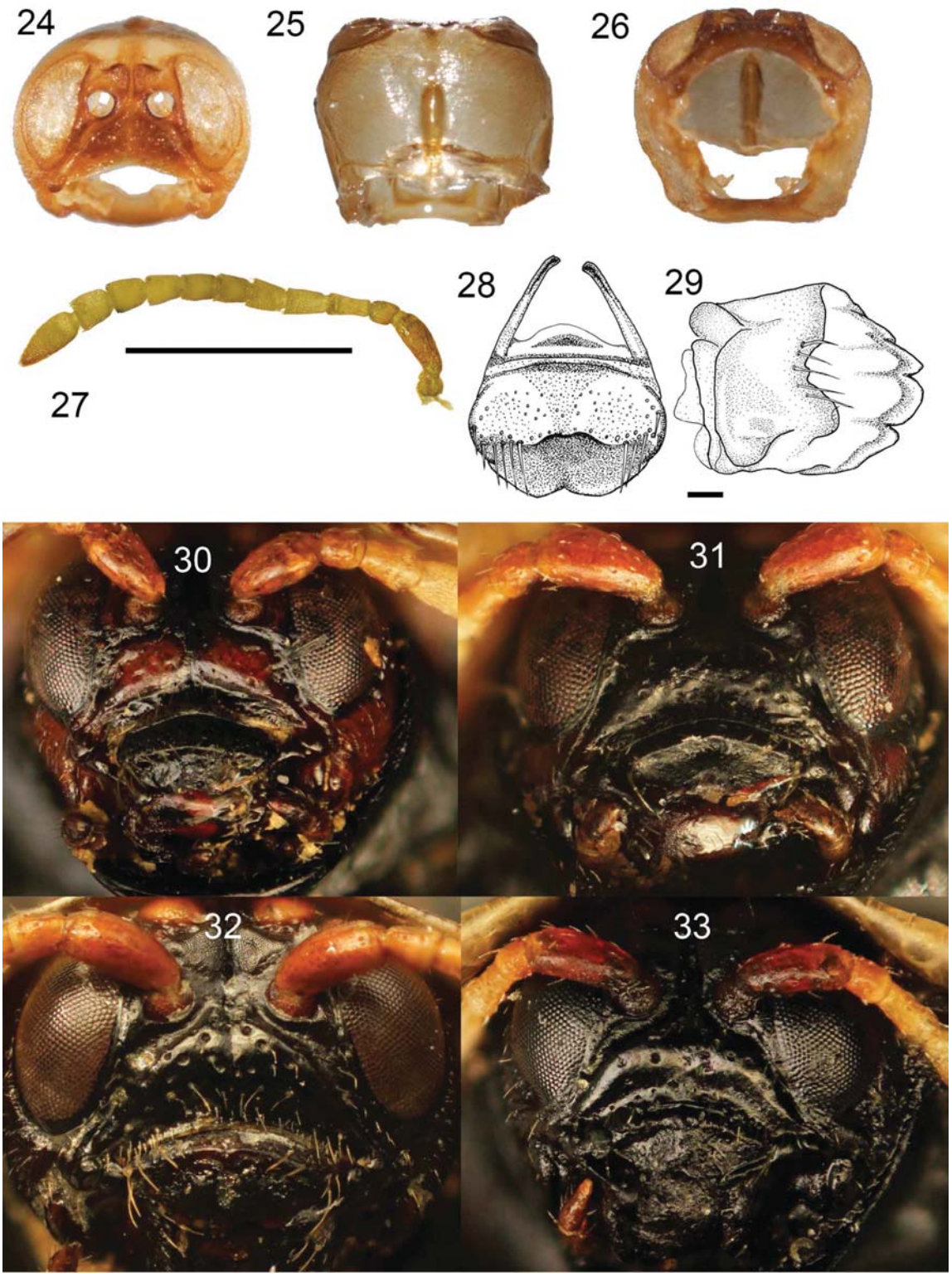

FIGURES 24–26. *Asteriza tainosa*, new species, head: 24, anterior view; 25, dorsal view; 26, ventral view (mouth fossa), scale bars = 1.0 mm; 27, antenna, scale bars = 1.0 mm; 28, labrum; 29, mandible, scale bars = 0.1 mm. Figs 30–33. Head (anterior view): 30, *Asteriza tainosa*, new species; 31, *Asteriza blakeae*, new species; 32, *Asteriza flavicornis*; 33, *Asteriza darlingtoni.*

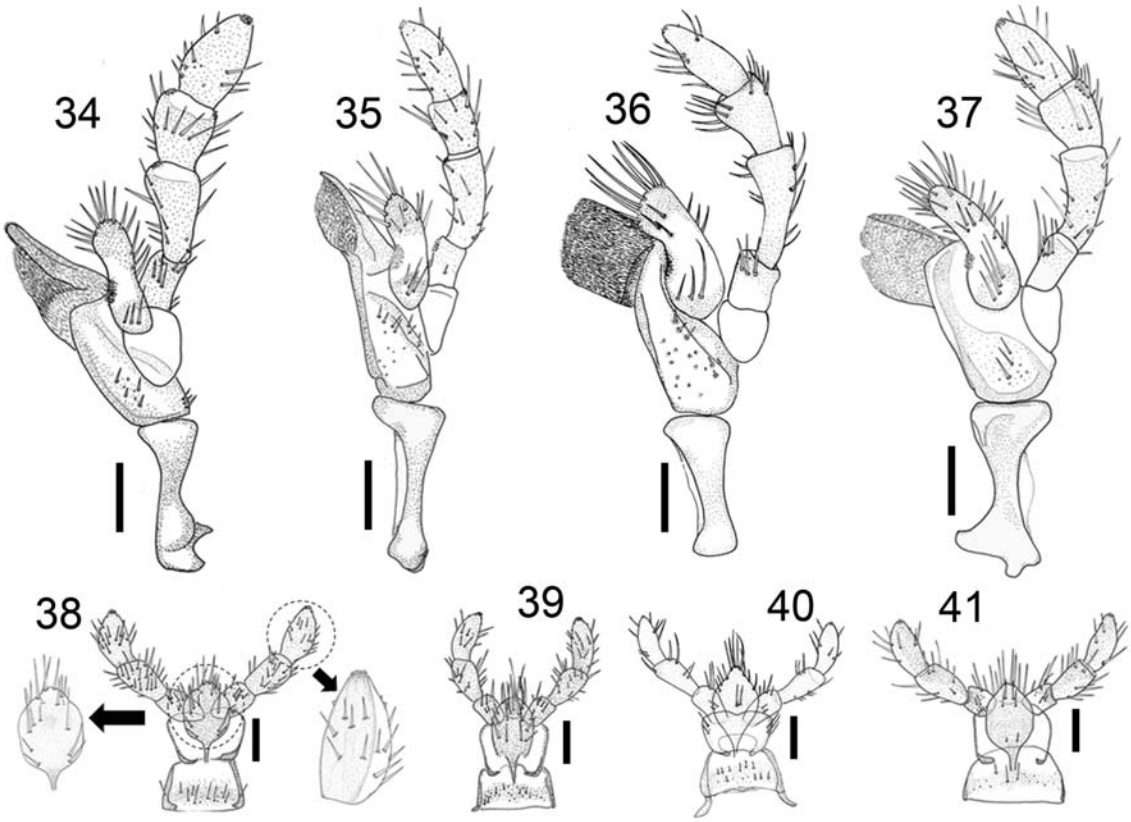

FIGURES 34–37. Maxillae: 34, *Asteriza tainosa*, new species; 35, *Asteriza blakeae*, new species; 36, *Asteriza flavicornis*; 37, *Asteriza darlingtoni*. Figs. 38–41. Labium. 38, *Asteriza tainosa*, new species, 39, *Asteriza blakeae*, new species, 40, *Asteriza flavicornis* 41, *Asteriza darlingtoni*. Scale bars = 0.1 mm.

Asteriza flavicornis (Olivier, 1790)

Cassida flavicornis Olivier 1790: 393 [original description], 1808: 957 [figure]; Staines & Whittington 2003: 3 [type catalog].

Asteriza flavicornis Chevrolat 1836: 372 [transfer]; Boheman 1854: 496 [description], 1856: 147 [checklist], 1862: 365 [description]; Gemminger & Harold 1876: 3660 [catalog]; Spaeth 1914: 122 [catalog]; Blackwelder 1946: 748 [checklist]; Wilcox 1975: 154 [catalog]; Borowiec 1996: 130 [checklist], 1999: 169 [catalog]; Chaboo 2000: 379 [outgroup in phylogenetic analysis]; Takizawa 2003: 97 [checklist]; Chaboo 2007: 23 [phylogeny]; Perez-Gelabert 2008: 125 [checklist]; Świętojańska & Windsor 2008: 655 [mature larvae, pupa, host plant]; Borowiec & Świętojańska 2011 [catalog].

Asteriza punctatissima Chevrolat 1836: 372 [checklist, cited with Klug as author]; Gemminger & Harold 1876: 3660 (*nomen nudum*).

Asteriza flavicornis var. *retigera* Chevrolat 1836: 372 [checklist; cited with Mannerheim as author]; Gemminger & Harold 1876: 3660 (*nomen nudum*).

Type. Lectotype (Fig. 1) and paralectotype (Fig. 2) in RSME, lacking locality information. Staines & Whittington (2003: 3) indicate the same information.

Diagnosis. *A. flavicornis* (Figs. 10–12) can be distinguished from *A. tainosa* **n. sp.** (Figs. 4–6) by the coloration of the pronotum and elytra that are less tan; from *A. blakeae* **n. sp.** (Figs. 7–8) by the elytral lateral margin that is less explanate, the pale pronotal lateral edges and bicolored femora; and from *A. darlingtoni* (Figs. 13–14) by the coloration and the shape between pronotal and elytral bases. The pronotum is nearly as wide as the elytral base, and together they form a nearly regular oval in dorsal view; the pronotal lateral margin is pale; the elytral punctures are more closely, regularly arranged; the dark markings on the elytra are interconnected, surrounding isolated pale blotches; the pale elytral markings are similar in size to those of the pronotal disc; each femur is black with the apical end reddish.

Redescription. *Adult*: Male (n=50) length 8.5–10.0 mm, width 7.2–8.0 mm; female (n=80) length 9.5–11.0 mm, width 8–10.0 mm. Body (Figs. 10–11) oval, slightly discontinuous between pronotal and elytral base in dorsal view; profile (Figs. 20–21) hemispherical with elytra slightly more extended than pronotum ventrad. Dorsal color mottled, black with irregular brown spots, shiny; pale color ranging from yellowish brown to reddish-brown (Figs. 10–11). Head entirely concealed in dorsal view, black; vertex with paired, tan, swollen regions. Frontoclypeus often divided by mesal sulcus or sulcus obliterated by punctures basally but apparent apically. Gena and subgena black or dark reddish-brown. Maxillary palpomeres III and IV (Fig. 36) occasionally with apical sensilla; III slightly curved, 2 times as long as II; IV 1.1 times longer than wide. Ligula (Fig. 40) apically rounded, coarsely setose; labial palpomere III 2.3 times as long as broad, with sensilla on apex, and with 2 individual sensilla subapically. Pronotum (Figs. 42–43) with anterior margin semicircular; posterolateral and posteromedial angles well developed; maximum width across posteromedial angles; dorsum smooth, without punctation or setation; anterior and lateral margins explanate; explanate portion slightly broader posteriad; anterior margin pale, translucent. Elytra (Figs. 51–52) moderately convex, with margins black with reddish brown edge, translucent in some specimens; explanate margin width less than one third elytron discal width.

Material examined. Lectotype, Dufrasne 1936–50, 236; no data (RSME: male); paralectotype, Dufrasne 1936–50, 235; no data (RSME: female); **Dominican Republic: Prov. Azua:** 8km N.E., Padre Las Casas, Rio Las Cuevas, 18˚ 46’ N., 70˚ 53’ W., Alt. 580 m, Oct 3–4 1991, C. Young, R. Davidson, J. Rawlins, Riparian growth in arid thorn scrub, hand collecting (CMNH: 10 males, 15 females; BYU: 2 females); **Prov. Independencia:** Rd. 47, between Los Pinos & Angel Felix, 760 m, 18˚ 36’ 98.6 N., 71˚ 45’ 55.6 W, 20 VI 2005 (CCC: 4 females); ESE Jiman, La Florida, 18˚14' N., 71˚44' W., 20m, moist site, 13 APR 1993, M. A. Ivie, D. Sikes, W. Lanier (WIBF: 4 males, 4 females); **Prov. Monte Cristi:** 5–9 km. N. Villa Elisa, 26 V 1992, col. M.C. Thomas (FSCA: 1 male, 1 female); 8 km. N. Villa Elisa, 31 V 1994, col. M.C. Thomas (FSCA: 2 males, 2 females); no data (ZMHB: 1 male, 1 female); **Prov. San Juan:** 28 km. S.E., San Juan, August 6, 1979, G. B. Marshall (WIBF: 1 female); St. Domingo, 2446, Gorham col. (USNM: 2 females); **Haiti: Prov. Ouquest:** Diquini, W.M. Mann, F. Monros col. 1959 (USNM: 1 female); Port au Prince, R.J. Crew, Wickman col. 1939 (USNM: 10 males, 15 females); Port au Prince, 2˚ 27’ 98 [no direction is provided on label], E.A. Klages, F. Monros col. 1959 (USNM: 3 males, 11 females; CUIC: 3 males, 2 females); Port au Prince [no direction is provided on label] (ZMHB: 1 male, 6 females); W.A. Hoffmann, Apr 16 1925, ex *Cordia mariani* (USNM: 4 males, 2 females); Coll. E. Friv. (HNHM: 1 female); no data (ZMHB: 9 males, 10 females).

Distribution. Dominican Republic: St. Domingo (Gemminger & Harold 1876), Azua (**range extension**), Independencia (**range extension**); **Haiti:** Port au Prince **(**Borowiec & Świętojańska 2011). Boheman (1854) indicated the locality Guyana, which Blake (1939) cited as the country of Guiana; Chaboo (2007: 234) also listed Guyana. Olivier (1790: 393) indicated the locality as “l’Amérique méridionale [South America], which referred to all of South America in the past. Based on the specimens we examined, *Asteriza* appears to be confined to Hispaniola. Olivier’s two type specimens (Figs. 1–2; RSME) lack locality labels (Olivier 1790).

Host plant. Boraginaceae: *Cordia* species (Świętojańska & Windsor 2008). One USNM specimen has a label with the host plant, *Cordia mariani*, but this is not an accepted name for any *Cordia* species.

Remarks. We hereby designate the male specimen as the lectotype (Fig. 1) from the two syntypes (RSME) because it is intact. The other syntype becomes the paralectotype; it is a female specimen (Fig. 2) lacking the abdomen.

Asteriza darlingtoni Blake, 1939

Asteriza darlingtoni Blake 1939: 238 [original description with figure]; Blackwelder 1946: 748 [checklist]; Wilcox 1975: 154 [catalog]; Borowiec 1996: 129 [checklist], 1999: 169 [catalog]; Takizawa 2003: 97 [checklist]; Perez-Gelabert 2008: 125 [checklist]; Borowiec & Świętojańska 2011 [catalog].

Type. Holotype (male, type number: MCZT_23637) and 2 paratypes in MCZ, url: http://insects.oeb.harvard.edu; 2 paratypes in USNM.

Diagnosis. This species is distinguished from the other three *Asteriza* species by the coloration and by the shape of the pronotal and elytral bases. The pronotum in dorsal view is moderately narrower than the elytral base (Figs. 13–14), not forming a nearly regular oval together with the elytra. The elytral punctures (Figs. 53–54) are

more sparsely and irregularly arranged; the pale markings of the elytral disc form numerous, irregularly shaped blotches, which are much larger than those of the pronotal disc in most specimens. Each femur is black, with the apex pale, similar to *A. flavicornis*; *A. blakeae* has pale reddish femora and (Fig. 15). The frontoclypeus (Fig. 33) is coarsely to moderately punctate and not divided by a mesal sulcus.

Redescription. *Adult*: Male (n=13) length 8.5–9.0 mm, width 7.5–8.0 mm; female (n=17) length 9.5–10.0 mm, width 8.0–8.5 mm. Body oval in dorsal view; pronotum and elytra slightly to moderately discontinuous, often more distinctly so in male (Figs. 13–14); profile hemispherical (Figs. 22–23), highest at middle of elytra. Head entirely concealed in dorsal view; gena and subgena black or dark reddish brown. Ligula with anterior margin slightly angled (Fig. 41). Pronotal disc slightly convex, black with brown blotches; anterior margin and edge slightly convex, translucent; lateral margin slightly depressed with edges curved upward, translucent and reddish. Elytra (Figs. 53–54) with brown spots larger and with punctures more sparse than in *A. flavicornis* (Figs. 51–52); brown spots often opalescent with small black spots; lateral reddish edge broader than in *A. tainosa*, **n. sp.** (Figs. 47–48) and *A. flavicornis* (Figs. 51–52) and narrower than in *A. blakeae*, **n. sp.** (Figs 49–50). Legs shiny and reddish brown with coxae and proximal half of femora black. Spermatheca falcate, with inner margin slightly longer and broader than in other *Asteriza* species (Fig. 70).

Material examined. Dominican Republic: Prov. La Vega: Constanza, 3−4,000 ft. VIII. 1938, Darlington (MCZ: 1 male, holotype; USNM: 1 female, paratype); Constanza to Jarabacoa 2−4,000 ft. Darlington (USNM: 1 male); 10 km. N.E. Constanza, May 25, 1978 C.W. & L.B., O'Brien & Marshall (WIBF: 1 female); 18 km. S.E. Constanza, August 4, 1979, C. W. O'Brien (WIBF: 1 female); Jarabacoa PN Armando Bermudez Los Tablones N 19˚ 3' 308, W 70˚ 53' 49 W, 20 VII 2002, col. Sardis Medrano (MHND: 1 male); Constanza Pinar Parejo, Valle Nuevo 10–12 VII 1998, S. Navarro y D. Veloz (MHND: 1 male, 1 female); Cordillera Central 4.1 km, SW E1 Convento, 18˚ 50' 37 N, 70˚ 42' 48 W, Alt. 1730m, V 31 2003, J. Rawlins, R. Davidson, C. Young, C. Nunez, P. Acevedo, dense secondary evergreen forest with pine, hand collecting (CMNH: 5 males, 2 females; BYU: 1 male, 2 females); Vic. Salta de Aguas Blancas, 19 VII 1996, M.C. Thomas (FSCA: 2 females); **Prov. Pedernales:** N. of Pedernales, border rd, Rio Banana, S. of Arroyos, 18˚09'291N, 71˚45'540 W, 21 JUL 1999, Ivie & Guerrero (WIBF: 3 males, 6 females); **Prov. San Cristóbal:** El Convento, *Pinus* forest on steep slopes above El Convento village, 1,700–1730 m, N 18˚ 50' 574, W. 70˚ 42' 189", 20 XI 2003, leg. T, Szűts (HNHM: 1 female).

Distribution. Dominican Republic: Prov. Pedernales and Prov. La Vega. Blake (1939) indicated two localities in La Vega—Constanza to Jarabacoa and Constanza; Borowiec (1999) indicated La Vega.

Remark. In contrast to Blake (1939), we found no consistent pattern of elytral brown spots and no significant difference in the aedeagus from the other *Asteriza* species.

Asteriza tainosa Shin, Chaboo & Clark, new species

Diagnosis. This species is distinguished by the coloration and swollen maxillary and labial palpi. The elytra (Figs. 4–5, 47–48) are mainly tan with black punctures and the anterolateral angle of the male elytra is less acute than in other species. Maxillary palpomeres III–IV (Fig. 34) and labial palpomere III (Fig. 38) are more swollen than in other *Asteriza* species. The frontoclypeus (Fig. 30) is finely and shallowly punctate, brown, and usually divided by a mesal sulcus.

Description. *Adult*: Male (n=85) length 9.0–9.5 mm, width 7.0–8.0 mm; female (n=110) length 10.0–11.5 mm, width 8.0–9.0 mm. Body oval, slightly discontinuous between pronotum and elytra, broadest at middle bulging area of elytra; profile (Figs. 16–17) hemispherical, highest at middle of elytra. Head entirely concealed in dorsal view; gena and subgena (Fig. 30) pale brown to brown. Maxillary palpomere III as long as broad; palpomere IV swollen, 1.5 times broader than long (Fig. 34). Labial palpomere III 1.5 times as long as broad; ligula with apex slightly angled (Fig. 38). Frontoclypeus finely and shallowly punctate, brown, usually divided by mesal sulcus (Fig. 30). Pronotum (Figs. 42–43) hemispherical in dorsal view with postero-medial angle; dorsum smooth and shiny; anterior margin slightly convex, translucent; lateral margin broader posteriad, slightly depressed with edges curved upward; yellow blotch pattern of pronotum more extensive than in other species. Thoracic sterna (Figs. 43, 46) shiny, black, medially flattened. Elytra tan, with each puncture and closely surrounding area black (Figs. 47–48). Legs shiny, reddish brown, with trochanters and proximal half of femora black (Fig. 6). Spermatheca falcate with inner margin curved; part near opening more sclerotized than in other *Asteriza* species (Fig. 67).

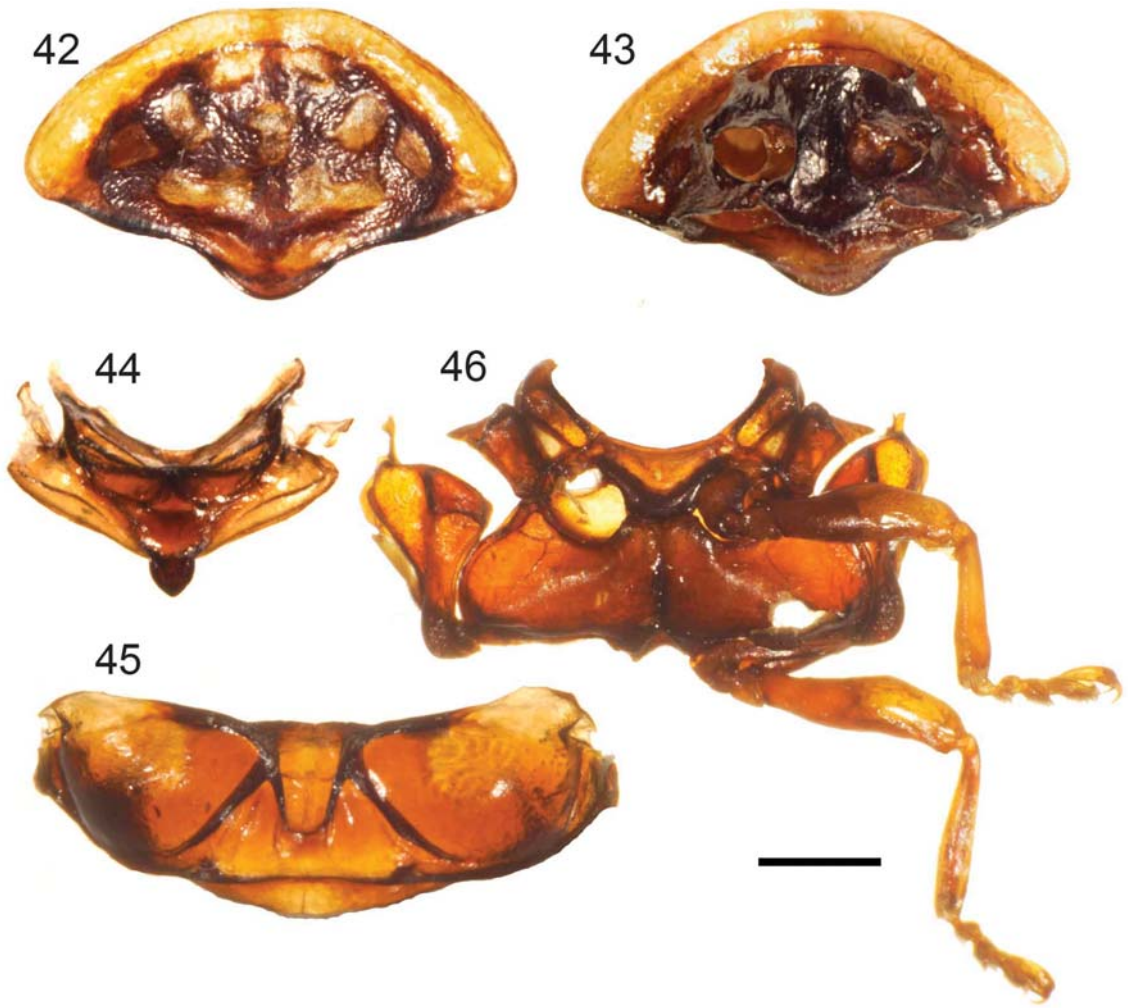

FIGURES 42–46. *Asteriza tainosa*, new species, thorax. 42, pronotum, 43, prosternum, 44, mesonotum, 45, metanotum, 46, meso-metasternum. Scale bars = 1.0 mm.

Type material. Holotype: Male. **Dominican Republic: Prov. Independencia:** Sierra de Bahoruco, North Slope, 13.5 km S.E. Puerto Escondido, N 18˚12'18, W 71˚31'08 W, Alt 1807 m, May 22–23 2004, C. Young, J. Fetzner, J. Rawlins, C. Nunez, Broadleaf *Pinus*, dense woodland, hand collecting (CMNH). Paratypes (192 specimens): **Dominican Republic: Prov. Independencia:** Rd191 Around Caseta No. 1, Parque Nacional Sierra de Bahoruce, 1,239 m, 18˚ 16 038 N, 71˚ 32' 691 W. 11–12 XII 2003, D. Perez, R. Bastardo, B. Hierro (AMNH: 1 male, 2 females); Sierra de Bahoruco, North Slope, 13.5 km SE, Puerto Escondido, 18˚12'18 N, 71˚31'08 W, Alt 1807 m, May 22–23 2004, C. Young, J. Fetzner, J. Rawlins, C. Nunez, Broadleaf *Pinus*, dense woodland, hand collecting (CMNH: 11 males, 16 females); **Prov. Moncion Prov.:** Manoncito, Santiago Rodriguez, R.D. 25 V 1980 (MHND: 41 males, 49 females); **Prov. Monte Cristi:** 5–9 km N. Villa Elisa 26 V 1992, col. M.C. Thomas (MHND: 2 males; FSCA: 1 male, 2 females); 5 km N. Villa Elisa 3 VI 1994, col. M.C. Thomas, (FSCA: 1 male); **Prov. Puerto Plata:** La Ceiba, Luperon, Rd. 21 XI 1981, col. Marcano (MHND: 1 male); **Prov. Sabaneta:** Los Ingenitos, Santiago Rodriguez r. d. 6 VII 1980 (MHND: 5 males, 8 females); Rio Gurabo Stgo Rdguez R.D. 5 VII 1980, col. Marcano (MHND: 1 male); Gurabo, Santiago Rodriguez, R.D. 5 VII 1980, col. Mota-Aquino (MHND: 5 males, 8 females); Sabana Las Caobas, STGO, R. D. 25 V 1980, col. Marcano, Abud-Mota and Reaynoso-Aquino (MHND: 7 males, 10 females); Sabana Las Caobas, STGO, R. D. 6 VII 1980, col. Marcano, Abud-Mota and Reaynoso-Aquino (MHND: 2 female); **Prov. Santiago:**D: 1 male); Gurabo, Santiago Rodriguez, R.D. 5 VII 1980, col. Mota-Aquino (MHND: 5 males, 8 females); Sabana Las Caobas, STGO, R. D. 25 V 1980, col. Marcano, Abud-Mota and Reaynoso-Aquino (MHND: 7 males, 10 females); Sabana Las Caobas, STGO, R. D. 6 VII 1980,

col. Marcano, Abud-Mota and Reaynoso-Aquino (MHND: 2 female); **Prov. Santiago:** S.J. Matas**,** Canafistol, Rd 25 V 1980, col. Marcano (MHND: 1 male); La Celestina S.J. Matas**,** , Rd. 30 VIII 1980 col. Marcano (MHND: 1 female); **Prov. Valverde:** El Cereado, Valverde, R.D. 2 I 1982, col. Marcano (MHND: 2 males, 2 females); **Haiti:** Prov. Sud-Est Massif de La Selle Morne d'Enfer 1850 m, 15 V 1984, M.C. Thomas (FSCA; 1 male, 1 female); Parc National La Visite vicinity park headquarter, 1880 m, 23 V 1984, col. M.C. Thomas (FSCA: 3 males, 8 females); Parc National La Visite between Park headquarter & Morne d'Enfer, 14 V 1984, M.C. Thomas (FSCA: 1 female).

Etymology. The species epithet is derived from the name Taínos, the original tribal inhabitants of Hispaniola before the arrival of Christopher Columbus in the New World (Saunders 2005).

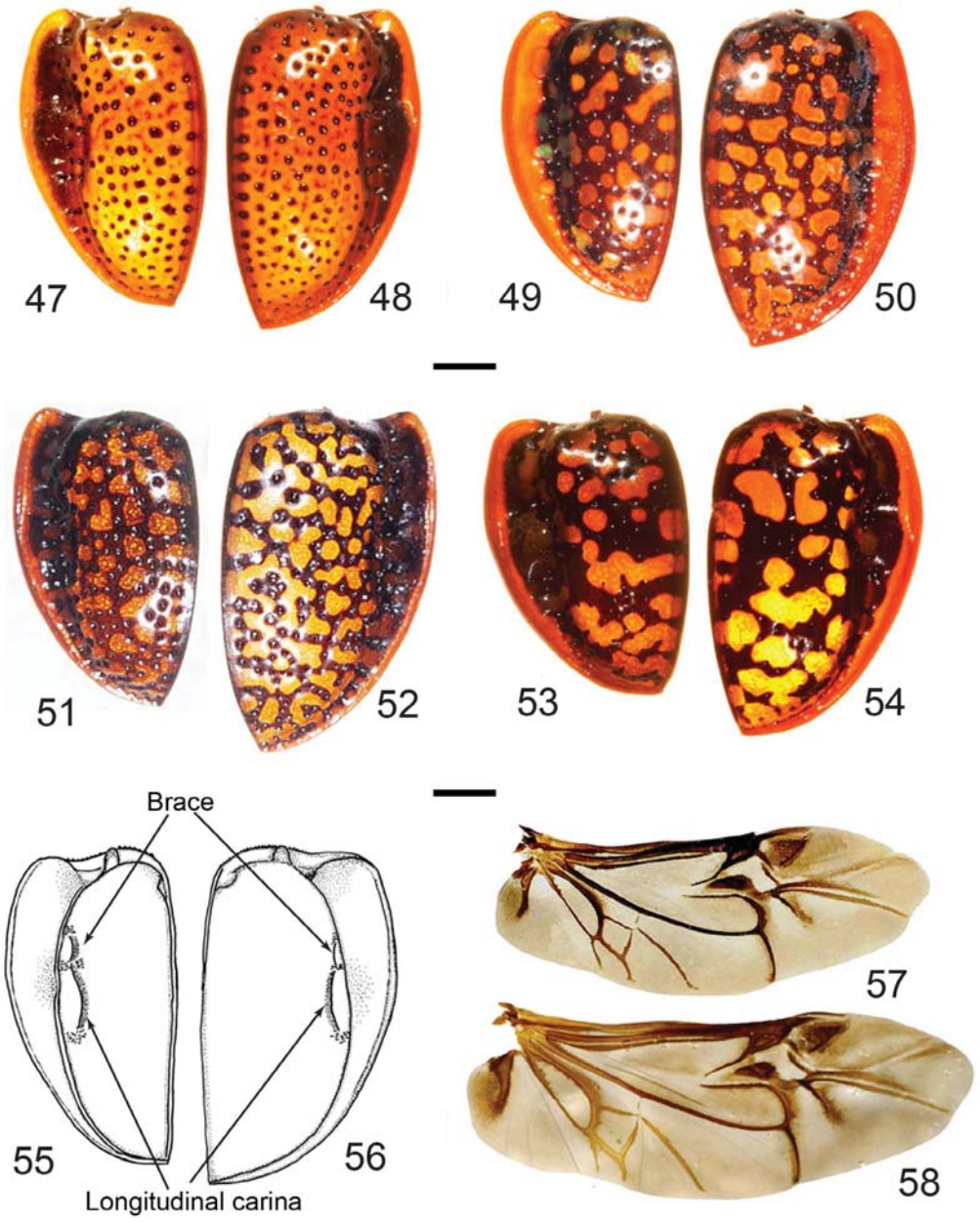

FIGURES 47–54. Elytra, dorsal view: *Asteriza tainosa*, new species, 47, male; 48, female; *Asteriza blakeae*, new species, 49, male; 50, female; *Asteriza flavicornis*, 51, male; 52, female; *Asteriza darlingtoni*, 53, male; 54, female. Figs. 55–56. Elytra, ventral view,: *Asteriza tainosa*, new species, 55, male; 56, female. Figs. 57–58. Hind-wings: *Asteriza tainosa*, new species, 57, male; 58, female. Scale bar = 1.0 mm.

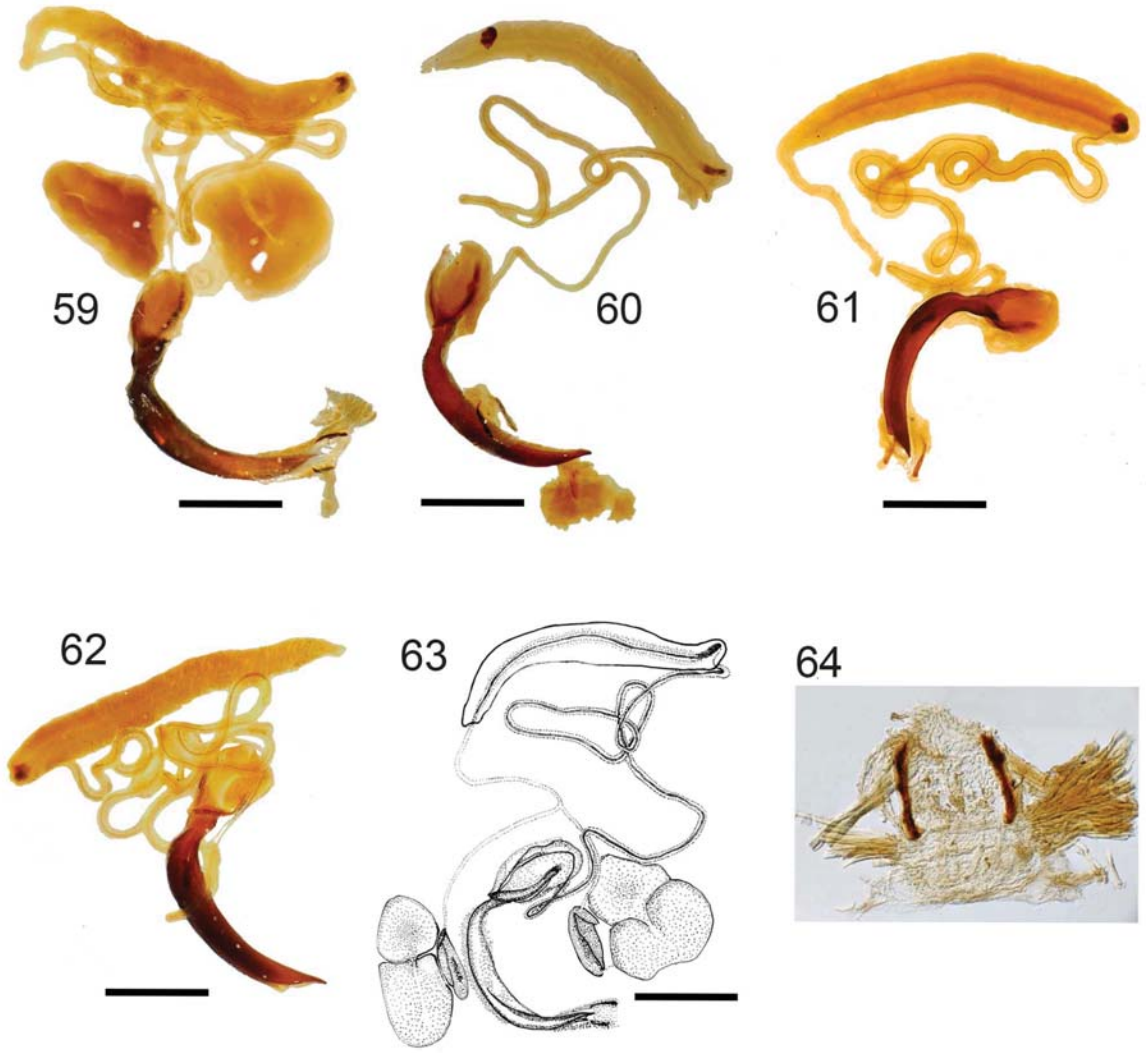

FIGURES 59–63. Male genitalia: 59, *Asteriza tainosa*, new species; 60, *Asteriza blakeae*, new species; 61, *Asteriza flavicornis*; 62, *Asteriza darlingtoni*; 63, *Asteriza tainosa*, new species, scale bars = 0.1 mm. Fig. 64. Spicules: *Asteriza tainosa*, new species.

Asteriza blakeae Shin, Chaboo & Clark, new species

Diagnosis. This species differs from the other three species by its coloration of the pronotal lateral margin, the elytral lateral margin and the femora. The pronotum (Figs. 7–8) is nearly as wide as the elytral base; in dorsal view it forms a nearly regular oval together with the elytra. The pronotal lateral margin is reddish brown and translucent; the elytral margin (Figs. 49–50) is also reddish and translucent without black coloration. The femora (Fig. 9) are mostly or entirely reddish brown.

Description. *Adult*: Male (n=3) length 9.0–9.5 mm, width 7.0–8.0 mm; female (n=7) length 9.8–11.3 mm, width 8.2–9.0 mm. Body (Figs. 7–8), oval or slightly discontinuous between pronotum and elytra, broadest at middle in dorsal view; profile hemispherical, highest at middle (Figs. 18–19). Head entirely concealed in dorsal view; gena and subgena black or dark reddish-brown (Fig. 31). Pronotum (Figs. 7–8) hemispherical with posteromedial angle in dorsal view; blotch pattern same as in *A. flavicornis*; lateral edges reddish, often translucent. Thoracic sterna shiny, black, flattened medially. Elytra (Figs. 7–8, 49–50) color mottled, black with irregular brown spots, shiny, punctate, with distinct lateral bulging areas; pale color ranging from yellowish-brown to red-

dish-brown; lateral margin reddish and transparent without black coloration. Legs (Fig. 9) shiny, reddish with coxae black. Spermatheca (Fig. 68) with inner margin long and narrow.

Type material. Holotype: Male. **Dominican Republic: Prov. Barahona:**, Eastern Sierra Bahoruco, Reserva Cachote 12.8 km NE, Paraiso, 18˚ 05' 54"N, 71˚ 11' 21 W, Alt. 1230m, 12 21 2004, C. Young, C, Nunez, J. Rawlins, J. Fetzner, Cloud forest with tree ferns, yellow pan trap (CMNH). Paratypes (7 specimens): **Dominican Republic: Prov. Barahona:** Eastern Sierra Bahoruco, Reserva Cachote 12.8 km NE, Paraiso, 18˚ 05' 54"N, 71˚ 11' 21 W, Alt. 1230m, 12 21 2004, C. Young, C, Nunez, J. Rawlins, J. Fetzner, Cloud forest with tree ferns, yellow pan trap (CMNH: male, 3 females; BYU: 1 female); Eastern Sierra Bahoruco, Reserva Cachote 12.8 km NE, Paraiso, 18˚ 05' 52 N, 71˚ 11' 19 W, 1198 m, 19–21 V 2004, C. Young, C, Nunez, J. Rawlins, J. Fetzner, semi-disturbed wet broadleaf, UV light (CMNH: 3 females);ca. 35 km N. Cabo Rojo, Las Abejas, 1250 m, 09 Sep 1988, M. Ivie, Philips & Johnson (WIBF: 1 male).

Etymology. The species epithet honors Doris H. Blake (1892–1978) for her valuable contributions on Caribbean Chrysomelidae (Froeschner *et al*. 1981; Bevelheimer 2007).

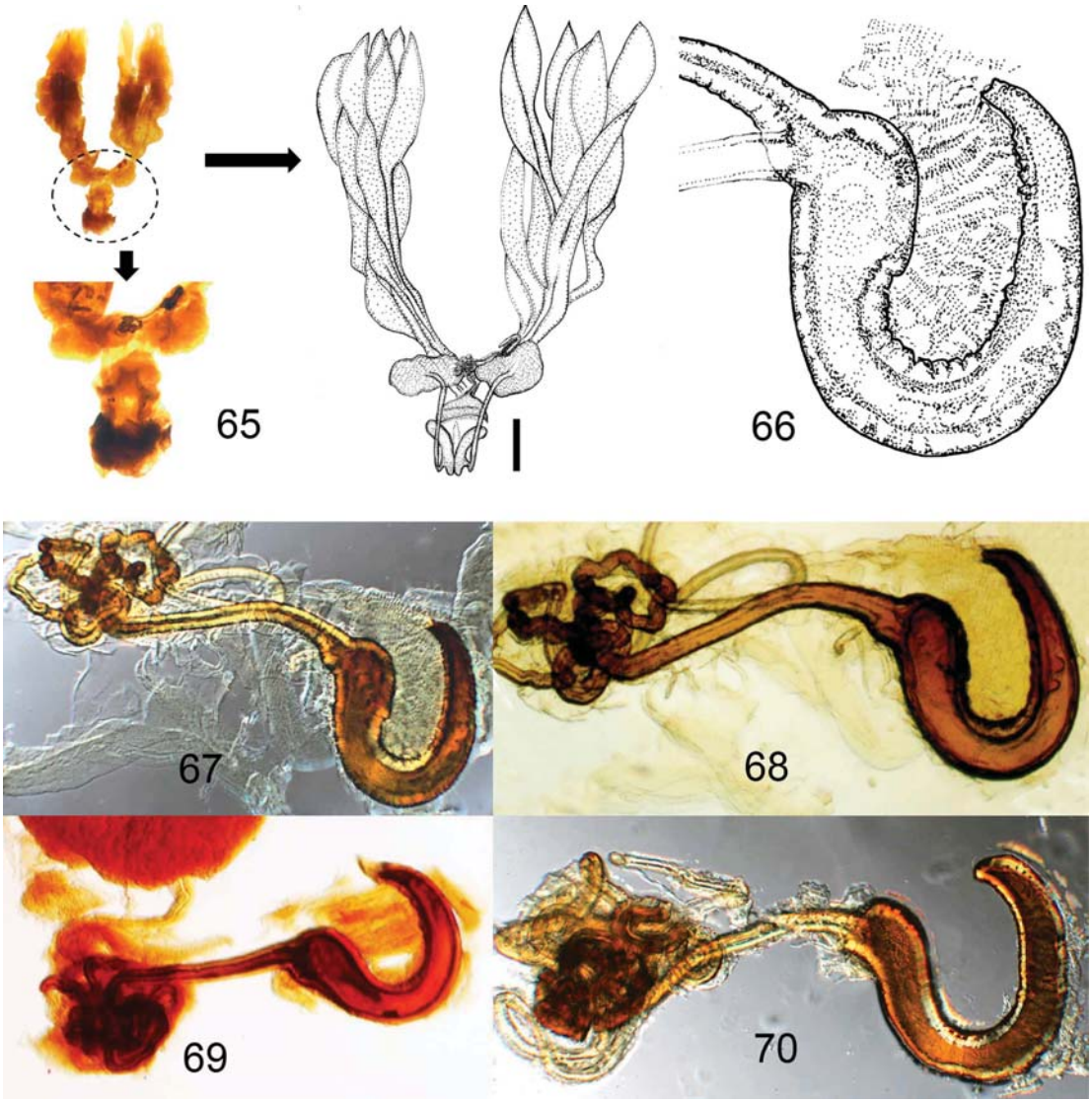

FIGURE 65. Female genitalia, *Asteriza blakeae*, new species, scale bar = 1.0 mm; Figs. 66–70, spermathecae: 66, *Asteriza blakeae*, new species; 67, *Asteriza tainosa*, new species; 68, *Asteriza blakeae*, new species; 69, *Asteriza flavicornis*; 70, *Asteriza darlingtoni*.

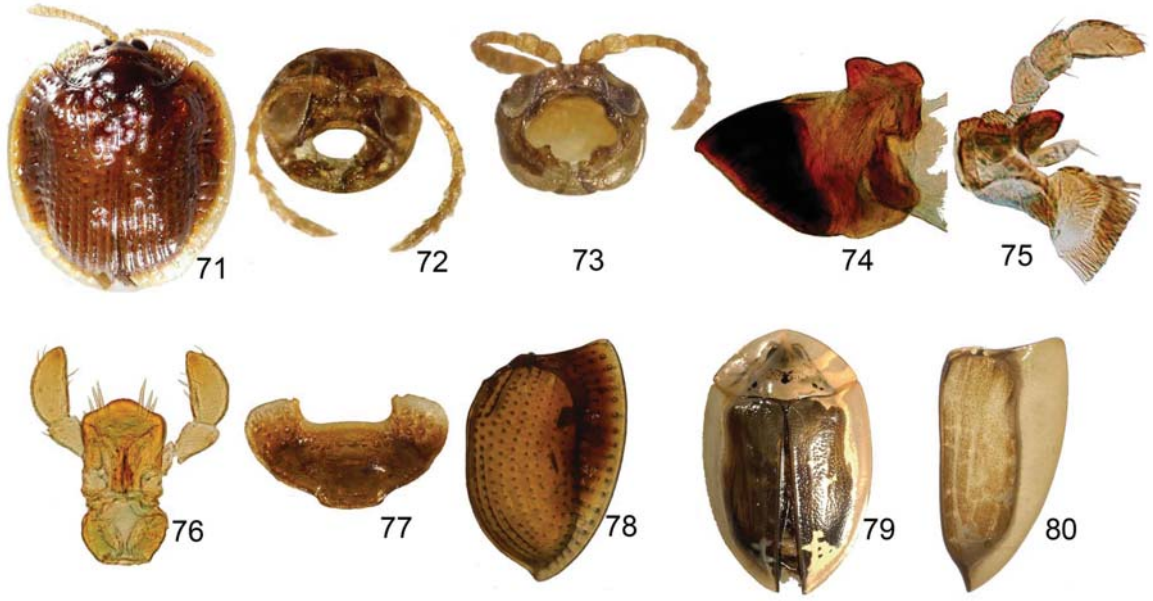

FIGURES 71–78. *Spaethiella* sp. (outgroup): 71, dorsal view; 72, head; 73, mouth fossa; 74, mandible; 75, maxilla; 76, labium; 77, pronotum; 78, elytron (ventral view). Figs. 79–80. *Physonota attenuata* (outgroup): 79, dorsal view; 80, elytron (ventral view).

Discussion

We found two most parsimonious trees (MPT) [Length = 19, consistency index (CI)=1, and retention index (RI)=1]; our characters were resolved unambiguously, which is reflected in the CI and RI values. The MPTs show the resolution of *Asteriza* species as (*A. darlingtoni* + *A. blakeae* **n. sp.**) + (*A. flavicornis* + *A. tainosa* **n. sp.**), or *A. blakeae* **n. sp.** + (*A. darlingtoni* + (*A. flavicornis* + *A. tainosa* **n. sp.**)). The close relationship of *Asteriza* with *Physonota attenuata* is supported by the characters of the head, mouthparts, and pronotum.

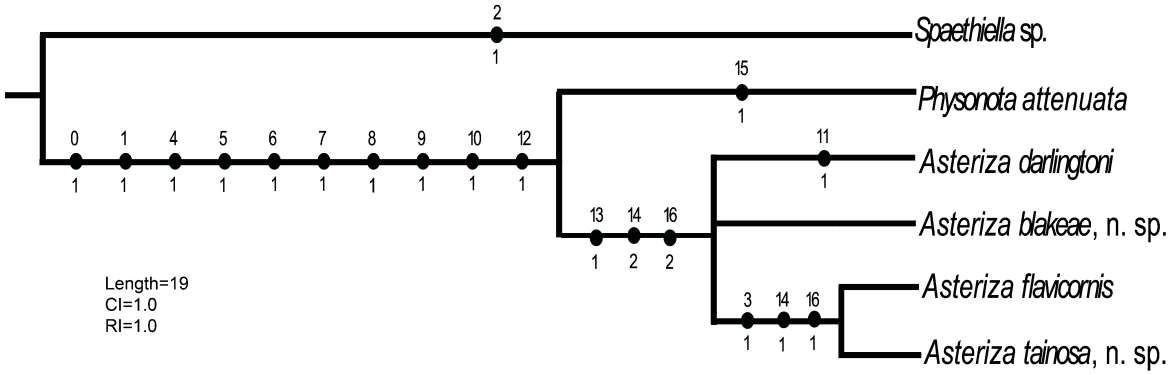

FIGURE 81. Cladogram of four species of *Asteriza* and two outgroups (*Spaethiella* sp. and *Physonota attenuta*). Black circles = unreversed changes; upper numbers = character numbers; lower numbers = character states.

The strict consensus topology (Fig. 81) shows the monophyly of *Asteriza* by the thickened elytral edge, narrowly explanate elytra, and elongate spermatheca. Historic distinguishing characters (thickened elytral edge and narrowly explanate elytra) of *Asteriza* are homoplasious across the subfamily Cassidinae (Chaboo 2007), but other characters, such as the protuberant frontoclypeus, form of the antennal bases, labral emargination, anteriorly angled

elytra basal margin, irregular elytral punctation (absence of regular striae and intervals), and long tarsomere IV, show that *Asteriza* is a derived cassidine.

The internal relationship among the four *Asteriza* species is weakly defined by the frontoclypeal and spermathecal characters. We identified absent and present as two states for the character of frontoclypeal mesal sulcus, and scored the state as present in *A. flavicornis* and *A. tainosa* **n. sp.** The sulcus is complete in *A. tainosa* **n. sp.** but in *A. flavicornis* the apical part is well defined and the basal part is sometimes disturbed basally by the punctation. The other characters for the species identification are mostly autapomorphies and do not resolve phylogenetic relationships. In contrast to the female genitalia, we found that the male genitalia in *Asteriza* do not offer any significant features for identification and the phylogenetic analysis.

TABLE 2. Characters used in the phylogenetic analysis of *Asteriza*.

Vertex, stridulatory file: 0, absent (Fig. 72); 1, present (Figs. 24–26).
Vertex, pair of bulging areas: 0, absent (Fig. 72); 1, present (Figs. 24, 30–33).
Frons: 0, depressed (Fig. 72); 1, not depressed (Figs. 24, 30–33).
Frontoclypeus, mesal sulcus: 0, absent (Fig. 72); 1, present (Figs. 30–33).
Antennomere I (scape): 0, rounded (Fig. 73); 1, elongate (Fig. 27).
Mouth fossa: 0, irregularly triangular (Fig. 73); 1, irregularly pentagonal (Fig. 26).
Mandible, number of teeth: 0, one (Fig. 74); 1, five (Fig. 29).
Lacinia shape: 0, oval (Fig. 75); 1, thin and extended (Figs. 34–37).
Ligula shape: 0, broad (Fig. 76); 1, oval (Figs. 38–41).
Ligula apical margin, sensilla: 0, absent (Fig. 76); 1, present (Figs. 38–41).
Pronotum, anterior margin: 0, discontinuous (Fig. 77); 1, continuous (Figs. 42, 79).
Pronotal and elytral base: 0, continuous (Figs. 4–5, 7–8, 10–11, 71, 79); 1, discontinuous (Figs 13–14).
Elytra, punctures: 0, striate (Fig. 71); 1, irregular (Figs. 47–54, 79).
Elytra, margin: 0, thin (Figs. 71, 79); 1, thickened (Figs. 47–54).
Elytra, ratio (of lateral margin/disc) at between lateral bulging areas: 0, broad (over 0.5) (Figs. 78, 80); 1, narrow (less than 0.33) (Figs. 6, 12); 2, slightly explanate (between 0.5 and 0.33) (Figs. 9, 15).
Elytra, brace: 0, present (Figs. 55–56, 78); 1, absent (Fig. 80).
Spermatheca, inner surface curve: 0, short and round; 1, long and round (Figs, 67, 69); 2, elongate (Figs. 68, 70).

TABLE 3. Character matrix of 17 morphological characters for four ingroup and two outgroup taxa. Character numbers correspond to characters discussed in Table 2.

Taxa	Characters																
	0	1	2	3	4	5	6	7	8	9	10	11	12	13	14	15	16
Spaethiella sp.	0	0	1	0	0	0	0	0	0	0	0	0	0	0	0	0	0
Physonota attenuata	1	1	0	0	1	1	1	1	1	1	1	0	1	0	0	1	0
Asteriza flavicornis	1	1	0	1	1	1	1	1	1	1	1	0	1	1	1	0	1
Asteriza darlingtoni	1	1	0	0	1	1	1	1	1	1	1	1	1	1	2	0	2
Asteriza tainosa	1	1	0	1	1	1	1	1	1	1	1	0	1	1	1	0	1
Asteriza blakeae	1	1	0	0	1	1	1	1	1	1	1	0	1	1	2	0	2

Acknowledgments

We thank John Rawlins and Robert Davidson (CMNH) for bringing the specimens to our attention. We thank the following curators and collections managers for loans of specimens: Jim Liebherr and Richard Hoebeke (CUIC); Alexander Konstantinov and David Furth (USNM); Paul Skelley (FSCA); Carmelo Nuñez (MHND); Michael A. Ivie (WIBF); Lee Herman and Safraz Lodhi (AMNH); and Otto Merkl (HMNN), as well as Santiago Zaragoza Caballero (Instituto de Biología, Colección Nacional de Insectos, Universidad Nacional Autónoma de México) for copying Duges's unpublished notes. We thank Steve Davis and Michael Engel (University of Kansas) for help on the Microptics photographic system; Graham E. Rotheray and Richard Lyszkowski (RSME) and Phil Perkins (MCZ) for loans of type specimens; and Charles D. Michener, Charles Staines, and Michael Schmitt for discussion.

This research is supported by NSF EPSCoR grant #66928 (CSC); CWS's visit to USNM was supported by a George Byers Endowment fund award. The research of SMC is supported by Brigham Young University.

Citations

Barber, H.S. (1946) Nomenclatorial note (Coleoptera: Cassidinae). *Revista de Entomología,* 17, 290–291.

Barber, H.S. & Bridwell, J.C. (1940) Dejean Catalogue names (Coleoptera). *Bulletin of the Brooklyn Entomological Society,* 35(1), 1–12.

Bevelheimer, S. (2007) *Doris Holmes Blake Papers, 1899–1985*, Smithsonian Institution Archives, Washington D.C. Available from http://siarchives.si.edu/findingaids/faru7310.htm#topofpage/ (August 1, 2011).

Blackwelder, R.E. (1946) Checklist of the coleopterous insects of Mexico, Central America, The West Indies and South America. Part 4. *United States National Museum, Bulletin,* 185, 551–763.

Blake, D.H. (1939) Eight new Chrysomelidae (Coleoptera) from the Dominican Republic. *Proceedings of Entomological Society of Washington,* 41, 231–239.

Boheman, C.H. (1854) *Monographia Cassididarum.* Tomus secundus. Holmiae, 506 pp. + 2 tab.

Boheman, C.H. (1856) *Catalogue of Coleopterous Insects in the Collection of the British Museum,* Part IX, Cassididae. London, 225 pp.

Boheman, C.H. (1862) *Monographia Cassididarum.* Tomus quartus. Holmiae, 504 pp.

Borowiec, L. (1995) Tribal classification of the cassidoid Hispinae (Coleoptera: Chrysomelidae). *In*: Pakaluk, J. & Ślipiński, S.A. (Eds.), *Biology, Phylogeny, and Classification of Coleoptera*, Papers Celebrating the 80th Birthday of Roy A. Crowson, Warszawa, pp. 541–558.

Borowiec, L. (1996) Faunistic records of Neotropical Cassidinae (Coleoptera: Chrysomelidae). *Polskie Pismo Entomologiczne,* 65, 119–251.

Borowiec, L. (1999) *A World Catalogue of the Cassidinae (Coleoptera: Chrysomelidae).* Biologica Silesiae, Wrocław, 476 pp.

Borowiec, L. & Świętojańska, J. (2011) *World Catalog of Cassidinae*, Wrocław, Poland. Available from: http://www.biol.uni.wroc.pl/cassidae/katalog%20internetowy/index.htm/ (August 1, 2011).

Bouchard, P., Bousquet, Y., Davies, A.E., Alonso-Zarazaga, M.A., John F. Lawrence, J.F., Lyal, C.H.C., Newton, A.F., Reid, C.A.M., Schmitt, M., Ślipiński. S.A., & Smith, A.B.T. (2011) Family-group names in Coleoptera (Insecta). *ZooKeys*, 88, 1–972.

Chaboo, C.S. (2000) Revision and phylogeny of the Caribbean genus *Elytrogona* (Coleoptera: Chrysomelidae: Cassidinae: Stolaini*). The Coleopterists Bulletin*, 54(3), 379–394.

Chaboo, C.S. (2004) Natural history observations in *Eurypepla calochroma* Blake (Chrysomelidae: Cassidinae: Physonotini). *The Coleopterists Bulletin,* 58(1), 71–78.

Chaboo, C.S. (2007) Biology and phylogeny of Cassidinae Gyllenhal (tortoise and leaf-mining beetles) (Coleoptera: Chrysomelidae). *Bulletin of the American Museum of Natural History,* 305, 1–250.

Champion, G.C. (1894) *Biologia Centrali-Americana. Insecta. Coleoptera. Volume VI. Part 2. Phytophaga. Cassididae and appendix to Hispidae*. pp.165–249 + tab. 5–13.

Chapuis, M.F. (1875) 11. Famille des Phytophages. *In*: Lacordaire, T. (Ed.), *Histoire Naturelle des Insectes. Genera des Coléopteres ou expos méthodique et critique de tous les genres proposés jusqu ici dans cet ordre d'Insectes.* Volume XI. A la Libraire Encyclopédique de Roret, Paris, 420 pp.

Chevrolat, A. (1834) *Coléopteres du Mexique.* Silvermann, Strasbourg, France, 211 pp.

Chevrolat, A. (1836) *Catalogue des Coléopteres de la collection de M. le Comte Dejean,* Troisieme édition, revue, corrigee et augmentee. Volume V. Paris, 443 pp.

Dugès, D.E. (1901) *Catálogo de la Colección de Coleópteros Mexicanos del museo nacional, formada y clasificada*. Segunda edicion, Num. 5, Imprenta del Museo Nacional, Mexico, 148 pp.

Evenhuis, N.L. (2011) *Abbreviations for Insect and Spider Collections of the World*, Honolulu, HI, USA. Available from: http://hbs.bishopmuseum.org/codens/codens-inst.html/ (August 1, 2011).

Froeschner, R.C., Froeschner, E.M.L. & Cartwright, O.L. (1981) Doris Holmes Blake, January 11, 1892–December 3, 1978. *Proceedings of the Entomological Society of Washington,* 83(3), 544–564.

Gemminger, M. & Harold, E. von. (1876) *Catalogus Coleopterorum hucusque descriptorum synonymicus et systematicus. Chrysomelidae (II), Languriidae, Erotylidae, Endomychidae, Coccinellidae, Corylophidae, Platypsyllidae.* Accedit. Index Generum universalis. Theodor Ackermann, Monachii: 3479–3822 + [2] pp.

Gistel, J. (1834) *Die Insecten-Doubletten aus der Sammlung des Grafen Rudolph von Jenison Walworth zu Regensburg, welche sowohl im Kauf als im Tausche abgegeben werden*, Nro. I. Käfer, München, II + 35 pp.

Goloboff, P.A. (1998) *Nona*. Computer software and documentation distributed by the American Museum of Natural History, New York.

Gyllenhal, L. (1813) *Insecta Suecica. Classis I. Coleoptera sive Eleuterata*, Tomus I, pars III. Scaris, 734 pp.

Hincks, W.D. (1952) The genera of the Cassidinae (Coleoptera: Chrysomelidae). *Transactions of the Royal Entomological Society of London,* 103, 327–358.

Hope, F.W. (1840) *The coleopterist's manual, part the third, containing various families, genera, and species, of beetles, recorded by Linneus and Fabricius. Also, descriptions of newly discovered and unpublished insects.* J.C. Bridgewater, London, UK, 191 + [3] pp.

International Commission of Zoological Nomenclature. (1999) *International Code of Zoological Nomenclature [ICZN]*. Fourth edition. The International Trust for Zoological Nomenclature, c/o Natural History Museum, London, i–xxix, + 306 pp.

Jeannel, R. (1955) *L'Edeage*. Museum National d'Histoire Naturelle, Paris, 155 pp.

Klug, K. (1829) Preissverzeichniss vorräthiger Insectendoubletten des Königl. Zoologischen Museums der Universität. Berlin, 18 pp.

Lawrence, J.F. & Britton, E.B. (1991) Coleoptera (beetles). *In*: Naumann, I.D. (Ed.), *The Insects of Australia*, Second edition. Volume II, Cornell University Press, Ithaca, New York, pp. 543–683.

Madge, R.B. (1988) The publication dates of Dejean's catalogues. *Archives of Natural History*, 15(3), 317–321.

Mannerheim, C.G. von (1825) Novae coleopterorum species imperii Rossici incolae descriptae, in Hummel. *Essais entomologiques*, 1(4), 19–41.

Monrós & Viana (1951) Las Cassidinae de la seccion "Hemisphaerotina" con revision de las especies Argentinas (Coleoptera, Cassidinae). *Acta Zoologica Lilloana*, 11, 367–395.

Nixon, K.C. (2002) *Winclada, Version 1.00.08*. Computer software and documentation. Available from: http://cladistics.com/ (August 1, 2011).

Olivier, A.G. (1790) *Encyclopédie Méthodique, Histoire Naturelle. Insectes.* Volume V. Paris, 793 pp.

Olivier, A.G. (1808) *Entomologie, ou histoire naturelle des Insectes, avec leur caracteres géneriques et spécifiques, leur description, leur synonymie, et leur figure enluminée. Coléopteres,* Volume VI. Paris, 613–1104 pp.

Perez-Gelabert, D.E. (2008) Arthropods of Hispaniola (Dominican Republic and Haiti): A checklist and bibliography. *Zootaxa,* 1831, 1–530.

Riley, E.G., Clark, S.M., Flowers, R.W. & Gilbert, A.J. (2002) 124. Chrysomelidae Latreille 1802. *In*: Arnett, R.H., Thomas, M.C., Skelley, P.E. & Frank, J.H. (Eds.), *American Beetles*, Volume 2, Polyphaga: Scarabaeoidea through Curculionoidea. CRC Press, Boca Raton, London, New York, Washington, pp.617–691.

Saunders, N.J. (2005) *The Peoples of the Caribbean*. ABC-Clio, Oxford, UK, 399 pp.

Seeno, T.N. & Wilcox, J.A. (1982) Leaf beetle genera. *Entomography,* 1, 1–221.

Spaeth, F. (1913) Kritische Studien über den Umfang und die Begrenzung mehrerer Cassiden-Gattungen nebst Beschreibung neuer amerikan. *Arten Archiv für Naturgeschichte*, 79, 126–164.

Spaeth, F. (1914) Chrysomelidae: 16. Cassidinae. *In*: Junk, W. & Schenkling, S. (Eds.), *Coleopterorum Catalogus*, Pars 62, Berlin, 182 pp.

Spaeth, F. (1942) Cassidinae (Coleoptera: Chrysomelidae). *In*: Titschack, E. (Ed.), *Beiträge zur Fauna Perus*, 2, 11–43.

Staines, C.L. (2010) Nomenclatural notes on Chalepini and Sceloenopliini (Coleoptera: Chrysomelidae: Cassidinae). *Insecta Mundi*, 0122, 1–2.

Staines, C.L. & Whittington, A.E. (2003) Chrysomelidae (Coleoptera) types in the Royal Museum of Scotland Collection. *Zootaxa,* 192, 1–8.

Sturm, J. (1843) *Catalog der Kaefer-Sammlung*. Nürnberg, Germany, 386 pp.

Świętojańska, J. & Windsor, D.L. (2008) Immature stages of *Asteriza flavicornis* (Olivier) and *Physonota alutacea* Boheman (Coleoptera: Chrysomelidae: Cassidinae). *Annales Zoologici*, 58, 641–665.

Takizawa, H. (2003) Check list of Chrysomelidae in West Indies (Coleoptera). *Hispaniolana*, Nueva Serie, 2, 1–125.

Verma, K.K. (2009) Retournement of the aedeagus in Chrysomelidae - revisited. *In*: Jolivet, P, Santiago-Blay, J. & Schmitt, M. (Eds.), *Research on Chrysomelidae*, Vol. 2. Brill, Leiden, The Netherlands, pp. 105–114.

Wilcox, J.A. (1975) Family 129. Chrysomelidae. *In*: Arnett Jr., R.H. (Ed.), *Checklist of the Beetles of North and Central America and the West Indies*. North American Beetle Fauna Series. Flora & Fauna Publications, Gainesville, pp. 166.

CHAPTER 2

A revision of the Neotropical tortoise beetle genus *Eurypedus* (Coleoptera: Chrysomelidae)

\

***** Formatted for submission to the journal *Canadian Entomologist.*

ABSTRACT

The genus *Eurypedus* Gistel was revised based on detailed morphological study including the mouthparts and genitalia. Besides previously known diagnostic characters such as an oblong and laterally parallel-sided body, narrow elytral lamella, narrow prosternal process between the procoxae, and angled pronotal base, new diagnostic characters were identified: antennal notches on the ventral surface of the antennomeres V–XI, a stridulatory file on the vertex and paired projections on the ventral surface of the pronotum. The distinct stridulatory file was found only in males. The number of ridges of the stridulatory file varied between 48 and 59. *Eurypedus thoni* Barber is synonymized with *E. peltoides* (Boheman). The remaining two species (*E. peltoides* and *E. nigrosignatus* (Boheman)) showed distinct distributions separated by the Amazon basin.

INTRODUCTION

The New World genus *Eurypedus* Gistel is little known and currently contains three recognized species (*E. nigrosignatus* (Boheman), *E. peltoides* (Boheman), *E. thoni* Barber). The current morphological circumscription of the genus is as follows: tarsomere IV without basal tooth, pronotal base emarginate with well-defined postero-lateral angles, oblong and laterally parallel-sided body, elytral lamella narrower than elytral inner marginal line, and prosternal process between procoxae narrower than trochanter (see Borowiec and Świętojańska 2014).

The first described species of *Eurypedus* was *Cassida oblonga* Sturm in Thon (1827). The original description included color paintings. Sturm was aware that his *C. oblonga* was a homonym of *C. oblonga* Illiger (see Illiger 1798), and also recognized that Illiger's *C. oblonga* was a junior synonym of *C. vittata* Villers. However, Sturm believed that his *C. oblonga* was a

valid name precisely because Illiger's *C. oblonga* was a junior synonym of *C. vittata*. In 1834, Gistel erected the genus *Eurypedus* to house *C. oblonga* as thereby creating the new combination *E. oblongus*. Unaware of Gistel's erection of *Eurypedus*, Sturm (1843) described *Ischyrosonyx* to house *C. oblonga*. Sturm's *Ischyrosonyx* was invalid because it was a synonym to the earlier erected *Eurypedus*. However, it was Sturm's *Ischyrosonyx* not *Eurypedus* that was used until Barber (1946). Boheman (1854) recognized a total of six species of *Ischyrosonyx* including five new species and provided a description for each (*I. oblonga, I. peltoides, I. inanis* Boheman, *I. discipennis* Boheman, *I. marginicollis* Boheman, *I. nigrosignata*). Spaeth (1914, 1915) reclassified *I. inanis* as a species of *Cistudinella* Champion owing to its rounded lateral body shape. He also synonymized *I. discipennis* and *I. marginicollis* with *I. nigrosignata* based on observations by Fritsche and considered *I. discipennis* and *I. marginicollis* to simply be different color morphs of *I. nigrosignata*. Barber (1946) recognized *Eurypedus* as a valid generic name and noted that *C. oblonga* by Sturm in Thon (1827) to be a primary homonym of *C. oblonga* Illiger (1798). Thus, Barber (1946) proposed *E. thoni* as the replaced name. Borowiec (1996) created the new combinations of two names (*E. nigrosignatus* and *E. oblongus*), and later (Borowiec 1999) designated a lectotype for *I. nigrosignata, I. discipennis*, *I. marginicollis* from syntype series, and *I. peltoides* from a syntype. Currently only three species of *Eurypedus* are valid (*E. nigrosignatus, E. peltoides,* and *E. thoni*).

Eurypedus was erected in Gistel (1834) without a formal description and the subsequent descriptions (Boheman 1854; Chapuis 1875) were limited to the general body shape and body coloration. The current morphological definition of *Eurypedus* by Borowiec and Świętojańska (2014) is still vague in term of distinguishing *Eurypedus* from other tortoise beetle genera. In

addition, the validity of each species in *Eurypedus* needs to be confirmed because diagnostic features are lacking for each species.

Herein, a detailed description of *Eurypedus* is provided with illustrations for mouthparts and genitalia included the first time. *Eurypedus thoni* is synonymized with *E. peltoides* based on continuous morphological color variation. Several new host plants are reported from the collecting data of the examined specimens. New morphological characters are provided and discussed. The distributions of valid species, based on the collecting locality from examined specimens and previously known data, are mapped.

MATERIAL AND METHODS

A total of 220 specimens including the name-bearing type specimens of six species were provided by the following collections:

AMNH: American Museum of Natural History, New York, New York, U.S.A.

DZUP: Universidade Federal do Paraná, Museu de Entomologia Pe. Jesus Santiago Moure, Curitiba Paraná, Brazil.

EGRC: Collection of Edward G. Riley, Texas, U.S.A.

FSCA: Division of Plant Industry, Florida State Collection of Arthropods, Gainesville, Florida, U.S.A.

HNHM: Hungarian Natural History Museum, Budapest, Hungary.

MCZ: Harvard University, Museum of Comparative Zoology, Cambridge, Massachusetts, U.S.A.

MNRJ: Universidade do Rio Janeiro, Museu Nacional, São Cristovão, Rio de Janeiro, Brazil.

NHRS: Naturhistoriska Riksmuseet, Stockholm, Sweden.

SEMC: Natual History Museum, University of Kansas, Lawrence, Kansas, U.S.A.

TAMU: Texas A abd M University, College Station, Texas, U.S.A.

USNM: National Museum of Natural History, Washington, D.C., U.S.A.

Descriptions were based on pinned and dissected specimens. For the description of the head, head appendages, and genitalia, the individual parts were treated in 5–10% KOH and dissected in distilled water, 95% alcohol, or glycerin. Dissected vouchers were preserved in glycerin. Specimens were examined with a Leica MZ16 stereomicroscope and an Olympus SZ30 stereomicroscope. Measurements were made with an ocular micrometer on a Leica DFC320 system attached to a Zeiss Axioskop 2 plus. Photographs were taken with a Microptics® camera system or a Leica DFC320 system attached to the Zeiss Axioskop 2 plus. For the scanning electron microscopy (SEM) images, head and antenna were mounted on SEM stubs using Pelco Tabs (carbon conductive tabs) and isopropanol-based colloidal graphite, and were coated with 30nm of gold for 60 seconds. SEM images were captured using a LEO 1550 FESEM in the Microscopy and Analytical Imaging Laboratory at the University of Kansas. For determining the number of lines on the stridulatory files, the images of the stridulatory files were taken with the Microptics® camera system; only stridulatory file ridges which are broader than long were counted.

The general terminology followed Lawrence and Britton (1991). The following terms used in this study deviate from the terms used in various published sources: **antennal notch** is used for the notched structures on the ventral surface of antennomeres V–XI (Figs. 24–27) instead of “antennal grooves” in Chaboo (2007) to distinguish them from the antennal grooves which are the paired antennae-receiving structures on the pronotal hypomeron or on each side of

the prosternum (Borowiec and Świętojańska 2014); **elytral lamella** is used instead of "elytral margin" or "elytra explanate margin" because the term "margin" should be more appropriately applied to where the dorsal and ventral plates meet; and **elytral medial marginal line** was used instead of "sutural interval" as used in the generic diagnosis of Borowiec and Świętojańska (2014) because "suture" should only be used for a line or structure demarcating segments (metameres) of the insect body.

For the distribution map (Fig. 41), the distribution of each species was marked as "**N**" for *E. nigrosignatus* and "**P**" for *E. peltoides* based on the locality data from previous studies (see Borowiec and Świętojańska 2014) and the specimens examined in this study. The localities were marked at the level of "Departamento," "Estatdo," or "Provincia" because most of the locality data on the labels from past studies and examined specimens were imprecise.

TAXONOMY

Subfamily Cassidinae Gyllenhal

Tribe Ischyrosonychini Chapuis

Eurypedus Gistel

(Figs. 1–40)

Eurypedus Gistel 1834: 31 [description, type species: *Cassida oblongus* Sturm in Thon (1827)]; Barber 1946: 290 [as valid name]; Seeno and Wilcox 1982: 175 [checklist]; Borowiec 1999: 171 [catalog]; Borowiec and Świętojańska 2014 [online catalog].

Ischyrosonyx Sturm [type species: *Ischyrosonyx oblonga* Sturm]: Dejean 1836: 370 [invalid generic name]; Sturm 1843: 273 [catalog]; Chapuis 1875: 382 [description]; Spaeth 1914: 65 [catalog]; Hincks 1952: 330 [key to tribes, genera list].

Type species

Cassida oblonga Sturm in Thon (1827) by monotypy (= *E. peltoides* (Boheman), see Remark section of *E. peltoides*).

Diagnosis

Eurypedus (Figs. 1–12) is distinguished from the other six genera of Ischyrosonychini (*Asteriza* Chevrolat, *Cistudinella*, *Enagria* Spaeth, *Eurypepla* Boheman, *Physonota* Boheman, and *Platycycla* Boheman) by its oblong and laterally parallel-sided body, elytral lamella narrower than elytral inner marginal line, and prosternal process between procoxae narrower than trochanter (Borowiec and Świętojańska 2014). It can also be distinguished by newly found diagnostic characters: presence of notches on the ventral surface of antennomeres V–XI (Figs. 24–27), and projections on each antero-lateral region of the prosternum on ventral surface of the pronotum each side (Figs. 29–30, marked by black arrow). The detailed morphological features of the head stridulatory files can also be used to distinguish *Eurypedus* from the other six genera of Ischyrosonychini including the sexual dimorphism with respect to the stridulatory file (Fig. 20–23), the number of ridges on the stridulatory file (48–59, Fig. 21), and the absence of a microtrichial patch on anterior portion of the stridulatory file (Fig. 20).

Description

Color (Figs. 1–12) mainly red to yellowish brown occasionally tan, with black marks; pronotal and elytral base with black spots or marked differently depending on individual; antennae black with brown setae; venter and legs generally shiny, black or blackish red, with basal half of each ventrite often brown to reddish brown; setae on tarsus reddish brown to tan. Body (Figs. 1–12) oblong with anterior margin of pronotum rounded or weakly sinuate, broadest between posterior 1/3 region of pronotum and middle of elytra in dorsal view; profile ovoid with pronotal anterior margin slightly lifted.

Head (Figs. 13–15) completely concealed by pronotum in dorsal view; shape roundly quadrate, broadest at middle, slightly broader than long in dorsal view with stridulatory file in postero-medial region of vertex. Frons triangular with upper margin slightly projected, sparsely punctuate, medially depressed by mid-frontal line; lateral region of frontal base disturbed by depression above condylic projection; clypeus slightly arched with indistinct frontoclypeal sulcus; inter-antennal region slightly broader than antennal socket. Eyes large, oval, bulging, located on upper antero-lateral region of head; inter-ocular area about 1.8 times as broad as eye diameter at broadest point in anterior view, slightly depressed with deep mid-cranial sulcus. Antennae (Figs. 24–27) reaching elytral base under pronotum; antennomere I oval, about 2 times longer than broad, about 2 times longer than antennomere II; antennomere II as long as broad or slightly longer than broad; antennomeres III–IV slender, slightly expanded apically; antennomere III shiny, sparsely setose; antennomere IV often more pubescent than antennomere III and less than antennomeres V–XI; each antennomeres V–XI pubescent with ventral notches; antennomere VII as long as broad; antennomeres VIII–X broader than long; antennomere XI 2 times as long as antennomere X.

Mouth fossa (Fig. 13) rounded subquadrate with upper half region broader and more sclerotized than lower half region. Labrum (Fig. 16) with basal half withdrawn under frontoclypeus (frons+clypeus); anterior 1/4 shifted ventrally, sparsely punctate with long setae, broadest before shifted line with anterior edge well-sclerotized; anterior margin emarginate medially with paired projections. Mandible (Fig. 17) well-sclerotized, fist-shaped, with 4 teeth; apical half shifted toward mouth fossa; basal half projected, sparsely punctate and setose. Maxilla (Fig. 18) long and slender; cardo distinctly narrower medially than base and apex; stipes slightly longer than cardo, narrower apically than base; lacinia membranous, petal-shaped, longer than galea, densely setose; galea 2-segmented with basal segment slightly longer than apical segment; apical segments oval, with long setae; palpus 4-segmented with palpifer laterally connected to middle of stipes; palpomere I triangular, slightly shorter than palpomere II; palpomere II slightly curved, longer than broad, slightly broader apically; palpomere III as long as palpomere II, broader apically with long setae near apex; palpomere IV elongate oval, about 1.5 times as long as palpomere III, with sensilla structure on apex. Labium (Fig. 19) with mentum withdrawn into prosternum; ligula oval with long setae on apical region; palpus 3-segmented; palpomere I quadrate, slightly broader apically; palpomere II irregularly quadrate, broader apically with outer length about 1.8 times as long as inner length, with long setae in apical region; palpomere III elongate oval, slight curved, sparsely setose with sensilla on apex.

Pronotum (Figs. 1–12) hemispherical in dorsal view, broadest near base or occasionally at level between of posterior 1/3 and base; basal line rounded with postero-medial region extended and broadly pointed; postero-lateral margin distinctly pointed; profile irregularly trapezoidal with rounded dorsal line, highest at base. Pronotal disc convex, smooth, finely punctate, often with shallow cleavage medially and depression in postero-medial region; pronotal

lamella distinct from discal area by depression except for anterior region; lateral lamella area lifted upward.

Prosternum (Figs. 29–30) convex, with distinct short collar; antero-lateral region extended on ventral surface of pronotum in terms of projections (marked by arrow); projections forming upper-lateral part of cervical cavity; tergosternal sulcus distinct; prosternal process smooth with arrow-shaped apex; arrow-shaped apex with lateral part distinctly depressed.

Mesonotum (Fig. 31) pentagonal with anterior apodemes well-developed; mesoscutellum well-sclerotized, triangular, convex with anterior half withdrawn into pronotal base. Mesosternum (Fig. 32) deeply notched in middle; mesepisternal ridge well defined; mesosternal process extended to middle of mesocoxal cavity, rigidly connected to metasternum.

Metanotum (Fig. 33) over 2 times broader than long; scutellar groove and scutoscutellar sulcus distinct. Metasternum (Fig. 32) flat or slightly convex medially with distinct longitudinal line, slightly broader posteriorly; anterior lateral region convex, extended anteriorly forming mesocoxal cavity.

Elytra (Figs. 1–12, 34) oblong, slightly convex, broadest near basal area, with each base of elytron rounded; basal line crenulated; surface shiny, finely punctate; punctures similarly sized; punctures forming striae, occasionally arranged irregularly in lateral region; elytral lamella narrow, distinct from elytral disc, continuous to rear end with edge thickened; brace (Fig. 34) distinct with posterior end weakly connected to longitudinal carina forming angle.

Legs (Figs. 29–30, 32) slender, shiny, extending beyond elytral margin when unfolded; trochanters elongate triangular; femora as broad as length of trochanter or slightly narrower, broadest at middle, much narrower toward base than distal end; mesotibia shorter than mesofemur (pro- and metatibia as long as each femur); tibiae broader apically with apicodorsal

end notched medially and projected laterally; apicolateral regions of tibia coarsely setose; tarsus dorsally convex, sparsely setose by long setae; ventral surface densely setose; tarsomere I small, hemispherical; tarsomere II weakly bilobed with apeces of lobe pointed, about 2 times as long as tarsomere I; tarsomere III deeply bilobed, 3 times as long as tarsomere I; tarsomere IV as long as tarsomere III, slender, slightly broader apically, covering the base of pretarsal claws; pretarsal claws robust, evenly curved, tapered.

Abdomen (Figs. 8, 11) covered by elytra, slightly elongate hemispherical, slightly convex medially, surface finely setose; each ventrite well-sclerotized with depression on each lateral region; ventrite I longest; ventrites II–IV subsequently shorter and narrower; ventrite V as long as ventrite IV with lateral depression more distinct.

Aedeagus (Figs. 35–38) curved in lateral view, slightly broader medially with aedeagal basal piece oval; apical end pointed; tegmen well-sclerotized, Y-shaped; spicule U-shaped with anterior end slightly extended (arrow marked); ejaculatory duct longer than base piece; seminal vesicle thin, slightly shorter than aedeagal base piece with sclerotized aedeagal bead (arrow marked) between ejaculatory duct and seminal vesicle.

Spermatheca (Figs. 39–40) falcate, short; basal part longer than apical part; receptacle fused to pump area with one opening; spermathecal duct long and coiled.

Remark

Antennal notches on the ventral surface of the antennomeres V–XI (Figs. 24–27) were also found in 10 species of *Cistudinella*—*C. apiata* (Boheman), *C. foveolata* Champion, *C. inanis* (Boheman), *C. lata* Spaeth, *C. lateripunctata* Spaeth, *C. notata* (Boheman), *C. obducta* (Boheman), *C. parva* (Wagener), *C. peruana* Spaeth, and *C. punctipennis* (Boheman) (personal

observation). The same antennal notches were also observed in other tortoise beetles (Chaboo 2007, Simões and Monné 2014). However, the numbers of antennomeres with antennal notches varied between seven (antennomeres V–XI) and five (antennomeres VII–XI) among tortoise beetles (see Chaboo 2007). The projection on each antero-lateral portion of the prosternum was found as a unique diagnostic character of *Eurypedus* (Figs. 29–30, marked by black arrow). These projections were only tenuously connected to the ventral surface of the pronotum.

Eurypedus peltoides (Boheman)

(Figs. 1–2, 6–8, 12, 13–19, 29, 31–34, 35–36, 39)

Cassida oblonga Sturm in Thon 1827: 112 [description with color painting, not *C. oblonga* in Illiger 1798].

Ischyrosonyx peltoides Boheman 1854: 323 [description]; Boheman 1856: 115 [checklist]; Boheman 1862: 283 [checklist]; Gemminger and Harold 1876: 3651[catalog]; Spaeth 1914: 65 [catalog].

Ischyrosonyx oblonga (Sturm): Boheman 1854: 322 [description with figure]; Boheman 1856: 115 [checklist]; Boheman 1862: 282 [checklist]; Gemminger and Harold 1876: 3651 [catalog]; Dohrn 1880: 156 [description of variation]; Spaeth 1914: 65 [catalog]; Chaboo 2007: 180 [phylogeny].

Eurypedus thoni Barber 1946: 291 [new species name for *Cassida oblonga* Sturm in Thon 1827]; Silva et al. 1968: 421 [faunistic record with host plant]; Borowiec 1999: 171 [catalog]; Borowiec 2002: 93 [faunistic record]; Borowiec 2009: 671 [faunistic record]; Sekerka 2004: 156 [Moravian museum collection]; Flinte et al. 2009: 587 [faunistic record];

Borowiec and Takizawa 2011: 447 [collection record]; Borowiec and Świętojańska 2014 [online catalog].

Ischyrosonyx thoni (Barber): Hincks 1952: 336 [key to tribes, genera list].

Eurypedus oblongus (Sturm): Borowiec 1996: 186 [faunistic record, new combination].

Eurypedus peltoides (Boheman): Borowiec 1999: 171 [catalog]; Borowiec and Świętojańska 2014 [online catalog].

Remark

Species should not be distinguished solely based on body coloration because color is variable among individuals in species of *Eurypedus* (see Spaeth 1915). In this study, *E. thoni* (Fig. 1) is synonymized with *E. peltoides* (Fig. 2) because of its continuous color variation (Figs. 12A–E). Boheman (1854) distinguished these two species based on their elytral colorations. The numerous black spots or marks were observed on all regions of the elytra in *E. thoni* (Fig. 1) but only three spots were exhibited in the anterior half of each elytron in *E. peltoides* (Fig. 2). However, the examined specimens of *E. thoni* exhibited various elytral colorations ranging from only two spots on umbones (Fig. 12 E) to most of the spots connected and forming an irregular shaped black spots on the elytra (Fig 12A). Two specimens of *E. peltoides* (Figs. 12D–12E) were examined including the lectotype. No additional specimens of *E. peltoides* were found. The coloration of the non-type specimen of *E. peltoides* (Fig. 12C) showed an additional faint black mark in the posterior region of the elytra in addition to the three black spots in the anterior half of each elytron, which was supposed not to exist in *E. peltoides*. These additional faint black spots were observed in most specimens of *E. thoni* as clear black spots in this study. Variation observed in pronotal shape, elytral depression around the mesoscutellum, and elytral discal shape

between the holotype of *E. thoni* (Figs. 1, 12A) and the lectotype of *E. peltoides* (Figs. 2, 12D) were considered to be non-significant because the vouchers of *E. thoni* examined in this study showed continuous variation in these features (Figs. 12A–12E). In addition, the distribution of *E. peltoides* is limited only to Saõ Paulo (Brazil) which is a part of the known distribution of *E. thoni*.

Type material

Lectotype of *E. peltoides* in NHRS. Mhm NHRS-JLKB 000020267. (Fig. 2, examined).

Type locality

Brazil.

Diagnosis

Eurypedus peltoides is easily distinguished from *E. nigrosignatus* by the shape of the prothorax and leg. The pronotal length is 0.55 times or less as long as broad at the broadest point; it is greater than 0.55 times as long as broad in *E. nigrosignatus*. The basal line of the pronotal hypomeron is less concave than in *E. nigrosignatus*. Tibial length is 3 times as long or longer than width of the distal apex; it is 2.5 times as long or shorter than width of the distal apex in *E. nigrosignatus* (Fig. 29).

Description

Adult (n=106) length 7.5–13.5mm, width 4.5–7.0mm (lectotype: length 11.5mm, width 6.7mm). Pronotum (Figs. 1–2, 6, 29) hemispherical with pronotal length 0.55 times as long as

broad at broadest point; pronotal disc convex with longitudinal cleavage medially; postero-medial region of pronotum flattened with shallow depression on each side; each basal line of pronotal hypomeron slightly concave with depth less than 0.35 times width of hypomeron at basal line. Elytral length about 1.35 times as long as broad at base with distinct medial marginal line on each elytron; medial marginal line marked by black coloration and depressed line by punctures; punctures on elytra disc evenly sized, forming striae, occasionally scattered; medial region of each elytral base slightly swollen; swollen region often located between two black marks when present. Tibiae elongate triangular in lateral view with length as long as 3 times distal width. Aedeagus curved, slightly narrower apically; basal piece longer than 3.5 times length of aedeagus; apex of media lobe pointed with angle less than 90˚.

Additional specimens examined

Argentina: Provincia de La Rioja, Guayapa, Patquía, 2439.47 (MCZ: 1); Provincia de La Rioja, Manantiales, xi.1946, T de Apostol (MCZ: 2); Provincia de Corrientes, Isla Apipé, xi.1945, Martinez, ex F Monro collection (USNM: 3); Provincia de Corrientes, Santo Tome, xi.1945, Martinez, ex F Monro collection (USNM: 3); xi.1963 MJ Viana (FSCA: 4); Provincia de Misiones, Santa Maria, xi.1958, MJ Viana (MNRJ: 2; FSCA: 8); Provincia de Misiones, Eldorado, 20.x.1983, A Kovacs (HNHM: 1); Provincia de Misiones, San Pedro, 1,000m, i.1956, ca. 630, DZUP, 148967 (DZUP: 1, head examined); Provincia de Misiones, San Pedro, i.1956, ca. 658, DZUP, 148968 (DZUP: 1); Provincia de Salta Güemes, K 15, 800 m, 22.i.1984, Bordon, DZUP, 148969 (DZUP: 1); Provincia de Tucumán, Tucumán , Colalao, i.1949, ca. 114, DZUP, 148970 (DZUP: 1); **Bolivia:** Departamento de Santa Cruz, 5km ESE, Warnes, Hotel Rio Selva, 20–21.x.2000, Morris/Wappes (BYU: 4); Departamento de Santa Cruz, 5km ESE Warnes, Hotel

Rio Selva, 3–4.xi.2001, 17° 33’ 695 S, 63° 11’ 981 W, 375m, MC Thomas (EGRC: 1); MM Reed, no detailed data (FSCA: 1); **Brazil:** Sturm, NHRS-JLKB 000020269 (NHRS: 1, Holotype of *E. thoni*, measured); Estado de Bahia (USNM: 1); Bahia, vii.1944 (AMNH: 1); Estado de Bahia, Barra-ES, Conc. DA, 5.v.1968, CT Elias and C Elias, DZUP, 148986 (DZUP: 1); Estado de Bahia, Cachoeira, 15.iii.1981, O Roppa (MNRJ: 1); Estado de Bahia, Cêrro Largo, x.1945, P Buck (MNRJ: 3); Estado de Espírito Santo, Linhares, 21.i.1977, J Becker (MNRJ: 1); Estado de Espírito Santo, Linhares, x.1970, B Silva (MNRJ: 1); Estado de Espírito Santo, Linhares, xi.1965, A Maller, DZUP, 148978, 148984 (DZUP: 2); Estado de Espírito Santo, Linhares, 18.i.1971, Alvarenga, DZUP, 148995 (DZUP: 3); Estado de Espírito Santo, Linhares, 11.xi.1970, Alvarenga, DZUP 148994 (DZUP: 7); Estado de Espírito Santo, Linhares, 21.xi.1971, JM Lima, DZUP 148985 (DZUP: 1); Estado de Espírito Santo, Pinheiro, 8.xi.1971, JM Lima, DZUP, 148982 (DZUP: 1); Estado de Espírito Santo, Pinheiro ES, 6.xi.1971, JM Lima, DZUP 148983 (DZUP: 2); Estado de Espírito Santo, Sooretama ES, Parque, 27.xi.1967, F Oliveira, DZUP, 148977, 148979, 148981, 148981 (DZUP: 4); Estado de Paraná, Maria Preta, O Monte-Minas (MNRJ: 1); Estado de Rio Grande do Sul, Porto Alegre xii. 2008, Rames, BCM (SEMC: 3 + 1♂1♀, dissected and examined); F Monros collection, no detailed data (USNM: 1, Fig. 12D); no data (EGRC: 1; HNHM: 1; MNRJ: 1).

Distribution

Argentina: Provincia de Corrientes (**new record)**; Provincia de Jujuy (**new record**); Provincia de Misione (Borowiec 1996); Provincia de La Rioja (**new record**); Provincia de Salta (Borowiec 2009); Provincia de Tucumán (**new record**). **Bolivia:** Departamento de Santa Cruz (Borowiec and Świętojańska 2014). **Brazil:** Estado de Bahia (**new record**); Estado de Espírito

Santo (**new record**); Estado de Minas Gerais (Boheman 1854); Estado de Paraná (**new record**); Estado de Rio de Janeiro (Flinte et al. 2009); Estado de Rio Grande do Sul (Borowiec 2009); Estado de Sao Paulo (Boheman 1854). **Paraguay:** Departamento de Concepción (Borowiec 1999).

Host plant

Boraginaceae: *Cordia ecalyculata* Vell. (Silva et al. 1968; Sekerka 2004).

***Eurypedus nigrosignatus* (Boheman)**

(Figs. 3–5, 9–11, 20–27, 30, 37–38, 40)

Ischyrosonyx nigrosignata Boheman 1854: 327, 1856: 116 [checklist], 1862: 283 [checklist]; Gemminger and Harold 1876: 3651 [catalog]; Champion 1894: 176 [faunistic record]; Spaeth 1914: 65 [catalog], 1915: 283 [description].

Ischyrosonyx discipennis Boheman 1854: 325, 1856: 115 [checklist], 1862: 283 [checklist]; Gemminger and Harold 1876: 3651 [catalog]; Spaeth 1914: 65 [catalog, aberration of *I. nigrosignata*], 1915: 283 [field observation note, aberration of *I. nigrosignata*].

Ischyrosonyx marginicollis Boheman 1854: 326, 1856: 116 [checklist], 1862: 283 [checklist]; Gemminger and Harold 1876: 3651; Spaeth 1914: 65 [catalog, aberration of *I. nigrosignata*], 1915: 283 [field observation note, aberration of *I. nigrosignata*].

Eurypedus nigrosignata (Boheman): Wilcox 1975: 154 [checklist]; Gomez et al. 1999: 1007 [larval biology].

Eurypedus nigrosignatus (Boheman): Borowiec 1996: 186 [faunistic record, new combination], 1999: 171 [catalog], 2002: 93 [faunistic record]; Gomez 2004: 489 [biology]; Chaboo 2007: 32 [egg figure]; Borowiec 2009: 671 [faunistic record]; Borowiec and Świętojańska 2014 [online catalog].

Type material

Lectotype of *I. nigrosignatus.* Type Dupont, NHRS-JLKB 000020273. Des. L. Borowiec (Fig. 3, measured) and four paralectotypes of *E. nigrosignatus*: Type Dupont, NHRS-JLKB 000020277. Des. L. Borowiec (measured); Guèrin, NHRS-JLKB 000020278. Des. L. Borowiec (measured); Guèrin, NHRS-JLKB 000020279. des. L. Borowiec (measured); Type Dupont, NHRS-JLKB 000020280 (measured) in NHRS.

Type locality

Colombia.

Diagnosis

Eurypedus nigrosignatus is easily distinguished from *E. peltoides* by the shape of prothorax and leg. The pronotal length is greater than 0.55 as long as broad at the broadest point; it is 0.55 times or less as broad as in *E. peltoides*. The basal line of the pronotal hypomeron is more concave than in *E. peltoides*. Tibial length is 2.5 times as long or slightly shorter than width of distal apex; it is 3 times as long or longer than the width of distal apex in *E. peltoides*.

Description

Adult (n=114) length 6.0–9.5mm, width 3.0–5.0mm (lectotype: length 7.5mm, width 3.7mm). Pronotum (Figs. 3–5, 9, 30) hemispherical with pronotal length longer than 0.55 times width of pronotum at the broadest point; pronotal disc convex with or without medial cleavage; postero-medial region of pronotum convex or flattened with shallow depression on each side; each basal line of pronotal hypomeron concave with depth about half width of hypomeron at basal line. Elytral length about 1.35 times as long as broad at base with distinct medial marginal line on each elytron; medial marginal line marked by marked by punctures and occasionally with black coloration; punctures on elytral disc evenly sized, forming striae; medial region of each elytra base convex with surface smooth, occasionally flattened. Tibiae elongate triangular in lateral view with length as long as or shorter than 2.5 times distal width. Aedeagus curved, slightly narrower apically; basal piece shorter than 0.3 times length of aedeagus; apex of median lobe broadly pointed with angle over 90˚.

Additional specimens examined

Brazil: (Estado de Amazonas or Estado de Minas Gerais) Capella, ex FC Bowditch collection (MCZ: 16, see Discussion). **Colombia:** Type Dupont, NHRS-JLKB 000020272, Des. L Borowiec (NHRS: 1, Lectotype of *E. discipennis*, measured); Type Dupont, NHRS-JLKB, 000020271. Des. L Borowiec (NHRS: 1, Lectotype of *E. marginicollis*, measured); Guèrin, NHRS-JLKB, 000020274, Des. L Borowiec (NHRS: 1, paralectotype of *E. marginicollis*, measured); Type Dupont, NHRS-JLKB, 000020275, Des. L Borowiec (NHRS: 1, paralectotype of *E. marginicollis*, measured); Type Dupont, NHRS-JLKB, 000020276, des. L Borowiec (NHRS: 1, paralectotype of *E. marginicollis*, measured); Puerto Colombia, 1986, J Bequaert (MCZ: 1); Departamento del Rio Magdalena, xi.1958, ca. 686, DZUP, 148973 (DZUP: 1).

Guatemala: Departamento de El Progreso, 94km road to Puerto Barrios, 14° 55’ 17 N, 89° 56’ 11 W, 19.vi.2002, WB Warner (EGRC: 5; TAMU: 2); Departamento de El Progreso, 103km Coban road, 2.vi.1991, R Anderson, thom scrub 91-43 (TAMU: 1); Departamento de Retalhuleu, Champerico, 3.viii.1905 (USNM: 2); Departamento de Zacapa, 7km West Teculutan, 25.vi.1993, 340m, R Brooks and J Ashe (SEMC: 2 + 2♂2♀, dissected for SEM and genitalia observation); intercepted in plane at Miami Florida, Byrd K Dozier, 31.vii.1969, in epiphytic Bromel ADS (EGRC: 2; FSCA: 3). **Honduras:** Department de Choluteca, 19.5km East Choluteca, Villa Gusdelupe, 5.vi.1993, FW Skillman Jr, Beating roadside vegetation (EGRC: 1; FSCA: 1). **Mexico:** Estado de Yucatán, 12km North of Quintana Roo Highway 295, 20.v.1987, DA Rider, EG Riley and TJ Riley (EGRC: 1). **Nicaragua:** Departamento de Esteli, Espinol, 21.i.1986, E Chavez, on *Tectona grandis* (USNM: 2); Departamento de León, Nagarote, 15.vii.1983, host plant *Melanthera aspera* (=*M. nivea*) (FSCA: 1); Departamento de León, x.1989, B Garcete (TAMU: 1; EGRC: 1); Departamento de Matagalpa, Carmen, 1.vii.1983, host plant *Cordia inermis* (FSCA: 4). **Panama:** Provincia de Chiriqua, Chiriqui (MCZ: 7, mislabeled as Costa Rica); Provincia de Colón, Coco solo Canal Zone, 30.v.1959, S Breeland (FSCA: 11); Provincia de Panama, Cerro Campana, 17.v.1993, F Andrews and A Gilbert (EGRC: 1); Provincia de Panama, Chepo, 3.vi.1993, F Andrews and A Gilbert (EGRC: 1); Provincia de Panama, 1km Eest of Chepo, 18.v.1993, EG Riley (EGRC: 3); Provincia de Panama, 21km SW of Chepo, 4.vii.1974, CWL O’Brien and Marshall (EGRC:1); Provincia de Panama, Chepo, 25.v.1996, DM Windsor (SEMC: 4); no detailed data, ex FC Bowditch collection (MCZ: 12). **Venezuela:** Estado Merida, San Juan, 25.vi.1983, Clark and Clark (BYU: 3; EGRC: 1); no detailed locality data, 11.v.1972, Zulia Urdaneta (USNM: 1); no detailed locality data, ex FC Bowditch collection (MCZ: 5); no detailed locality data, ex FC Bowditch collection (MCZ: 4).

Distribution

Brazil: Estado de Amazonas or Estado de Minas Gerais, Capella (inclear for Estado level, see discussion). **Colombia:** Departamento del Magdalena (Borowiec 1996). **Guatemala:** Departamento de El Progreso (**new record**); Departamento de Retalhuleu (**new record**); Departamento de Zacapa (Borowiec 1996). **Honduras** (**new record**)**:** Departamento de Choluteca (**new record**). **Mexico:** Estado de Yucatán (**new record**). **Nicaragua:** Departamento de Chontales (Champion 1854); Departamento de Esteli (**new record**); Departamento de Leon (**new record**); Departamento de Matagalpa (**new record**). **Panama:** Provincia de Chiriqua (**new record**); Provincia de Colón (**new record**); Provincia de Panama (Windsor et al. 1992). **Venezuela**: Estado Merida (Borowiec 2002).

Host plant

Asteraceae: *Melanthera nivea* (L.) Small (**new record**). Boraginaceae: *Cordia spinescens* L. (Windsor et al. 1992), *Cordia currasavica* (Jacq.) Roem. and Schult. (Gomez et al. 1999; Gomez 2004); *Cordia inermis* (Mill.) I. M. Johnst. (**new record**). Verbenaceae: *Tectona grandis* L. f. (see Discussion)

DISCUSSION

The tribal name Ischyrosonychini was designated for *Ischyrosonyx* (= *Eurypedus*) and later included *Cistudinella*. However, the current concept of Ischyrosonychini includes two other groups (*Asteriza* Chevrolat and the physonotines—*Enagria* Spaeth, *Eurypepla Boheman*, *Physonota* Boheman, and *Platycycla* Boheman) (Borowiec and Świętojańska 2014). However,

the monophyly of the current concept of Ischyrosonychini is only weakly supported and no synapomorphy appears to support the group (Borowiec 1995). As a putative synapomorphy of Ischyrosonychini, the head stridulatory file was observed in all current genera in Ischyrosonychini (Schmitt 1994, Shin et al. 2012). In addition, the morphological features of the stridulatory files can be also used to distinguish *Eurypedus* from other genera in Ischyrosonychini. In *Eurypedus*, stridulatory files were present on males (Figs. 20–21) and absent on females (Figs. 22–23), whereas obvious stridulatory files were found in both males and females in all species of *Asteriza* (Shin et al. 2012). *Eurypedus* showed a smaller number (up to 59) of ridges on the stridulatory files compared to the species of Ischyrosonychini with stridulatory file with over 100 file ridges (Schmitt 1994, Shin et al. 2012).

Stridulation is produced when two structures (stridulatory file and plectrum) are being rubbed against each other. Based on the location of the stridulatory file on the head in *Eurypedus*, a band-like structure with projected anterior and posterior margins on the ventral surface of the pronotum was found as putative plectral structure (Figs. 29–30). Similar structures were observed in *Asteriza* in the same location with only one projected line (Shin et al. 2012).

In the taxonomic history of *Eurypedus*, color variation caused an increase in the species number. The color variation is more pronounced in *E. nigrosignatus* than in *E. peltoides.* Color variation in *E. nigrosignatus* ranges from the elytra and pronotum being without any black marks to completely black except for lamellae; in *E. peltoides*, elytra may exhibit only one black mark on each umbo or have numerous black marks irregularly fused. No significant character of coloration was found that would distinguish between the species.

According to Morrone (2001), Latin America including the Caribbean is divided into three biogeographical regions: Nearctic, Neotropics, and the Andes. Based on the known distributions

and the collecting information from the examined specimens, *Eurypedus* is distributed only in Morrone's Neotropical region (Fig. 41). However, 16 specimens of *E. nigrosignatus* with the printed label "Capella, Brazil, FC Bowditch" (marked as N? in Fig. 41) were in the collection of the MCZ. The collecting locality of these specimens requires confirmation. Apart from those 16 specimens from Capella, Brazil, none of the other 98 specimens of *E. nigrosignatus* examined in this study were collected from or south of the Amazon Basin. This suggests that the distributions of two species of *Eurypedus* are likely separated by the Amazon Basin.

The distribution of *E. peltoides* mirrors the distribution of its host plant (*C. ecalyculata*) (GBIF 2015). The distribution of *E. nigrosignatus* also correspondes to the distribution of its host plants (*M. nivea, C. spinescens, C. inermis*) except for *C. currasavica,* which is a Panamanican endemic species. However, the distribution across the Andes, the Greater Antilles, North region of Mexico, and Florida, USA of *M. nivea, C. spinescens,* and *C. inermis* are slightly broader than the distribution of *E. nigrosignatus* (GIBF 2015). This indicates that the distribution of each species is limited not only by the host plant(s) but also by other environmental factors. There were two specimens of *E. nigrosignatus* collected on *T. grandis* (common name: Teak, Verbenaceae) from Nicaragua. The original distribution of *T. grandis* is in Southeast Asia and it is exotic to many countries in Africa and the New World for different purposes (Tewari 1992). *Tectona grandis,* as a host plant of *E. nigrosignatus,* needs to be confirmed by determining if *E. nigrosignatus* actually feeds on this tree or was only collected from this tree.

ACKNOWLEDGMENTS

The author is grateful to K. Jensen and M. S. Engel (University of Kansas) for their general comments and assistance, and to the curators, collections managers, and institutions for

the loan of specimens: Lee Herman (AMNH); Lucia Massutti Almeida (DZUP); Edward G. Riley (EGRC, TAMU); Michael Thomas (FSCA); Ottö Merkl (HNHM); Philip Perkins (MCZ); Miguel Monné (MNRJ); Johannes Bergsten and Bert Viklund (NHRS); David Furth, Alexander Konstantinov, and Steven Lingafelter (USNM).

This research was partially supported by the Program of Entomology, Department of Ecology and Evolutionary Biology, University of Kansas and is a contribution of the Division of Entomology, University of Kansas Natural History Museum.

CITATIONS

Barber, H.S. 1946. Nomenclatorial note (Coleoptera, Cassidinae). Revista de Entomologia, **17**: 290–291.

Boheman, C.H. 1854. Monographia Cassididarum. Tomus secundus. Holmiae.

Boheman, C.H. 1856. Catalogue of coleopterous insects in the collection of the British Museum, Part IX, Cassididae. S. Bagster and Sons, TYP., London.

Boheman, C.H. 1862. Monographia Cassididarum. Tomus quartus. Holmiae.

Borowiec, L. 1995. Tribal classification of the cassidoid Hispinae (Coleoptera: Chrysomelidae). *In* Biology, Phylogeny, and Classification of Coleoptera. *Edited by* J. Pakaluk and and S.A. Ślipiński. Papers Celebrating the 80th Birthday of Roy A. Crowson, Warszawa. pp. 541–558.

Borowiec, L. 1996. Faunistic records of Neotropical Cassidinae (Coleoptera: Chrysomelidae). Polskie Pismo Entomologiczne, **65**: 119–251.

Borowiec, L. 1999. A World Catalogue of the Cassidinae (Coleoptera: Chrysomelidae). Biologica Silesiae, Wrocław.

Borowiec, L. 2002. New records of Neotropical Cassidinae, with description of three new species (Coleoptera: Chrysomelidae). Genus, **13**: 43–138.

Borowiec, L. 2009. New records of Neotropical Tortoise beetles (Coleoptera: Chrysomelidae: Cassidinae). Genus, **20**:615–722.

Borowiec, L., and Takizawa, H. 2011. Neotropical tortoise beetles in the Amazon Insectarium, Tokyo, Japan with description of nine new species (Coleoptera: Chrysomelidae: Cassidinae). Genus, **22(3)**: 427–484.

Borowiec, L., and Świętojańska, J. 2014. Cassidinae of the World – an interactive manual (Coleoptera: Chrysomelidae) [online]. Available from http://www.biol.uni.wroc.pl/cassidae/katalog%20internetowy/index.htm [accessed 1 July, 2015]

Chaboo, C.S. 2007. Biology and phylogeny of Cassidinae Gyllenhal (tortoise and leaf-mining beetles) (Coleoptera: Chrysomelidae). Bulletin of the American Museum of Natural History, **305**: 1–250.

Champion, G.C. 1894. Biologia Centrali-Americana Insecta Coleoptera, Volume VI. Part 2. Phytophaga. Cassididae and appendix to Hispidae. R. H. Porter, London.

Chapuis, M.F. 1875. 11. Famille des Phytophages. *In* Histoire Naturelle des Insectes. Genera des Coléopteres ou exposé méthodique et critique de tous les genres proposés jusqu'ici dans cet ordre d'Insectes. Volume XI. *Edited by* T. Lacordaire. A la Libraire Encyclopédique de Roret Paris.

Dejean, M. 1836. Catalogue des Coléopteres de la collection de M. le Comte Dejean, 2nd édition. Paris, Livr. **5**: 361–442.

Dohrn, C.A. 1880. Exotisches. Entomologische Zeitung, herausgegeben von dem entomologischen Vereine zu Stettin, **41**: 149–157.

Flinte, V., Borowiec, L., de Freitas, S., Viana, J.H., Fernandes, F.R., Nogueira-de-Sá, F., Valverde de Macedo, M., and Monteiro, R.F. 2009. Tortoise beetles of the State of Rio de Janeiro, Brazil (Coleoptera: Chrysomelidae: Cassidinae). Genus, **20(4)**: 571–614.

GBIF. 2015. Global Biodiversity Information Facility [online]. Available from http://www.gbif.org/ [accessed 21 April 2015].

Gemminger, M. and von Harold, E. 1876. Catalogus Coleopterorum hucusque descriptorum synonymicus et systematicus. Tom. XII. Chrysomelidae (Pars II), Languriidae, Erotylidae, Endomychidae, Coccinellidae, Coryophidae, Platypsyllidae. Accedit Index Generum universalis. Monachii, **12**: 3479–3822.

Gistel, J. 1834. Die Insecten-Doubletten aus der Sammlung des Grafen Rudolph von Jenison Walworth zu Regensburg, welche sowohl im Kauf als im Tausche abgegeben werden, Nro. I. Käfer, München.

Gómez, N.E., Witte, L., and Hartmann, T. 1999. Chemical defense in larval tortoise beetles: essential oil composition of fecal shields of *Eurypedus nigrosignata* and foliage of its host plant, *Cordia curassavica*. Journal of Chemical Ecology, **25(5)**: 1007–1027.

Gómez, N.E. 2004. Survivorship of immature stages of *Eurypedus nigrosignatus* Boheman (Chrysomelidae: Cassidinae: Physonotini) in Central Panama. The Coleopterists Bulletin, **58(4)**:489–500.

Hincks, W.D. 1952. The genera of the Cassidinae (Coleoptera: Chrysomelidae). Transactions of the Royal Entomological Society of London, **103**: 327–358.

Illiger, J.K.W. 1798. Verzeichniss der Käfer Preussens. Halle.

Lawrence, J.F., and Britton, E.B. 1991. Coleoptera (beetles). *In* The Insects of Australia, Second edition. Volume II, *Edited by* I. D. Naumann. Cornell University Press, Ithaca, New York, 543–683.

Morrone, J.J. 2001. Biogeografía de América Latina y el Caribe. MabdT–Manuales abd Tesis SEA, volume 3. Zaragoza.

Schmitt, M. 1994. Stridulation in leaf beetles (Coleoptera, Chrysomelidae) *In* Novel aspects of the biology of Chrysomelidae. *Edited by* P.H. Jolivet, M. Schmitt and E. Petitpeierre. Kluwer Academic Publisher, the Netherlands. pp 319–325.

Seeno, T.N., and Wilcox, J.A. 1982. Leaf beetle genera. Entomography **1**: 1–221.

Shin, C., Chaboo, C.S., and Clark, S.M. 2012. Phylogenetic revision of the Hispaniolan endemic genus *Asteriza* Chevrolat, 1836 (Coleoptera: Chrysomelidae: Cassidinae: Ischyrosonychini). Zootaxa, **3227**: 34–53.

Simões, M.V.P. and Monné, M.L. 2014. Taxonomic Revision of the genus *Mesomphalia* Hope, 1839 (Insecta, Coleoptera, Chrysomelidae). Zootaxa, 3835(2)**: 151**–197.

Sekerka, L. 2004. Species of Cassidinae and Hispinae contained in the Moravian Museum Collection in Brno (Coleoptera, Chrysomelidae). Acta Musei Moraviae Scientiae biologicae, **89**: 117–165.

Silva, A.G.d'A., Gonçalves, C.R., Galvão, D.M., Gonçalves, A.J., Gomes, J., Silva, M.N., Simoni L. 1968. Quarto catálogo dos insetos que viviem nas plantas do Brasil. Seus parasitos e predadores. Parte II 1.° Tomo. Ministério da Agricultura, Laboratório Central de Patologia Vegetal, Rio de Janeiro.

Spaeth, F. 1914. Chrysomelidae: 16. Cassidinae. *In* Coleopterorum Catalogus, Pars 62. *Edited by* W. Junk and S. Schenkling. Berlin.

Speath, F. 1915. Neue Cassidinen (Coleoptera). Stettiner Entomologische Zeitung, **76**:265–290.

Sturm, J. 1827. 4. Coleoptera Jenae. *In* Abbildungen ausländischer Insecten. *Edited by* T. Thon. 4 pp + 6 pls.

Sturm, J. 1843. Catalog der Kaefer-Sammlung. Nürnberg. Germany.

Tewari, D.N. 1992. A monograph on teak (*Tectona grandis* Linn. F.). International Book Distributors.

Wilcox, J.A. 1975. Family 129. Chrysomelidae. *In* Checklist of the Beetles of North and Central America and the West Indies. North American Beetle Fauna Series. *Edited by* R.H. Arnett Jr. Flora and Fauna Publications, Gainesville.

Windsor, D.M., Riley, E.G., and Stockwell, H.P. 1992. An introduction to the biology and systematics of Panamanian Tortoise Beetles (Coleoptera: Chrysomelidae: Cassidinae). *In* Insects of Panama and Mesoamerica, Selected studies. *Edited by* D. Quintero and A. Aiello. Oxford University Press, Oxford, 372–391.

LIST OF FIGURES

Figs. 1–5. Type specimens. 1. Holotype of *E. thoni*. 2. Lectotype of *E. peltoides*. 3. Lectotype of *E. nigrosignatus*. 4. Lectotype of *E. discipennis*. 5. Lectotype of *E. marginicollis*.

Figs. 6–8. *E. peltoides*. 6. Dorsal view. 7. Lateral view. 8. Ventral view. 9–10. *E. nigrosignatus*. 9. Dorsal view. 10. Lateral view. 11. Ventral view. 12A–E. Color and morphological variation of *E. peltoides*.

Figs. 13–15. Head of *E. peltoides*. 13. Dorsal view. 14. Anterior view. 8. Ventral view (mouth fossa). 16–19. Mouthparts of *E. peltoides*. 16. Labrum. 17. Mandible. 18. Maxilla. 19. Labium. 20–23. Stridulatory files of *E. nigrosignatus* 20. Male (head dorsal view). 21. Stridulatory file (male). 22. Faint stridulatory file (female). 23. Female (head dorsal view). 24–27. Antenna of *E. nigrosignatus*. 24. Antenna (ventral view). 25. Antennomeres IV–VI. 26. Antennomere XI. 27. Ventral notch (antennomere VI).

Figs. 29–30. Prosternum. 29. *E. peltoides.* 30. *E. nigrosignatus*. 31–34. *E. nigrosignatus*. 31. Mesonutum. 32. Complex of meso- and metasternum. 33. Metanotum. 34. Elytra (ventral view).

Figs. 35–38. Male genitalia. 35. Aedeagus of *E. peltoides* (ventral view, arrow: gastrale spiculum). 36. Aedeagus of *E. peltoides* (lateral view). 37. Aedeagus of *E. nigrosignatus* (ventral view, arrow: seminal vesicle). 38. Aedeagus of *E. nigrosignatus* (lateral view). 39–40. Spermathecae. 39. *E. peltoides*. 40. *E. nigrosignatus*.

Fig. 41. Distribution of *E. nigrosignatus* (**N**) and *E. peltoides* (**P**); **N?** indicates 12 specimens of *E. nigrosignatus* from Museum of Comparative Zoology.

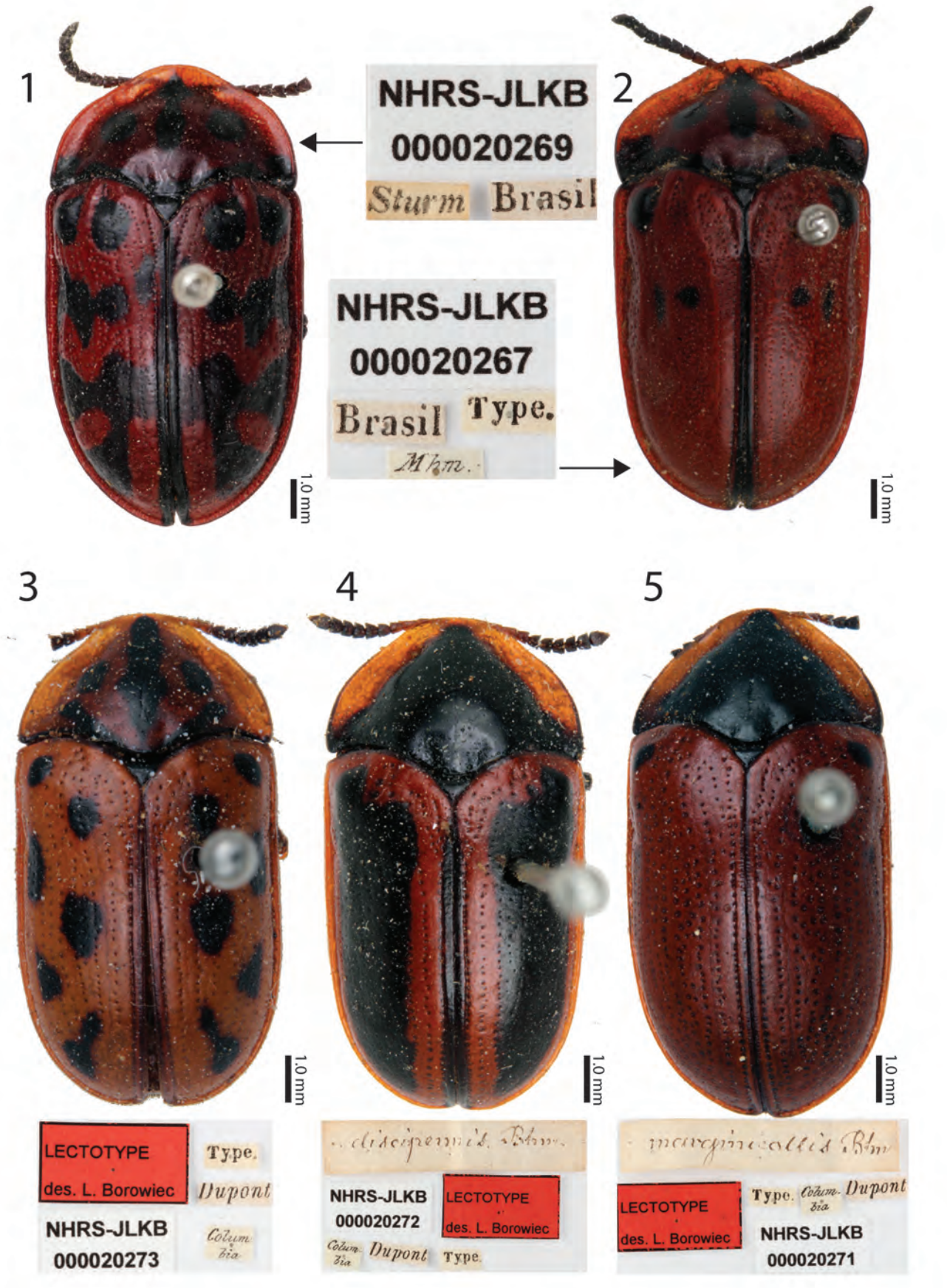
1
NHRS-JLKB
000020269
Sturm Brasil
NHRS-JLKB
000020267
Brasil Type.
Mhn.
2
1.0 mm
1.0 mm
3
4
5
1.0 mm
1.0 mm
1.0 mm
LECTOTYPE
des. L. Borowiec
Type.
Dupont
NHRS-JLKB
000020273
Colum-bia
discipennis Blm.
NHRS-JLKB
000020272
LECTOTYPE
des. L. Borowiec
Colum-bia Dupont Type.
marginicollis Blm.
LECTOTYPE
des. L. Borowiec
Type. Colum-bia Dupont
NHRS-JLKB
000020271


6
7
1.0 mm
8
9
10
1.0 mm
11
12
A
B
C
D
E

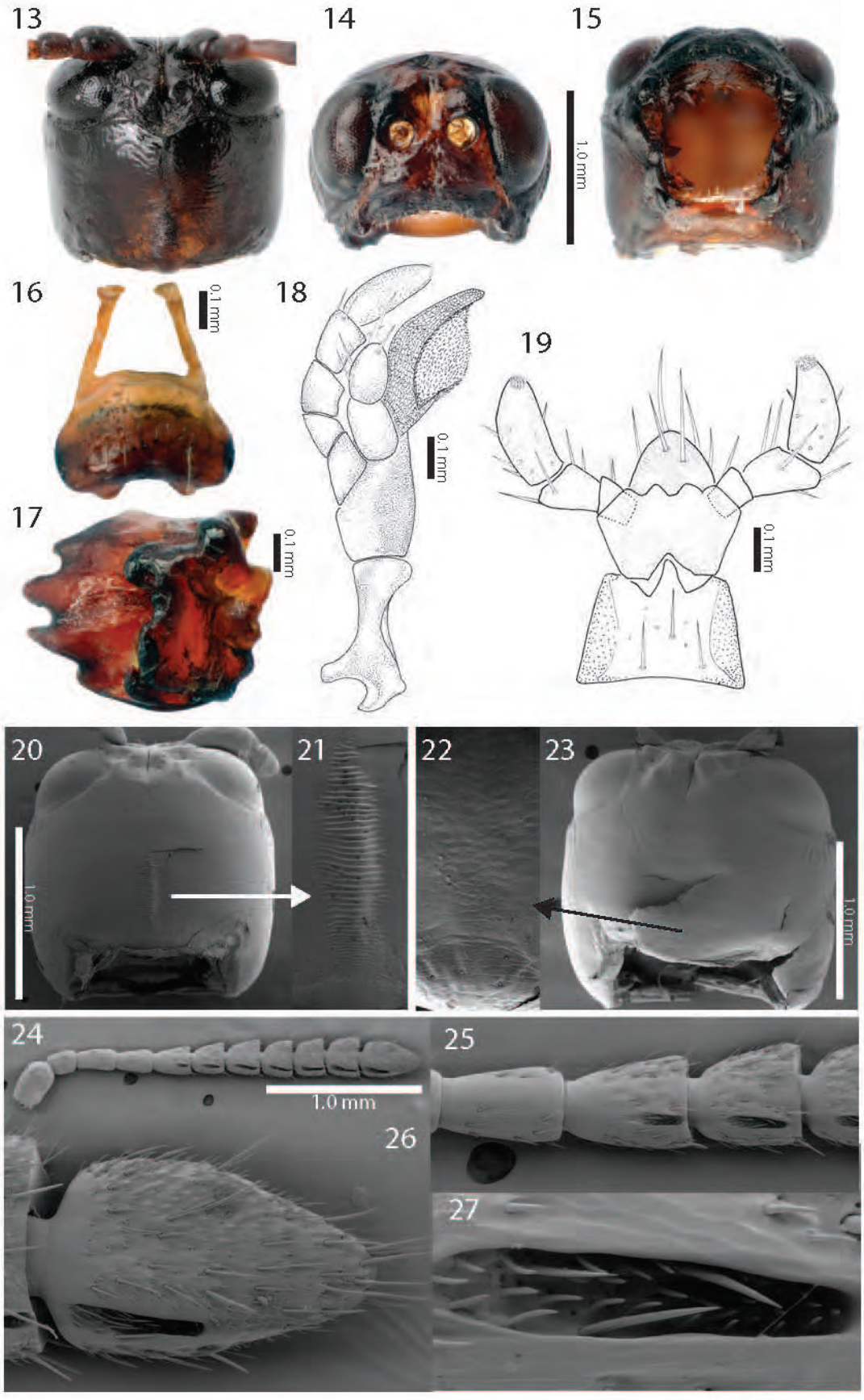
13
14
15
1.0 mm
16
0.1 mm
18
0.1 mm
19
0.1 mm
17
0.1 mm
20
21
1.0 mm
22
23
1.0 mm
24
1.0 mm
26
25
27

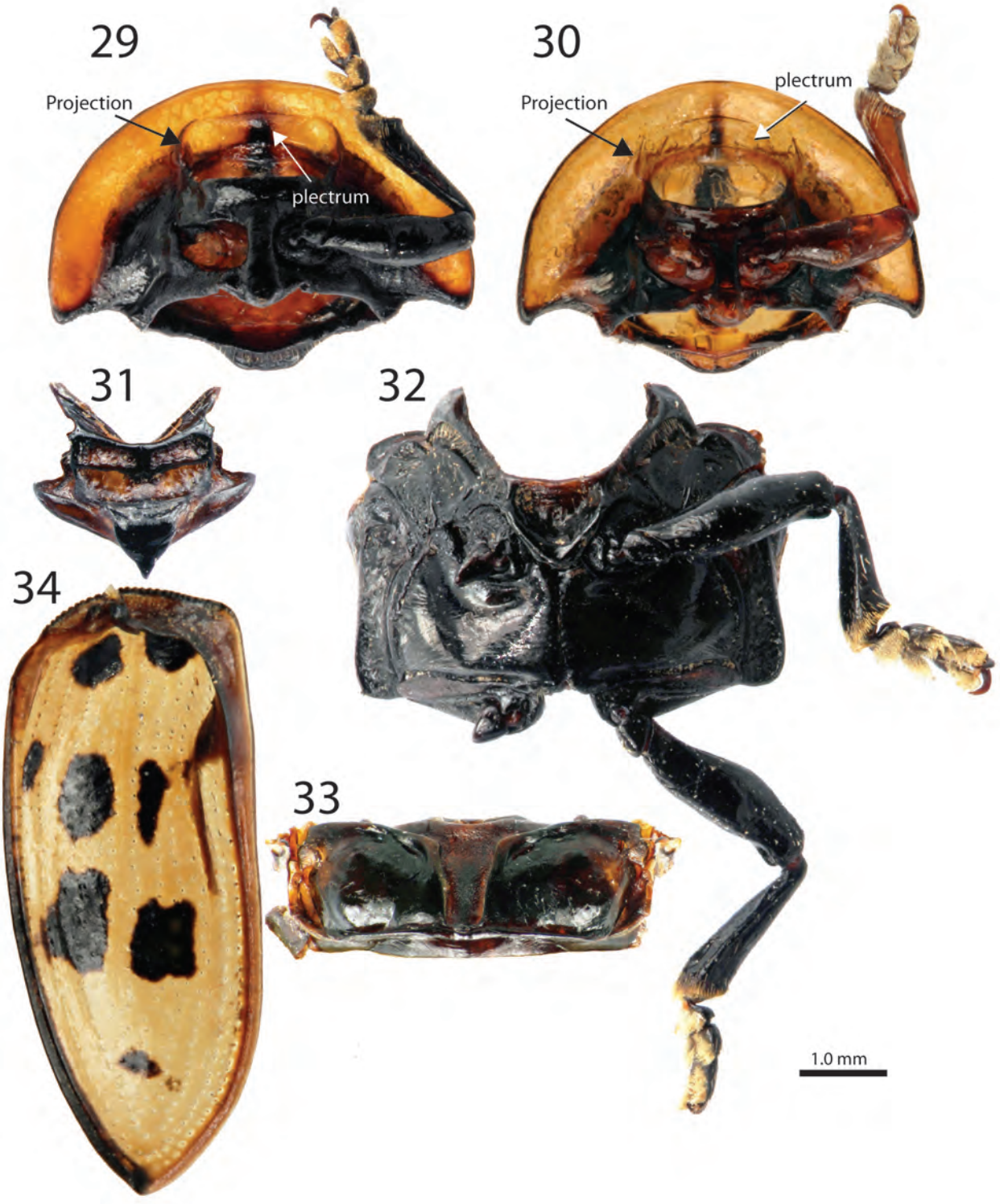
29
Projection
plectrum
30
Projection
plectrum
31
32
34
33
1.0 mm

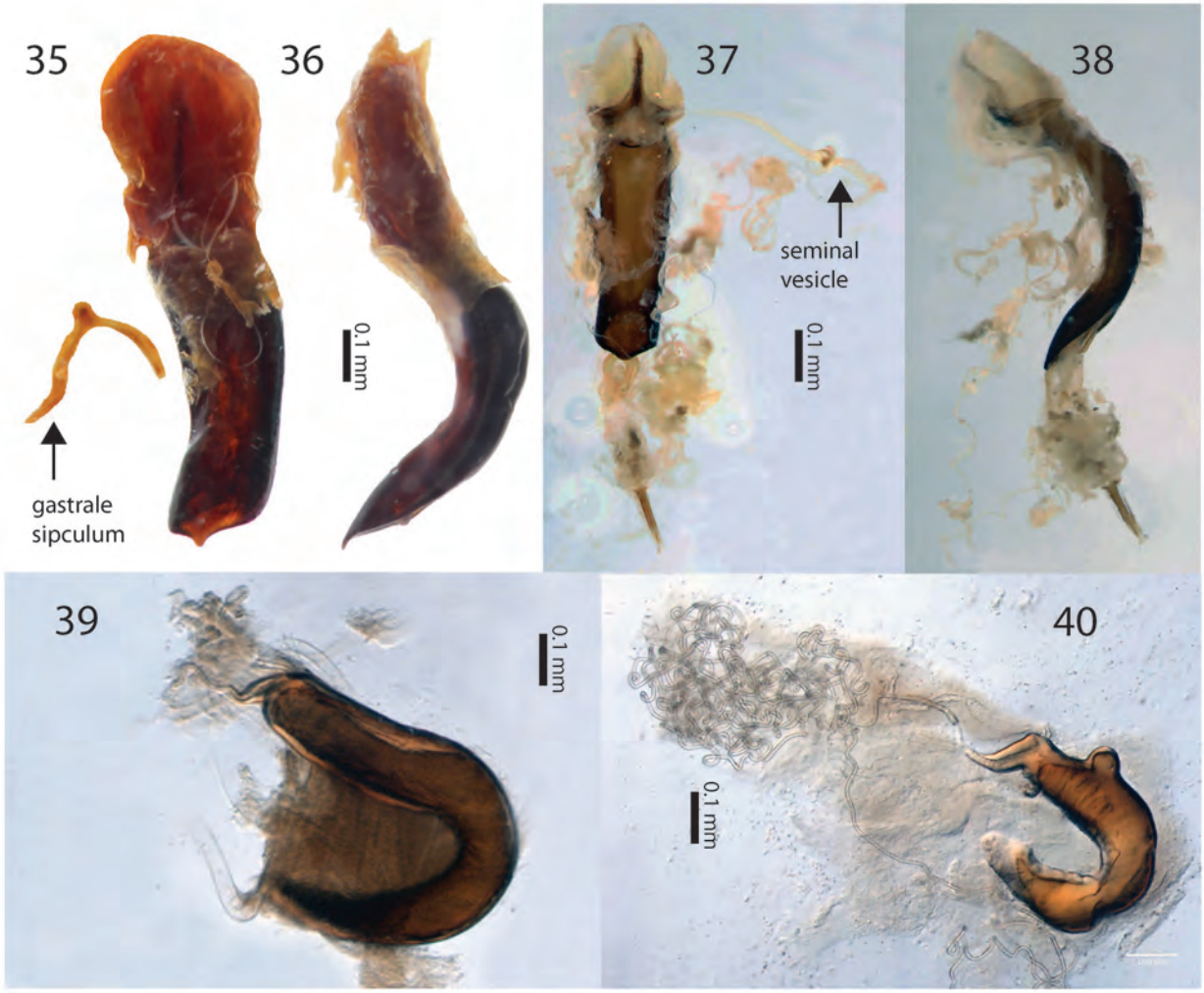
35
gastrale
sipculum
36
0.1 mm
37
seminal
vesicle
0.1 mm
38
39
0.1 mm
40
0.1 mm


Mexico
Belize
Honduras
Guatemala
El Salvador
Nicaragua
Costa Rica
Panama
Venezuela
Guyana
Suriname
French Guiana
Colombia
Ecuador
Peru
"Amazon Basin"
Brazil
Bolivia
Paraguay
Chile
Uruguay
Argentina
N: Eurypedus nigrosignatus
P: Eurypedus peltoides

CHPATER 3

Phylogeny of the tortoise beetle tribe Ischyrosonychini based on morphological data (Coleoptera: Chrysomelidae)

***** Formatted for submission to the journal *Coleopterists Bulletin.*

ABSTRACT

A cladistic analysis was performed with 155 morphological characters and 84 species representing 34 genera in 10 tribes of tortoise beetles (Cassidinae). The taxon sampling was exclusively designed to test the monophyly and validity of each genus in the tribe Ischyrosonychini as it is currently constituted. The result indicated that the tribe Ischyrosonychini should include only those species of *Cistudinella* and *Eurypedus*, and the tribe Asterizini was recovered to include *Asteriza*, *Enagria*, *Eurypepla*, *Physonota*, and *Platycycla* as its constituent genera. Within the clade of Asterizini, *Enagria* and *Physonota* were synonymized with *Asteriza*. In term of tribal level relationships, Asterizini and Ischyrosonychini are more closely related to Eugenysini, Goniocheniini, Mesomphaliini, and Omocerini than to Aspidimorphini, Cassidini and Dorynotini with which they were previously allied. The characters of the head stridulatory file and the associated plectral structure appeared to be phylogenetically informative. The distributions of Asterizini and Ischyrosonychini s. str. were illustrated along with the phylogeny.

INTRODUCTION

The subfamily Cassidinae is the second most speciose lineage of leaf beetles with about 6,000 described species (Borowiec & Świętojańska 2014, Staines 2014), and comprises the tortoise beetles and leaf-mining beetles (Borowiec 1995a, Hsiao & Windsor 1999, Chaboo 2007, Borowiec & Świętojańska 2014, Staines 2014). Both tortoise beetles and leaf-mining beetles are distributed worldwide although the tribal diversity is higher in tropical regions (Borowiec & Świętojańska 2014, Staines 2014). In the taxonomic history of Cassidinae, the tortoise beetles and the leaf-mining beetles have been classified separately because of their distinct body forms.

The tortoise beetles, as their common name implies, have a round body often with broad lamellae on the pronotum and elytra, whereas the leaf-mining beetles have an elongate body without lamellae. The subfamily Cassidinae was proposed by Gyllenhal (1813) for only the tortoise beetles. In the same publication he established the subfamily Hispinae for the leaf-mining beetles, a system variously modified over the years (see review in Chaboo 2007, table 1): together as a superfamily Cassidoidea, as independent families from Chrysomelidae, as independent subfamilies within Chrysomelidae, as independent tribes within Clytrinae (= Clytrini in Cryptocephalinae), and an unranked group "Cryptostomes" owing to the withdrawn basal half of the labrum. Chen (1940) revised Cassidinae to include both the tortoise beetles and leaf-mining beetles. Staines (2002) clarified the nomenclatural priority for Cassidinae over Hispinae for the combined group. Still, "cassidines" (referring to tortoise beetles) and "hispines" (referring to leaf-mining beetles) are often used to distinguish between the two body shapes, even though body shape appears to have evolved independently in several different tribes. for example, several species of hispine, such as *Adalurnus rotunatus* Maulik (Alurnini), exhibit the body forms typical of the tortoise beetles (Staines 2014). Moreover, the tribe Imatidiniini includes beetles of both leaf-mining and tortoise beetle body shapes (Borowiec & Świętojańska 2014, Staines 2014). Currently, Borowiec & Świętojańska (2014) listed 14 tribes of tortoise beetles and Staines (2014) listed 24 tribes of leaf-mining beetles. Imatidiini and Spilophorini are included in both classifications.

Background for the tribe Ischyrosonychini

The New World tribe Ischyrosonychini is a little-known group with 69 described species in seven genera (Borowiec & Świętojańska 2014). The tribe traditionally was recognized as three

distinct lineages (Hincks 1952): the traditional Ischyrosonychini Chapuis (*Cistudinella* Champion and *Eurypedus* Gistel), Asterizini Hincks (*Asteriza* Chevrolat), and Physonotini Hincks (*Enagria* Spaeth, *Eurypepla* Boheman, *Physonota* Boheman, and *Platycycla* Boheman) (Figs. 1–7). The traditional Ischyrosonychini were first recognized with *Ischyrosonyx* Sturm (junior synonym of *Eurypedus*) by its oblong body; semi-circular pronotum with postero-lateral region acute; pronotum entirely covering head in dorsal view; and slightly convex body in lateral view (Chapuis 1875). When the tribe Ischyrosonychini was proposed, the physonotines and *Asteriza* were classified as members of "Cassidites" (= Cassidini) (Chapuis 1875). Spaeth (1942) proposed Physonototitae without description, and listed only *Physonota dilatata* Kirsch as its member. However, Physonototitae was an unavailable family-group name due to the lack of a description (ICZN, Art. 13.1). Hincks (1952) described and defined Physonotini by their broad elytral lamellae; yellow antennae with black distal antennomeres; and yellow and opalescent body color. Asterizini were also recognized by Hincks (1952) and diagnosed by narrow elytral lamellae with thickened lateral margins; broad, flat and arrow-shaped prosternal process; and the coloration (opalescent elytra and yellow antennae with three reddish proximal antennomeres). The traditional classification (Ischyrosonychini, Physonotini, and Asterizini) was used until the first phylogenetic study of Cassidinae at the tribal level by Borowiec (1995a) (Figs. 8–10).

Three phylogenetic analyses have been conducted focusing at the tribal level in Cassidinae (Borowiec 1995a, Hsiao & Windsor 1999, Chaboo 2007), but no consistent patterns were recovered. The inconsistency in those phylogenies have resulted in an ambiguous classification for Cassidinae. However, the three traditional subgroups of Ischyrosonychini were always nested with seven other tortoise beetle tribes (Aspidimorphini, Cassidini, Dorynotini, Eugenysini, Goniocheniini, Mesomphaliini, and Omocerini) but no consistent phylogenetic

placement was recovered for Ischyrosonychini in relation to these seven tribes (Borowiec 1995a, Hsiao & Windsor 1999, Chaboo 2007).

The notion of a close relationship among Asterizini, Ischyrosonychini, and Physonotini was first introduced by Borowiec (1995a, Figs. 8–10), and later by Hsiao & Windsor (1999). Borowiec created a data matrix for 21 tribes with 20 morphological characters from the couplets in the identification key of Hincks (1952), but without examining actual specimens. The characters and character states used by Borowiec (1995a) were too simplified and the couplets from Hincks (1952) were actually based on a study by Spaeth that was unpublished due to the bombing of Vienna during World War II (Hincks 1952). Borowiec (1995a) provided two phylogenies one each based on Spaeth's original couplets (Fig. 8) and Hincks' modified version (Fig. 9). The phylogeny based on Spaeth's couplets showed monophyly of the three traditional groups (Ischyrosonychini + (Asterizini + Physonotini)) (Fig. 8, boxed). In the phylogeny based on Hincks' couplets, the three traditional groups appeared as a paraphyletic group (Dorynotini + Physonotini + (Asterizini + Ischyrosonychini) + (Cassidini + Basiptini + (Aspidimorphini + Charidotini))) (Fig. 9, boxed). Borowiec (1995a) concluded that Asterizini, Ischyrosonychini, and Physonotini were closely related, but without synapomorphies at the tribal level, and suggested uniting them under the oldest name Ischyrosonychini (Fig. 9, boxed). Hsiao & Windsor (1999) performed a molecular phylogenetic analysis using 12s mtDNA sequence data. In this study, 47 species representing both leaf-mining beetles and tortoise beetles were included, with a species of Donaciinae as outgroup. Their study included a species each of *Eurypedus* and *Physonota*, and suggested the possible monophyly of Ischyrosonychini. However, the taxon sampling in Hsiao & Windsor (1999) was restricted to mainly the Panamanian fauna and the number of examined species was not sufficient to demonstrate phylogenetic relationships.

Chaboo (2007) performed a phylogenetic analysis of 98 species in 94 genera representing the full diversity of Cassidinae and six species from other subfamilies as outgroups, and using 210 characters from adult morphology, larval morphology, and biology. Chaboo (2007) included four species from four genera of Ischyrosonychini (*Asteriza*, *Eurypedus*, *Eurypepla*, and *Physonota*); these four species were placed on different branches on the terminal polytomy of the derived tortoise beetles in Aspidimorphini, Basiprionotini, Cassidini, Dorynotini, Eugenysini, Goniocheniini, Mesomphaliini, and Omocerini.

Goals

Phylogenetic relationships among tribes of tortoise beetles and the monophyly of each tribe is not well understood (Borowiec 1995a, Hsiao & Windsor 1999, Chaboo 2007). In particular, the monophyly of Ischyrosonychini was only weakly supported and largely without evidence (Borowiec 1995a). The unresolved relationship among the tortoise beetle tribes was mainly caused by a lack of phylogenetic studies and insufficient taxon sampling in the previous studies (Borowiec 1995a, Hsiao & Windsor 1999, Chaboo 2007). In addition, developing and understanding morphology have also been overlooked due to the distinct external morphology of each species or each group. To determine whether Ischyrosonychini is a monophyletic group and the phylogenetic position within the tortoise beetles, a study focusing on the phylogeny of Ischyrosonychini needs to be conducted with new morphological characters and sufficient taxon sampling.

This study had with five goals: **1)** to identify morphological characters and associated character states for phylogenetic analysis; **2)** to test the monophyly of Ischyrosonychini in a framework of comprehensively sampled tortoise beetles; **3)** to illuminate the phylogenetic

relationships among the three traditional subgroups of Ischyrosonychini; **4)** to define the generic boundaries within Ischyrosonychini; and **5)** to determine the placement of Ischyrosonychini in relation to other tortoise beetle tribes.

Herein a phylogenetic analysis was performed with adult morphological data. The morphological characters used in previous studies (Borowiec 1995, Chaboo 2007) were reviewed and compared to the characters used in this study. The gastral spiculum of the male genitalia and the head stridulatory file were introduced for the first time to be utilized in phylogenetic analysis. The distributions of the species in Ischyrosonychini were illustrated along with the phylogeny.

MATERIALS AND METHODS

The list of the examined specimens, characters and associated character states, and the data matrix are provided as Appendices 1, 2 and 3. In total 164 specimens from 11 collections were examined. For more detailed morphological examination, selected specimens were prepared for scanning electron microscopy, low vacuum scanning electron microscopy, and histological sectioning. Collection acronyms are as follow:

AMNH: American Museum of Natural History, New York, NY, USA

ASUT: University of Arizona, Frank M. Hasbrouck Insect Collection, Tempe, AZ, USA

EGRC: Edward G. Riley Collection, Texas A&M University, College Station, TX, USA

FSCA: Florida State Collection of Arthropods, Gainesville, FL, USA

LACM: Los Angeles County Museum of Natural History, Los Angeles, CA, USA

MNRJ: University of Rio de Janeiro, National Museum, Sao Cristovão, Rio de Janeiro, Brazil

MUSM: San Marcos University Natural History Museum, Lima, Peru

SEMC: Natural History Museum, University of Kansas, Lawrence, KS, USA

TAMU: Texas A&M University, College Station, TX, USA

UNAM: The National University of Mexico, Mexico DF, Mexico

USNM: National Museum of Natural History, Washington, DC, USA

Taxon Sampling

Taxon sampling was mainly focused on members of the Ischyrosonychini. For the other tribes, taxa were chosen based on the phylogenies of Borowiec (1995a, Fig. 10), Hsiao & Windsor (1999), and Chaboo (2007). Due to the ambiguous phylogenetic relationship of Ischyrosonychini with other tortoise beetle groups, eight tribes (Aspidimorphini, Basiprionotini, Cassidini, Dorynotini, Eugenysini, Goniocheniini, Mesomphaliini, and Omocerini) were also treated as part of the ingroup. For outgroups, two species of Hemisphaerotini (*Hemisphaerota cyanea* (Say) and *Hemisphaerota* sp.) were selected because these two tribes have unambiguously been considered as basal groups to Ischyrosonychini and eight tribes which were always nested with Ischyrosonychini in previous studies (Borowiec 1995a, Hsiao & Windsor 1999, Chaboo 2007). In total, 84 species representing 34 genera from 10 tribes were included in the analysis: four species were unidentified in species level. In general, the type genus of each tribe and the type species of 27 out of 34 genera were examined for nomenclatural stability (examined genera with non-type species: *Hemisphaerota* Monros & Viana, *Laccoptea* Boheman (Aspidimorphini), *Eurypedus* and *Eurypepla* (Ischyrosonychini), *Chelymorpha* Chevrolat and *Stola*s Billberg (Mesomphaliini), and *Canistra* Erichson (Omocerini)).

The sampling included 51 out of 67 described species in all seven genera (ca. 76%) of Ischyrosonychini and an unidentified species of *Physonota* (indicated as "*Physonota* sp."). The type species of each genus was included in the analysis except for *Ed. thoni* Barber and *El.*

jamaicensis (Linnaeus). *Eurypedus thoni* was excluded because it was synonymized with *Ed. peltoides* (Boheman) (Shin 2015). *Eurypepla calochroma* (Blake) was selected as sole representative of the genus among the four species of *Eurypepla*. The four species of *Eurypepla* might be conspecific, with morphological variation in body size, dark spots on pronotum and elytra, and different body shape based on sex (Woodruff 1979, personal observation with type specimens and multiple voucher specimens of each species). Currently, *Cistudinella* comprises 15 described species. Among the 15 species, four species of *Cistudinella* seemed to be either misclassified or junior synonyms of other species: *C. bahiana* Spaeth was considered as a species of Cassidini based on the photographs of the lectotype; *C. biguttata* Hincks was considered as a female specimen of *C. inanis* (the lectotype of *C. inanis* was a male); and *C. bipunctata* (Kirsch) and *C. rufitarsis* Spaeth were considered different color morphotypes of *C. notata* (personal comment by Lukas Sekerka, and comparison with the photographs of the type specimens). The recalculated taxon sampling for Ischyrosonychini, excluding those listed above, is 51 out of 60 species (ca. 84%) and an unidentified species of *Physonota*.

For Dorynotini, Goniocheniini, and Omocerini, at least one species from each genus was examined except for a monotypic genus *Heteronychocassis* Spaeth (Dorynotini) because its classification at the tribal level remains uncertain (Simões & Sekerka 2014). Limited taxon sampling was applied for Aspidimorphini, Cassidini, Eugenysini, and Mesomphaliini. For Aspidimorphini (285 described species in six genera), three species of *Aspidimorpha* Hope and a species of *Laccoptera* were selected because *Aspidimorpha* (199 described species) and *Laccoptera* (66 described species) are larger than the other four genera in diversity, and the distinct general morphology between these two genera (Borowiec & Świętojańska 2014). In addition, these selected species in Aspidimorphini represent different regions: *Aspidimorpha*

dissentanea Boheman and *Laccoptera murrayi* Boheman are distributed in Africa; *Aspidimorpha miliaris* (Fabricius) is distributed in Southern Asia and South-East Asia; and *Aspidimorpha* sp. is distributed in South-East Asia (Borowiec & Świętojańska 2014). Cassidini is the largest tribe among the tortoise beetle tribes (about 1300 described species in 87 genera), and morphological disparity among the genera and species is as diverse as its diversity (Borowiec & Świętojańska 2014). In addition, Cassidini is the only tortoise beetle tribe whose members are distributed in both Old World and New World (Borowiec & Świętojańska 2014). In the analysis, three species of Cassidini (*Cassida nebulosa* Linnaeus, *Charidotis miniata* Boheman, and *Coptocycla undecimpunctata* (Fabricius)) were selected to represent different regions and previously known subgroups. *Cassida nebulosa* is distributed widely in Palearctic, and the species of *Charidotis* Boheman and *Coptocycla* Chevrolat are distributed in Neotropics (Borowiec & Świętojańska 2014). Moreover, *Charidotis* and *Coptocycla* are the type genera of *Charidotitae* and *Coptocyclitae* respectably (subgroups of Cassidini). Eugenysini is a small tribe with 34 described species in three genera (Borowiec & Świętojańska 2014). In the analysis, *Agenysa connectens* (Baly) was selected because Eugenysini has been considered as a subgroup of Mesomphaliini (Borowiec 1995a, Hsiao & Windsor 1999, Chaboo 2007). Mesomphaliini is the second largest tribe among the tortoise beetle tribes (about 550 described species in 25 genera) and distributed only in New World (Borowiec & Świętojańska 2014). The several mesomphaliine genera exhibit unique morphology from other mesomphaliine genera due to flightlessness (extremely convex body with fused elytra in *Convexocoleus* Shin, *Elytrogona* Chevrolat and *Stoiba* Spaeth) (Shin 2012, Shin & Chaboo 2012) and maternal care (extremely expanded elytral lamellae in *Acromis* Chevrolat, *Omaspides* Chevrolat and *Paraselenis* Spaeth) (Chaboo et al. 2014). The members in Mesomphaliini with these unique morphological features were excluded for taxon sampling

because a combination of unique morphological features might affect the resolution of the phylogeny. In addition, 10 genera in Mesomphaliini comprise of less than five described species, which indicates the distinct morphological disparity among the genera (Borowiec & Świętojańska 2014). Besides *Mesomphalia gibbosa* (Fabricius) (type genus and type species), *Chelymorpha cassidea* (Fabricius) and a species of *Stola*s were selected in the analysis. The species of *Chelymorpha* and *Stolas* are distributed widely in New World: the distributions of most mesomphaliine genera are limited to small areas (Borowiec & Świętojańska 2014). In addition, these two genera are the type genera of Chelymorphites and Stolaini (junior synonyms of Mesomphaliini).

Terminology

The following abbreviations for generic names in the Ischyrosonychini were used: *Asteriza* (***A.***), *Cistudinella* (***C.***), *Enagria* (***En.***), *Eurypepla* (***El.***), *Eurypedus* (***Ed.***), *Physonota* (***Ph.***) and *Platycycla* (***Pl.***). The generic names in other tribes were fully spelled out.

The terminology for morphological features in the tortoise beetles was not consistently applied. The terminology for the external morphology and the genitalia are redefined and compared with previous studies, and new characters introduced. Morphological features are illustrated with *Ph. alutacea* Boheman as an exemplar. Suggested terms are indicated by in boldface.

General morphology and terminology of tortoise beetles (illustrated with *Ph. alutacea*)

Head (Figs. 17–19). On the head of tortoise beetles only four line structures are observed (Figs. 17–19). The **epicranial sulcus** (Fig. 18, **Ecs**) is an upside down Y-shaped line. The upper

part (one line) of the epicranial sulcus is also called the **coronal sulcus** (Fig. 18, **Cs**) (= "mid-cranial suture" + "mid-frontal sulcus" in Chaboo 2007), while the paired lines in the lower portion are called the **frontal sulcus** (Fig. 18, **Fs**) (= "frontogenal sulcus" in Chaboo 2007). The frontal sulci are divided from the coronal sulcus by the **antennal sockets** (Fig. 18, **Atsk**). On the ventral surface of the head capsule, both sides of the gena are connected to the gula by gular sulci. The **gular sulci** (Fig. 19, **Gs**) (= "gular suture" in Chaboo 2007) can be either present or absent between the mentum and head fossa. Applying a strict conceptual distinction between "suture" (line structure between metameric segments) and "sulcus" (any lines generally by invagination with antecosta for muscle attachment), the line structure between the **gula** (Fig. 19, **G**) and **gena** should properly be considered to be sulci. Here, a new term, the "**mid-frontal line**" (Fig. 18, **mfl**), is used for the longitudinal line on the medial region of the frons (= "mid-frontal sulcus" in Shin et al. 2012). This line structure is not invaginated (without antecosta) and its presence varies among individuals (absent, shallowly depressed or clearly lined, Shin et al. 2012). Tortoise beetles possess only the frons, vertex, and gena. Other regions of the head, such as subgena, postgena, occiput, and postocciput, which are divided by sutures or sulci, are missing. The dorsal region (Fig. 17) of the head is defined as the **vertex** and the lateral regions are defined as the **gena**. However, the distinction between the vertex and gena is ambiguous. The **stridulatory files** (Fig. 17, **Sf**) are found only on the postero-medial region of the vertex among tortoise beetles (Schmitt 1994, Wessel 2006, Shin et al. 2012). The number of **file ridges** (= "striae" in Gahan 1920, Chaboo 2007) on the stridulatory files varies among tortoise beetles. The **frons** (Fig. 18, **F**) is triangular or pentagonal and clearly defined in most tortoise beetles; it can be distinguished laterally by the frontal sulci (occasionally indistinct) and ventrally by the **clypeus** (Fig. 18, **Cl**). Several authors used the term **frontoclypeus** (Fig. 18, **Fcl**) (Chaboo 2007,

Shin & Chaboo 2012, Shin et al. 2012, Simões & Monné 2014) for the complex of the fused frons and clypeus, these are demarcated only by a shallow epistomal sulcus. In *Ph. alutacea*, the clypeus is flattened and the **epistomal sulcus** (Fig. 18, **Ecs**) (= "clypeal groove" in Borowiec 1995b, "epistomal suture" in Chaboo 2007) (Fig. 18) is indistinct. The members of the tribe Aspidimorphini and Cassidini may have an expanded clypeus over the basal region of the labrum. This expanded clypeus also has been called the "horizontal clypeus" and diagnosed as a putative synapomorphy of Aspidimorphini and Cassidini (Riley 1986, Borowiec 1995a, Borowiec & Świętojańska 2014).

Antenna (Fig. 20). The detailed morphology of the antennae was well-documented with illustrations by Chaboo (2007). Tortoise beetles possess either incrassate, weakly serrate, or elongate antennae. The incrassate and weakly serrate antennae are more common than elongate antennae among tortoise beetles and often flattened dorso-ventrally. The elongate antennae are not flattened and generally much longer than 2 times the length of the head. The **scape** (Fig. 20, **Sp**) (= antennomere I) is elongate and oval, and the **pedicel** (Fig. 20, **Pc**) (= antennomere II) is oval and as long as or slightly longer than broad in most tortoise beetles. Some tortoise beetles exhibit the **antennal notches** (= "antennal groove" or "ventro-marginal grooves" in Chaboo 2007, "antennal suture" in Simões & Monné 2014) between antennomeres V–XI or VI(VII)–XI (not observed on *Ph. alutacea*). The term **antennal groove** (= "lateral groove" in Chaboo 2007) (indistinct in *Ph. alutacea*) had previously been used for the antennal-receiving structure on the lateral sides of prosternum in Borowiec & Świętojańska (2014). *Physonota alutacea* possesses antennae with seven pubescent distal antennomeres (IV–XI), and the dark coloration on the

ventral surface of the scape and three distal antennomeres. The length of the antennae is as long as or slightly shorter than two times the length of the head.

Mouth fossa and mouth-parts (Figs. 19, 21–24). The orientation of the **mouth fossa** (Fig. 19, **Mf**) in tortoise beetles has been described as hypognathous (Chaboo 2007) or opisthognathous (Chapuis 1874, Chen 1940, 1964, 1985, Riley et al. 2002). The mouthparts are oriented ventrally on the head. The head is partially or completely covered by the pronotum and faces ventrally. Because of the direction of the head, the mouthparts are located posteriorly. However, the mouth orientation should be referred as **hypognathous** based on its location on the head. The general structure of the mouthparts in tortoise beetles is conserved and the terminology has been consistent. The basal region of the labrum is inserted in the head capsule and articulates with the clypeus (Figs. 17, 21).

This inserted **labrum** (Fig. 21) has been used as a diagnostic feature for “Cryptosomata” (currently the subfamily Cassidinae, tortoise beetles + leaf-mining beetles) (Chapuis 1874). The anterior region of the labrum is exposed and shifted ventrally (Fig. 21). The shape of the exposed region is round (often the lateral contour is straight) and medially concave (narrow, flat, broad) or occasionally sinuate.

The **mandible** (Fig. 22) shows more variation than the other mouthparts. The basal groups such as members of Hemisphaerotini (based on the phylogeny in Borowiec 1995a) possess a laterally elongate mandible with one or few teeth (see Chaboo 2007). The more derived tortoise beetles, including physonotines, possess a fist-shaped mandible (Fig. 22) (Shin & Chaboo 2012, Shin et al. 2012, Simões & Monné 2014). The apical half of the mandible is shifted and parallel to the face. Tortoise beetles with the fist-shaped mandibles possess several

teeth, or the teeth may be fused (Chaboo 2007). *Physonota alutacea* possesses five teeth on each mandible. An additional structure is the **horizontal ridge** (Fig. 22, **hr**) (= "horizontal thickening" in Shin & Chaboo 2012) on the upper part in the basal half of the mandible and present in tortoise beetles with the fist-shaped mandibles (Shin & Chaboo 2012, Shin et al. 2012). The horizontal ridge is generally located next to the mandibular tooth II.

The **maxilla** (Fig. 23) is comprised of the cardo, stipes, lacinia, galea, and maxillary palpus. The **cardo** (Fig. 23, **Cd**) is elongate and narrower medially than the distal and proximal regions. The **stipes** (Fig. 23, **St**) is elongate and triangular. The cardo and stipes are similar in length. The **lacinia** (Fig. 23, **La**) is either lobe-shaped (Chaboo 2007) or petal-shaped among tortoise beetles (Shin & Chaboo 2012, Shin et al. 2012), and covered by scale-like fine setae. The setae on the lacinia are much shorter than the setae on the galea and maxillary palpus. The **galea** (Fig. 23, **Ga**) is generally a lobe-shaped structure undivided in *Ph. alutacea* and the species of *Asteriza* (Shin et al. 2012), and two segmented (as "basigalea" and "distigalea" in Chaboo 2007) in other tortoise beetles (Chaboo 2007, Shin & Chaboo 2012, Simões & Monné 2014). In the segmented galea, the basal half (= "basigalea") is more sclerotized and darker than the apical half (= "distigalea"). The **maxillary palpus** (Fig. 23, **Mp**) is 4-segmented in tortoise beetles and connected to the **palpifer** (Fig. 23, **Pf**) on the stipes. The length and shape of each maxillary palpomere are different among species.

The **labium** (Fig. 24) is divided into four parts: mentum, prementum, ligula, and labial palpus. The **mentum** (Fig. 24, **Mt**) is quadrate and connected to the gula. The **prementum** (Fig. 24, **pMt**) is as broad as the mentum and bearing the pairs of the labial palpi antero-laterally and the ligula medially. The width of the **ligula** (Fig. 24, **Lg**) is different among species and the apex of ligula may be rounded or acute. The **palpiger** (Fig. 24, **Pg**) (articulating sclerite between

palpus and prementum) is missing or partially fused in tortoise beetles (palpiger was mis-marked on the labial palpomere I in Chaboo 2007). In *Ph. alutacea*, the palpiger is fused to the prementum. The **labial palpus** (Fig. 24, **Lp**) is 3-segmented. The shape and length of the labial palpomeres are different among species.

Prothorax (Figs. 11–13, 25). The shape of prothorax is varied among tortoise beetles. In *Ph. alutacea*, the **pronotum** (Figs. 11–13) is semicircular and divided two different regions: (pronotal) **disc** (Fig. **Pd**) and **lamella** (Fig. 11, **Pl**). The term "disc" has been used consistently and it is defined by the inner region that separates the dorsum and tergum. The lamella is the explanate area surrounding the anterior and lateral portion of the disc. Several terms have been used for lamella such as margin or explanate margin (Chaboo 2007, Borowiec & Świętojańska 2011, 2013, 2014, Shin & Chaboo 2012, Shin et al 2012). The margin was defined as "a more or less narrow part of a surface within the edge" (Nichols 1989; p. 422), which made it difficult for readers to distinguish it from the edge. In this study, the term "margin" was thought to be the same as the edge. In *Ph. alutacea*, the pronotal disc and lamella are well distinguished by the texture of the surface, convexity, and depressed line between them. In many tortoise beetles, the head is covered completely or partially by the pronotum in dorsal view. The morphological features of the pronotum, such as the anterior marginal line (by the degree of covering head), postero-lateral angle (pointed or round), lateral line, basal line of pronotal disc, have been used in identification and phylogenetic analyses (Chaboo 2007, Shin & Chaboo 2012, Shin et al. 2012, Shin 2013, Borowiec & Świętojańska 2014). The basal region of the pronotal disc is not surrounded by the lamella. The **basal line** of the pronotum (Fig. 25) in *Ph. alutacea* and most other tortoise beetles is often marked by a black line. In this study, the **anterior line** of pronotum

(Fig. 25) is defined as the anterior line between the lateral edges of the head cavity because the morphological variation was found consistently in that region. The **lateral line** of lamella (Fig. 25) is defined as between the anterior and basal lines. On the ventral surface of the pronotum, a **dorsal head cavity line** (Fig. 25, **dhcl**) is observed connecting to the anterior line (edge) of the prosternum in the physonotines and the species of *Asteriza* (Shin et al. 2012). This projected dorsal head cavity line is thought to function as the plectrum for the head stridulatory file in *Ph. alutacea*. The other tortoise beetles (whether the stridulatory file is present or not), including Ischyrosonychini s. str., possess band-like dorsal head cavity line by two projected lines.

The **prosternum** (Fig. 25) is often shorter than the length of the pronotal disc in tortoise beetles. The anterior edge of the prosternum often forms an expanded structure (= **prosternal collar** (Fig. 25, **PrSc**) in Chaboo 2007, Borowiec & Świętojańska 2014). This collar structure varies in length and its continuity with the ventral surface of the pronotum. The **prosternal process** (Fig. 25, **PrSp**) is located between the procoxal cavities. The width, length, surface texture, and shape of the prosternal process vary. The posterior half of the procoxal cavity is closed by the **hypomeron** (Fig. 25, **hym**) as a form of lobe (= lobe of hypomeron (Fig. 25, **hyml**) in Chaboo 2007) and the hypomeron is fused or connected on the postero-lateral lobes of the prosternal process. The prosternum and pronotal hypomeron are clearly distinguished by a **tergosternal sulcus** (Fig. 25, **TSs**) at the anterior region of the procoxal cavity.

Meso- and metathorax (Figs. 26–29). The **mesonotum** (Fig. 26) is an acute pentagonal sclerite with the paired **anterior mesonotal processes** (Fig.26, **antMsp**), the paired **postnatal elytral processes** (Fig. 26, **ptelp**), and the posterior angle of the **mesoscutellum** (Fig. 26, **Msstl**). The anterior mesonotal process varies in length. In the middle of the mesoscutum, the

longitudinal mesothoracic sulcus (Fig. 26, **lgMsths**) (= “longitudinal mesothoracic suture” in Chaboo 2007) is formed and generally terminates anterior to the mesoscutellum. The paired **elytral axillary cords** (Fig. 26, **axlc**) originate from the lateral portions of the mesoscutellum. The **metanotum** (Fig. 27) is much broader than long and only weakly sclerotized. In the antero-medial region, a short **prescutum** (Fig. 27, **psut**) is present; it is distinguished from the metascutum by the **anterior costal suture**. The **metascutum** (Fig. 27, **Mtsut**) is divided medially by the **metascutellar groove** (Fig. 27, **stlg**). The surface of each lateral region of the metascutum is smooth and slightly convex. The metascutellar groove is well-defined by a paired **alar ridge** (Fig. 27, **arr**) (= “alacristae” in Chaboo 2007) on each side, and which curves antero-laterally. The **metascutellum** (Fig. 27, **Mtstl**) is narrower than the metascutum. The anterior region of the metascutellum is emarginated by the metascutellar groove. The pterothoracic ventrites are actually the combined procoxal elements (Lawrence et al. 2000). Here, meso- and metaventrite were used for these ventral sclerites instead of “mesosternite” and “metasternite” in Chaboo (2007), Shin & Chaboo (2012), Shin et al. (2012), and Shin (2013).

The medial region of the **mesoventrite** (Fig. 28, **MsV**) is generally covered by the posterior region of the prosternal process. The shape of the mesoventrite is rounded triangular and narrow. The mesoventrite is connected to the mesoepisternum laterally and the anterior edge of the metaventrite between the mesocoxal cavities. The **mesepisternum** (Fig. 28, **Msest**) is divided into two different portions by the **mesepisternal ridge** (Fig. 28, **Msestr**). The anterior region of the mesepisternum is concave, and covered by the posterior ridge of the hypomeron. The **mesepimeron** (Fig. 28, **Msem**) is quadrate and laterally broadening. The medial edge on the mesepimeron is adjacent to the metaventrite and the posterior edge is connected to the metepisternum and metepimeron.

The **metaventrite** (Fig. 28, **MtV**) is broader than long with a **discrimen** (Fig. 28, **dicm**) medially (= “medial longitudinal line” in Chaboo 2007). The surface of the metaventrite might be rounded or flat. In *Ph. alutacea*, the surface is flattened laterally, forming an **angular projection** (Fig. 28, **anp**) (from Sanderson 1948) at the postero-lateral edges. The **metepisternum** (Fig. 28, **Mtest**) is located between the metaventrite and metespimeron. The metepisternum is divided into anterior and posterior regions by a projected line. The anterior region of the metepisternum is broader than long and the surface is flattened. The posterior region is longer than broad and medially narrower. The **metepimeron** (Fig. 28, **Mtem**) is shorter than the metepisternum, laterally connected to the metepisternum.

The **metendosternite** (Fig. 29) (= “metafurca” in Chaboo 2007) is little studied in tortoise beetles. The **stalk** (Fig. 29, **stl**) (also called “stem”, see Velázquez de Castro 1998) is triangular and arises from the ventral surface of the postero-medial region of the metaventrite. The stalk is connected to the middle of paired **sheaths** (Fig. 29, **sht**) which are weakly sclerotized and divided by the **longitudinal flange** (Fig. 29, **lonfl**). Paired **anterior tendons** (Fig. 29, **anttd**) arise from the antero-medial region of each sheath. The lateral apex of each sheath bears the **arm** (Fig. 29, **arm**) and **hemiductus** (Fig. 29, **hmdt**). In Chaboo (2007), the term “lamina” was used for the complex of the stalk and sheath. In Simões & Monné (2014), “lamina” was used for the arm and “brace” was used for the hemiductus.

Elytra (Figs. 11, 30). In dorsal view, two different regions can be distinguished: the **(elytral) disc** (Fig. 11, **Ed**) and **lamella** (Fig. 1, **El**). The term “elytral lamella(e)” is used to avoid confusion between the edge and margin as in the pronotum. In the humeral region, the **umbo(nes)** (Fig. 11, **Und**) (= “humerus” in Chaboo 2007) is observed. On the ventral surface of

each elytron, a narrow **epipleuron** is located; the length of the **epipleural ridge** (Fig. 30, **epr**) is shorter than half the length of the elytron in the physonotines. On the ventral surface of the elytral disc near the epipleural ridge, the **brace** (Fig. 30, **br**) and **longitudinal carina** (Fig. 30, **logc**) are observed. The base of the brace is connected to the epipleuron. The longitudinal carina often is absent in many species of tortoise beetles. The connection and angle between the brace and longitudinal carina vary among tortoise beetles.

Hindwing (Fig. 31). The general morphology and venation of the **hindwing** are similar among the tortoise beetles but the terminology for venation has been poorly documented and inconsistently applied (Chaboo 2007, Simões & Monné 2014). Several tortoise beetles, which have lost the ability to fly, show extremely divergent morphologies: a lobe-like structure in species of *Elytrogona* Chevrolat (vestigial hindwing) and half-sized wings in species of *Stoiba* Spaeth (brachypterous hindwing) (Shin & Chaboo 2012). Most tortoise beetles possess the fully-developed hindwings (Fig. 31). The **costa** (Fig. 31, **C**) and **subcosta** (Fig. 31, **sC**) are fused near the wing base. The **radius** (Fig. 31, **R**) is distinct and fused near the radial cell with the Costa+Subcosta. The **radial cell** (Fig. 31, **rc**) is triangular and formed by the complex of the Cost+Subcosta+Radius, the **proximal edge of the radial cell** (Fig. 31, **pe**)**,** and **distal edge of the radial cell** (Fig. 31, **de**). The proximal edge and distal edge of the radial cell are fused forming the **radius recurrent vein** (Fig. 31, **Rr**). The **radial fold** is found next to the distal apex of the radial cell. In the distal 1/3 region of the hind wing, two stripes are observed: **postradial stripe** (Fig. 31, **pst**) and **medial stripe** (Fig. 31, **mst**). The **cubitus** (Fig. 31, **Cu**) is distinct and divided into two different veins: the **median+radius cross vein** (Fig. 31, **rm**) and **first cubital vein** (Fig. 31, **Cu1**). The **anal cell** (Fig. 31, **ac**) is long and oval, and located near the hindwing

base with three wing veins: **first anal vein** (Fig. 31, **A1**), **second anal vein** (Fig. 31, **A2**), and **third anal vein** (Fig. 31, **A3**). The first and the second anal veins are connected by the **first anal cross vein** (Fig. 31, **a1**) and **second anal cross vein** (Fig. 31, **a2**).

Legs (Figs. 32–33). The morphology of the legs in tortoise beetles is conserved. The **procoxa** and **mesocoxa** are oval, and the **metacoxa** is medially round and narrows laterally. The **trochanter** of each leg is small and triangular. The **femur** (Fig. 32, **fm**) and **tibia** (Fig. 32, **tb**) of each leg is similar in length (occasionally tibiae are distinctly short than the femur in the front and middle legs). **Tarsomere I** (Fig. 33, **tsm1**) is round or triangular. **Tarsomere II** (Fig. 33, **tsm2**) is weakly bilobed, longer than the tarsomere I. **Tarsomere III** (Fig. 33, **tsm3**) deeply is bilobed with its length either reaching the bases of the pretarsal claws or the apexes of the pretarsal claws. In *Ph. alutacea*, the apexes of tarsomere III reach to the base of the pretarsal claws. **Tarsomere IV** is completely fused with tarsomere V in Cassidinae. **Tarsomere V** (Fig. 33, **tsm5**) is as long as or slightly longer than tarsomere III. Several distinct morphological features are found on the apex of tibia, tarsomere V, and **pretarsal claw (= ungues)** (Fig. 33, **prtscl)**. These features include a spine on the anterior side of tibial apexes of all legs in *Ph. calcarata* (Boheman) and *Ph. maculiventris* (Boheman), paired teeth or projections on the apex of the tarsomere V in the species of *Enagria* Spaeth, tooth on each base of the pretarsal claw in the members of Mesomphaliini and Eugenysini, and the micropectinate structure on the pretarsal claws in some species of Aspidimorphini and Cassidini (Riley 1986, Świętojańska 2001, Shin & Chaboo 2012).

Abdomen (Fig. 16). The morphology of the **abdomen** is conserved among tortoise beetles. In ventral view, five **ventrites** are observed (= sternites III–VII). Each ventrite is slightly convex in the medial region with a shallow depression on each side. The ventrite I and II are fused with or without a depressed line.

Male genitalia (Fig. 34). The male genitalia of tortoise beetles are laid laterally and they rotate when they protract for mating (= "deversement" in Verma 2009, Shin et al. 2012). The male genitalia consist of three parts: internal reproductive organs, aedeagus, and gastral spiculum. The internal organs consist of the **ejaculatory duct** (Fig. 34, **ejcd**), **seminal vesicle** (Fig. 34, **smv**) and two pairs of **testes** (Shin et al. 2012). The seminal vesicle may be as thin as the ejaculatory duct (as in *Ph. alutacea*) or as thick as the median lobe of the aedeagus as in *Asteriza* (Shin et al. 2012). The aedeagus is divided into three different structures: phallobase, median lobe, and tegmen. The **phallobase** (Fig. 34, **pb**) is incomplete oval. The **median lobe** (Fig. 34, **ml**) is well-sclerotized with pointed apex. The **tegmen** (Fig. 34, **tgm**) is Y-shaped. The **manubrium** (Fig. 34, **mnb**) is a part of the tegmen which is the unpaired process. The gastral spiculum is a modification of the 9th abdominal segment supporting the genitalia from below (Pajni & Bansal 1974). In most tortoise beetles, a V-shaped **gastral spiculum** (Fig. 32, **gasp**) (= spiculum gastrale) is found on the membrane surrounding the median lobe near the anus. Most morphological studies of tortoise beetles failed to observe the gastral spiculum. The anterior tip of the gastral spiculum which is V-shaped in *Ph. alutacea*, can be slightly extended, and therefore Y-shaped in other taxa. In species of *Asteriza*, the gastral spiculum exists as paired arms (= "spicule" in Shin et al 2012). The angle between the arms and shape of the arms (straight, curved, or slight sinuate) varies depending on species.

Female genitalia (Fig. 35). The internal reproductive organs of the female in tortoise beetles are well documented in Chaboo (2007) and Shin et al. (2012). The **spermatheca** is found near the common oviduct in the ventral space of the abdomen. The spermathecal system is divided into four different parts. The **vasculum** (Fig. 35, **vscl**) (= "pump" in Chaboo 2007) is a well-sclerotized pocket-shaped structure. The **velum** (= "apical appendix" in Chaboo 2007) is an additional sclerotized structure on the apex of the vasculum, which is absent *Ph. alutacea*. The **ampulla** (Fig. 35, **amp**) (= "receptacle" in Chaboo 2007) is a chamber between the vasculum and spermathecal duct, which can vary in shape and length. The **ductus glandula** (Fig. 35, **dtgd**) (= "gland" in Chaboo 2007) is a vascular structure which generally arises on the ampulla and is less sclerotized than the spermathecal duct. The **spemathecal duct** (Fig. 35, **sptd**) varies in length and shape (coiled, loosely sinuated, strongly or loosely tangled) among tortoise beetles. External features were scored for all specimens prior to dissection.

Dissection of Specimens

For dissection, the specimens were separated into their major parts (i.e., head, pronotum, pterothoracic complex, and abdomen). The separated parts were treated in 5–10% KOH (duration varied depending on the specimen) and dissected in distilled water, 95% alcohol, or glycerin. Dissected vouchers were preserved in glycerin. Specimens were examined with a Leica MZ16 stereomicroscope and an Olympus SZ30 stereomicroscope. Photographs were taken with a Microptics® camera system and a Leica DFC320 system attached to the Zeiss Axioskop 2 plus.

Scanning Electron Microscopy and Low-Vacuum Scanning Electron Microscopy

Stridulatory files on the head were observed in 63 out of 84 species under the light microscope, and the details were coded from the microscopic images. Due to sexual dimorphism of the head stridulatory file in some species (absent or less conspicuous in females), the characters were collected mainly from male specimens.

To illustrate the morphological variation in the stridulatory files, a male specimen of a species in each genus of Ischyrosonychini (*A. flavicornis* (Olivier), *C. foveolata* Champion, *En. ovata* Boheman, *El. calochroma*, *Ed. nigrosignatus* (Boheman), *Ph. alutacea*, and *Pl. deruta* Boheman) was prepared for scanning electron microscopy (**SEM**). The heads were mounted on aluminum stubs using adhesive Pelco tabs and isopropanol-based colloidal graphite. Specimen was coated with 30nm thickness of gold. Scanning electron microscopic images were captured using a LEO 1550 FESEM. A female specimen of *Ed. nigrosignatus* was also prepared for SEM to illustrate the sexual dimorphism on the head stridulatory file. For the other examined species with both male and female specimens (52 species), which were not prepared for SEM, male specimens were prepared for low-vacuum (= non-coating) scanning electron microscopy (**nSEM**); females of four species (*C. lata* Spaeth, *C. parva* (Wagener), *Ph. cerea* Boheman, and *Ph. vittifera* Sapeth) were examined in case when male specimens were not available.

Number of Stridulatory File Ridges

The number of stridulatory file ridges was counted from the images by SEM and nSEM on screen. The character states for ridge numbers (Ch.#34) were determined only by the ridge numbers from *Asteriza*, *Cistudinella*, *Enagria*, *Eurypepla*, *Eurypedus*, *Physonota*, and *Platycycla* because the sampling focused mainly on Ischyrosonychini (Figs. 36–37). The overall range of the ridge numbers in Ischyrosonychini was between 48 and 270. The ridge number was

considered to be discrete because breaks were shown in numbers among the groups or species of *Cistudinella* and *Physonota*. Based on the distribution of the ridge numbers (Figs. 36–37), at least three breaks were observed (between 57–79, 100–106, and 208–235). These breaks were used to define each character state in ridge number.

Histological Sectioning of Head and Pronotum

To illustrate the morphology of the sagittal section of the stridulatory file (Chs.# 28 and 33) and the dorsal head cavity line (Ch.# 83), male specimens of *Ed. nigrosignatus* and *Ph. alutacea* were prepared for histological sectioning to illustrate the stridulatory file and associated plectral structure on the ventral surface of the pronotum. Separated parts (head + pronotum) from the dried specimens were preserved in xylene overnight at room temperature, transferred to a xylene/paraffin (1:1) solution for 6~ hours twice in an oven (59˚C), transferred to 100% paraffin for 12~ hours 2 times in an oven (59 ˚C), and embedded in paraffin. The paraffin embedded specimens were sectioned at 10μm thickness using an Olympus CUT4060 retracting rotary microtome. The sections were cleared in xylene, stained with Gill's hematoxylin, counterstained with eosin, and mounted under coverslips in Canada balsam. Stained sections were digitally photographed with a Leica DFC230 camera mounted on a Zeiss Axioskop 2 plus compound microscope utilizing the Leica Firecam software. Measurements were made with Imag J, and Adobe Photoshop CS5 was used for enhancing the images.

Data Matrix and Cladistic Analysis

For the phylogenetic analysis, a data matrix was created (Appendix 3) for 84 tortoise beetles species using 155 morphological characters (Appendix 2).

In total, 155 characters were coded for each species: 26 characters from head capsule (ca. 16.8%), nine characters from head stridulatory file (ca. 5.8%), 15 characters from antennae (ca. 9.7%), 15 characters from mouthparts (ca. 9.7%), 30 characters from prothorax (ca. 19.3%), six characters from meso- and metathoracic complex (3.9%), four characters from abdomen (ca. 2.6%), nine characters from legs (ca. 5.8%), 31 characters from elytra (20%), five characters from male genitalia (ca. 3.2%), and six characters from female genitalia (ca. 3.9%). The number of the characters with binary character states was 100. The other 55 characters were coded with more than two character states: 33 characters with three states, 16 characters with four states, three characters with five states, two characters with six states, and one characters with seven states. An inapplicable character state was coded with "–" in the data matrix and treated as a separate character state.

The completed data matrix contained 866 missing characters (ca. 6.65%) and 513 inapplicable character states (about 3.92%). The analysis was performed in NONA (Goloboff 1998) through Winclada version 10.00.08 (Nixon 2002). Among the two outgroup *Hemisphaerota* species, *Hemisphaerota cyanea* was selected as outgroup for the analysis. All characters were weighted equally and unordered (Fitch optimization) to avoid bias. The parsimony ratchet was used to find the most parsimonious tree (Nixon 2002). As the setting for the tree-finding analysis, five trees were held per run, 16 (ca. 10%), 32 (ca. 20%) or 48 (ca. 30%) characters sampled with 10,000 replicates for each analysis, and with multi-ratcheting (five runs with five simultaneous threads). To acquire the support values for branches, bootstrap and jackknife analyses were performed in Winclada. In both analyses, 10,000 replicates were performed and the bootstrap and jackknife values were collected from the replicates. Bremer

Support values were acquired from 50,000 holds by allowing 10-step suboptimal trees and the range of the value was marked between 1 and 10.

Distribution Mapping

The distribution maps were provided only for the species of Ischyrosonychini. The distribution maps were compiled based on the locality data from Borowiec & Świętojańska (2014) and the locality data from those specimens examined in this study. The boundaries for mapping were mainly determined by Morrone (2001), and modified to include the distribution of species included in this study. Northeastern part of U.S.A. with the southern region of Canada (distribution of *Ph. helianthi* (Randall) and *Ph. unipunctata* (Say)), and South Florida (distribution of *El. calochroma*) which were not included in Morrone (2001), were determined each as a separate region.

RESULTS

Phylogeny of Ischyrosonychini (Figs. 38–39)

Four most parsimonious trees 1518 steps in length were recovered. In the strict consensus tree of these four trees, only two polytomies were present: one among the species of *Chlamydocassis* Spaeth (Goniocheniini) and one among the species of *Physonota* (Ischyrosonychini). Outgroup (two species of *Hemisphaerota*) was defined from the ingroup taxa (clade #1) by 27 synapomorphies including 11 non-homoplastic morphological features (Chs.#49(0), 52(1), 53(0), 56(0), 57(0), 66(2), 84(1), 88(0), 89(0), 99(0), 146(3)). The supporting values for the ingroup (clade #1) are 94 (bootstrap), 94(jackknife), and 4(Bremer support): following support values are indicated in parentheses in order of bootstrap, jackknife and Bremer

support. Clade #2 was defined by five synapomorphies (Chs.#21(0): expanded clypeus over labrum, 51(0): round antero-lateral line of labrum, 54(0): presence of mandibular tooth I, 74(2): convex anterior line of pronotum and 95(0): short anterior mesonotal process).

Among the taxa in clade #2, the basal group comprised four species representing four genera of Dorynotini (clade #3). The monophyly of Dorynotini was supported by six synapomorphies (Chs.#65(1): medially broadened pronotum, 78(1): angled postero-lateral edges of pronotum, 82(1): incontinuous pronotum lamella toward base, 115(1): laterally expanded elytral lamella, 119(1): angulate elytra in profile, and 122(1): absence of latero-middle bulging area on elytra). The support values for clade #3 are 94, 94, and 4.

Clade #4 (support values: -, - ,2) was supported by four synapomorphies (Chs.#22(1): presence of vertex lobe, 38(1): dorso-ventrally flattened antennae, 41(1): antennomere IV as long as or longer than 2 times length of pedicel, and 60(2): mandibular tooth III larger than other teeth. Clade #4 was a complex of the members in Aspidimorphini and Cassidini. Clade #5 (support values: 63, -, 2) was supported by three synapomorphies (Chs.#3(1): presence of projected orbital lines on posterior region of compound eyes, 16(1): elevated upper region of frons, and 98(1): presence of projection in the antero-medial region of mesoventrite). Neither Aspidimorphini (*Aspidimorpha* and *Laccoptera*) nor Cassidini (*Cassida*, *Charidotella* and *Coptocycla*) were monophyletic. The taxa in clade #6 were all New World tribes. Clade #6 (support values: -, -, 3) was supported by six synapomorphies (Chs.#9(1): half of interocular distance as broad as diameter of compound eye, 10(0): compound eyes located above upper tangent line of mouth fossa, 18(1): middle region of frons swollen, 20(1): surface between lower region of frons and clypeus flattened, 101(2): each abdominal ventrite black with posterior region brown, and 146(1): Y-shaped gastral spiculum).

Physonotines (*Enagria*, *Eurypepla*, *Physonota*, and *Platycycla*) were grouped with four species of *Asteriza* (clade #7) (support values: 76, 59, 4). Clade #7 were shown to be the sister group of clade #9 (Omocerini + Goniocheniini + Mesomphaliini + Eugenysini + *Cistudinella* + *Eurypedus*, unordered list). Clade #7 was supported by six synapomorphies (Chs.#29(0): broadest region of stridulatory file found in anterior 1/3 region, 30(0): length of stridulatory file longer than half length of head, 61(0): undivided maxillary galea, 70(1): length of pronotal disc longer than half width of pronotal disc, 83(0): one project line as dorsal head cavity line on ventral surface of pronotum, and 87(0): pronotal collar continuous to ventral surface of pronotum. The physonotines and four species of *Asteriza* did not group with *Cistudinella* and *Eurypedus*.

Clade #9 (support values: 61, -, 3) was supported by nine homoplastic synapomorphies (Chs.#4(0): coronal sulcus extending over posterior tangent line of compound eyes, 42(2): antennomeres III–X completely black, 64(0): triangular labial palpomere I, 71(0): absence of pronotal anterior lamella, 74(1): anterior line of pronotum flat or slightly concave which allowed part of compound eyes exposed in dorsal view, 76(1): posterior half of lateral line in pronotum round and parallel towards base, 78(0): postero-lateral edges of pronotum pointed, 106(0): length of mesotibia as long as or slightly shorter than length of mesofemur, and 147(1): arms of gastral spiculum round). The tribe Omocerini (clade #10) (support values: 76, 52, 5) was placed as the basal group within clade #9 and its monophyly was supported by 12 synapomorphies (Chs.#6(3): faintly and irregularly depressed dorsal surface of head, 23(2): presence of more than one head trichobothria between upper region of compound eyes, 29(2): broadest region of stridulatory file in posterior 1/3 region, 36(1): length of antenna longer than 2 times length of head, 38(0): unflattened (round) antennae, 62(1): maxillary galea flat and square, 89(1): width of prosternal

process between procoxal cavities as broad as or broader than width of procoxal cavity, 93(2): posterior half of prosternal process depressed, 95(1): length of anterior mesonotal process as long as or longer than length of lateral line of mesoscutum, 98(1): presence of antero-medial projection on mesoventrite, 116(1): elytral base distinctly broader than pronotal base, and 129(1): punctures on elytra coarse).

Clade #11 is a complex of members in the Eugenysini, Goniocheniini, Mesomphaliini, as well as *Cistudinella* and *Eurypedus*. Clade #10 (-, -, 1) was supported by four synapomorphies (Chs.#22(0): absence of vertex lobe, 79(0): each side of basal line of pronotum concave, 113(0): angle between pretarsal claws less than 90˚, and 154(2): spermathecal duct loosely tangled). *Herissa pantherina* (Blanchard) (monotypic genus of Goniocheniini) was recovered to be the sister group of the remaining members of clade #11. In this study, the tribe Goniocheniini appeared to be paraphyletic because clade #12 (Mesomphaliini + Eugenysini) and clade #13 (*Cistudinella* and *Eurypedus*) were nested within taxa of Goniocheniini. Clade #12 (support values: 83, 76, 2) was supported by nine synapomorphies including three non-homoplastic synapomorphies (Chs.#112(1): presence of basal tooth on pretarsal claw, 140(1): epipleural ridge extending over middle of elytra, and Ch.#91(3): absence of postero-lateral lobes on prosternal process).

The monophyly of the current concept of Ischyrosonychini (*Asteriza, Cistudinella, Enagria, Eurypedus, Eurypepla, Physonota,* and *Platycycla*) was not supported in this study. Clade #13 (*Cistudinella* + *Eurypedus*) (support values: 75, 57, 4) was supported by seven synapomorphies (Chs.#4(1): short coronal sulcus, 37(1): serrate antennomere III–X, 66(3): pronotal surface punctate, 71(1): presence of anterior lamella of pronotum, 128(0): punctures on elytra forming striae, 130(0): intervals between punctures on elytra broader than 5 times diameter

of puncture and , 150(0): loop-shaped spermathecal vasculum). Clade #13 showed a closer relationship with members of Eugenysini, Goniocheniini, and Mesomphaliini than with clade #7 (physonotines + *Asteriza*).

Generic Boundaries of the Target Taxa (Figs. 38–39)

In clade #7, *Pl. deruta* (monotypic genus) and *El. calochroma* were found to be two independent basal lineages, and *El. calochroma* was sister to clade#8 which included the members of *Asteriza*, *Enagria* and *Physonota*. The later clade (support values: 51, -, 3) was supported by six synapomorphies (Chs.#4(0): coronal sulcus extending over the posterior tangent line of compound eyes in dorsal view, 7(0): presence of seatae on dorso-medial region of head, 24(1): head trichobothrium on vertex lobe, 90(0): width between postero-lateral lobes of prosternal process narrower than width of procoxal cavity, 106(0): mesotibia as long as or slightly shorter than mesofemur, and 154(3): spermathecal duct long and irregularly curved but not tangled nor coiled). The four species of *Asteriza* (support value: 100, 100, 10) were placed as a derived group in clade#8. The two species of *Enagria* (support value: 100, 100, 10) were placed together among the species of *Physonota* (Fig. 38).

Both *Cistudinella* and *Eurypedus* (clade #13) were recovered as reciprocally monophyletic (Figs. 38–39). The monophyly of *Cistudinella* (support value: 78, 66, 7) was supported by a combination of ten homoplastic synapomorphies (Chs.#9(0), 29(2), 42(1), 54(1), 80(1), 88(1), 103(0), 124(0), 133(0), 148(0)). The monophyly of *Eurypedus* (support values: 100, 100, 10) was supported by 28 synapomorphies including two non-homoplastic synapomorphies (Chs.#33(1): presence of intervals between ridges on stridulatory file, and 86(1): presence of prosternal antero-lateral projections on ventral surface of pronotum).

DISCUSSION

Comparisons of Phylogenetic Relationships with Previous Studies

There have been only three phylogenetic studies conducted that addressed the phylogenetic relationships at the tribe level in Cassidinae (Borowiec 1995a, Hsiao & Windsor 1999, Chaboo 2007). However, among the tortoise beetle tribes, the phylogeny suggested by Borowiec (1995a, Fig. 10) has been widely accepted. There were two fundamental differences between the present phylogeny and the phylogeny by Borowiec (1995a, Fig. 10): **1)** the physonotines and *Asteriza* (clade #8) did not group with clade #13 (*Cistudinella* + *Eurypedus*); **2)** the target taxa (clades #7 and #13) formed a clade with the members of Eugenysini, Goniocheniini, Mesomphaliini and Omocerini. In the previous phylogenetic studies (Borowiec 1995a, Hsiao & Windsor 1999), the target taxa (clade #7 and #13) were either sister to Aspidimorphini, Cassidini or Dorynotini, or they formed a clade with these tribes. The close relationship of Ischyrosonychini (clades #7 and #13) to Eugenysini, Goniocheniini, Mesomphaliini, and Omocerini observed in this study may have been the result of the addition of new morphological characters used in this study and the re-interpretation of previous character states. Interestingly, in the phylogeny based on Spaeth's couplets in Borowiec (1995a, Fig. 8), Ischyrosonychini appeared as a monophyletic group and they formed a clade with Eugenysini, Goniocheniini, Mesomphaliini, and Omocerini.

The monophyly of Omocerini (clade #10) was confirmed in this study with a species from each of all seven genera. This tribe appeared as the basal group in clade #9. The monophyly of Omocerini also appeared in Hsiao & Windsor (1999) and Chaboo (2007) with a species of each from two genera (*Discomorpha* Cheverolat and *Omocerus* Cheverolat) and a species of

each from four genera (*Canistra* Erichson, *Cyclosom*a Guérin, *Discomorpha* and *Polychalca* Chevrolat) respectively. However, in Borowiec (1995a), the monophyly of Omocerini and the relationship to Goniocheniini and Mesomphaliini were unclear. Borowiec (1995a) treated the lineage of Omocerini + Goniocheniini as "Omocerini" (in Fig. 10), speculating that Omocerini was a derived group within "Omocerini", and indicated paraphyly of Goniocheniini. Borowiec also suggested that paraphyly of "Omocerini" (= Omocerini + Goniocheniini) related to Mesomphaliini.

In clade #11, only the monotypic genus *Herissa* Spaeth (Goniocheniini) was found as the sister group to the other taxa including other members of Goniocheniini, as well as Mesomphaliini, Eugenysini, *Cistudinella*, and *Eurypedus*. In clade #11, Goniocheniini and Mesomphaliini appeared to be paraphyletic: *Cistudinella* and *Eurypedus* formed a clade, and the only sampled species of Eugenysini was grouped with the members of Mesomphaliini. This unclear phylogenetic relationship within clade #11 was thought to be caused of: **1)** a lack of a synapomorphies for the Goniocheniini, and **2)** the similar external morphology between the species of *Goniochenia* Weise and *Mesomphalia* Hope. According to Borowiec (1995a), species of Goniocheniini were defined by the absence of apomorphies from Omocerini (with antennae slightly telescoped, with six proximal antennomeres glabrous) and Mesomphaliini (pretarsal claws with teeth). In addition, the members of *Goniochenia* and *Mesomphalia* exhibited very distinct morphologies from the other genera in each tribe but these two genera exhibited similar morphologies despite each classified in a different tribe. The similar morphology between the species of *Goniochenia* and *Mesomphalia* could also be implied from the taxonomic history of the species of *Goniochenia*. Seven species (out of 13) of *Goniochenia* were originally described as species of *Mesomphalia* (Borowiec & Świętojańska 2014). In this study, *Goniochenia*

quadraticollis (Boheman) was sister to clade #12 (Mesomphaliini + Eugenysini). *Agenysa connectens* (Eugenysini) was placed among the members of Mesomphaliini and sister taxon to a species of *Stolas*. The similar relationship of Eugenysini among with the members of Mesomphaliini appeared in Borowiec (1995a), Hsiao & Windsor (1999), and Chaboo (2007). Borowiec (1995a) treated the members of Eugenysini as a subset of Mesomphaliini and suggested a close relationship with the genus *Stolas* Billberg, which agreed with this study.

Phylogenetic Relationships within the Target Group

In clade #7 (Figs. 38–39), *Pl. deruta* and *El. calochroma* were separated by several autapomorphies from clade #8 (*Asteriza* + *Enagria* + *Physonota*). Both *Eurypepla* and *Platycycla* were recognized as distinct genera.

Boheman (1854, 1856, 1862) described 26 out of 39 species in *Physonota*. Boheman divided the members of *Physonota* into four different subgroups by overall morphological features:

Subgroup 1: oval body, convex profile (see Ch.#118(2)), elytral lateral margin broadly round and elytral posterior apex around (see Ch.#138(0)): this group was further divided further by the presence of the black marks on pronotum (see Chs.#68(1), 69(1)).

Subgroup 2: oval body and elytral posterior apex pointed (see Ch.#138(1)): subgroup 2 was further divided by the presence of the black marks on pronotum (see Chs.#68(1), 69(1)).

Subgroup 3: body round and elytra less convex (see Ch.#118(0 or 1)): subgroup 3 was further divided by presence of the spine on anterior apex of tibia (see Ch.#109(1)).

Subgroup 4: angled profile on elytra (see Ch.#119(1)).

Boheman's subgroups were not recovered in this study except for subgroup 4, which was recovered as the basal group of clade #8 (*Ph. cerea* Boheman, *Ph. citrina* Boheman, *Ph. nitidicollis* Boheman, and *Ph. sublaevigata* Spaeth).

The clades of *Asteriza* (four species) and *Enagria* (two species) placed among species of *Physonota*: *Physonota* appeared to be paraphyletic. *Enagria* was treated as a subgenus of *Physonota* in Hincks (1952) and Seeno & Wilcox (1982). The monophyly of *Enagria* was well-supported among species of *Physonota* in this study. The most interesting placement within clade #8 was that of *Asteriza* as the most derived species within clade #8. The four species of *Asteriza* exhibit a distinct morphology such as thickened elytral margin, bigger puncture size, and black coloration (except for *A. tainosa* Shin et al.) from the other members in clade #7, which classified *Asteriza* separately from the physonotines In addition, their distribution is limited to Hispaniola (Shin et al. 2012), and where none of the other species in clade #8 are found.

Both *Cistudinella* and *Eurypedus* in clade #13 (Figs. 38–39) were shown to be monophyletic. Interestingly, *C. inanis*, first described by Boheman (1854) as *Ischyrosonyx* Strum (junior synonym of *Eurypedus*) because of it similar morphology to *Eurypedus*, placed deeply among species of *Cistudinella*.

Systematics

The current concept of the tribe Ischyrosonychini was shown to be not monophyletic. The tribal name **Ischyrosonychini** should be applied only to the members in clade #13 (*Cistudinella* + *Eurypedus*). The tribal name **Asterizini** sensu Hincks (1952) (type genus: *Asteriza*) should be resurrected for the members in clade #7. The genus *Physonota* was paraphyletic, when excluding

Asteriza and *Enagria*, and so *Physonota* and *Enagria* are here considered synonyms of ***Asteriza*** as the oldest name.

Tribe Ischyrosonychini Chapuis 1875

Ischyrosonychites Chapuis 1875: 382.

Ischyrosonychini: Seeno & Wilcox 1982: 175; Borowiec 1995a: 556; Hsiao & Windsor 1999: 43; Chaboo 2007: 180; Bouchard et al. 2011: 516; Borowiec & Świętojańska 2014 (online catalog).

Physonotini: Borowiec 1999: 169; Chaboo 2007.

Diagnosis: Ischyrosonychini are distinguished from other tortoise beetle tribes by the following combination of characters: round anterior line of pronotum which covers head completely in dorsal view (in Dorynotini, Omocerini, Goniocheniini, Eugenysini, and most species of Mesomphaliini the transverse or concave anterior line of the pronotum allows part of the compound eyes to be exposed in dorsal view); angled postero-lateral edges of pronotum (in Aspidimorphini, Cassidini, and Asterizini where the postero-lateral edges of the pronotum are rounded); antennal notches on ventral surface of the antennomeres III–XI (in Dorynotini, Eugenysini, Mesomphaliini, Omocerini, Asterizini, and most species of Cassidini and Aspidimorphini there are no antennal notches); head stridulatory file present (in Dorynotini, Omocerini and most species of Mesomphaliini there is no stridulatory file); simple pretarsal claws (in Mesomphaliini and Eugenysini the pretarsal claws are toothed); and two-lined (band-like) dorsal head cavity line on ventral surface of pronotum (in Asterizini with there is one projected line).

Type genus: *Ischyrosonyx* Sturm 1843 (junior synonym of *Eurypedus* Gistel 1834).

Genera included:

***Cistudinella* Champion 1894**

Cistudinella Champion 1894: 164 (type species: *Cistudinella foveolata* Champion 1894, by monotypy); Spaeth 1914: 64; Hincks 1952: 336, 1956: 553 (key to species); Seeno & Wilcox 1982: 175; Borowiec 1999: 169; Borowiec & Świętojańska 2014 (online catalog).

***Eurypedus* Gistel 1834**

Eurypedus Gistel 1834: 31; Barber 1946: 290 (as valid name); Seeno & Wilcox 1982: 175; Borowiec 1999: 171; Borowiec & Świętojańska 2014 (online catalog); Shin 2015.

Ischyrosonyx Sturm 1843: 273 (type species: *Eurypedus thoni* Barber 1946 = *Cassida oblonga* Sturm in Thon 1827 not Illiger 1798, by monotypy); Chapuis 1875: 382; Spaeth 1914: 65; Hincks 1952: 336.

Remark: There is no need to update the generic diagnosis for the genera in Ischyrosonychini. The couplet #3 in Borowiec (1995a) for Ischyrosonychini can still be used to distinguish between *Cistudinella* and *Eurypedus*.

Tribe Asterizini Hincks 1952

Asterizini Hincks 1952: 330; Seeno & Wilcox 1982: 175; Chaboo 2007: 172.

Physonotitae Spaeth 1942: 32 (unavailable family-group name, Art. 13.1).

Physonotini Hincks 1952: 329; Seeno & Wilcox 1982: 175; Borowiec 1999: 169; Hsiao & Windsor 1999: 43; Chaboo 2007. **n. syn.**

Ischyrosonychini: Borowiec 1995a: 556; Bouchard et al. 2011: 516; Borowiec & Świętojańska 2014 (online catalog)

Remark: Both Asterizini and Physonotini were erected in Hincks (1952). Asterizini was chosen over Physonotini because new circumscription of *Asteriza* includes the members of *Physonota*.

Diagnosis: Asterizini are distinguished from other tortoise beetle tribes by the following combination of characters: round anterior line of pronotum which covers head completely in dorsal view (in Dorynotini, Omocerini, Goniocheniini, Eugenysini, and most species of Mesomphaliini the transverse or concave anterior line of the pronotum allows part of the compound eyes to be exposed in dorsal view); round postero-lateral regions of pronotum (in Dorynotini, Omocerini, Goniocheniini, Eugenysini, and most species of Mesomphaliini with there are postero-lateral edges of the pronotum angled or pointed, flattened antennae with no antennal notches on ventral surface of antennomeres III–XI (in Ischyrosonychini, Goniocheniini, and some species of Cassidini and Aspidimorphini antennal notches are present and often with unflattened antennae); head stridulatory file present (in Dorynotini, Omocerini, and most species of Mesomphaliini there are no stridulatory file); simple pretarsal claws (in Mesomphaliini and Eugenysini have toothed pretarsal claws); and projected dorsal head cavity line on ventral surface of pronotum (in all other tortoise beetle tribes there is a two-lined (band-like) dorsal head cavity line).

Type genus: *Asteriza* Chevrolat in Dejean 1836.

Genera included:

***Asteriza* Chevrolat in Dejean 1836**

Asteriza Chevrolat in Dejean 1836: 372, 1837: 396 (type species: *Cassida flavicornis* Olivier, 1790 by monotypy); Chapuis 1875: 387; Spaeth 1914: 122; Hincks 1952: 336; Seeno & Wilcox 1982: 175; Borowiec 1999a: 169; Shin et al. 2012: 34; Borowiec & Świętojańska 2014 (online catalog).

Physonota Boheman 1854: 190 (type species: *Physonota alutacea* Boheman 1854, designated by Hincks 1952: 336); Chapuis 1875: 386; Champion 1894: 165; Spaeth 1914: 62; Hincks 1952: 336; Balsbaugh & Hays 1972: 191; Seeno & Wilcox 1982: 175; Borowiec 1999a: 172; Borowiec & Świętojańska 2014 (online catalog). New synonymy.

Enagria Spaeth 1913: 139 (type species: *Physonota ovata* Boheman 1854 by original designation), 1914: 61; Hincks 1952: 336 (as subgenus of *Physonota*); Seeno & Wilcox 1982: 175 (as subgenus of *Physonota*); Borowiec 1999a: 171; Borowiec & Świętojańska 2014 (online catalog). New synonymy.

Physonaspis Spaeth in Hincks 1952: 345 (as subgenus of *Physonota*, type species: *Omoplata calcarata* Boheman, 1854 by monotypy); Hincks 1952: 336 (as subgenus of *Physonota*); Seeno & Wilcox 1982: 175 (as subgenus of *Physonota*).

Remark: The names of the former members in *Enagria* and *Physonota* need to be recombined under *Asteriza*. The new combinations of the species in *Asteriza* are provided in table 1. The concept of *Asteriza* changes by incorporating *Enagria* and *Physonota*. Shin et al. (2012) defined *Asteriza* by oval body, hemispherical pronotum, pale antennae with scape, pedicel and often antennomere III shiny red to reddish brown and apical half of last antennomere tanned, elytral lamella being less than half width of discal area, mottled elytra by yellow and black coloration, bulging structure between elytral disc and elytral lamella in middle, thickened edge of elytral lamella, and moderately punctured elytra with punctures scattered. However, couplets #5 and 6 in Borowiec (1995) for Ischyrosonychini can still be used (after replacing *Asteriza* for *Physonota*) to identify the genus.

Diagnosis: The new concept of *Asteriza*, now including those species from *Enagria* and *Physonota* is oval body, antennomere III longer than pedicel (antennomere II), basal four or five antennomeres glabrous, and half width of elytral disc broader than width of elytral lamella at posterior tangent line of umbo. *Asteriza* are distinguished from *Eurypepla* and *Platycycla* by the following combination: antennomere III longer than pedicel (in *Eurypepla* antennomere III is as long as pedicel); half width of elytral disc narrower than elytral lamella at the posterior tangent line of umbones (in Platycycla elytral lamella is broader than the half width of the disc at the posterior tangent line of the umbones); and basal four or five antennomeres glabrous (in Platycycla basal three antennomeres are glabrous).

***Eurypepla* Boheman 1854**

Eurypepla Boheman 1854: 236 (type species: *Cassida jamaicensis* Linnaeus 1758, designated by Hincks 1952: 336); Chapuis 1875: 384; Spaeth 1914: 61; Hincks 1952: 336 (as subgenus of *Physonota*); Seeno & Wilcox 1982: 175 (as subgenus of *Physonota*); Borowiec 1999: 172; Borowiec & Świętojańska 2014 (online catalog).

Platycycla Boheman 1854

Platycycla Boheman 1854: 240 (type species: *Platycycla deruta* Boheman 1854, by monotypy); Chapuis 1875: 385; Spaeth 1914: 61; Hincks 1952: 336 (as subgenus of *Physonota*); Seeno & Wilcox 1982: 175 (as subgenus of *Physonota*); Borowiec 1999: 177.

Morphological Characters

Most of the characters used in this study have been used in previous descriptions, diagnoses, and phylogenetic studies of Cassidinae (see comments of each character in Appendix 2). Borowiec (1995a) compiled a morphological data matrix with 20 characters (0 to 19) for 21 tribes. This data matrix included two tribes of the leaf-mining beetles (hispines) and the morphological characters of both adult and larva. Thirteen characters (Ch.#0, 4, 5, 6, 7, 8, 9, 10, 15, 16, 17, 18, 19) in his data matrix were not considered in this study because they were used to distinguish between leaf-mining and tortoise beetles, among tortoise beetle tribes which were not included in this study, or taken from larval morphology and host plant information. Character #3 (length of clypeus) in Borowiec (1995a) was also excluded because its character states were ambiguous and were considered duplicated with character #2 (horizontal clypeus). Therefore, only six characters in Borowiec (1995a) were modified and used in this study (Chs.#1, 2, 11, 12, 13, 14). These characters have been considered the major factors in adult morphology that have

been used to determine tortoise beetles lineages. Since Borowiec's phylogenetic study (1995a) was conducted based on the morphological features extracted from the couplets in the identification key in Hincks (1952), these characters were too simple and too widely applied to all members in each tribe. These characters and transitions of the character states are discussed below based on the taxa and phylogeny in this study.

Character #1 in Borowiec (1995a): head exposition in dorsal view: This character was modified as pronotum shape with three different states (Ch.#74). The phylogeny in this study showed that the pronotum completely covering the head in dorsal view (Ch.#74(2)) grouped clade #2 (Fig. 40). The pronotum partially covering the head (Ch.#74(1)) was shared by members of clade #9. However, transitions to Ch.#74(0) in four genera of Omocerini (*Cyclosoma*, *Discomorpha*, *Omocerus*, and *Polychalca*) and Ch.#74(2) in *Eurypedus* were observed within clade #9.

Character #2 in Borowiec (1995a): horizontalization of clypeus. The expanded clypeus over the labrum (Ch.#21(0)) was thought to be a synapomorphy in some lineages of Aspidimorphini and Cassidini (Riley 1986, Borowiec 1995a). In this study, this character was only coded for whether the inferior margin was expanded on the labrum despite its length. The expansion of the clypeus on the labrum appeared to be one of the synapomorphies for clade #2. Several lineages in clade #9 (*Canistra osculatii* Guérin, *Carlobruchia tricostata* (Spaeth), *Cassidinoma denticulate* (Boheman) (Omocerini), *Herissa pantherina* (Goniocheniini), Mesomphaliini, *Agenysa caedemadens* (Lichtenstein) (Eugenysini)) possessed the alternate state (Ch.#21(1)).

Character #11 in Borowiec (1995a): width of elytra lamella. The character was modified and applied in this study with four states (Ch.#132). In this study, the width of the elytral lamella

was measured at the posterior tangent line of umbones only on females due to sexual dimorphism on body shape and elytral lamella (Ch.#124). The species with sexual dimorphism of the elytral lamella showed that males possessed wider elytral lamellae than females (Shin et al. 2012). In addition, the morphology of the tortoise beetles without the sexual dimorphism on elytral lamella possessed more elongate body shape, which was thought to be the body shape of females in the species with the sexual dimorphism on body shape. In this study, the width of the elytral lamella appeared to be uninformative character to resolve relationships at the tribal level.

Character #12 in Borowiec (1995a): modification of pretarsal claw. The character of modification of the pretarsal claw was also used this study (Ch.#112). Three character states were applied (simple, toothed, and micropectinate). Most of the examined species possessed the simple pretarsal claws (Ch.#112(0)) except for the species of Mesomphaliini and Eugenysini with toothed pretarsal claws (Ch.#112(1)) and the species of Aspidimorphini with the micropectinate pretarsal claws (Ch.#112(2)). The monophyly of Aspidimorphini was not supported by the micropectinate pretarsal claws but the monophyly of Mesomphaliini + Eugenysini (clade #12) was supported by toothed pretarsal claws.

Character #13 in Borowiec (1995a): distance or angle between pretarsal claws. This character was modified with four states (Ch.#113). The angle between pretarsal claws appeared to be uninformative for the phylogenetic relationship in this study. However, the adjacent pretarsal claws were shown as a derived state within Dorynotini (clade #3).

Character #14 in Borowiec (1995a): extension of tarsomere III. Borowiec (1995a) suggested that “expanded last tarsal segment” as the apomorphic character state. He coded Eugenysini with this derived state. The statement should be clarified. The last tarsal segment should indicate the tarsomere V. Based on the tarsal morphology of Eugenysini, it should be

inferred as “elongate tarsomere III” because the lobes of the tarsomere III in Eugenysini extend anteriorly and those cover the pretarsal claws laterally (if the tarsomere V extended, the pretarsal claws would be more exposed). In this study, the same character and character states were applied (Ch.#110). However, an elongate tarsomere III (Ch.#110(0)) was also observed among the members of Aspidimorphini, Cassidini, and Dorynotini.

Characters of two structures (gastral spiculum and head stridulatory file) were used in tortoise beetles for the first time. Three different shapes of the gastral spiculum were observed among the tortoise beetles (Ch.#146). The outgroup taxa possessed the Y-shaped gastral spiculum (Ch.#146(0)). This structure was absent in Dorynotini (clade #3) and Aspidimorphini + Cassidini (clade #5). Within clade #9, the morphology of the gastral spiculum appeared to be uninformative on phylogenetic relationship. The paired arms of the gastral spiculum (Ch.#146(2)) were only found within clade #7.

Head stridulatory files (Figs. 42–57) were observed in several tribes within clade #6. Specifically, all species of clade #7 (Asterizini), #10 (Omocerini) and #13 (Ischyrosonychini) possessed the stridulatory file (Fig. 58). Based on the morphological variation and sexual dimorphism in the head stridulatory files, nine characters were applied in this study (Chs.#27–35). Omocerini (clade #10) and *Cistudinella* possessed the stridulatory files with the broadest point in the posterior 1/3 region (Ch#29(2), Figs. 42, 50, 59). The space between the files ridges (Fig. 18, 26, Ch.#33.(1)) was observed only in *Eurypedus*. The character state of the number of file ridges (Ch#34, Fig. 60) was consistent with minor numbers of character state transitions in generic or tribal levels in the target taxa: two species of *Eurypedus* shared the number of files ridges less than 60 (Ch#34(0)); nine species of *Cistudinella* possess the number of file ridge either between 80 and 90 (Ch#34(1)) or between 100 and 210 (Ch#34(2)); and the members of

clade #7 (Asterizini) shared the number of file ridge between 100 and 210 (Ch#34(2)), except for two species with the number of file ridge over 230 (Ch#34(3)).

The plectral structure on the ventral surface of the pronotum appeared to be an important character for clade #7 (Asterizini). A single projected line serving as the plectrum (Figs. 62, 64: marked by red arrow) was observed in all species in Asterizini, which appeared to be the unique non-homoplastic synapomorphy for clade: a plectrum made up of with two projected lines (Figs. 63, 65: marked by blue arrow) was observed all other tortoise beetles in this study; whether possessing the stridulatory file on the head or not.

Besides the variation in the morphology of the stridulatory files, a microtrichial patch anterior to the stridulatory file (Ch#24(1)) (Figs. 45–49, 53–57, marked by yellow arrow) was observed in all species in Asterizini and Cassidini, and some members in other tribes (three species Aspidimorphini, one species of Goniocheniini and two species of Omocerini); this patch was absent in species of *Cistudinella* and *Eurypedus* (Figs. 42–44, 50–52), and all the other tortoise beetles in this study.

Biogeography

The members of the Asterizini (clade #7, Fig. 66) are distributed between Peru (*Ph. dilatata*, not included in this study) and the southeastern region of Canada (Borowiec & Świętojańska 2014). The species diversity is said to be highest in Oaxaca and Veracruz, Mexico (Borowiec & Świętojańska 2014). In clade #7, no significant trend in distribution was found (Fig. 66). However three interesting observations about the distribution in the phylogenetic context can be made. Two species from the northeastern U.S.A. and southeastern Canada (*Ph. helianthi* (Randall) and *Ph. unipunctata* (Say)) showed an unusual distribution, separate from

those other species in Asterizini. Four species of *Asteriza* (an endemic Hispaniolan group) appeared as the terminal group of clade #7. None of the other species in clade #7 were distributed in Hispaniola, suggesting a single invasion. The species of *Eurypepla* are disjunctly divided in Yucatan, Cuba, Jamaica, and South Florida (Borowiec & Świętojańska 2014): none of other species of Asterizini was distributed in where the species of *Eurypepla* were distributed. Woodruff (1976) mentioned that the Geiger tree (*Cordia sebestena* Linnaeus, the only host plant of the species of *Eurypepla*) was distributed in South America, West Indies, and Yucatan, Mexico, and introduced in Florida Keys in the early 19th century. This suggests that *Eurypepla* in Florida was also introduced in Florida with the Geiger tree.

Species in the Ischyrosonychini (clade #13) (Fig. 67) were mostly distributed between Yucatan, Mexico and South America. The distributions of the two species in *Eurypedus* were distinctly divided by the Amazon Basin (Shin 2015). Most of the species of *Cistudinella* were distributed in South America. Four species of *Cistudinella* (*C. lata*, *C. obducta* (Boheman), *C. peruana* Spaeth, *C. plagicollis* Spaeth (not included in this study)) were distributed to the west of the Andes. Two species of *Cistudinella* (*C. foveolata* and *C. parva*) were distributed in Central America and the northern part of South America. The other species of *Cistudinella* overlapped with the distribution of *Ed. peltoides*. Among the species of *Cistudinella*, *C. obducta* was distributed in the largest area including some regions of the Amazon Basin (Fig. 67, purple regions on the map). Besides *C. obducta*, none of species in *Cistudinella* was collected in the Amazon Basin, which was similar to the distribution of the species in *Eurypedus*. The similar distribution between *Cistudinella* and *Eurypedus* might imply that the Amazon Basin might have formed after those two genera were separate, and functioned as a geographical barrier for the species in each genus.

ACKNOWLEDGMENTS

The author is grateful to Kirsten Jensen and Michael S. Engel (University of Kansas) for their excellent guidance for this article; Lee Herman and Sarfraz Lodhi (AMNH), Sang-Mi Lee (ASUT), Edward G. Riley (EGRC, TAMU), Michael Thomas (FSCA), Brian Brown and Weiping Xie (LACM), Miguel A. Monné (MNRJ), Gerardo Lamas (MUSM), Santiago Caballero Zaragoza and Sara Lopez (UNAM) and David Furth, Alexander S. Konstantinov, Steve W. Lingafelter (USNM) for the specimen loans; and Lukas Sekerka (National Museum, Prague, Czech Republic), Marianna Simões and Mabel Alvarado (University of Kansas) for providing general comments and the photographs of the type specimens. This study was supported by the Entomology program, Department of Ecology and Evolutionary Biology and the Biodiversity Institute of the University of Kansas.

CITATIONS

Balsbaugh, E.U. Jr. & Hays, K.L. 1972. The leaf beetles of Alabama (Coleoptera: Chrysomelidae). Auburn University (Alabama) Agricultural Experiment Station Bulletin, 441: 1–223.

Barber, H.S. 1946. Nomenclatorial note (Coleoptera, Cassidinae). Revista de Entomologia, 17: 290–291.

Boheman, C.H. 1854. Monographia Cassididarum. Tomus secundus. Officina Nordstedtiana, Holmiae. 506 pp. + 2 pls.

Boheman, C.H. 1856. Catalogue of Coleopterous Insects in the Collection of the British Museum, Part IX, Cassididae. London, 225 pp.

Boheman, C.H. 1862. Monographia Cassididarum. Tomus quartus. Officina Nordstedtiana, Holmiae, 504 pp.

Borowiec, L. 1995a. Tribal classification of the cassidoid Hispinae (Coleoptera: Chrysomelidae). In: Biology, Phylogeny, and Classification of Coleoptera. (eds.) Pakaluk, J. & Ślipiński, S.A., Muzeum I Instytut Zoologii, Warszawa, 541–558.

Borowiec, L. 1995b. Two new species of *Physonota* Boh. from Mexico, and notes on *Ph. cerea* Boh. (Coleoptera: Chrysomelidae: Cassidinae). Genus, 6(3–4): 429–439.

Borowiec, L. 1999. A World Catalogue of the Cassidinae (Coleoptera: Chrysomelidae). Biologica Silesiae, Wrocław, 479 pp.

Borowiec, L. & Świętojańska, J. 2011. The tortoise beetles of Madagascar (Coleoptera: Chrysomelidae: Cassidinae), Part 1: Basiprionotini, Aspidimorphini, and Cassidini (except the genus *Cassida*). Polish Taxonomical Monographs, Polish Taxonomical Society, 18: 1–246.

Borowiec, L. & Świętojańska, J. 2013. The tortoise beetles of Madagascar (Coleoptera: Chrysomelidae: Cassidinae), Part 2: Cassidini, the genus *Cassida* Linnaeus. Polish taxonomical monographs, Polish Taxonomical Society, 20: 1–293.

Borowiec, L. & Świętojańska, J. 2014. Cassidinae of the World – an interactive manual (Coleoptera: Chrysomelidae). Available from http://www.biol.uni.wroc.pl/cassidae/katalog%20internetowy/index.htm (Accessed: July 1, 2015).

Chaboo, C.S. 2007. Biology and phylogeny of Cassidinae Gyllenhal (tortoise and leaf-mining beetles) (Coleoptera: Chrysomelidae). Bulletin of the American Museum of Natural History, 305: 1–250.

Chaboo, C.S., Frieiro-Costa, F.A., Gómez-Zurita, J. & Westerduijn, R. 2014. Origins and diversification of subsociality in leaf beetles (Coleoptera: Chrysomelidae). Journal of Natural History, Volume 48: 2325–2367.

Champion, G.C. 1894. Biologia Centrali-Americana, Insecta Coleoptera, Volume VI. Part 2. Phytophaga (part). (ed.) Porter, R.H., Zoologia, London, 249 pp. + 13 pls.

Chapuis, M.F. 1874. Famille des Phytophages. In: Histoire Naturelle des Insectes. Genera des Coléoptères ou exposé méthodique et critique de tous les genres proposés jusqu'ici dans cet ordre d'Insectes. Volume X. (eds.) Lacordaire, T.H., A la Libraire Encyclopédique de Roret, Paris, 455 pp.

Chapuis, M.F. 1875. Famille des Phytophages. In: Histoire Naturelle des Insectes. Genera des Coléoptères ou exposé méthodique et critique de tous les genres proposés jusqu'ici dans cet ordre d'Insectes. Volume XI. (eds.) Lacordaire, T.H., A la Libraire Encyclopédique de Roret Paris, 420 pp.

Chen, S. 1940. Attempt at a new classification of the leaf beetles. Sinensia, 11: 451–481.

Chen, S. 1964. Evolution and classification of the chrysomelid beetles. Acta Entomologica Sinica, 13(4): 469–483.

Chen, S. 1985. Phylogeny and classification of the Chrysomeloidea. Entomography, 3: 465–475.

Crowson, R.A. 1981. The Biology of the Coleoptera. Academic Press, London, 802 pp.

Dumortier, B. 1963. Morphology of sound emission apparatus in Arthropoda. In: Acoustic Behaviour of Animals. (ed.) Brusenl, R.G., Elsevier Publishing Company, New York, 277–345.

Gahan, C.J. 1900. Stridulation organs in Coleoptera, Transaction of the Royal Entomological Society of London, 48: 433–452.

Gistel, J. 1834. Die Insecten-Doubletten aus der Sammlung des Grafen Rudolph von Jenison Walworth zu Regensburg, welche sowohl im Kauf als im Tausche abgegeben werden, Nro. I. Käfer. Druck von George Jaquet, München, 35 pp.

Goloboff, P.A. 1998. NONA. Available from: http://www.cladistics.com/aboutNona.htm (Accessed: February 17 2015).

Gyllenhal, L. 1813. Insecta Svecica. Classis I. Coleoptera sive Eleuterata. Tomus I, Pars III. Litteris F. J. Leverentz, Scaris, 734 pp.

Hincks, W.D. 1952. The genera of the Cassidinae (Coleoptera: Chrysomelidae). Transactions of the Royal Entomological Society of London, 103: 327–358.

Hincks, W.D. 1956. Some Neotropical Cassidinae (Col., Chrysom.) in the Museum G. Frey. Entomologisch Arbeiten aus dem Museum G. Frey Tutzing bei München, 7: 545–559.

Hsiao, T.H. & Windsor, D.M. 1999. Historical and biological relationships among Hispinae inferred from 12S mtDNA sequence data. In: Advances in Chrysomelidae Biology 1. (ed.) Cox, M.L., Backhuys Publishers, Leiden, 39–50.

International Commission of Zoological Nomenclature [ICZN]. 1999. International Code of Zoological Nomenclature, [fourth edition]. International Trust for Zoological Nomenclature, London, i–xxix, + 306 pp.

Iturralde-Vinent, M.A. & MacPhee, R.D.E. 1999. Paleogeography of the Caribbean region: Implications for Cenozoic biogeography. Bulletin of the American Museum of Natural History, 238: 1–**95.**

Lawrence, J.G., Hastings, A.M., Dallwitz, M.J., Paine, T.A. & Zurcher, E.J. 2000. Beetles of the world. A key and information system for families and subfamilies. Version 1.0 for Microsoft Windows. CSIRO publishing, Canberra. [Compact Disc].

Linnaeus, C. 1758. Systema naturae per regna tria naturae, secundum classes, ordines, genera, species, cum characteribus, differentiis, synonymis, locis. Tomus I. Editio decima, reformata. Laurentii Salvii, Holmiae, 824 pp.

Morrone, J.J. 2001. Biogeografía de América Latina y el Caribe. M&T–Manuales & Tesis SEA, volume 3, Zaragoza, 148 pp.

Nixon, K. C. 2002. Winclada. Available from: http://www.cladistics.com/aboutWinc.htm (Accessed: February 17 2015).

Olivier, A.G. 1790. Encyclopédie Méthodique, Histoire Naturelle. Insectes, Volume V. Chez Panckoucke, Paris, 793 pp.

Pajni, H.R. & Bansal, R.K. 1974. Gastral spiculum in Chrysomelidae (Coleoptera). International Journal of Insect Morphology and Embryology. Volume 3, 2: 225–229

Pongrácz, A. 1935. Die eozäne Insektenfauna des Geiseltales. Nova Acta Academiae Caesareae Leopoldino-Carolinae Naturae Curiosorum (Neue Folge), 2: 485–572 + 1–7 pls.

Riley, E.G. 1986. Review of the tortoise beetle genera of the tribe Cassidini occurring in America, North of Mexico (Coleoptera: Chrysomelidae: Cassidinae). Journal of the New York Entomological Society, 94(1): 98–144.

Rossetti, D.F. & Valeriano, M.M. 2007. Evolution of the lowest Amazon basin modeled from the integration of geological and SRTM topographic data. Catena, 70: 253–265.

Sanderson, M.W. 1948. Larval, pupal, and adult stages of North American *Physonota* (Chrysomelidae). Annals of the Entomological Society of America, 41(4): 468–477.

Seeno, T.N. & Wilcox, J.A. 1982. Leaf beetle genera. Entomography, 1: 1–221.

Schmitt, M. 1994. Stridulation in leaf beetles (Coleoptera, Chrysomelidae). In: Novel aspects of the biology of Chrysomelidae. (eds.) Joliver, P.H., Cox, M.L. & Petitpierre, E., Kluwer Academic Publisher, Netherlands, 319–325.

Shin, C. 2013. A new genus of mesomphaliine tortoise beetle (Coleoptera: Chrysomelidae), with description of a new flightless species from Haiti. The Coleopterists Bulletin, 67(4): 521–531.

Shin, C. 2015. A revision of the Neotropical tortoise beetle genus *Eurypedus* (Coleoptera: Chrysomelidae). (a chapter of the Ph.D. thesis, unpublished)

Shin, C. & Chaboo, C.S. 2012. A revision and phylogenetic analysis of *Stoiba* Spaeth 1909 (Coleoptera: Chrysomelidae). Zookeys, 224: 1–36.

Shin, C., Chaboo, C.S. & Clark, S.M. 2012. Phylogenetic revision of the Hispaniolan endemic genus *Asteriza* Chevrolat, 1836 (Coleoptera: Chrysomelidae: Cassidinae: Ischyrosonychini). Zootaxa, 3227: 34–53.

Simões, M.V.P. 2014. Taxonomic revision of the genus *Paranota* Monrós and Viana, 1949 (Coleoptera: Chrysomelidae: Cassidinae: Dorynotini). The Coleopterists Bulletin, 68(4): 631–655.

Simões, M.V.P. & Monné, M.L. 2014. Taxonomic revision of the genus *Mesomphalia* Hope, 1839 (Insecta, Coleoptera, Chrysomelidae). Zootaxa, 3835(2): 151–197.

Simões M.V.P. & Sekerka, L. 2014. Redescription of *Heteronychocassis acuticollis* Spaeth, 1915 (Coleoptera: Chrysomelidae: Cassidinae). The Coleopterists Bulletin, 68(3):407–410.

Spaeth, F. 1913. Kritische Studien über den Umfang und die Begrenzung mehrerer Cassiden-Gattungen nebst Beschreibung neuer amerikan. Arten. Archiv für Naturgeschichte,79: 126–164.

Spaeth, F. 1914. Chrysomelidae: 16. Cassidinae. In: Coleopterorum catalogus, Pars 62. (eds.) Junk, W. & Schenkling, S., Einzel-Preis, Berlin, 182 pp.

Spaeth, F. 1942. Cassidinae (Coleoptera: Chrysomelidae). In: Beiträge zur Fauna Perus nach der Ausbeute der Hamburger Süd Peru-Expedition 1936, anderer Sammlungen, wie auch auf Grund von Literaturangaben, (ed.) Titschack, E., Verlag von Gustav Fischer, Jena, 2: 11–43.

Staines, C.L. 2002. The New World tribes and genera of hispines (Coleoptera: Chrysomelidae: Cassidinae). Proceedings of the Entomological Society of Washington, 104: 721–784.

Staines, C.L. 2014. Hispines of the world. Available from http://idtools.org/id/beetles/hispines/index.php (Accessed: July 1, 2015).

Sturm, J. 1827. Coleoptera Jenae. In: Abbildungen ausländischer Insecten. (ed.) Thon, T., Caoekeaschen, Jena, 4 pp + 6 pls.

Sturm, J. 1843. Catalog der Kaefer-Sammlung. Nürnberg. Germany, 386 pp. + 17 pls.

Świętojańska, J. 2001 A revision of the tribe Aspidimorphini of the Oriental region (Coleoptera: Chrysomelidae: Cassidinae). Polskie Towarzystwo Taksonomiczen, Genus (Supplement), 318 pp. + 18 pls.

Nichols, S.W. 1989. The Torre-Bueno glossary of entomology, Revised Edition of A Glossary of Entomology by J.R. de la Torre-Bueno (1937) including Supplement A by G.S. Tulloh, (ed.) Schuh, R.T., The New York Entomological Society incorporating the Brooklyn Entomological in cooperation with the American Museum of Natural History, 1–840.

Verma, K.K. 2009. Retournement of the aedeagus in Chrysomelidae — revisited. In: Research on Chrysomelidae, Volume 2. (eds.) P. Jolivet, J. Santiago-Blay & M. Schmitt. Brill, Leiden, 105–114.

Velázquez de Castro, A.J. 1998. Morphology and taxonomy of the genus *Sitona* Germar, 1817. (I): the metendosternite (Coleoptera: Curculionidae). Atti del Museo Regionale di Scienze Naturali, Torino, 109–123.

Wessel, A. 2006. Stridulation in the Coleoptera — An overview. In: Insect sound and communication (Physiology, Behaviour, Ecology and Evolution). (eds.) Drosopoulos, S. & Claridge, M.F., Taylor & Francis Group, Boca Raton, FL, 397–404.

Woodruff, R.E. 1976. The tortoise beetles of Florida III, *Eurypepla calochroma floridensis* Blake (Coleoptera: Chrysomelidae). Entomology Circular, Florida Department of Agriculture & Consumer Service, 163: 1–2.

LIST OF FIGURES

Figs. 1–7. Dorsal habitus of the target taxa. 1. *Cistudinella foveolata* Champion, 2. *Eurypedus nigrosignatus* (Boheman), 3. *Asteriza flavicornis* (Olivier), 4. *Enagria ovata* Boheman 5. *Eurypepla calochroma* (Blake) 6. *Physonota alutacea* Boheman 7. *Platycycla deruta* Boheman.

Figs. 8–10. Phylogenetic hypotheses of tortoise beetle tribes in Borowiec (1995a). 8. Phylogeny based on Spaeth's key, 9. Phylogeny based on Hincks' key, 10. Phylogeny proposed by Borowiec.

Figs. 11–16. *Physonota alutacea* Boheman. 11–13. dorsal view (**Ed**: elytral disc, **El**: elytral lamella, **Elmm**: elytral medial margin, **Pd**: pronotal disc, **Pl**: pronotal lamella, **Umb**: umbo), 14–15. lateral view. 14. round dorsal line, 15. slightly angled dorsal line, 16. ventral view.

Figs. 17–19. Head of *Physonota alutacea* Boheman. 17. dorsal view (**Ce**: compound eye, **Sf**: stridulatory file, **Vxl**: vertex lobe), 18. frontal view (**Atsk**: antennal socket, **Cl**: clypeus, **Cs**: coronal sulcus, **Ecs**: epicranial sulcus, **ess**: epistomal sulcus, **F**: frons, **Fcl**: frontoclypeus, **Fs**: frontal sulcus, **mfl**: mid-frontal line, **Vxl**: vertex lobe), 19. ventral view (**G**: gula, **Gs**: gular sulcus, **Mf**: mouth fossa).

Figs. 20–24. Antenna and mouthparts of *Physonota alutacea* Boheman. 20. Antenna (**Pc**: pedicel; **Sp**: scape), 21–24. Mouthparts. 21. labrum, 22. madible (**hr**: horizontal ridge),

23. maxilla (**Cd**: cardo, **Ga**: galea, **La**: lacinia, **Mp**: maxillary palpus, **Pf**: palpifer, **St**: stipes), 24. labium (**Lg**: ligula, **Lp**: labial palpus, **Mt**: mentum, **Pg**: palpiger, **pMt**: prementum).

Figs. 25–27. Thoracic segements of *Physonota alutacea* Boheman. 25. Prothorax (ventral view) (**dhcl**: dorsal head cavity line, **Hc**: head cavity, **hym**: hypomeron, **hyml**: hypomeral lobe, **PrS**: prosternum, **PrSc**: prosternal collar, **PrSp**: prosternal process), 26. mesonotum (**antMsp**: anterior mesonotal process, **axlc**: axillary cord, **lgMsths**: longitudinal mesothoracic sulcus, **Msstl**: mesoscutellum, **Mssut**: mesoscutum, **ptelp**: postnatal elytral process), 27. metanotum (**arr**: alar ridge, **Mtnpc**: metanotal postnatal cleft, **Mtstl**: metascutellum, **Mtsut**: metascutum, **psut**: prescutum, **stlg**: scutellar groove).

Figs. 28–29. Thoracic segements of *Physonota alutacea* Boheman. 28. Meso-, metaventrite complex (**anp**: angular projection, **dicm**: discrimen, **Msem**: mesempimeron, **Msest**: mesoepisternum, **Msestr**: mesoepisternal ridge, **MsV**: mesoventrite, **Mtest**: metepisternum, **Mtem**: metepimerom, **MtV**: metaventrite), 29. Metendosternite (**anttd**: anterior tendon, **arm**: arm, **hmdt**: hemiductus, **lonfl**: longitudinal flange, **sht**: sheath, **stl**: stalk).

Figs. 30–33. Thoracic appendages of *Physonota alutacea* Boheman. 30. hingwing (**A1**: 1st anal vein, **A2**: 2nd anal vein, **A3**: 3rd anal vein, **A4**: 4th anal vein, **a1-a2**: 1st-2nd anal cross vein, **ac**: anal cell, **af**: anal fold, **C**: costa, **Cu**: cubitus, **Cu1**: 1st cubital vein, **de**: distal edge of radial cell, **M2**: 2nd meidan vein, **mst**: medial stripe, **pe**: proximal edge of radial

cell, **pst**: postradial stripe, **R**: radius, **rc**: radial cell, **rm**: radiomeida vein, **rf**: radial fold, **Rr**: radial recurrent vein, **sC**: subcostal). 31. Elytron (ventral view) (**br**: brace, **epr**: epipleural ridge, **logc**: longitudinal carina). 32. (hind) leg (**cx**: coxa, **trct**: trochanter, **fm**: femur, **tb**: tibia). 33. (hind leg) tarsus and pretarsus (**tsm**: tarsomere, **prtscle**: pretarsal claw).

Figs. 34–35. Genitalia of *Physonota alutacea* Boheman. 34. aedeagus (**pd**: phallobase, **ejad**: ejaculatory duct, **ml**: median lobe, **mnb**: manubrium, **gasp**: gastral spiculum, **smv**: seminal vesicle, **tgm**: tegmen), 35. spermatheca (**amp**: ampulla, **dtgd**: ductus glandula opening, **sptd**: spermathecal duct, **vscl**: vasculum).

Figs. 36–37. Graphs representing the distribution of the stridulatory file ridge number in target taxa. 36. File ridge numbers by genus, 37. Graph by number of species based on ridge number.

Fig. 38. Phylogenetic hypothesis based on a strict consensus tree resulted from parsimony analysis with dorsal habitus of selected taxa: illustrated species are indicated by # next to the species name; the order of the dorsal habitus images are up to bottom and left to right; the numbers in the grey circles indicate the clade number; the boxes with the solid colors indicate the monophyletic tribes; the boxes with the dotted lines indicate non-monophyletic tribes; for the species of non-monophyletic tribe are indicated by the initial of the tribal name next to the species names.

Fig. 39. Strict consensus tree of four most parsimonious trees conducted in this study with the character number, character states and support values: only unambiguous characters are marked on the tree; the numbers in the grey circles indicate the clade number; each character number is located above the circle and each character state is located below the circle; the white circles indicates homoplastic synapomorphies and the black circle indicates non-homoplastic synapomorphies; support values (Bootstrap, Jackknife, Bremer Support) are located under each node in red; the monophyletic groups are boxed by the solid color and the non-monophyletic groups are boxed by the dotted lines.

Figs. 40–41. Strict consensus tree with the character state transitions on the branches and taxa names. 40. Character #74 (shape of anterior line of pronotum): green (state 0); blue (state 1); black (state 2), 41. Character#146 (shape of gastral spiculum): green (state 0); blue (state 1); black (state 2); brown (state 3); pink (missing data or ambiguous state).

Figs. 42–49. SEM images of the heads. 42. *Cistudinella foveolata*, 43. *Eurypedus nigrosignatus* (male with stridulatory file), 44. *Eurypedus nigrosignatus* (female without stridulatory file), 45. *Asteriza flavicornis*, 46. *Enagria ovata*, 47. *Eurypepla calochroma*, 48. *Physonota alutacea*, 49. *Platycycla deruta*.

Figs. 50–57. SEM images of the stridulatory files. 50. *Cistudinella foveolata*, 51. *Eurypedus nigrosignatus* (male with stridulatory file), 52. *Eurypedus nigrosignatus* (female without stridulatory file), 53. *Asteriza flavicornis*, 54. *Enagria ovata*, 55. *Eurypepla calochroma*, 56. *Physonota alutacea*, 57. *Platycycla deruta*: arrows indicate the microtrichial patches.

Figs. 58–59. Strict consensus tree with the character state transitions on the branches and taxa names. 58. Character #27 (stridulatory file): green (state 0); blue (state 1); pink (missing data or ambiguous state), 59. Character#29 (broadest region of stridulatory file): green (state 0); blue (state 1); black (state 2); pink (missing data or ambiguous state).

Figs. 60–61. Strict consensus tree with the character state transitions on the branches and taxa names. 60. Character #34 (number of striae): green (state 0); blue (state 1); black (state 2); red (state 3); pink (missing data, non-applicable data or ambiguous state), 61. Character#83 (Shape of dorsal head cavity line on ventral surface of pronotum = plectrum): green (state 0); blue (state 1).

Figs. 62–63.Ventral view of the prothorax. 62. *Physonota alutacea*, 63. *Eurypedus nigrosignatus* (arrow indicates plectrum (dorsal head cavity line)). 64–65. Sagittal section of head with pronotum (stained by hematoxylin with counterstained by eosin). 64. *Physonota alutacea*, 65. *Eurypedus nigrosignatus* (arrow indicates plectrum (dorsal head cavity line)).

Fig. 66. Clade #7 (Asterizini) with distributional mapping: the previous generic names (*Physonota* and *Enagria*) are used. The regions in the map was mainly determined by Morrone (2001), and modified based on the distribution of each species in this study.

Fig. 67. Clade #11 with distributional mapping for clade #13 (Ischyrosonychini). The regions in the map was mainly determined by Morrone (2001), and modified based on the distribution of each species in this study.


1
2
3
4
5
6
7

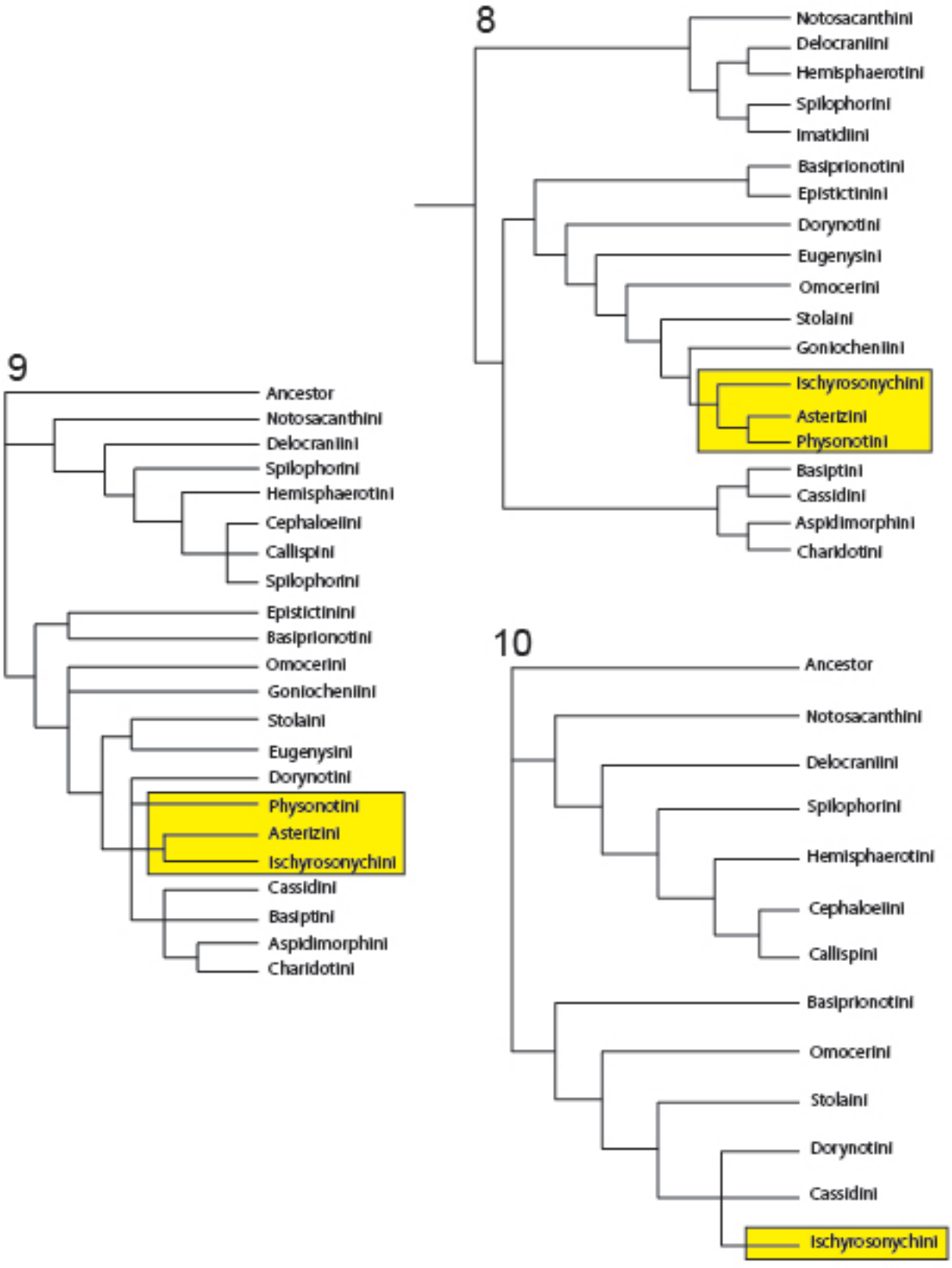
8
Notosacanthini
Delocraniini
Hemisphaerotini
Spilophorini
Imatidiini
Basiprionotini
Epistictinini
Dorynotini
Eugenysini
Omocerini
Stolaini
Goniochenilini
Ischyrosonychini
Asteriziini
Physonotini
Basiptini
Cassidini
Aspidimorphini
Charidotini
9
Ancestor
Notosacanthini
Delocraniini
Spilophorini
Hemisphaerotini
Cephaloeiini
Callispini
Spilophorini
Epistictinini
Basiprionotini
Omocerini
Goniochenilini
Stolaini
Eugenysini
Dorynotini
Physonotini
Asteriziini
Ischyrosonychini
Cassidini
Basiptini
Aspidimorphini
Charidotini
10
Ancestor
Notosacanthini
Delocraniini
Spilophorini
Hemisphaerotini
Cephaloeiini
Callispini
Basiprionotini
Omocerini
Stolaini
Dorynotini
Cassidini
Ischyrosonychini

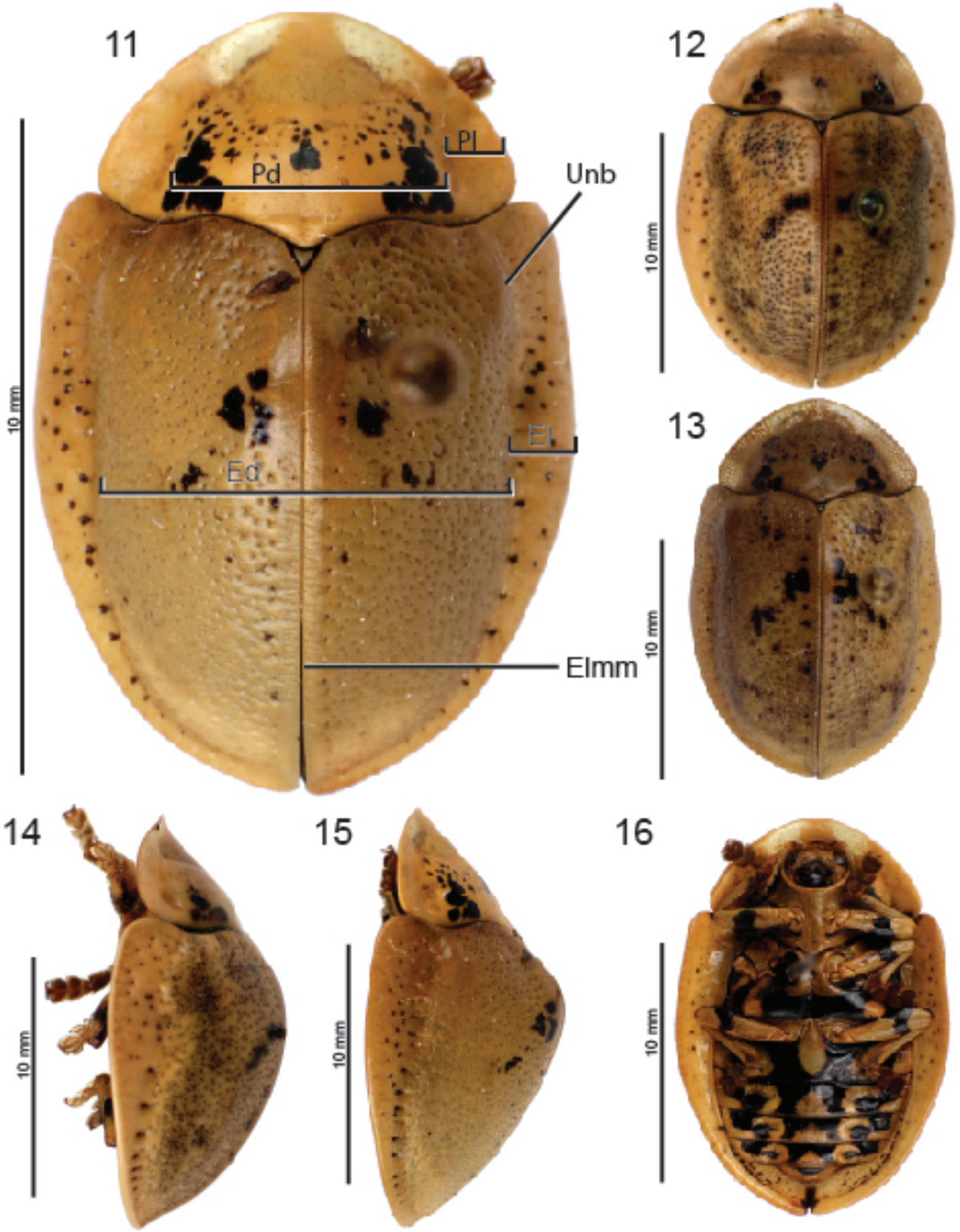
11
Pl
Pd
Unb
El
Ed
Elmm
10 mm
12
10 mm
13
10 mm
14
10 mm
15
10 mm
16
10 mm

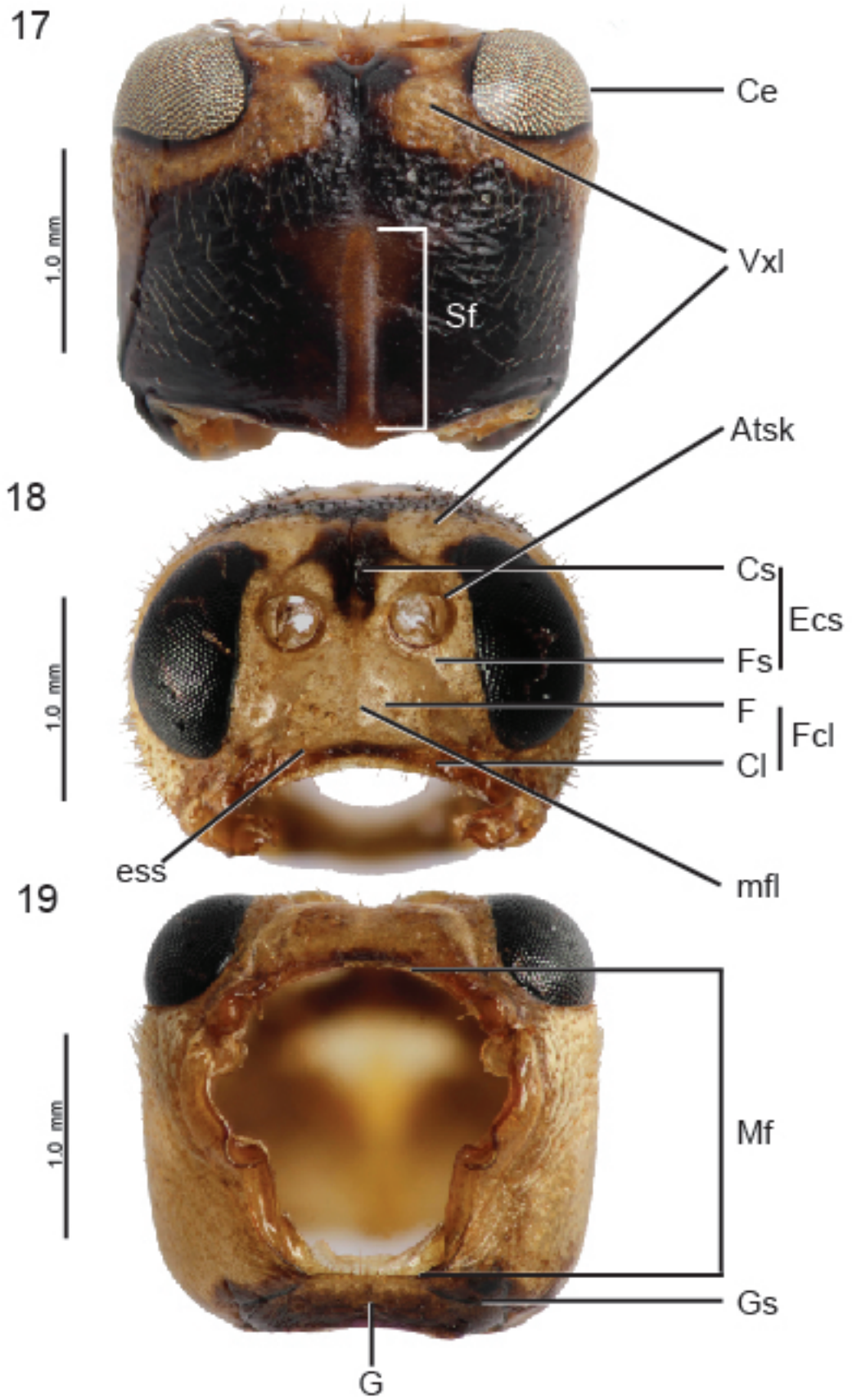
17
1.0 mm
Ce
Vxl
Sf
Atsk
18
1.0 mm
Cs
Ecs
Fs
F
Fcl
Cl
ess
mfl
19
1.0 mm
Mf
Gs
G

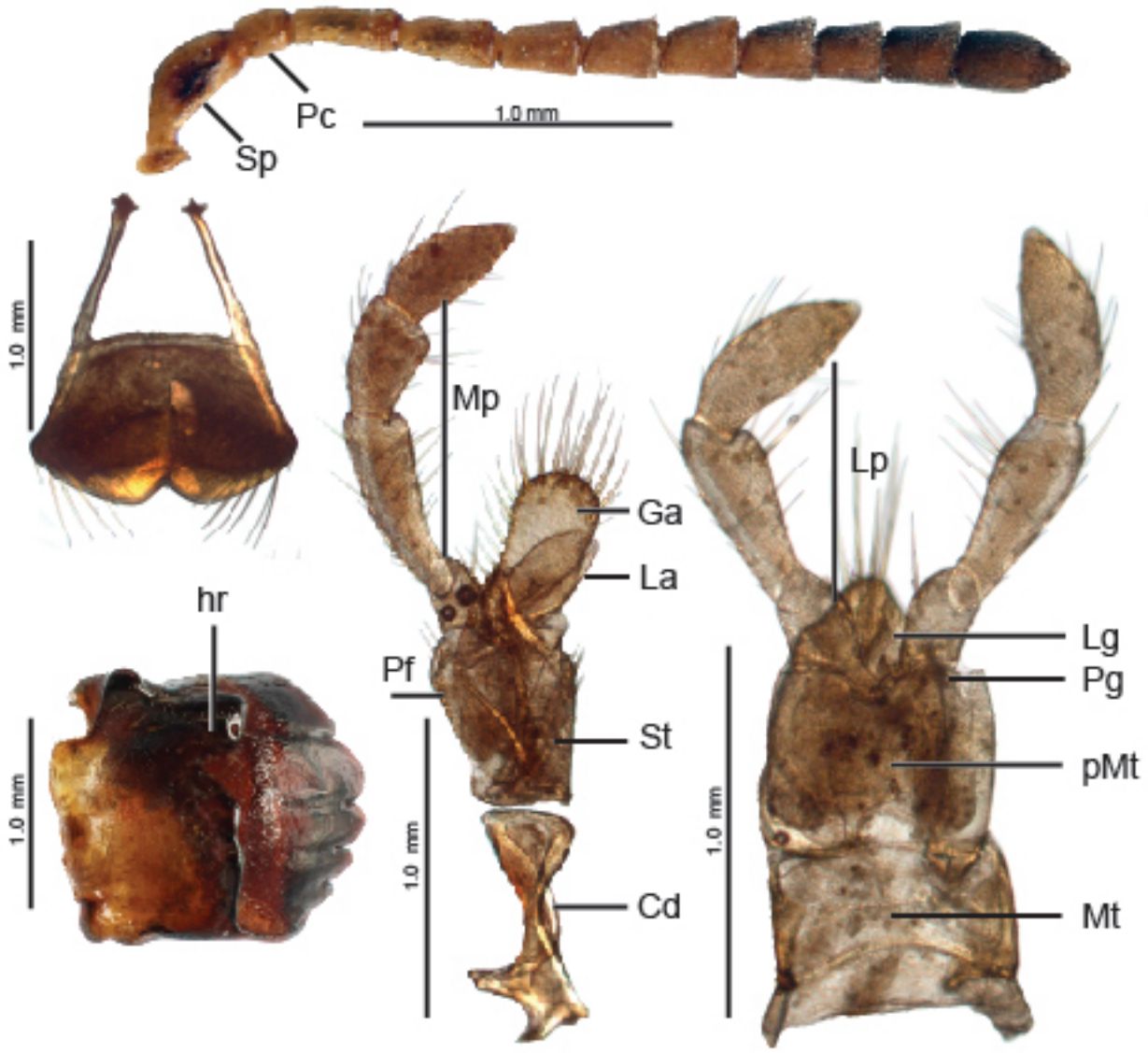
Pc
Sp
1.0 mm
1.0 mm
Mp
Ga
La
Pf
St
Cd
1.0 mm
hr
1.0 mm
Lp
Lg
Pg
pMt
Mt
1.0 mm

25

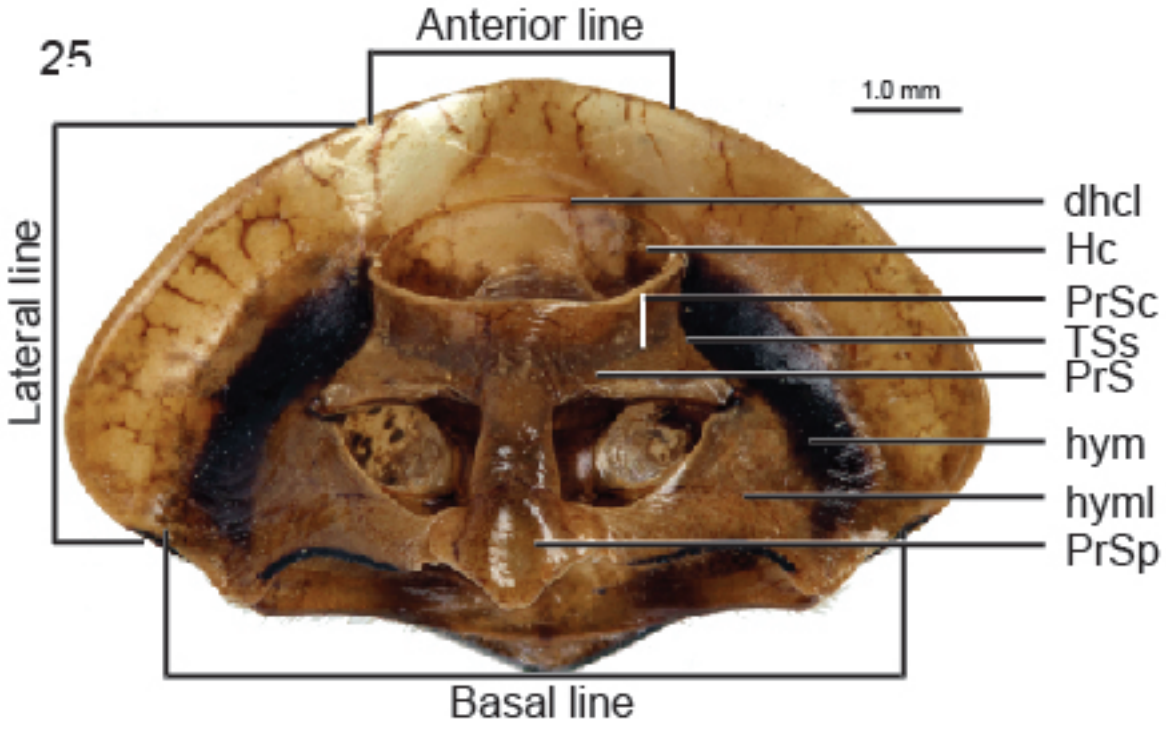
Anterior line
1.0 mm
Lateral line
dhcl
Hc
PrSc
TSs
PrS
hym
hyml
PrSp
Basal line

26

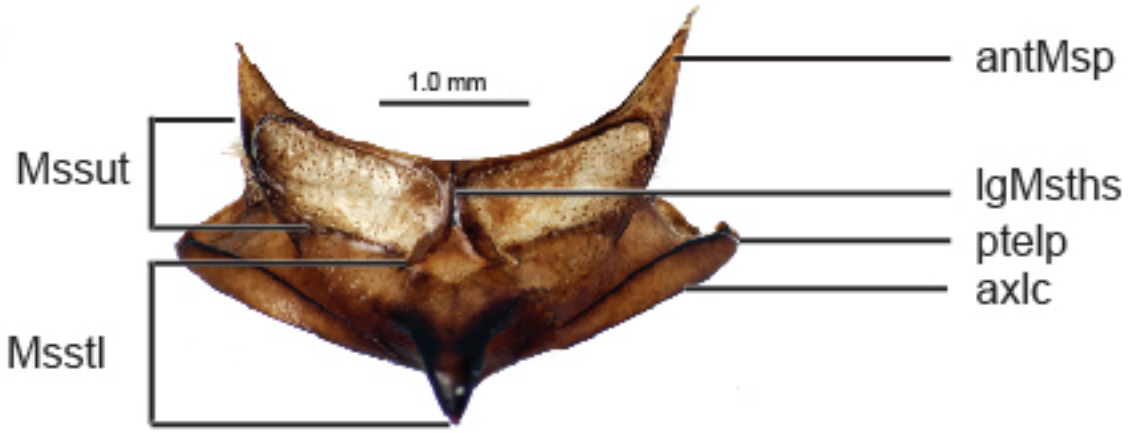
1.0 mm
Mssut
Msstl
antMsp
lgMsths
ptelp
axlc

27

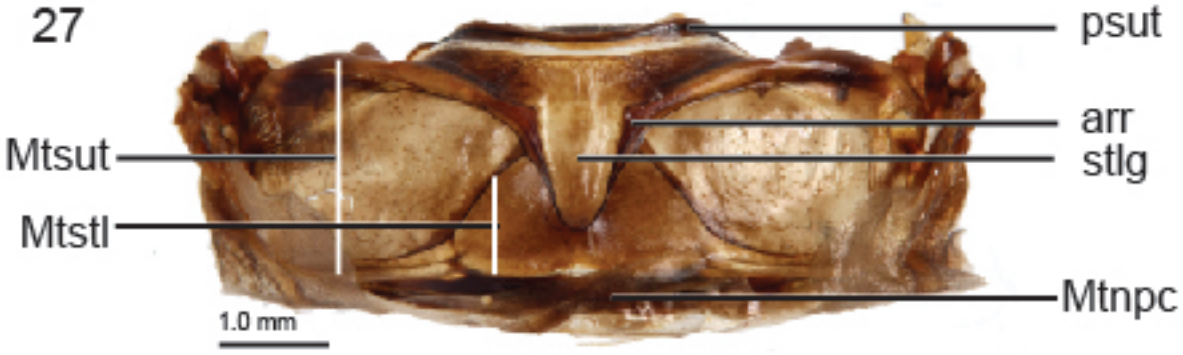
psut
arr
stlg
Mtsut
Mtstl
Mtnpc
1.0 mm

28

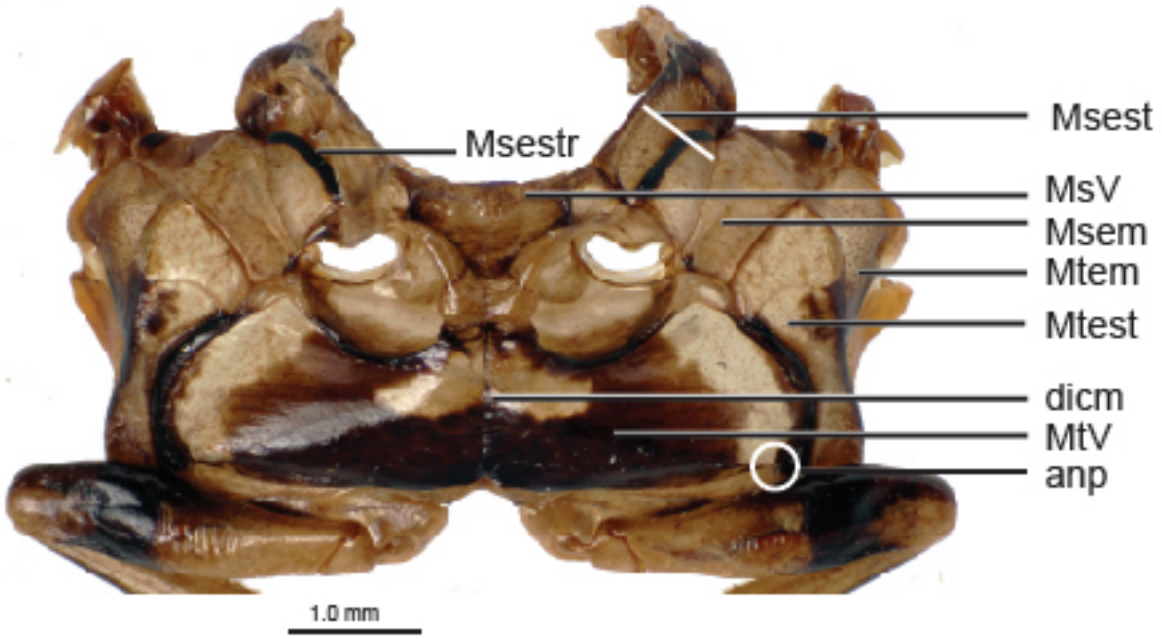
Msestr
Msest
MsV
Msem
Mtem
Mtest
dicm
MtV
anp
1.0 mm

29

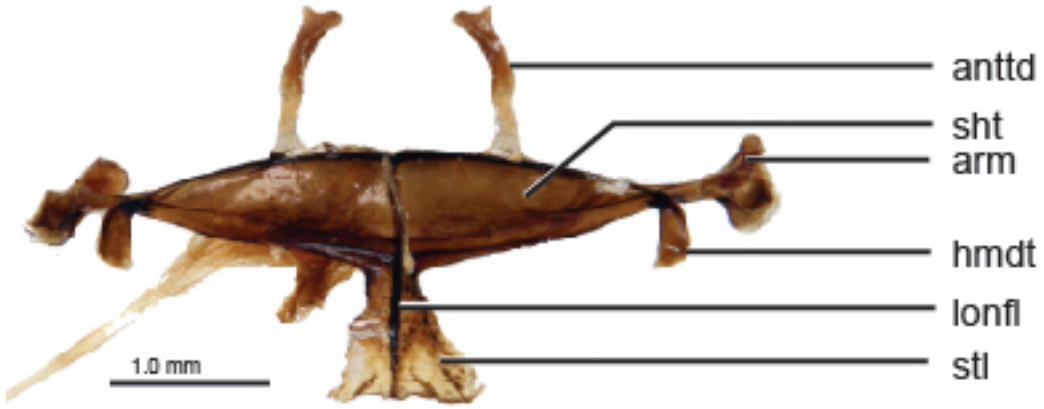
anttd
sht
arm
hmdt
lonfl
stl
1.0 mm

30

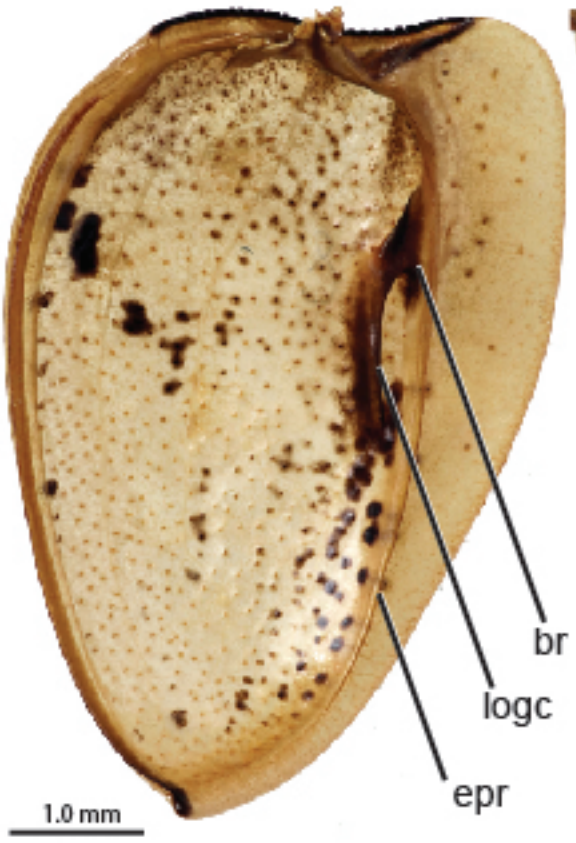
br
logc
epr
1.0 mm

32


cx
trct
fm
1.0 mm
tb

33

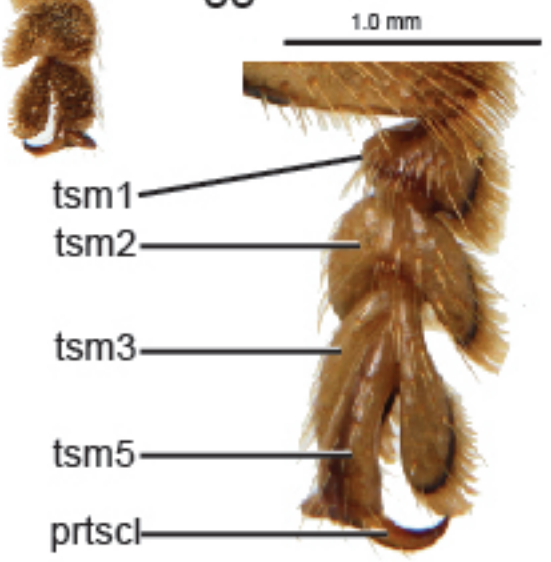
1.0 mm
tsm1
tsm2
tsm3
tsm5
prtscl

31

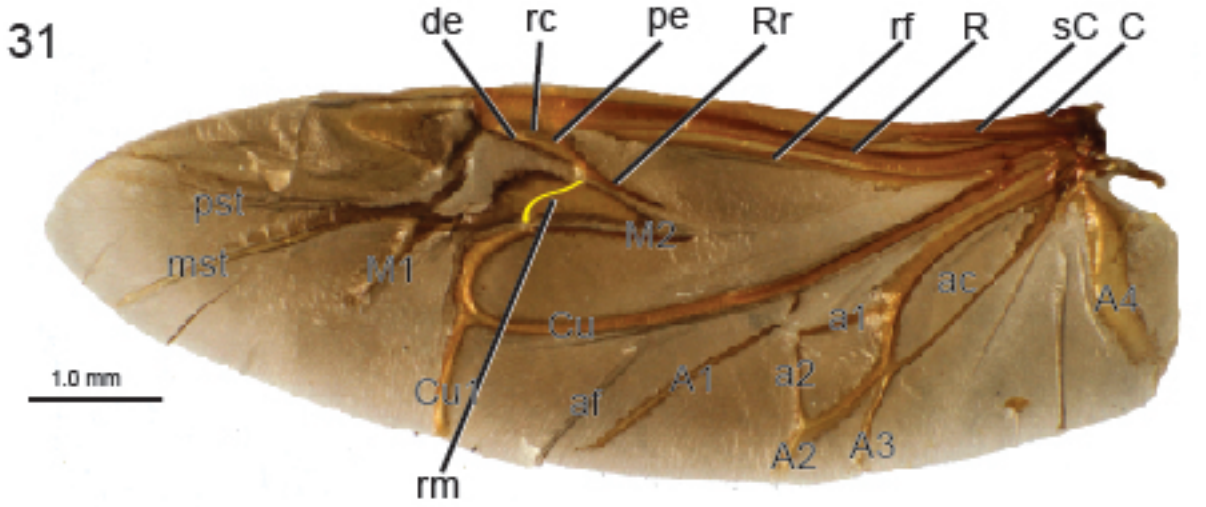
de
rc
pe
Rr
rf
R
sC
C
pst
mst
M1
M2
Cu
Cu1
a1
A1
a2
ac
A4
A2
A3
rm
1.0 mm

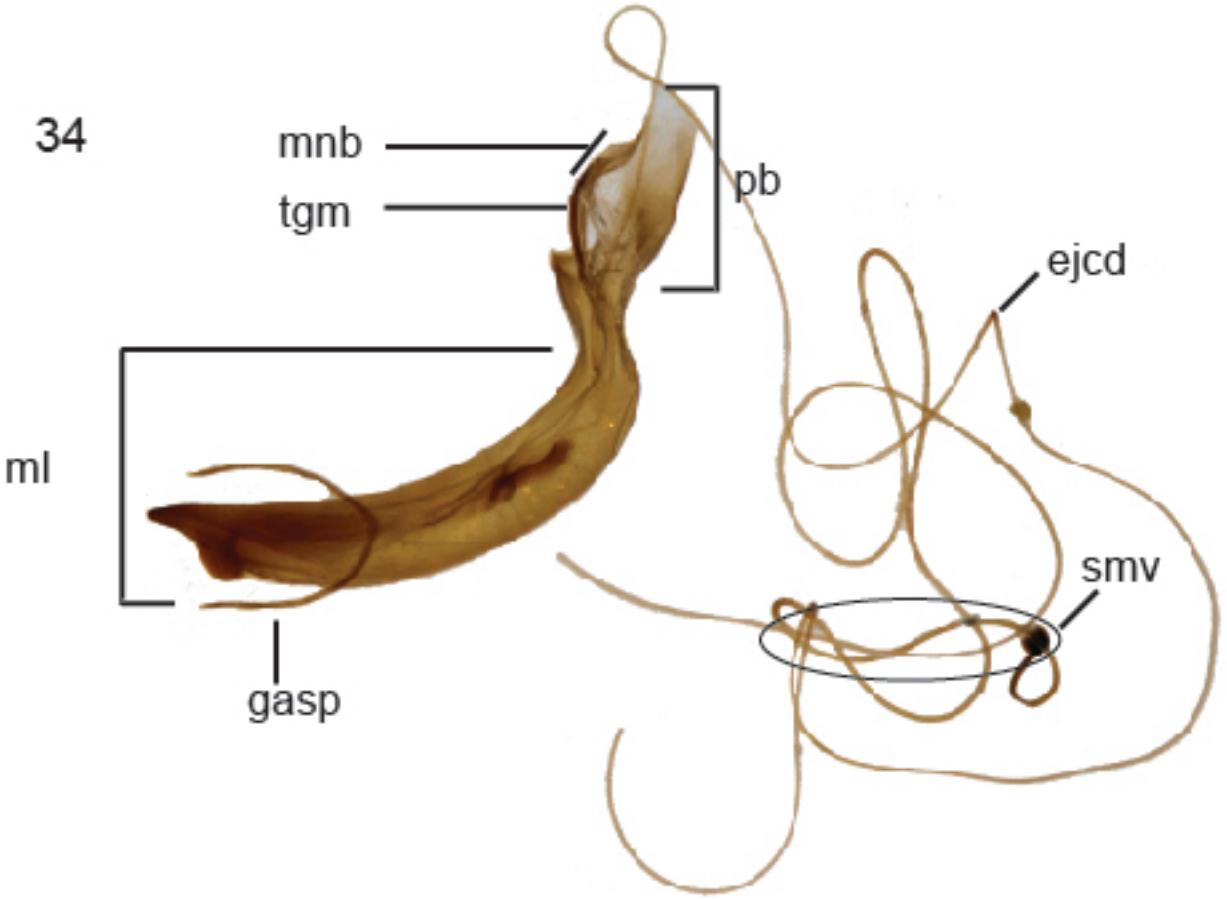
34
mnb
tgm
pb
ejcd
ml
smv
gasp

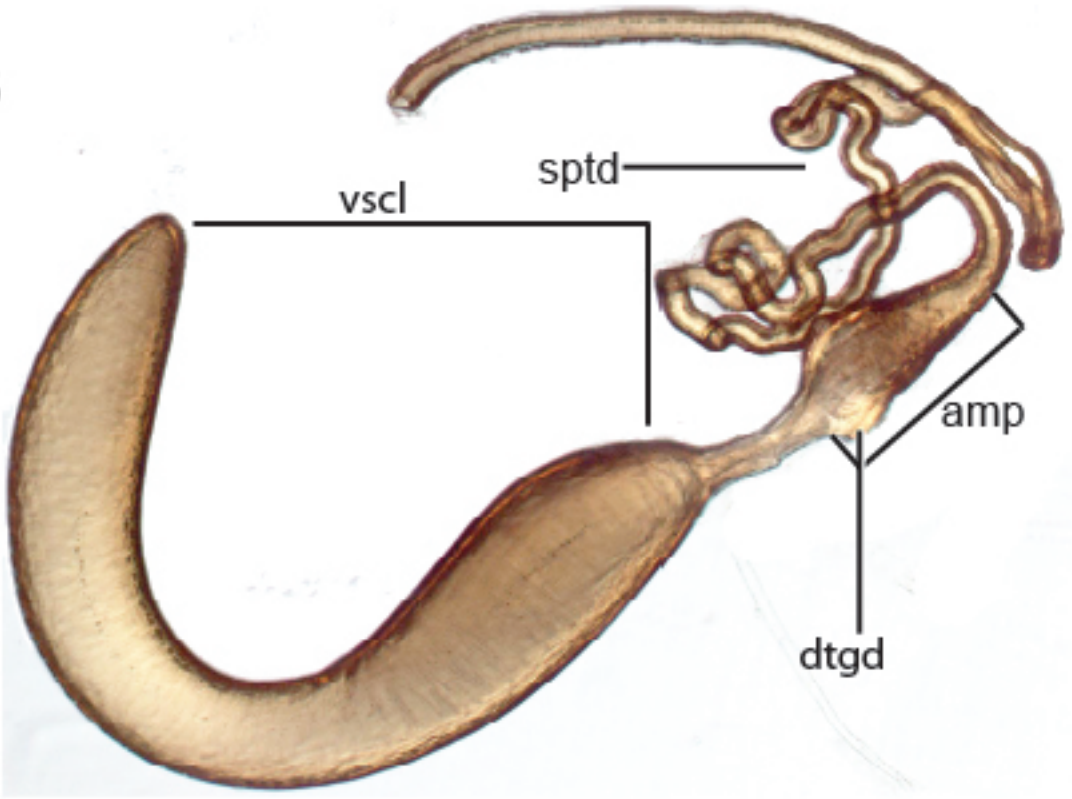
35
sptd
vscl
amp
dtgd

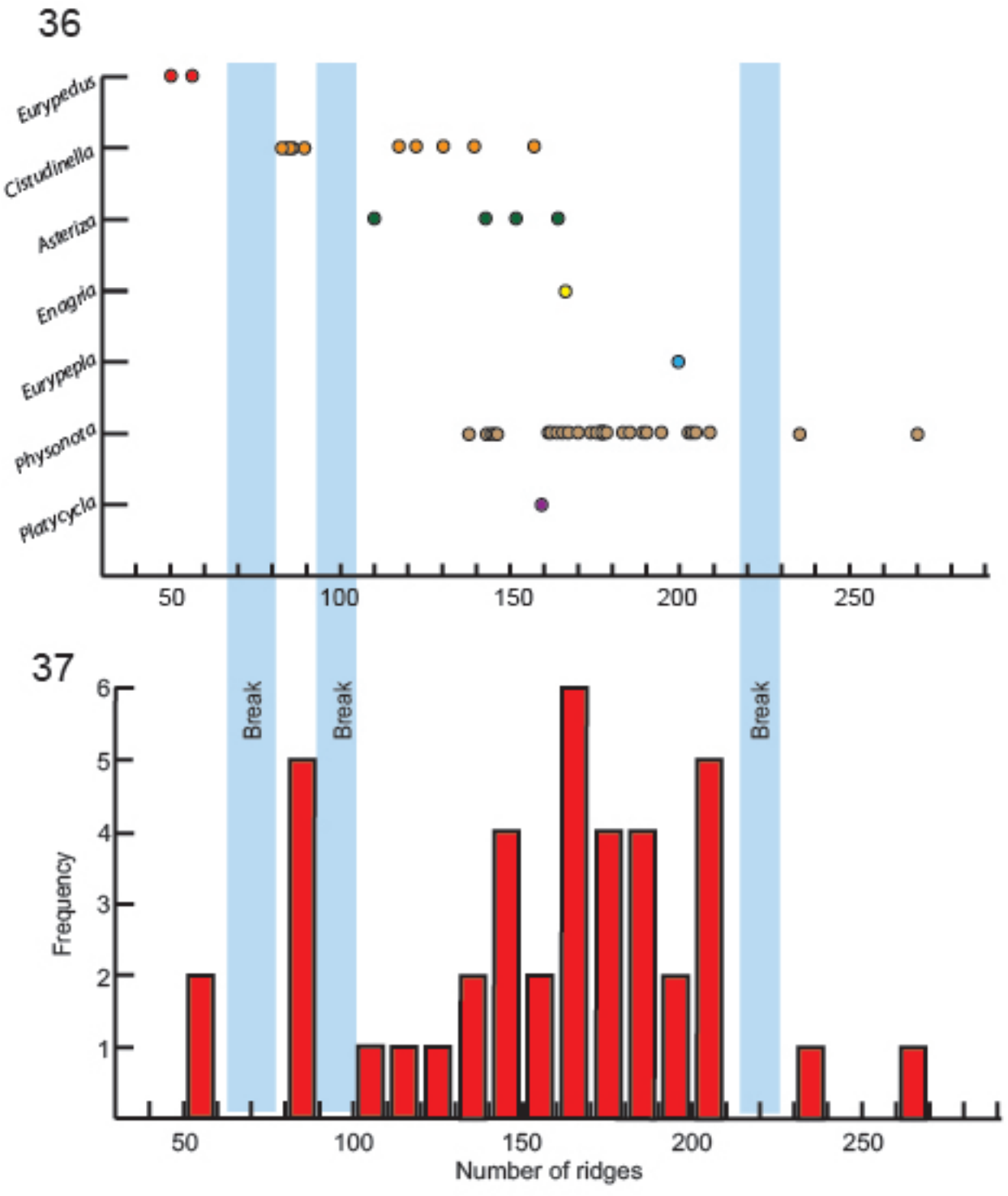
36
Eurypedus
Cistudinella
Asteriza
Enagria
Eurypepla
physonota
Platycycla
50
100
150
200
250
37
Break
Break
Break
Frequency
1
2
3
4
5
6
50
100
150
200
250
Number of ridges

38

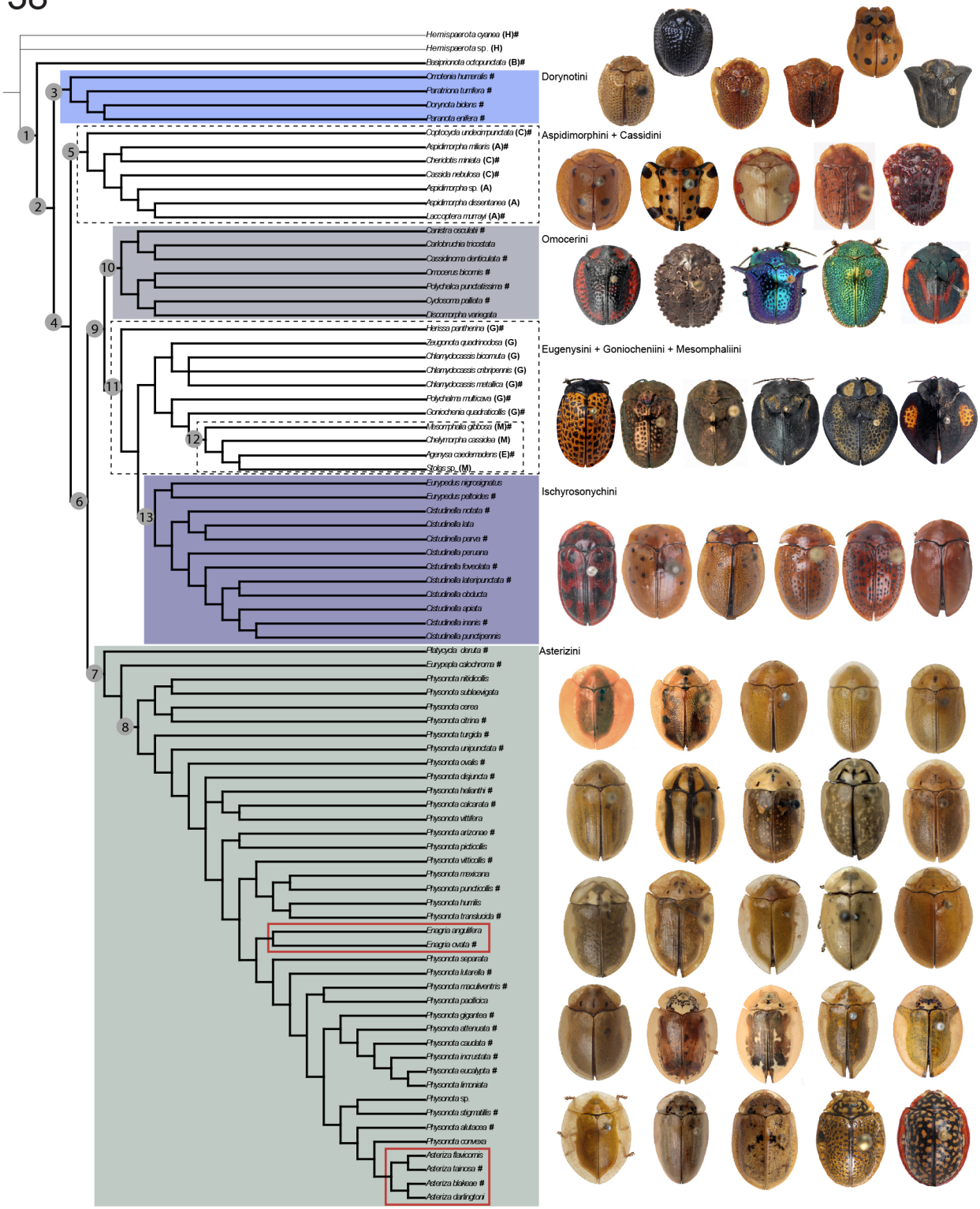
Hemispaerota cyanea (H)#
Hemispaerota sp. (H)
Basiprionota octopunctata (B)#
Omfalenia humeralis #
Paratriona tumifera #
Dorynota bidens #
Peranomota emfera #
Dorynotini
Coptocycla undecimpunctata (C)#
Aspidimorpha miliaris (A)#
Chendotis miniata (C)#
Cassida nebulosa (C)#
Aspidimorpha sp. (A)
Aspidimorpha dissentanea (A)
Laccoptera murrayi (A)#
Aspidimorphini + Cassidini
Canistra osculati #
Carlobruchia tricostata
Cassidinorma denticulata #
Omocerus bicornis #
Polychalca punctatissima #
Cyclosoma pallata #
Discomorpha variegata
Omocerini
Herissa penthremia (G)#
Zeugonota quadrinodosa (G)
Chlamydocassis bicornuta (G)
Chlamydocassis cribripennis (G)
Chlamydocassis metallica (G)#
Polychalma multicava (G)#
Goniocheria quadraticollis (G)#
Mesomphalia globosa (M)#
Chelymorpha cassidea (M)
Agenysa caedemadens (E)#
Stolas sp. (M)
Eugenysini + Goniocheniini + Mesomphaliini
Eurypedus nigrosignatus
Eurypedus pallicides #
Ostodinella notata #
Ostodinella lata
Ostodinella parva #
Ostodinella peruana
Ostodinella foveolata #
Ostodinella latenpunctata #
Ostodinella obducta
Ostodinella apicata
Ostodinella inanis #
Ostodinella punctipennis
Ischyrosonychini
Platycycla deruta #
Eurypepla calochroma #
Physonota nitidicollis
Physonota subleavigata
Physonota corea
Physonota citrina #
Physonota turgida #
Physonota unipunctata #
Physonota ovalis #
Physonota disjuncta #
Physonota helianthi #
Physonota calcarata #
Physonota vittifera
Physonota arizonae #
Physonota pedicollis
Physonota vitticollis #
Physonota mexicana
Physonota punctipollis #
Physonota humilis
Physonota translucida #
Emagria angulifera
Emagria ovata #
Physonota separata
Physonota lutarella #
Physonota maculiventris #
Physonota pacifica
Physonota gigantea #
Physonota attenuata #
Physonota caudata #
Physonota incrustata #
Physonota eucalypta #
Physonota limoniata
Physonota sp.
Physonota stigmatilis #
Physonota alutacea #
Physonota convexa
Asteriza flavicornis
Asteriza fainosa #
Asteriza blakeae #
Asteriza darlingtoni
Asterizini

39

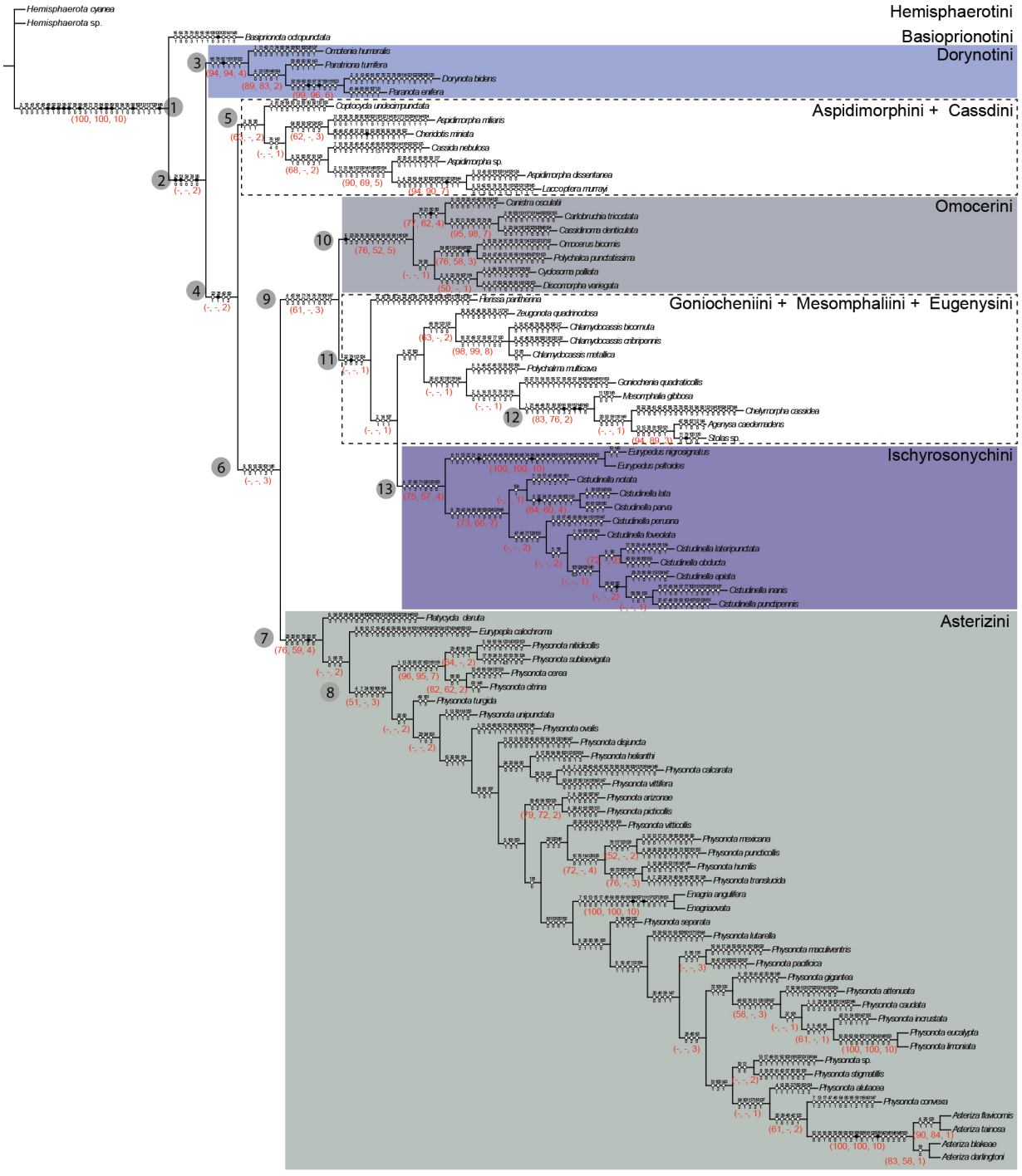
Hemisphaerotini
Basioprionotini
Dorynotini
Aspidimorphini + Cassdini
Omocerini
Goniocheniini + Mesomphaliini + Eugenysini
Ischyrosonychini
Asterizini
Hemisphaerota cyanea
Hemisphaerota sp.
Basiprionota octopunctata
Ornotenia humeralis
Paratriona turnifera
Dorynota bidens
Paranota enifera
Coptocycla undecimpunctata
Aspidimorpha miliaris
Cheridotis miniata
Cassida nebulosa
Aspidimorpha sp.
Aspidimorpha dissentanea
Laccoptera murrayi
Canistra osculati
Carlobruchia tricostata
Cassidinorma denticulata
Omocerus bicornis
Polychalca punctatissima
Cyclosoma pallata
Discomorpha variegata
Florissa panthenina
Zeugomota quadrimodosa
Chlamydocassis bicornuta
Chlamydocassis cribripennis
Chlamydocassis metallica
Polychalma multicava
Goniochenia quadraticollis
Mesomphala gibbosa
Chelymorpha cassidea
Agenysa caedemadens
Stolas sp.
Eurypedus nigrosignatus
Eurypedus peltoides
Cistudinella notata
Cistudinella lata
Cistudinella parva
Cistudinella peruana
Cistudinella foveolata
Cistudinella lateripunctata
Cistudinella obducta
Cistudinella apicata
Cistudinella inanis
Cistudinella punctipennis
Platycycla deruta
Eurypepla calochroma
Physonota nitidicollis
Physonota subleavigata
Physonota cerea
Physonota atrima
Physonota turgida
Physonota unipunctata
Physonota ovalis
Physonota disjuncta
Physonota helianthi
Physonota calcarata
Physonota vittifera
Physonota arizonae
Physonota picticollis
Physonota viticollis
Physonota mexicana
Physonota punctiicollis
Physonota humilis
Physonota translucida
Enagria angulifera
Enagrioovata
Physonota separata
Physonota lutarella
Physonota maculiventris
Physonota pacifica
Physonota gigantea
Physonota attenuata
Physonota caudata
Physonota incrustata
Physonota eucalypta
Physonota limoniata
Physonota sp.
Physonota stigmatilis
Physonota alutacea
Physonota convexa
Asteriza flavicornis
Asteriza tarinosa
Asteriza blakeae
Asteriza darlingtoni

40

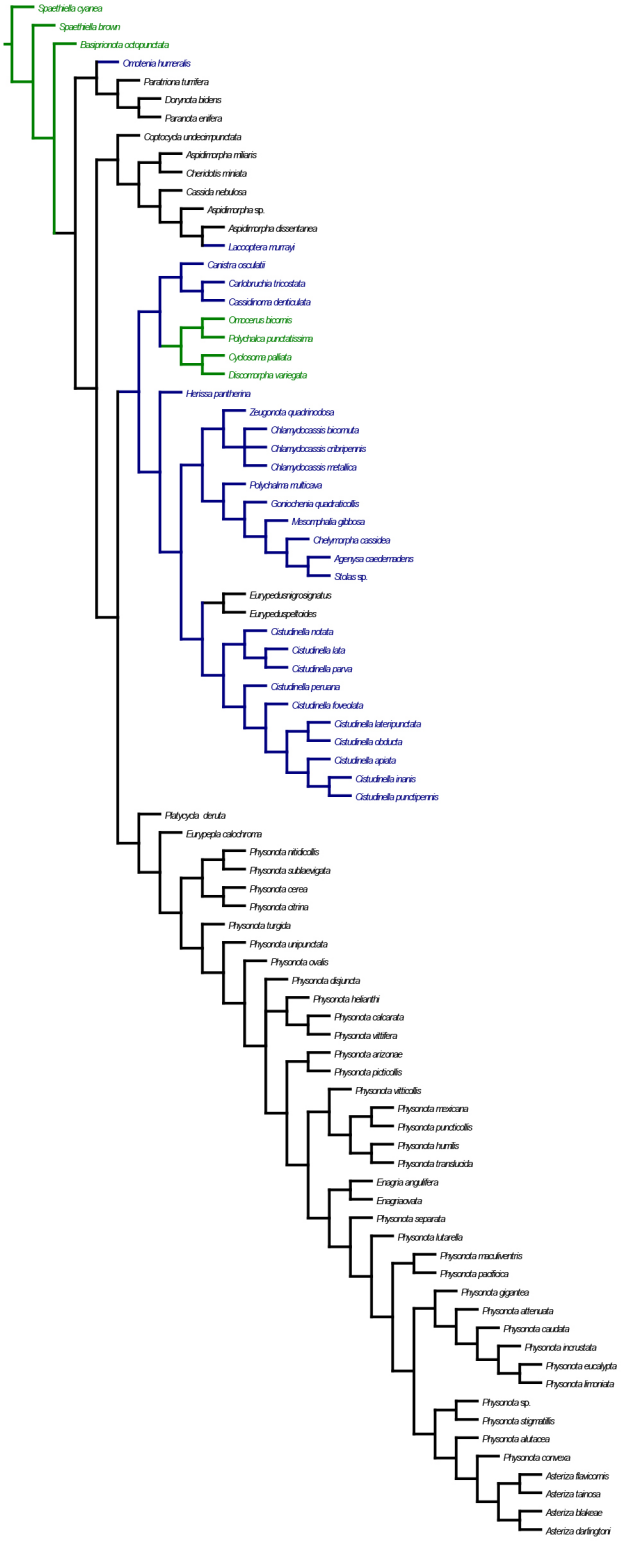
Spaethiella cyanea
Spaethiella brown
Basprionota octopunctata
Omotenia humerals
Paratriona turrifera
Dorynota bidens
Paranota enifera
Coptocycla undecimpunctata
Aspidimorpha miliaris
Cheridotis minuta
Cassida nebulosa
Aspidimorpha sp.
Aspidimorpha dissentanea
Laccoptera murrayi
Canistra oculati
Carlobruchia tricostata
Cassidinoma denticulata
Omocerus bicornis
Polychalca punctatissima
Cyclosoma pallida
Discomorpha variegata
Heressa panthenina
Zeugonota quadrinodosa
Chlamydocassis bicornuta
Chlamydocassis cribripennis
Chlamydocassis metallica
Polychalma multicava
Goniochenia quadraticollis
Mesomphalia gibbosa
Chelymorpha cassidea
Agenysa caedemaculens
Stolas sp.
Eurypedus nigrosignatus
Eurypedus peltoides
Cistudinella notata
Cistudinella lata
Cistudinella parva
Cistudinella peruana
Cistudinella foveolata
Cistudinella lateripunctata
Cistudinella obducta
Cistudinella apicata
Cistudinella inanis
Cistudinella punctipennis
Platycycla deruta
Eurypepla calochroma
Physonota nitidicollis
Physonota sublaevigata
Physonota cerea
Physonota atrima
Physonota turgida
Physonota unipunctata
Physonota ovalis
Physonota disjuncta
Physonota helianthi
Physonota calcarata
Physonota vittifera
Physonota arizonae
Physonota picticollis
Physonota viticollis
Physonota mexicana
Physonota punctacollis
Physonota humilis
Physonota translucida
Enagria angulifera
Enagria ovata
Physonota separata
Physonota lutarella
Physonota maculiventris
Physonota pacifica
Physonota gigantea
Physonota attenuata
Physonota caudata
Physonota incrustata
Physonota eucalypta
Physonota limoniata
Physonota sp.
Physonota stigmatilis
Physonota alutacea
Physonota convexa
Asteriza flavicornis
Asteriza tainosa
Asteriza blakeae
Asteriza darlingtoni

41

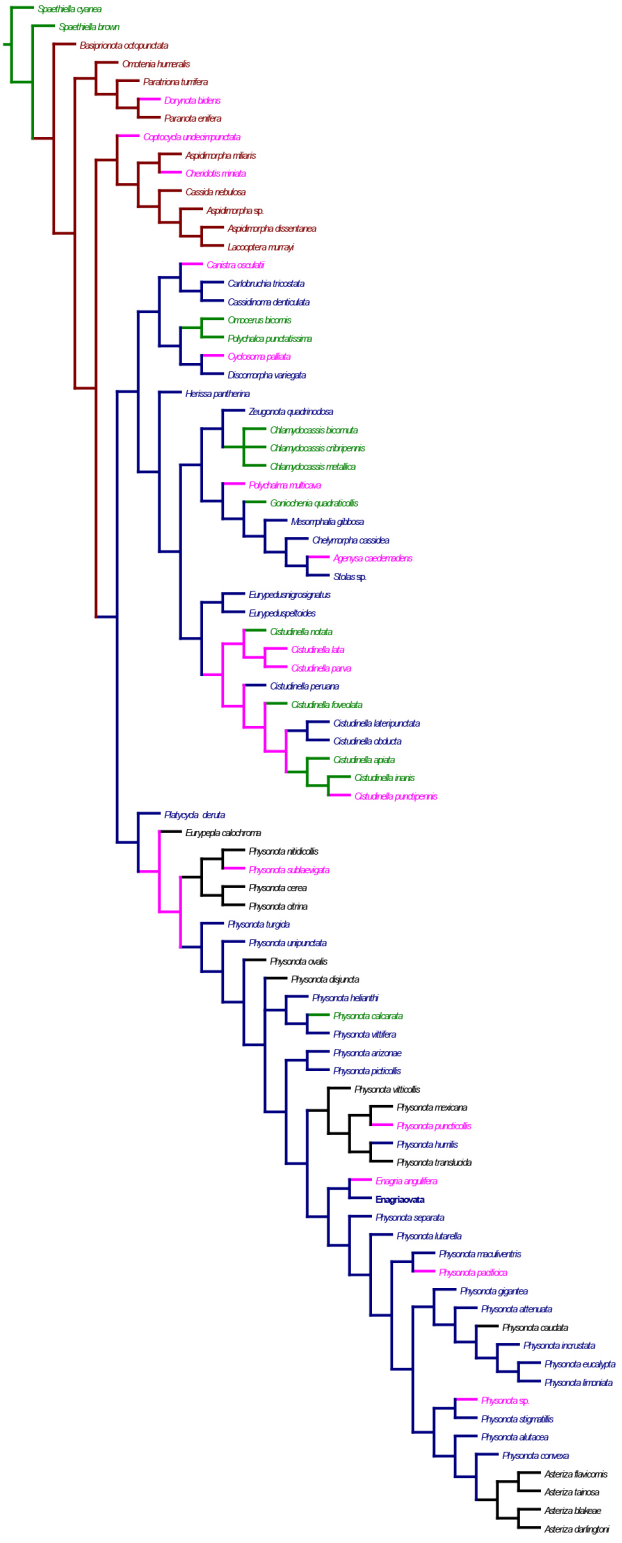
Spaethiella cyanea
Spaethiella brown
Basprionota octopunctata
Omotenia humerals
Paratriona turrifera
Dorynota bidens
Paranota enifera
Coptocycla undecimpunctata
Aspidimorpha miliaris
Cheridotis minuta
Cassida nebulosa
Aspidimorpha sp.
Aspidimorpha dissentanea
Laccoptera murrayi
Canistra oculati
Carlobruchia tricostata
Cassidinoma denticulata
Omocerus bicornis
Polychalca punctatissima
Cyclosoma pallida
Discomorpha variegata
Heressa panthenina
Zeugonota quadrinodosa
Chlamydocassis bicornuta
Chlamydocassis cribripennis
Chlamydocassis metallica
Polychalma multicava
Goniochenia quadraticollis
Mesomphalia gibbosa
Chelymorpha cassidea
Agenysa caedemaculens
Stolas sp.
Eurypedus nigrosignatus
Eurypedus peltoides
Cistudinella notata
Cistudinella lata
Cistudinella parva
Cistudinella peruana
Cistudinella foveolata
Cistudinella lateripunctata
Cistudinella obducta
Cistudinella apicata
Cistudinella inanis
Cistudinella punctipennis
Platycycla deruta
Eurypepla calochroma
Physonota nitidicollis
Physonota sublaevigata
Physonota cerea
Physonota atrima
Physonota turgida
Physonota unipunctata
Physonota ovalis
Physonota disjuncta
Physonota helianthi
Physonota calcarata
Physonota vittifera
Physonota arizonae
Physonota picticollis
Physonota viticollis
Physonota mexicana
Physonota punctacollis
Physonota humilis
Physonota translucida
Enagria angulifera
Enagria ovata
Physonota separata
Physonota lutarella
Physonota maculiventris
Physonota pacifica
Physonota gigantea
Physonota attenuata
Physonota caudata
Physonota incrustata
Physonota eucalypta
Physonota limoniata
Physonota sp.
Physonota stigmatilis
Physonota alutacea
Physonota convexa
Asteriza flavicornis
Asteriza tainosa
Asteriza blakeae
Asteriza darlingtoni

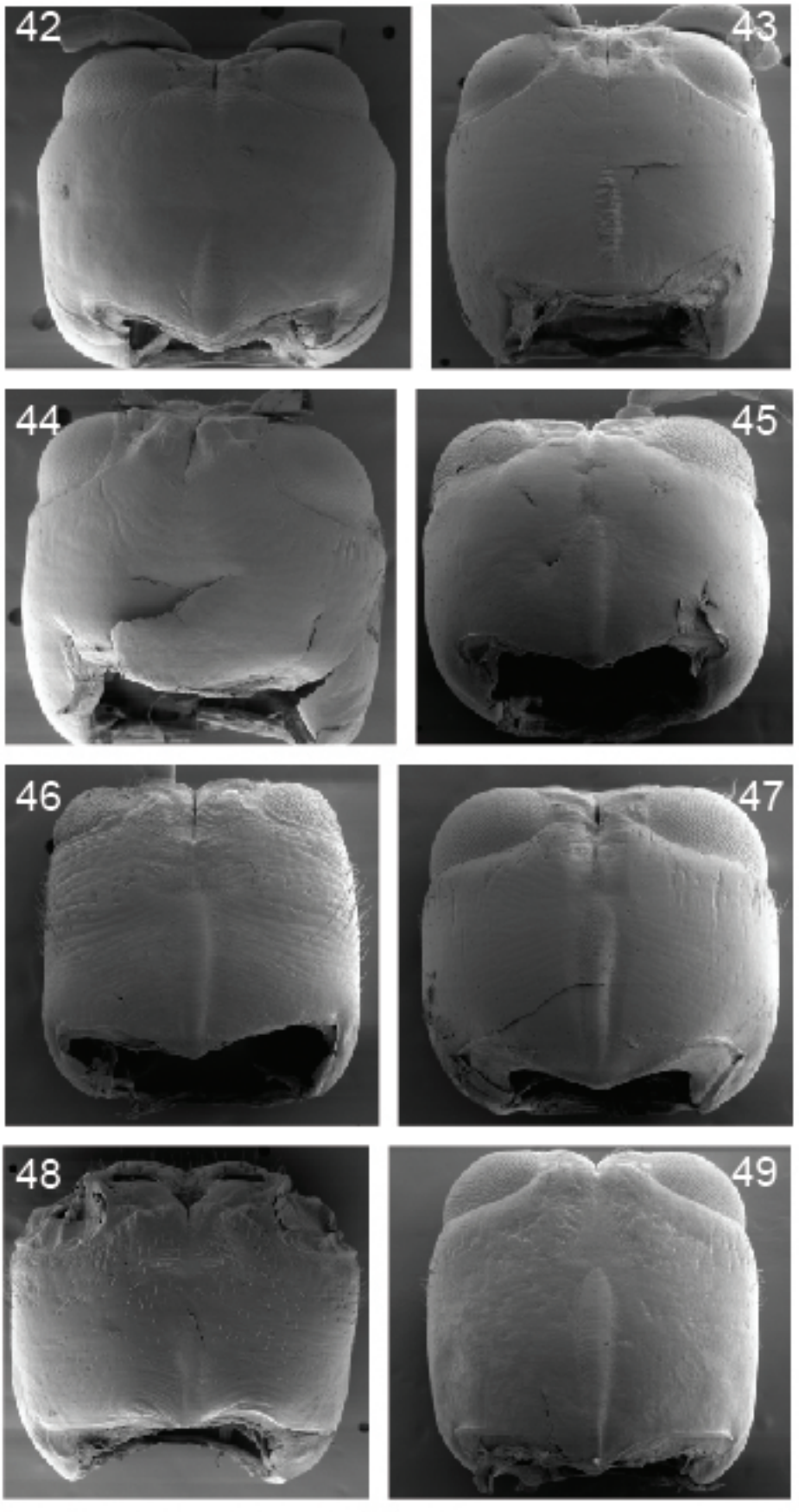
42
43
44
45
46
47
48
49

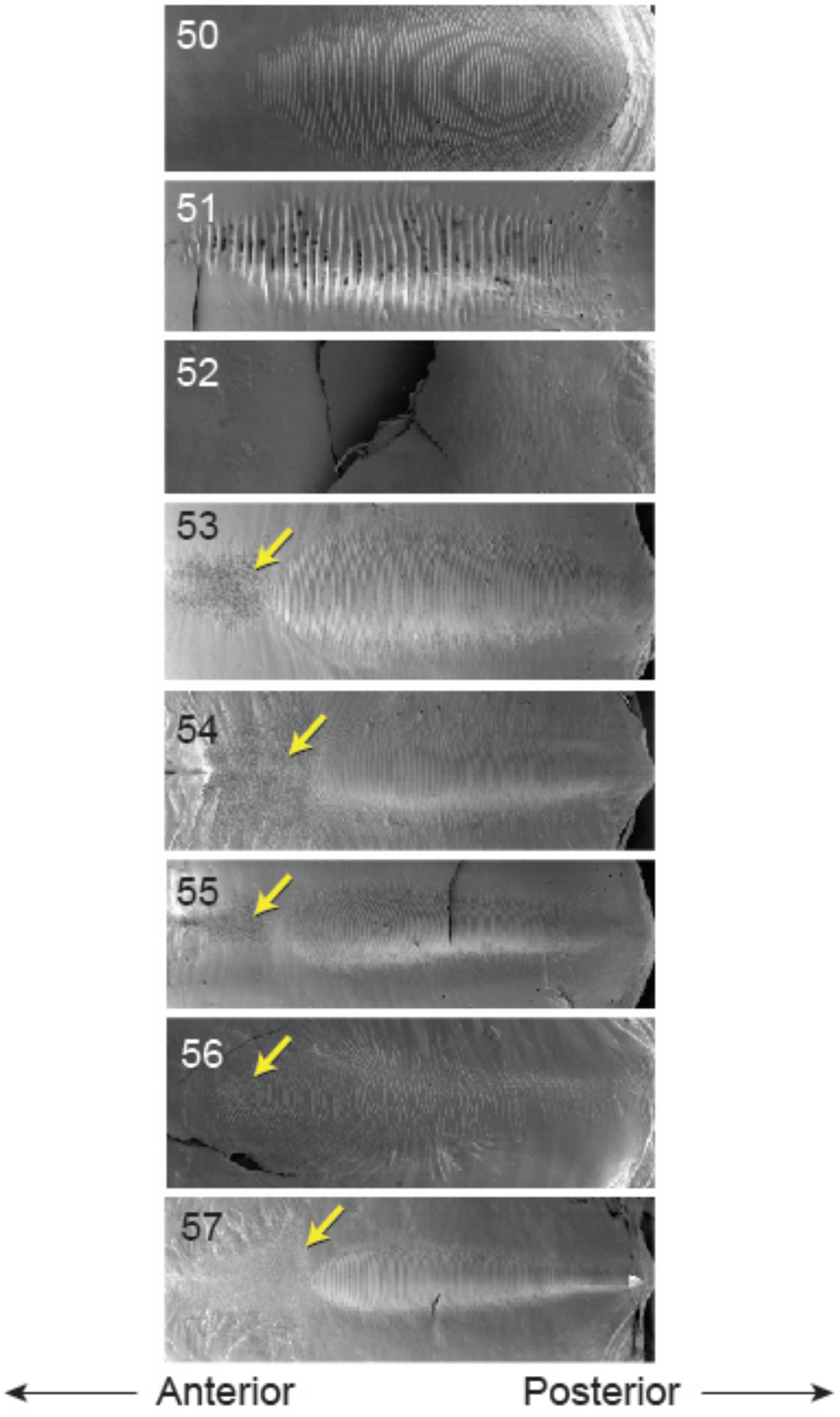
50
51
52
53
54
55
56
57
Anterior
Posterior

58

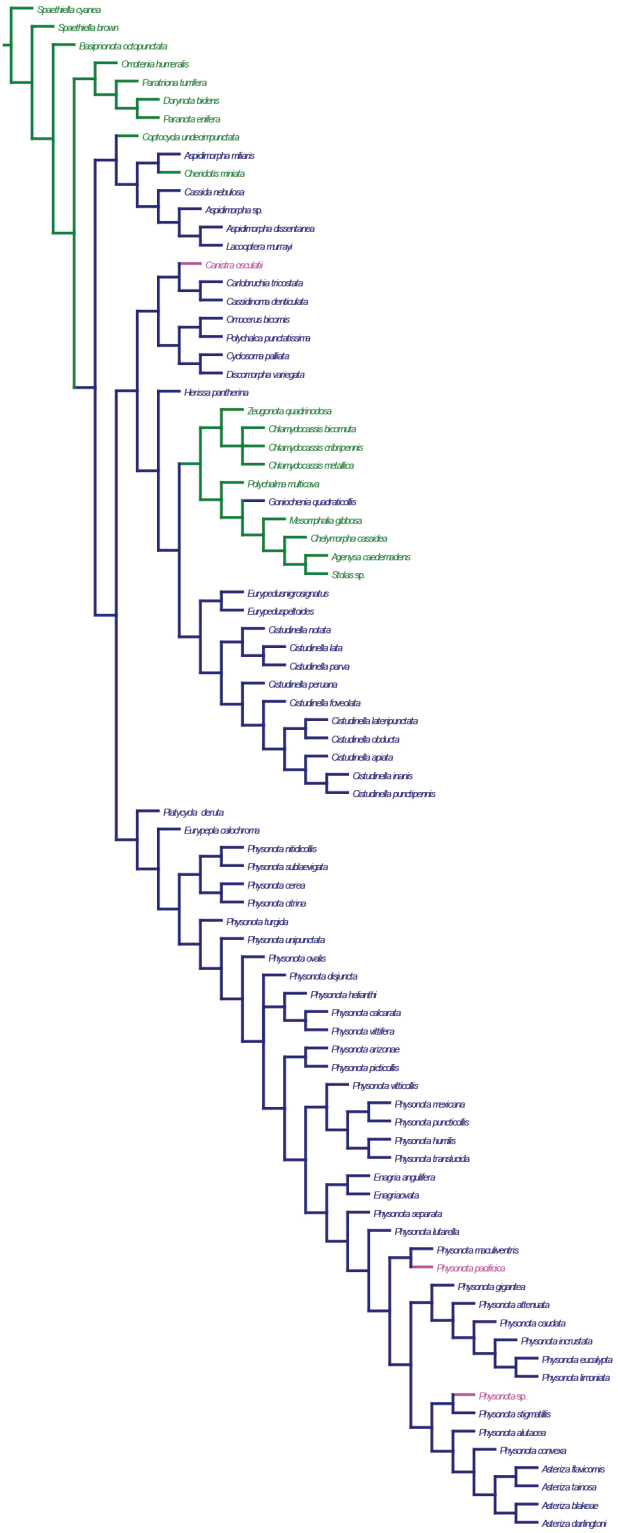
Spaethiella cyanea
Spaethiella brown
Basiprionota octopunctata
Omrotenia humerales
Paratriona turrifera
Dorynota bidens
Paranota enifera
Coptocycla undecimpunctata
Aspidimorpha miliaris
Cheridotis miniata
Cassida nebulosa
Aspidimorpha sp.
Aspidimorpha dissentanea
Lacoptera murrayi
Canistra oculata
Carlobruchia tricostata
Cassidinoma denticulata
Omocerus bicornis
Polychalca punctatissima
Cyclosoma pallida
Discomorpha variegata
Heressa panthemina
Zeugonota quadrinodosa
Chlamydocassis bicornuta
Chlamydocassis cribripennis
Chlamydocassis metallica
Polychalma muticava
Goniochenia quadraticollis
Mesomphalia gibbosa
Chelymorpha cassidea
Agenysa caedemadens
Stolas sp.
Eurypedunigrosignatus
Eurypedupelfoides
Cistudinella notata
Cistudinella lata
Cistudinella parva
Cistudinella peruana
Cistudinella fovelata
Cistudinella laterpunctata
Cistudinella obducta
Cistudinella apicta
Cistudinella inanis
Cistudinella punctipennis
Platycyda deruta
Eurypepla calochroma
Physonota nitidicollis
Physonota sublaevigata
Physonota cerea
Physonota obnina
Physonota turgida
Physonota unipunctata
Physonota ovalis
Physonota disjuncta
Physonota helianthi
Physonota calcarata
Physonota vittifera
Physonota arizonae
Physonota picticollis
Physonota viticollis
Physonota mexicana
Physonota punctacollis
Physonota humilis
Physonota translucida
Eriagria angulifera
Eriagriaovata
Physonota separata
Physonota lutarella
Physonota maculiventris
Physonota pacifica
Physonota gigantea
Physonota attenuata
Physonota caudata
Physonota incrustata
Physonota eucalypta
Physonota limoniata
Physonota sp.
Physonota stigmatilis
Physonota alutacea
Physonota convexa
Asteriza flavicornis
Asteriza tainosa
Asteriza blakeae
Asteriza darlingtoni

59

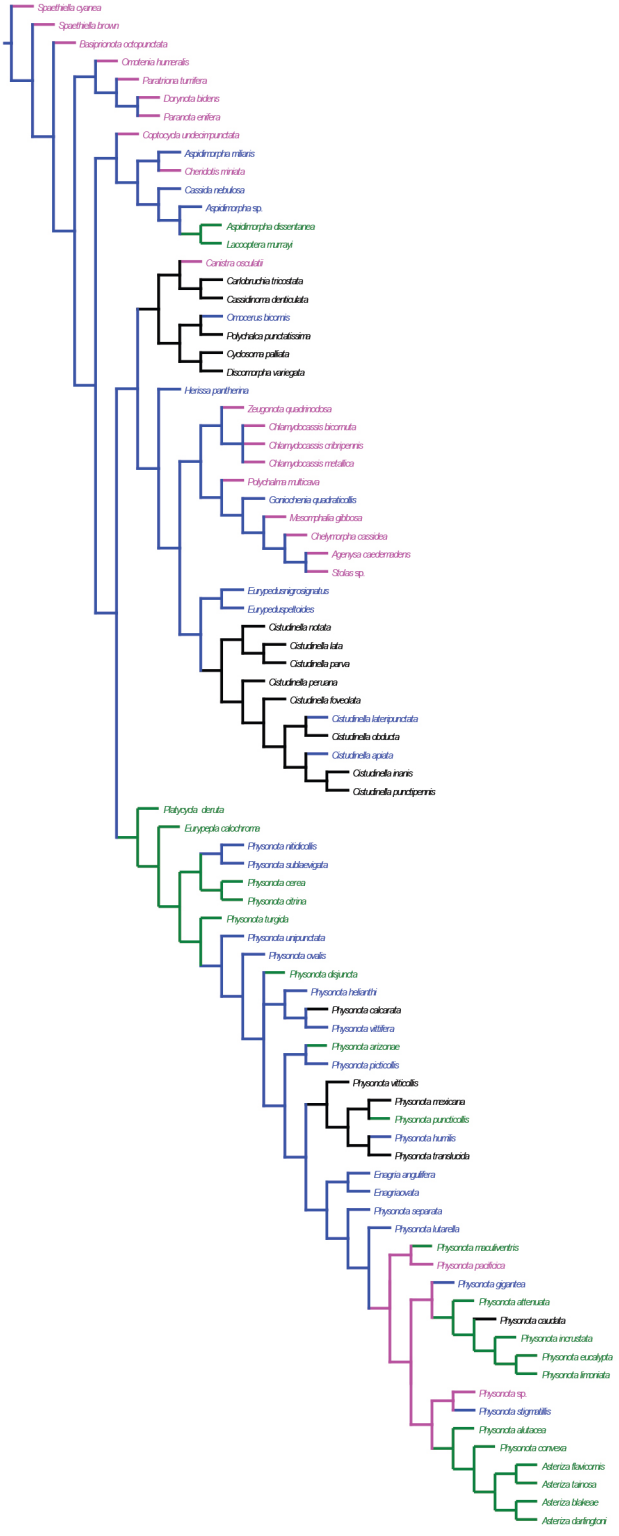
Spaethiella cyanea
Spaethiella brown
Basiprionota octopunctata
Omrotenia humerales
Paratriona turrifera
Dorynota bidens
Paranota enifera
Coptocycla undecimpunctata
Aspidimorpha miliaris
Cheridotis miniata
Cassida nebulosa
Aspidimorpha sp.
Aspidimorpha dissentanea
Lacoptera murrayi
Canistra oculata
Carlobruchia tricostata
Cassidinoma denticulata
Omocerus bicornis
Polychalca punctatissima
Cyclosoma pallida
Discomorpha variegata
Heressa panthemina
Zeugonota quadrinodosa
Chlamydocassis bicornuta
Chlamydocassis cribripennis
Chlamydocassis metallica
Polychalma muticava
Goniochenia quadraticollis
Mesomphalia gibbosa
Chelymorpha cassidea
Agenysa caedemadens
Stolas sp.
Eurypedunigrosignatus
Eurypedupelfoides
Cistudinella notata
Cistudinella lata
Cistudinella parva
Cistudinella peruana
Cistudinella fovelata
Cistudinella laterpunctata
Cistudinella obducta
Cistudinella apicta
Cistudinella inanis
Cistudinella punctipennis
Platycyda deruta
Eurypepla calochroma
Physonota nitidicollis
Physonota sublaevigata
Physonota cerea
Physonota obnina
Physonota turgida
Physonota unipunctata
Physonota ovalis
Physonota disjuncta
Physonota helianthi
Physonota calcarata
Physonota vittifera
Physonota arizonae
Physonota picticollis
Physonota viticollis
Physonota mexicana
Physonota punctacollis
Physonota humilis
Physonota translucida
Eriagria angulifera
Eriagriaovata
Physonota separata
Physonota lutarella
Physonota maculiventris
Physonota pacifica
Physonota gigantea
Physonota attenuata
Physonota caudata
Physonota incrustata
Physonota eucalypta
Physonota limoniata
Physonota sp.
Physonota stigmatilis
Physonota alutacea
Physonota convexa
Asteriza flavicornis
Asteriza tainosa
Asteriza blakeae
Asteriza darlingtoni

60

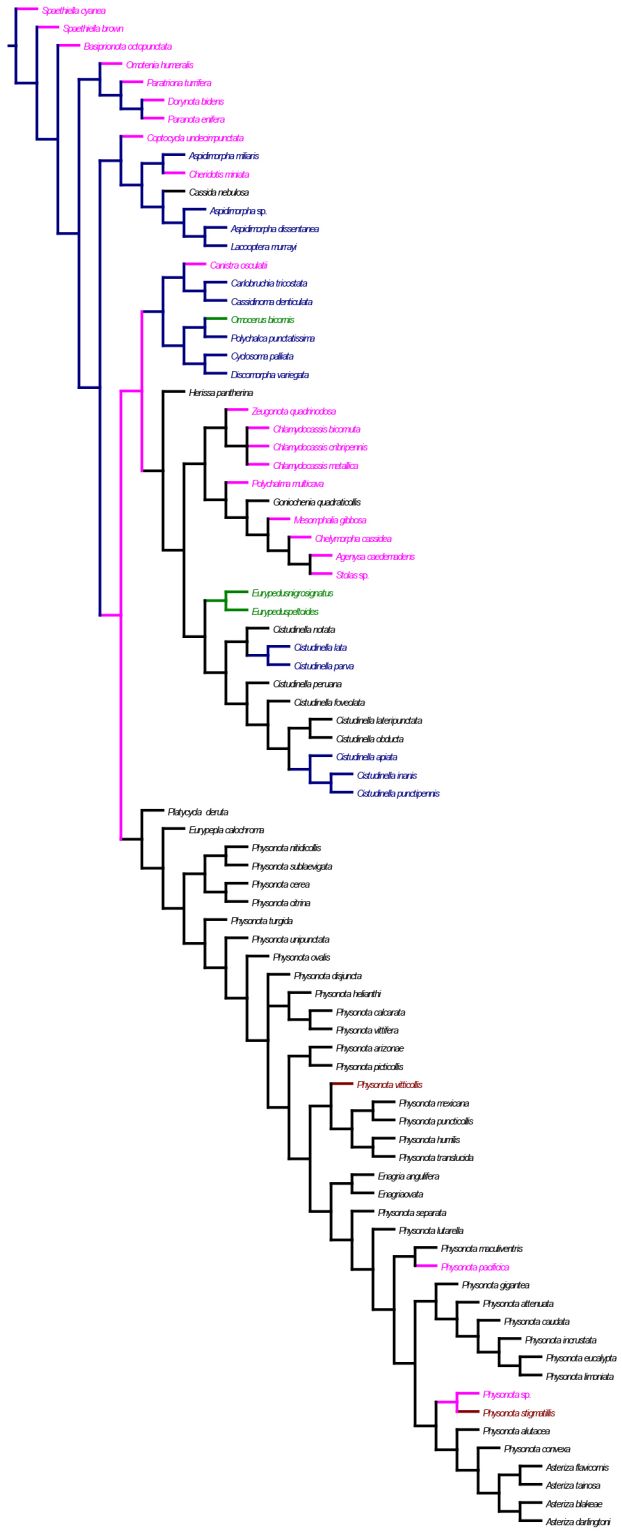
Spaethiella cyanea
Spaethiella brown
Basipronota octopunctata
Omotenia humeralis
Paratriona tumifera
Dorynota bidens
Paranota emifera
Coptocycla undecimpunctata
Aspidimorpha milanis
Cheridotis minuta
Cassida nebulosa
Aspidimorpha sp.
Aspidimorpha dissentanea
Laccoptera murrayi
Canistra osculati
Carlobruchia tricostata
Cassidinoma denticulata
Omocerus bicornis
Polychalca punctatissima
Cyclosoma pallida
Discomorpha variegata
Herissa pantherina
Zeugonota quadrinodosa
Chlamydocassis bicornuta
Chlamydocassis cribripennis
Chlamydocassis metallica
Polychalma multicava
Goniochenia quadraticollis
Mesomphalia gibbosa
Chelymorpha cassidea
Agenysa caedemadens
Stolas sp.
Eurypedus nigrosignatus
Eurypedus pefloides
Cistudinella notata
Cistudinella lata
Cistudinella parva
Cistudinella peruana
Cistudinella fovelata
Cistudinella laterpunctata
Cistudinella obducta
Cistudinella apiata
Cistudinella inanis
Cistudinella punctipennis
Platycycla deruta
Eurypepla calochroma
Physonota nitidicollis
Physonota subbaevigata
Physonota cerea
Physonota citrina
Physonota turgida
Physonota unipunctata
Physonota ovalis
Physonota disjuncta
Physonota helianthi
Physonota calcarata
Physonota vittifera
Physonota arizonae
Physonota picticollis
Physonota viticollis
Physonota mexicana
Physonota punctacollis
Physonota humilis
Physonota translucida
Enegnia angulifera
Enegnia ovata
Physonota separata
Physonota lutarella
Physonota maculiventris
Physonota pacifica
Physonota gigantea
Physonota attenuata
Physonota caudata
Physonota incrustata
Physonota eucalypta
Physonota limoniata
Physonota sp.
Physonota stigmatilis
Physonota alutacea
Physonota convexa
Ateriza flavicornis
Ateriza tainosa
Ateriza blakeae
Ateriza darlingtoni

61

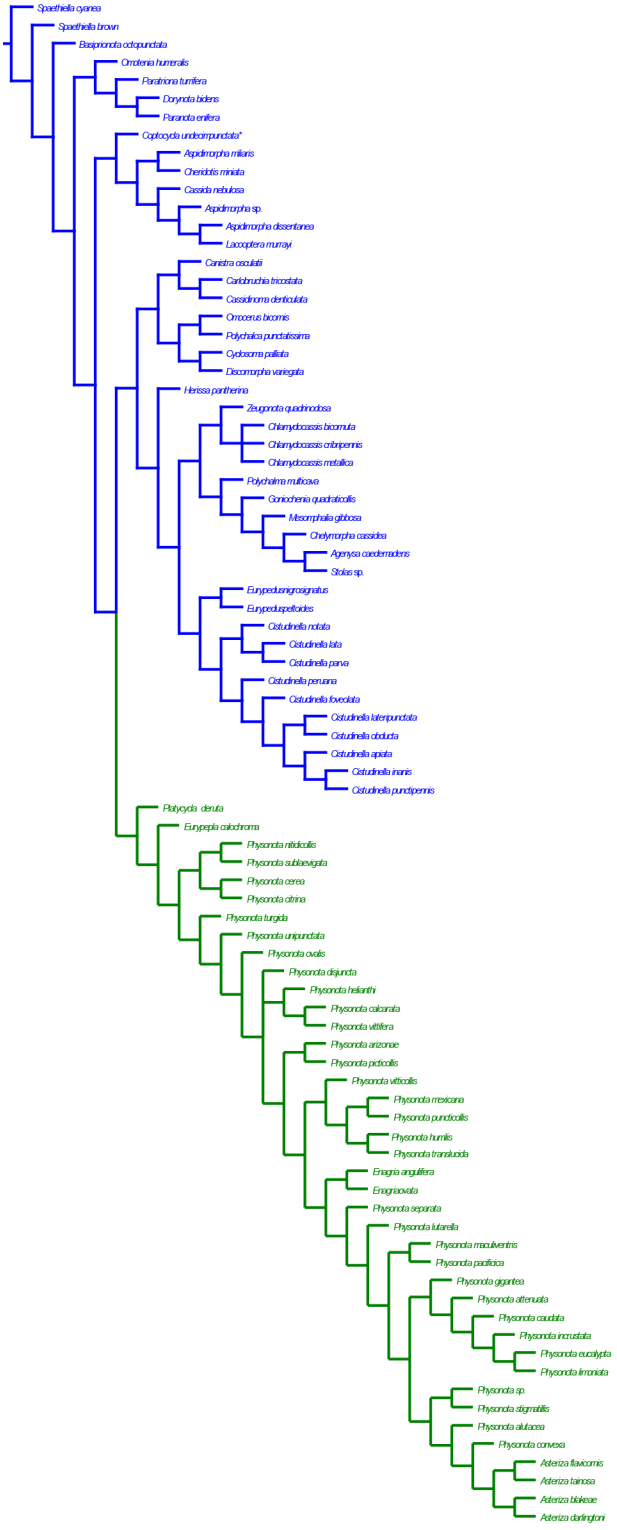
Spaethiella cyanea
Spaethiella brown
Basipronota octopunctata
Omotenia humeralis
Paratriona tumifera
Dorynota bidens
Paranota emifera
Coptocycla undecimpunctata*
Aspidimorpha milanis
Cheridotis minuta
Cassida nebulosa
Aspidimorpha sp.
Aspidimorpha dissentanea
Laccoptera murrayi
Canistra osculati
Carlobruchia tricostata
Cassidinoma denticulata
Omocerus bicornis
Polychalca punctatissima
Cyclosoma pallida
Discomorpha variegata
Herissa pantherina
Zeugonota quadrinodosa
Chlamydocassis bicornuta
Chlamydocassis cribripennis
Chlamydocassis metallica
Polychalma multicava
Goniochenia quadraticollis
Mesomphalia gibbosa
Chelymorpha cassidea
Agenysa caedemadens
Stolas sp.
Eurypedus nigrosignatus
Eurypedus pefloides
Cistudinella notata
Cistudinella lata
Cistudinella parva
Cistudinella peruana
Cistudinella fovelata
Cistudinella laterpunctata
Cistudinella obducta
Cistudinella apiata
Cistudinella inanis
Cistudinella punctipennis
Platycycla deruta
Eurypepla calochroma
Physonota nitidicollis
Physonota subbaevigata
Physonota cerea
Physonota citrina
Physonota turgida
Physonota unipunctata
Physonota ovalis
Physonota disjuncta
Physonota helianthi
Physonota calcarata
Physonota vittifera
Physonota arizonae
Physonota picticollis
Physonota viticollis
Physonota mexicana
Physonota punctacollis
Physonota humilis
Physonota translucida
Enegnia angulifera
Enegnia ovata
Physonota separata
Physonota lutarella
Physonota maculiventris
Physonota pacifica
Physonota gigantea
Physonota attenuata
Physonota caudata
Physonota incrustata
Physonota eucalypta
Physonota limoniata
Physonota sp.
Physonota stigmatilis
Physonota alutacea
Physonota convexa
Ateriza flavicornis
Ateriza tainosa
Ateriza blakeae
Ateriza darlingtoni

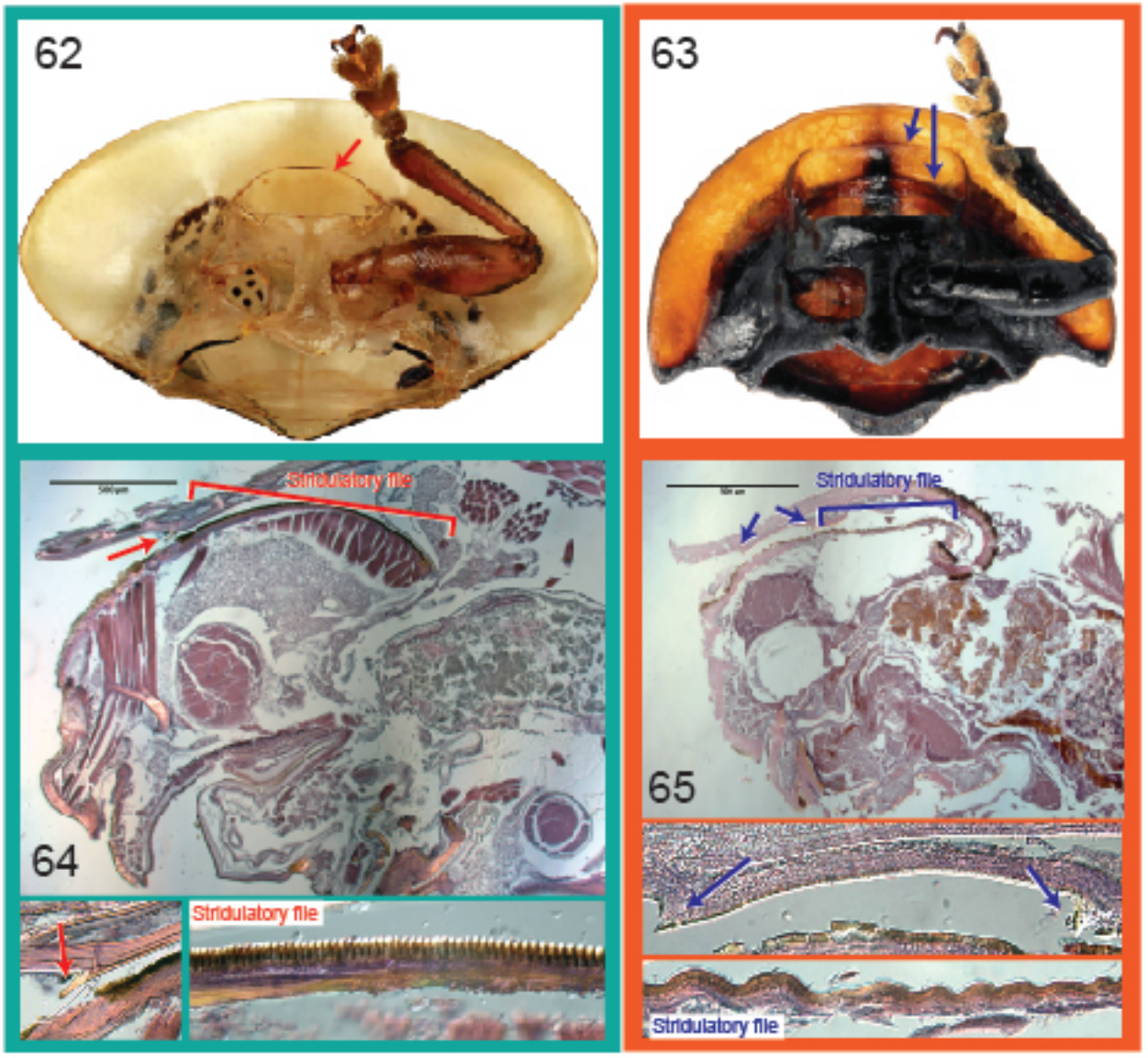
62
63
Stridulatory file
64
65
Stridulatory file
Stridulatory file
Stridulatory file

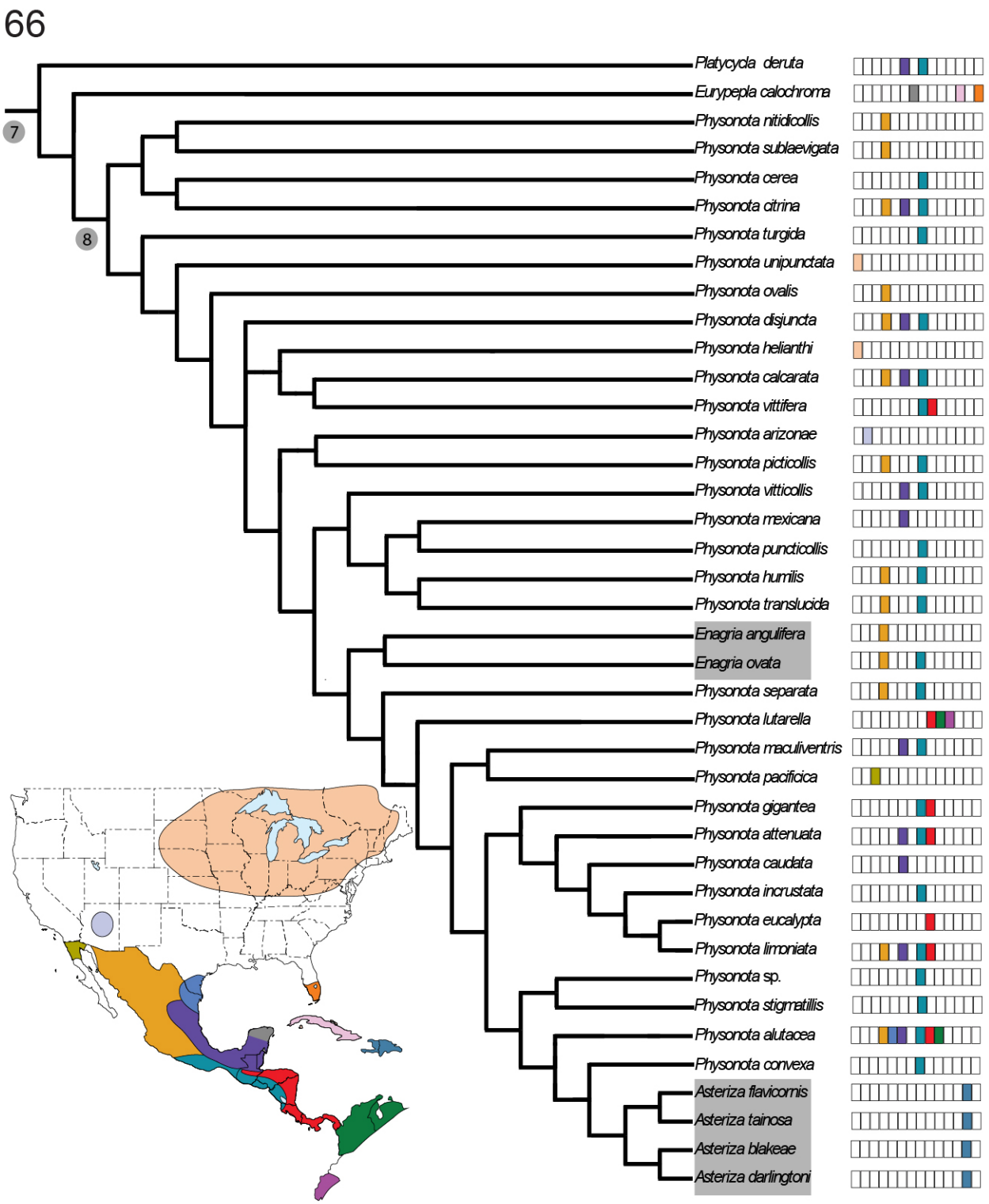
66
7
8
Platycycla deruta
Eurypepla calochroma
Physonota nitidicollis
Physonota sublaevigata
Physonota cerea
Physonota citrina
Physonota turgida
Physonota unipunctata
Physonota ovalis
Physonota disjuncta
Physonota helianthi
Physonota calcarata
Physonota vittifera
Physonota arizonae
Physonota picticollis
Physonota vitticollis
Physonota mexicana
Physonota puncticollis
Physonota humilis
Physonota translucida
Enagria angulifera
Enagria ovata
Physonota separata
Physonota lutarella
Physonota maculiventris
Physonota pacificica
Physonota gigantea
Physonota attenuata
Physonota caudata
Physonota incrustata
Physonota eucalypta
Physonota limoniata
Physonota sp.
Physonota stigmatillis
Physonota alutacea
Physonota convexa
Asteriza flavicornis
Asteriza tainosa
Asteriza blakeae
Asteriza darlingtoni

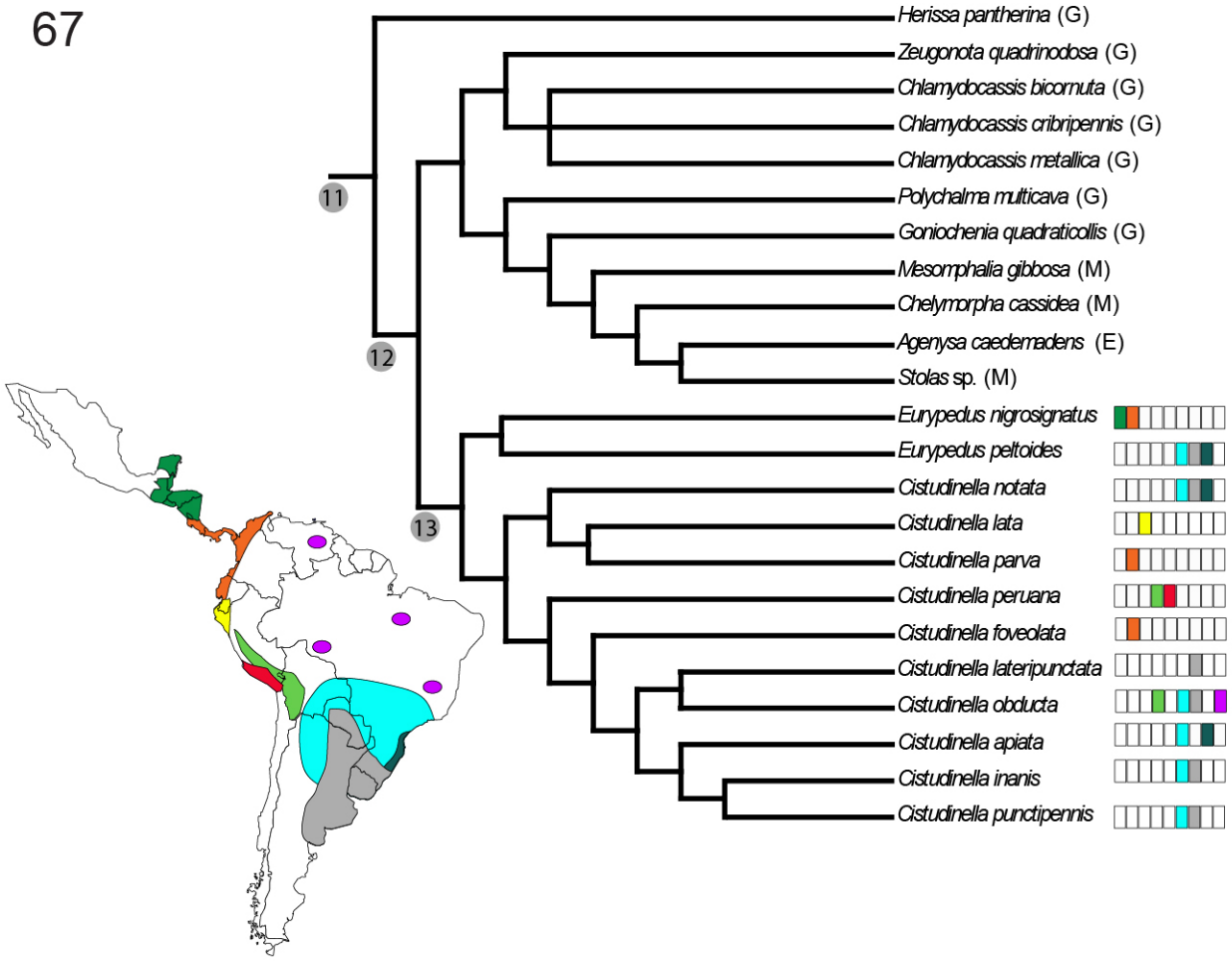
67
11
12
13
Herissa pantherina (G)
Zeugonota quadrinodosa (G)
Chlamydocassis bicornuta (G)
Chlamydocassis cribripennis (G)
Chlamydocassis metallica (G)
Polychalma multicava (G)
Goniochenia quadraticollis (G)
Mesomphalia gibbosa (M)
Chelymorpha cassidea (M)
Agenysa caedemadens (E)
Stolas sp. (M)
Eurypedus nigrosignatus
Eurypedus peltoides
Cistudinella notata
Cistudinella lata
Cistudinella parva
Cistudinella peruana
Cistudinella foveolata
Cistudinella lateripunctata
Cistudinella obducta
Cistudinella apiata
Cistudinella inanis
Cistudinella punctipennis

Table 1. List of the species in *Asteriza* with new combination.

Original Name	New Combination
Asteriza darlingtoni Blake	*Asteriza darlingtoni* Blake
Asteriza flavicornis (Olivier)	*Asteriza flavicornis* (Olivier)
Asteriza tainosa Shin et al.	*Asteriza tainosa* Shin et al.
Asteriza blakeae Shin et al.	*Asteriza blakeae* Shin et al.
Enagria angulifera Spaeth	*Asteriza angulifera* (Spaeth) **n. comb.**
Enagria ovata Boheman	*Asteriza ovata* (Boheman) **n. comb.**
Physonota alutacea Boheman	*Asteriza alutacea* (Boheman) **n. comb.**
Physonota arizonae Schaeffer	*Asteriza arizonae* (Schaeffer) **n. comb.**
Physonota attenuate Boheman	*Asteriza attenuate* (Boheman) **n. comb.**
Physonota breviuscula Boheman	*Asteriza breviuscula* (Boheman) **n. comb.**
Physonota caudata Boheman	*Asteriza caudata* (Boheman) **n. comb.**
Physonota cerea Boheman	*Asteriza cerea* (Boheman) **n. comb.**
Physonota citrina Boheman	*Asteriza citrina* (Boheman) **n. comb.**
Physonota citronella Boheman	*Asteriza citronella* (Boheman) **n. comb.**
Physonota convexa Borowiec	*Asteriza convexa* (Borowiec) **n. comb.**
Physonota dilatata Kirsch	*Asteriza dilatata* (Kirsch) **n. comb.**
Physonota disjuncta (Chevrolat)	*Asteriza disjuncta* (Chevrolat) **n. comb.**
Physonota eucalypta Boheman	*Asteriza eucalypta* (Boheman) **n. comb.**
Physonota flavago Boheman	*Asteriza flavago* (Boheman) **n. comb.**
Physonota gigantean Boheman	*Asteriza gigantean* (Boheman) **n. comb.**
Physonota helianthi (Randall)	*Asteriza helianthi* (Randall) **n. comb.**
Physonota humilis Boheman	*Asteriza humilis* (Boheman) **n. comb.**
Physonota incrustata Boheman	*Asteriza incrustata* (Boheman) **n. comb.**
Physonota limoniata Boheman	*Asteriza limoniata* (Boheman) **n. comb.**
Physonota lutarella Boheman	*Asteriza lutarella* (Boheman) **n. comb.**
Physonota maculiventris Boheman	*Asteriza maculiventris* (Boheman) **n. comb.**
Physonota mexicana Boheman	*Asteriza mexicana* (Boheman) **n. comb.**
Physonota nitidicollis Boheman	*Asteriza nitidicollis* (Boheman) **n. comb.**
Physonota ovalis Boheman	*Asteriza ovalis* (Boheman) **n. comb.**
Physonota ovipennis Champion	*Asteriza ovipennis* (Champion) **n. comb.**
Physonota pacifica Spaeth	*Asteriza pacifica* (Spaeth) **n. comb.**
Physonota pellucida Wagener	*Asteriza pellucida* (Wagener) **n. comb.**
Physonota perampla Champion	*Asteriza perampla* (Champion) **n. comb.**
Physonota picticollis Boheman	*Asteriza picticollis* (Boheman) **n. comb.**
Physonota plana Boheman	*Asteriza plana* (Boheman) **n. comb.**
*Physonota puncticollis B*orowiec	*Asteriza puncticollis* (Borowiec) **n. comb.**
Physonota separate Boheman	*Asteriza separate* (Boheman) **n. comb.**
Physonota stigmatilis Boheman	*Asteriza stigmatilis* (Boheman) **n. comb.**
Physonota sublaevigata Spaeth	*Asteriza sublaevigata* (Spaeth) **n. comb.**
Physonota translucida Boheman	*Asteriza translucida* (Boheman) **n. comb.**
Physonota turgida Boheman	*Asteriza turgida* (Boheman) **n. comb.**
Physonota unipunctata (Say)	*Asteriza unipunctata* (Say) **n. comb.**
Physonota vitticollis Boheman	*Asteriza vitticollis* (Boheman) **n. comb.**
Physonota vittifera Spaeth	*Asteriza vittifera* (Spaeth) **n. comb.**

Appendix 1. Specimens Examined

The tribes are listed alphabetically as are the species within each tribe. The type species were indicated next to the species name. “SEM” and “nSEM” are used to indicate specimens used for scanning electron microscopic images or non-coating scanning electron microscopic images.

Outgroups

Tribe Hemisphaerotini Monrós & Viana

Hemisphaerota cyanea (Say)

No locality data (SEMC: 1♂1♀, dissected)

Hemisphaerota sp.

No locality data (SEMC: 1♂1♀, dissected)

Ingroups

Tribe Aspidimorphini Chapuis

Aspidimorpha dissentanea Boheman

Liberia: no detailed locality data, OF Cook (USNM: 1♂1♀, dissected, nSEM)

Aspidimorpha miliaris (Fabricius) type species

Java: Tjipajung, III 10 1957, CL Klein, ex Lima beans (SEMC: 1♂, dissected, nSEM)

Aspidimorpha sp.

Philippines, Canaoalan Binmaley Pongasina, “Phil. ld.”, III 6 1936, Benito Abalos (SEMC: 1♀, dissected, nSEM); Philippines: Lamao, Luzon, III–VI 1911, CV Piper (USNM: 1♂1♀, dissected)

Laccoptera murrayi Boheman

Cameroon: Nanga Ebobo, Dr. Lenczy, 1959 ex F Monrós collection (USNM: 1♂1♀, dissected, nSEM)

Tribe Basiprionotini Gressitt

Basiprionota octopunctata (Fabricius) type species

No locality data, Gorham, acc. 68498 (USNM: 1♂, dissected)

Tribe Cassidini Gyllenhal

Cassida nebulosa Linnaeus type species

Sweden: no detailed locality data (SEMC: 1♂1♀, dissected, nSEM)

Charidotis miniata Boheman type species

Brazil: Rio de Janeiro, Corcovado, XI 8 1975, MA Monné & CA Campos Seabra (MNRJ: 1♀, dissected)

Coptocycla undecimpunctata (Fabricius) type species

Brazil: Amazonas, Estrada Manaus-Itacoatiara, "KM 64 Areal", IX 19 1977, J Becker (MNRJ: 1♀, dissected)

Tribe Dorynotini Monrós & Viana

Dorynota bidens (Fabricius) type species

Brazil: Espírito Santo, Córrego do Ita, XI 1981, HW Saar (MNRJ: 1 specimen, sex undetermined); Espírito Santo, Linhares, Parque Sooretama, X 1968, FM Oliveira (MNRJ: 1 specimen, sex undetermined)

Omotenia humeralis (Olivier) type species

Haiti: Port au Prince, II 27 1998, EA Klages (USNM: 2♂1♀, dissected)

Paranota ensifera (Boheman) type species

Paraguay: Paraguarí, Sapucay, III, WTFoster (USNM: 1♂1♀, dissected)

Paratriona turrifera (Boheman) type species

Cuba: Cayamas ESA Schwarz (USNM: 1♂1♀, dissected)

Tribe Eugenysini Hincks

Agenysa connectens (Baly) type species

Peru: Junin, Sani Beni, X 16 1935, F Woytkowski (SEMC: 1 specimen, sex undetermined)

Tribe Goniocheniini Spaeth

Chlamydocassis bicornuta (Boheman)

Brazil: Para, Belem, I 24 1969, L & CWO Brien (FSCA: 1 specimen, sex undetermined)

Chlamydocassis cribripennis (Boheman)

Boliva: Santa Cruz, Lomas de Arena Biological Park, II 10 1999, LA Stage (FSCA: 1 specimen, sex undetermined)

Chlamydocassis metallica (Klug) type species

Bolivia: Santa Cruz, Bueno Vista, 380 m, II 20 1999, L Stange, Malaise trap (FSCA: 1♂1♀, dissected)

Goniochenia quadraticollis (Boheman) type species

"Maromba (Itatlala), E. Rio, VII 29 1952, C Lelte & Seabraz e Zikka" (MNRJ: 1♂, dissected, nSEM); Brazil: Rio de Janeiro, florersta da Tujica, IV 1951, CAC Seabra (MNRJ: 1♀, dissected)

Herissa pantherina (Blanchard) type species

Brazil: Mato Grosso, Maracaju, II 1937, ex Monrós collection (USNM: 1♂, dissected, nSEM); Mato Grosso, Maracaju, XI 1938, ex Monrós collection (USNM: 1♀, dissected)

Polychalma multicava (Latreille) type species

Panama: Canal Zone, Pipeline road, 10 mi NW from Gamboa, VI 9 1978, NR Woodey (USNM: 2 specimens, sex undetermined)

Zeugonota quadrinodosa (Boheman) type species

Brazil: Goias, Goiatuba, I 1952, A Maller (MNRJ: 1♂, dissected); Goias, Goiatuba, II 1941 (MNRJ: 1♀, dissected)

Tribe Ischyrosonychini Chapuis

Asteriza blakeae Shin, Chaboo & Clark

Dominican Republic: Barahona, Eastern Sierra, Bahoruco, Reserva Cachote 12.8 km NE, Paraiso, 18°05'54"N, 71°11'21"W, 1,230 m, XII 21 2004, C Young, C Nunez, J Rawlins & J Fetzner, Cloud forest with tree ferns, yellow pan trap (SEMC: 1♂1♀, ♂, dissected, SEM)

Asteriza darlingtoni Blake

Dominican Republic: La Vega, Cordillera Central, 4.1 km SW, 18°50'37"N, 70°42'48"W, 1,730 m, V 31 2003, J Rawlins, R Davidson, C Young, C Nunez & P Acevedo (SEMC: 1♂1♀, dissected, nSEM)

Asteriza flavicornis (Olivier) type species

Dominican Republic: Azua: 8 km NE, Padre Las Casas, Rio Las Cuevas, 18°46'N, 70°53'W, 580m, Oct 3–4 1991, C Young, R Davidson & J Rawlins, Riparian growth in arid thorn scrub, hand collecting (SEMC: 1♂1♀, dissected, nSEM)

Asteriza tainosa Shin, Chaboo & Clark

Dominican Republic: Independencia: Sierra de Bahoruco, North Slope, 13.5 km SE, Puerto Escondido, 18°12'18"N, 71°31'08"W, 1,807 m, May 22–23 2004, C Young, J Fetzner, J Rawlins & C Nunez, Broadleaf *Pinus* sp., dense woodland (SEMC: 1♂1♀, dissected, nSEM)

Cistudinella apiata (Boheman)

Brazil: Rio de Janeiro, Corcovado, XI 1957, Alvaranga & Saabra (MNRJ: 1♂, dissected, nSEM); Rio de Janeiro, Corcovado, X 1958, Alvaranga & Saabra (MNRJ: 1♀, dissected)

Cistudinella foveolata Champion type species

Panama: Panama, Canal Zone, Calyton observatory, 11 VI 1976, E Riley (EGRC: 1♂1♀, dissected, SEM)

Cistudinella inanis (Boheman)

Brazil: Santa Catarina, Nova Teutonia, 300–500 m, I 1974, F Plaumann (EGRC: 1♂, dissected, nSEM); Argentina: Misiones, San Ignacio, IX 1955, A Maller (MNRJ: 1♀, dissected)

Cistudinella lata Spaeth

Panama: Chiriqui, La Fortuna, Divide Trall, XII 8 1988, DM Windsor (EGRC: 1♀, dissected, nSEM)

Cistudinella lateripunctata Spaeth

Brazil: Santa Catarina, Nova Teutonia, 300–500 m, I 1970, F Plaumann (EGRC: 1♂, dissected, nSEM); Argentina: Misiones, “Dept. Concep-Sta. Maria”, XI-1958, MJ Viana (FSCA: 1♀, dissected)

Cistudinella notata (Boheman)

Brazil: Nova, Teutonia 300–500 m, XI 1974, F Plaumann, (EGRC: 1♂1♀, dissected, nSEM)

Cistudinella obducta (Boheman)

Brazil: Rondonia, 62 km SW, Ariquemes, near Fazenda Rancho Grande, X 20–31 1997, BK Dozier (FSCA: 1♂1♀, dissected, nSEM)

Cistudinella parva (Wagener)

Ecuador: Pastaza, Rio Negro, 4,000 ft.,VII 1 1980, CM. Stevens (FSCA: 1♀, dissected, nSEM)

Cistudinella peruana Spaeth

Peru: no detailed locality data (MUSN: 1♂1♀, dissected, nSEM)

Cistudinella punctipennis (Boheman)

Brazil: Rio Grande, Guanabara, X 1989, ES Lima (MNRJ: 1♀, dissected, nSEM)

Eurypedus nigrosignatus (Boheman)

Guatemala: Zacapa, 7 km W Teculutan, VI 25 1993, R Brooks & JS Ashe (SEMC: 2♂2♀, dissected, SEM, histological sectioning)

Eurypedus peltoides (Boheman)

Brazil: Rio Grande do Sul, Porto Alegre, XII 2008, BCM Rames (SEMC: 1♂1♀, dissected, nSEM)

Enagria angulifera Spaeth

Mexico: Mexico DF, Temascal Tepec, 1931, GB Hinton (UNAM: 1♀, nSEM)

Enagria ovata Boheman type species

Mexico: Mexico DF. Pedregal de San Angel, VIII 27 1976 (UNAM: 1♂, dissected, nSEM); Puebla, Tecamachalco 8 mi NE, VII 3 1963 (SEMC: 1♀, dissected)

Eurypepla calochroma (Blake)

USA: Florida, Davie, University of Florida parking lot, IV 25 2013, C Shin (SEMC: 2♂2♀, dissected, SEM)

Physonota alutacea Boheman type species

Nicaragua: Granada, Reserva Silvestre Privada Domitila, VI 4 2011, C Shin (SEMC: 2♂2♀, dissected, SEM, histological sectioning)

Physonota arizonae Schaeffer

USA: Arizona, Pima County, 2.1 mi S of Gibbon, Mt. Santa Catalina, 3,200 ft., VII 29 1972, on *Ambrosia ambrosiodes*, G. Lasalle & M. Kolner (ASUT: 1♂1♀, dissected, nSEM)

Physonota attenuata Boheman

Nicaragua: Granada, Reserva Silvestre Privada Domitila, VI 4 2011, C Shin (SEMC: 2♂2♀, dissected, nSEM)

Physonota calcarata (Boheman)

Mexico: Jalisco, 0.2 mi from Nayarit st. line hwy #1511, VIII 1963, G Byers (SEMC: 1♂1♀, dissected, nSEM)

Physonota caudata Boheman

Mexico: Vera Cruz, Jalapa, ex Gorham collection acc. 68498 (USNM: 1♂1♀, dissected, nSEM)

Physonota cerea Boheman

Mexico: Oaxaca, 7 mi S from Juchatengo, 4,000 ft., VIII 10 1970, E Fisher & P Sullivan (LACM: 1♂1♀, dissected, nSEM)

Physonota citrina Boheman

El Salvador: Santa Ana, Metapan, “Had”, Montecristo, 2,300 m, Cloud Forest, III 2 1972, SL Steinhauser (FSCA: 1♂1♀, dissected, nSEM)

Physonota convexa Borowiec

Mexico: Jalisco, Chamela Field Station, VII 11 1989, AR Alsina, C Michner & R Brooks, malaise trap #018 (SEMC: paratype ♂, dissected, nSEM; paratype ♀, genitalia information from Borowiec 1995b)

Physonota disjuncta (Chevrolat)

Mexico: Michoacan, Morelia, IX 4 1938, LJ Lipovsky (SEMC: 1♂1♀, dissected, nSEM)

Physonota eucalypta Boheman

Mexico: Vera Cruz, Chiapaz (USNM: 1♂, dissected, nSEM); Guatemala: 1908, R Guerin ex Monrós collection (USNM: 1♀, dissected)

Physonota gigantea Boheman

Nicaragua: Granada, Reserva Silvestre Privada Domitila, VI 4 2011, C Shin (SEMC: 2♂2♀, dissected, nSEM)

Physonota helianthi (Randall)

USA: New York, Cadosia, VIII 3 1930, KF Chamberlain (SEMC: 1♂, dissected); No locality data (SEMC: 1♀, dissected, nSEM)

Physonota humilis Boheman

Mexico: Aguscalientes, 10 mi NE from Calvillo, VII 5 1984, Carroll, Schaffner & Friedlander (TAMU: 1♂1♀, dissected, nSEM)

Physonota incrustata Boheman

Mexico: Sinaloa,La Capilla del Taxte, 1020 m, Highway 40, oak/pine forest, III 5 1992, JD Boone, RS Peigler & WS Sear (TAMU: 1♂, dissected, nSEM); no locality data (UNAM: 1♀, dissected)

Physonota limoniata Boheman

Guatemala: 39 km from Guatemala–San Salvador, E Barrera & F Arias (UNAM: 1♂, dissected, nSEM); no locality data (SEMC: 1♀, dissected)

Physonota lutarella Boheman

Panama: Bocas Del Toro, 2.3 mi N from Continental Divide, V 27 1993, E Riley (EGRC: 1♂, dissected, nSEM)

Physonota maculiventris Boheman

Mexico: Chiapas, Sumidero, Canyon near Tultitlan Gutierrez, 4,000 ft., VI 19 1986, DB Thomas (EGRC: 1♂, dissected, nSEM); Oaxaca, 32 mi S from Valle Nacional, 7,000 ft., V 21 1971, Bright (EGRC: 1♀, dissected)

Physonota mexicana Boheman

Mexico: Guanajuato, 2 mi W from Delores Hidalgo, VII 5 1985, J Schaffner (TAMU: 1♂, dissected, nSEM); Hidalgo, Apam, IX 4 1952, McGregor (CNIN: 1♀, dissected)

Physonota nitidicollis Boheman

Mexico: Morelos, 18˚ 53’ 20.5”N 98˚ 44’ 4.1” W, “BPE”, “TETE 1912”, X 1 2004, E. Moreno (UNAM: 1♂, dissected, nSEM); Michoacan, 16 mi W from Zitacuaro, VIII 31 1938, LJ Lipovsky (SEMC: 1♀, dissected)

Physonota ovalis Boheman

Mexico: Chihuahua, Ojito, Santa Barbara, “Kilo 36”, 6,900 ft., VIII 17 1947, GM Bradt (AMNH: 1♂1♀, dissected, nSEM)

Physonota pacifica Spaeth

Mexico: Baja California, Nogales, IV 4 1942, on Cactus (USNM: 1 specimen, sex undetermined); Sinaloa, Los Mochis, III 1923, RH Van Zwaluwenburg (USNM: 1 specimen, sex undetermined); Sinaloa, Mazatilan, IX 2 1965, on Bromeliad orchid, W Jackson (USNM: 1 specimen, sex undetermined); Sonora, Empalme, Cochore Beach, VII 26 1952, P&C Vaurie (AMNH: 1 specimen, sex undetermined); Sonora, Guaymas, VII 18 1954, M Cazier, W Gertaoh & Bradts (AMNH: 2 specimens, sex undetermined)

Physonota picticollis Boheman

Mexico: Sinaloa (SEMC: 1♂1♀, dissected, nSEM)

Physonota puncticollis Borowiec

Mexico: Hidalgo, 21 mi NE from Huichapanm 6,650 ft., Highway 45, VII 26 1982, C&L O’Brien & G Wibmer (EGRC: 1♀, dissected, nSEM)

Physonota separata Boheman

Mexico: Morelos, Tepoztlan, VI 15 1993, D Furth (USNM: 1♂, dissected, nSEM); Chihuahua, near Sonora border, 4 mi N from Los Chinacas, 4,910 ft. VII 9–10 1989, S McCleve (EGRC: 1♀, dissected)

Physonota stigmatillis Boheman

Mexico: Guerrero, Acahuizotla, 22 VI 1982, L Torres (UNAM: 1♂, dissected, nSEM); Chiapas, Reserva El Ocote, XII 2–10 1998, G Ortega, E barrera, & A Casasola (UNAM: 1♀, dissected)

Physonota sublaevigata Spaeth

Mexico: Jalisco, 4 mi W from Mazamitla, X 1950, 6,600 ft., AA Alcorn (SEMC: 1♀, dissected, nSEM)

Physonota translucida Boheman

Mexico: Mexico, Tejupilco, “3960 pas”, VII 1932 (EGRC: 1♂, dissected, nSEM); Puebla, Atexcoco, III 12 1994, E Barrera & C Mayorga (UNAM: 2♀, dissected)

Physonota turgida Boheman

Mexico: Durango, 24 mi W from La Ciudad, 7,000 ft., VI 20 1964, LA Kelton (EGRC: 1♂, dissected, nSEM); Jalisco, LaBarca,hwy #85-2, VII 10 1985, GW Byers, at light (SEMC: 1♀, dissected)

Physonota unipunctata (Say)

No locality data (SEMC: 1♂1♀, dissected, nSEM)

Physonota vitticollis Boheman

Mexico: Jalisco, Jocotepec, VIII 15 1987, B Gill (EGRC: 1♂, dissected, nSEM); Oaxaca, 19 miles S from San Miguel Suchixtepec, VII 17 1985, Jones & Schaffner (TAMU: 1♀, dissected)

Physonota vittifera Spaeth

Nicaragua: Jinotega, El Jaguar, Coffee finca, 4,356 ft., XII 3–8 2005, DG Marqua (TAMU: 1♂, dissected, nSEM)

Physonota sp.

Mexico: Chiapas, Cerro Hueco, 5 km S from Tuxtla Gutierrez, VII 23 1992, B Gomez (UNAM: 1♂1♀)

Platycycla deruta Boheman type species

Mexico: Vera Cruz, St. Lugrecia, FK Knab (UNAM: 1♂, dissected, SEM); Vera Cruz, San Cayetano, VIII 1958, F Torres (UNAM: 1♀, dissected)

Tribe Mesomphaliini Hope

Chelymorpha cassidea (Fabricius)

USA: no detailed locality data (SEMC: 1♂1♀, dissected)

Mesomphalia gibbosa (Fabricius) type species

Brazil: Rio de Janeiro, Paineiras, IX 28 1954, J Becker (MNRJ: 1♂, dissected); Rio de Janeiro, florersta da Tujica, IV 1980, B Silva (MNRJ: 1♀, dissected)

*Stola*s sp.

Costa Rica: Cartago, Turrialba, VII 5 1963, 1950 ft., CD Michener et al. (SEMC: 1 specimen, sex undetermined)

Tribe Omocerini Hincks

Canistra osculatii Guérin

No locality data (SEMC: 1♂, dissected)

Carlobruchia tricostata (Spaeth) type species

Argentina: Jujuy, IV 10 1927, RC Shannon (USNM: 1♂1♀, dissected, nSEM)

Cassidinoma denticulata (Boheman) type species

Paraguay: Paraguarí, Sapucay, II 13 1903, WT Foster (USNM: 1♂, dissected, nSEM); Argentina: Misiones, Pastoreo Grande, II 1954, WT Foster, ex Monrós collection (USNM: 1♀, dissected)

Cyclosoma palliata (Fabricius) type species

Brazil: Para, Obidos, I 1956, FM Oliveira (MNRJ: 1♂, dissected, nSEM); Para, Obidos, IX 1953, FM Oliveira Para (MNRJ: 1♀)

Discomorpha variegata (Linnaeus) type species

No locality data (SEMC: 1♂1♀, dissected, nSEM)

Omocerus bicornis (Linnaeus) type species

Brazil: Para, Mocajuba, Mangabeira, VI 1953, Orisando Rego (MNRJ: 1♂, dissected, nSEM); Para, Obidos, VI 1979, B Silva (MNRJ: 1♀, dissected)

Polychalca punctatissima (Wolf) type species

Brazil: Baiha, Conceição do Almeida, II 19 1978, J Becker (MNRJ: 1♂, dissected, nSEM); No locality data (SEMC: 2♀, dissected)

Appendix 2. Characters and Associated States Used in Phylogenetic Analysis

[Character 1] **Length of head:** the length was measured at the medial longitudinal line of the head and the width was measured at the posterior tangent line of the compound eyes in dorsal view (Fig. 17).

0: longer than broad

1: as long as broad or broader than long

[Character 2] **Connection between facial area, and dorsal and lateral areas on head:** this character was a modified version of characters # 28 and #36 (supraorbital ridge and sulcus) in Chaboo (2007) because the supraorbital sulci were formed by the projected line between the facial area and dorsal and lateral areas. Herein those were considered as one character.

0: smoothly connected (Fig. 17)

1: face separated from dorsal and lateral areas by projected line (Shin 2015, figs. 13–14).

[Character 3] **Projected orbital behind compound eyes on head in dorsal view**: this character was used in Chaboo (2007, Ch.#35) as orbital sulcus with the same states.

0: absent

1: present (Chaboo 2007, fig. 42G).

[Character 4] **Length of coronal sulcus on head in dorsal view:** this character was used in Chaboo (2007, Ch.#31) as head cranial suture with the same states.

0: reaching to or extending over posterior tangent line of compound eyes (Fig. 17)

1: short, terminating before posterior tangent line of compound eyes (Shin 2015, fig. 13)

[Character 5] **Surface of antero-medial region of posterior tangent line of compound eyes on head in dorsal view.**

0: depressed (Shin 2015, fig. 13)

1: slightly convex or flat

[Character 6**] Surface of postero-medial region of posterior tangent line of compound eyes on head in dorsal view.**

0: smooth (Shin 2015, fig. 42)

1: transversely lined (Fig. 46)

2: irregularly depressed (Fig. 49)

3: longitudinally striate

[Character 7] **Setae on dorso-medial surface of head in dorsal view:** these setae should be considered separately from those on temporal area (found in all examined specimens in this study) and the microtrichial patch on the vertex (Ch.#25).

0: present (Figs. 17–19)

1: absent (Shin 2015, fig. 13)

[Character 8] **Distance between antennal sockets on head in frontal view:** this character was used in Chaboo (2007, Ch.#51). The character states were modified because hispines (with diameter 2 times broader than diameter of antennal socket) were not examined in this study.

0: narrower than diameter of antennal socket (Chaboo 2007, fig. 43H)

1: as broad as diameter of antennal socket (Fig. 18)

2: broader than diameter of antennal socket

[Character 9] **Width between coronal sulcus and medial margin of compound eye on head in frontal view:** width was measure at mid-level.

0: narrower than diameter of compound eye (Chaboo 2007, fig. 43H)

1: as broad as diameter of compound eye (Fig. 18)

2: boarder than diameter of compound eye (Chaboo 2007, fig. 43A)

[Character 10**] Location of compound eye at inferior tangent line with mouth fossa on head in frontal view:** Chaboo (2007, Ch.#71) used a similar character with the states based on the location of antennal insertion. In tortoise beetles, the locations of the antennal sockets do not vary. In this study, the location of the compound eyes was determined relative to the mouth fossa.

0: above mouth fossa (Fig. 18)

1: meeting or overlapping with mouth fossa (Chaboo 2007, fig. 44E)

[Character 11] **Visibility of head capsule (temporal area) behind compound eyes in frontal view:** Chaboo (2007, Ch.#38) used a similar character with two character states (compound eyes protuberant or not). Herein, the measurement for the protuberant compound eyes was clarified based on the visibility of the head capsule (temporal area) in frontal view.

0: temporal areas not visible (Fig. 18)

1: temporal areas exposed laterally (Shin 2015, fig. 14)

[Character 12] **Shape of frons on head in frontal view:** this character was used in Chaboo (2007, Ch.#65) as the length of the frontoclypeus and hypostomal area (= bottom line). Length was measured at the medial line and the width was measured at the bottom line.

0: as long as or longer than broad (Chaboo 2007, fig. 44D)

1: broader than long (Fig. 18)

[Character 13] **Shape of frontal sulcus on head in frontal view:** Chaboo (2007, Ch.#37) used a similar character with three states (triangular, upside-down triangular, and faint), which was more focused on the shape of the frons. In this study, the character was more focused on the lateral margin of the sulcus.

0: straight (Shin 2015, Fig. 14)

1: convex (round) (Shin et al. 2012, fig. 33)

2: disconnected (only upper part of each side present by faint line) (Fig. 18)

[Character 14] **Depression above mouth fossa at low-lateral regions of frons on head in frontal view:** this depression should be distinguished from the depressions associated with condylic projections adjacent to the mouth fossa.

0: absent (Fig. 18)

1: present (Shin 2015, fig. 14)

[Character 15] **Shape of upper part of frons on head in frontal view:** the upper part (angle) was formed by the frontal sulci, and observed between the antennal sockets in tortoise beetles.

0: pointed (Shin et al. 2012, fig. 24)

1: rounded

2: upper angle remained open (often with medial longitudinal line) (Fig. 18)

[Character 16] **Surface of upper region of frons on head in frontal view:** this character was used in Chaboo (2007, Ch.#68) as whether the surface of the frons was on the same plane of the antennal base or not. In this study, this character focused on the surface of each region on the frons (see also Chs#18 and 20 in this study).

0: flattened (Fig. 18)

1: elevated (Chaboo 2007, fig. 45D)

[Character 17] **Punctures on surface of frons on head in frontal view:** irregular punctation often formed irregular depressions. Those depressions were also considered as punctures.

0: present (Fig. 18)

1: absent

[Character 18] **Surface of frons at middle region on head in frontal view** (see Ch#16 in this study).

0: flattened or slightly depressed (Fig. 18)

1: swollen

[Character 19] **Medial longitudinal line of frons on head in frontal view:** the same character was used in Chaboo (2007, Ch.#30) as the midfrontal sulcus.

0: absent (Shin et al. 2012, fig. 31)

1: present (Shin et al. 2012, figs. 30, 32)

[Character 20] **Surface between lower region of frons and clypeus on head in frontal view:** the clypeus was always flattened (if present) and it was a good indicator for measuring the surface of the lower region in front (see Chs#16 and 18 in this study).

0: only clypeus flattened (Shin et al. 2012, fig. 30)

1: both lower region of frons and clypeus flattened (fig. 18)

[Character 21] **Expansion of inferior margin of clypeus on labrum in frontal view:** Borowiec (1995a) used this character (ch.#2) as clypeus horizontalization.

0: present (often only small portion expanded) (Shin et al. 2012, fig. 30)

1: absent (Shin 2013, figs. 20–22)

[Character 22] **Vertex lobe between compound eye and coronal sulcus on head in dorsal or frontal view:** vertex lobe was considered to be a modification of the surface between the compound eye and the coronal sulcus. The size and shape varied when it was present.

0: absent (Shin 2015, figs. 13–14)

1: present (Figs. 17–18)

[Character 23] **Head trichobothria in dorsal view:** the head trichobothria were only found in the medial upper regions between the compound eyes in tortoise beetles.

0: absent

1: present (only one) (Chaboo 2007, figs. 44A, C, F)

2: present (more than one) (Chaboo 2007, fig. 59D)

[Character 24**] Head in dorsal view, location of head trichobothria:** in the outgroup (two species of *Hemisphaerota*), similar trichobothria were found under the antennal sockets. However, those were considered non-homologous structures from those in ingroup species in this study (coded as inapplicable for two species of *Hemisphaerota*). This character was also coded as inapplicable for *Herissa pantherina* due to the absence of the trichobothria in this species.

0: adjacent to compound eyes (Chaboo 2007, figs. 44A, C, F)

1: distant from compound eyes (Fig. 18)

[Character 25] **Microtrichial patch on vertex of head in dorsal view:** the shape of the patch, size patch and number of fine setae varied among species. In few species (such as *Physonota alutacea*), it was shown as a few fine setae not as a patch (Fig. 56). However, those fine setae on the patch were easily distinguished by their short length from the other setae on head (see Ch#7 in this study).

0: absent (Figs. 50–52)

1: present (Figs. 53–57, marked by yellow arrow)

[Character 26] **Extension of coronal sulcus to microtrichial patch on vertex of head in dorsal view:** microtrichial patch were found only on the middle region of the head. When the patch and the coronal sulcus were connected, the fine setae located in the sulcus. Species without the microtrichial patch were coded as inapplicable (see Ch#25 in this study).

0: reaching to microtrichial patch (Fig. 47)

1: coronal sulcus and microtrichial patch separate (Fig. 45)

[Character 27] **Stridulatory file on postero-medial region in dorsal surface of head:** the stridulatory files were always observed on the postero-medial region of the head in dorsal view among tortoise beetles.

0: absent (Shin & Chaboo 2012, fig. 44)

1: present (Figs. 50–51, 53–57)

[Character 28] **Convexity of stridulatory file on head in dorsal view:** a convex stridulatory file was easily distinguished from a flat one when the head was observed in frontal or lateral view. Species without the stridulatory files were coded as inapplicable (see Ch#27 in this study).

0: convex (Fig. 18)

1: flat

[Character 29] **Broadest region of stridulatory file on head in dorsal view:** this character was used to define the shape of the stridulatory file. Species without the stridulatory files were coded as inapplicable (see Ch#27 in this study).

0: in anterior 1/3 region (Fig. 55)

1: in medial 1/3 region (Fig. 51)

2: in posterior 1/3 region (Fig. 50)

[Character 30] **Length of stridulatory file compared to length of head:** species without the stridulatory files were coded as inapplicable (see Ch#27 in this study).

0: longer than half length of head (Fig. 49)

1: as long as or shorter than half length of head (Fig. 42)

[Character 31] **Stridulatory file, posterior extension:** state 0 was applied when the posterior end of the stridulatory file was convex with clear ridges. Species without the stridulatory files were coded as inapplicable (see Ch#27 in this study).

0: reaching posterior margin of head (Fig. 49)

1: not reaching posterior margin of head (Fig. 43)

[Character 32] **Shape of file ridges on stridulatory file in male:** species without the stridulatory files were coded as inapplicable (see Ch#27 in this study).

0: clear (Fig. 57)

1: faint or irregular (Fig. 56)

[Character 33] **Space between file ridges on stridulatory file:** species without the stridulatory files were coded as inapplicable (see Ch#27 in this study).

0: absent (Fig. 51)

1: present (Figs. 53–54)

[Character 34**] Number of file ridges on stridulatory file:** the character states were defined by the frequency graphs of the ridge numbers. Species without the stridulatory files were coded as inapplicable (see Ch#27 in this study).

0: less than 60 (Fig. 51)

1: between 80 and 90 (Fig. 50)

2: between 100 and 210 (Fig. 53)

3: more than 230

[Character 35] **Stridulatory file in female:** a clear stridulatory file was always observed in male when a species possesses the stridulatory file. However, different shaped stridulatory files were observed in females of six species in this study. Species without the stridulatory files were coded as inapplicable (see Ch#27 in this study).

0: absent

1: present (only present in male, faint or absent in female) (Figs. 51–52)

2: present (female with clear file with less number of ridges than male)

[Character 36] **Antennal length:** Chaboo (2007, Ch.#49) used this character with two states based on the relative length with pronotum. In this study, it was modified and is presented as relative to the length of the head.

0: as long as or shorter than 2 times length of head (Shin & Chaboo 2012, figs. 44–46)

1: longer than 2 times length of head (Simões & Monné 2014, fig. 98)

[Character 37] **Shape of antennomeres III–X:** Chaboo (2007, Ch.#60) used a similar character with two states (apex wider than base, apex as wide as base). In this study, the shape was observed only of antennomeres III–X because antennomeres I, II, and XI were always elongate or oval in all species examined.

0: quadrate (or simple) (Shin & Chaboo 2012, figs. 44–46)

1: slightly serrate (Shin 2015, fig. 24)

[Character 38] **Antennal dorso-ventral flattening:** to distinguish the states for this character, the antennae should be examined at different angles.

0: absent (Simões & Monné 2014, fig. 98)

1: present (Shin 2015, fig. 24)

[Character 39] **Color of ventral surface of scape (antennomere I):** this character was used mainly for the physonotines. Nineteen species with black or dark scape were coded as inapplicable.

0: pale or brown (Shin & Chaboo 2012, figs. 44–46)

1: darker (only ventral surface) (Fig. 20)

[Character 40] **Length of antennomere III:** Chaboo (2007, Ch.#56) used this character based on the relative length with the scape. In this study, the length of the antennomere III was determined as relative to the length of the pedicel. The length of the pedicel was used because it was more consistent than the length of the scape among tortoise beetles.

0: as long as or shorter than pedicel

1: longer than pedicel, shorter than 2 times length of pedicel (Shin 2015, fig. 24)

2: longer than 2 times length of pedicel (Shin 2013, fig. 16)

[Character 41] **Length of antennomere IV** (see Ch.#40 in this study).

0: longer than pedicel, shorter than 2 times length of pedicle (Shin 2013, fig. 15)

1: as long as or longer than 2 times length of pedicel (Shin 2013, fig. 16)

2: as long as or shorter than pedicel (Chaboo 2007, fig. 48C)

[Character 42] **Color of ventral surface of antennomeres III–X:** this character was used to distinguish among species of *Physonota* in Boheman (1854). The antennomere XI was excluded because the dark coloration only on antennomere XI was often found independently among tortoise beetles (Shin et al. 2012). The pedicel was also excluded because it is always brown in species with pale yellow or pale brown antennae.

0: uniformly pale yellow to pale brown (Shin & Chaboo 2012, figs. 44–46)

1: color mixed (proximal antennomeres pale with distal antennomeres black) (Fig. 20)

2: completely black or dark brown (Shin 2013, fig. 16)

[Character 43] **Number of antennomeres with dark or black ventral surface between antennomeres III–X:** the number was counted starting at antennomere X. Species with uniformly brown or black antennae were coded as inapplicable (see Ch.#42 in this study).

0: 1

1: 2

2: 3

3: 4

4: 5

5: 6

[Character 44] **Antennal notches on ventral surface of antennomeres at posterior side:** Chaboo (2007, Ch.#59) used this character as “ventromarginal grooves” (see Chs# 45 and 46 in this study).

0: absent (Fig. 20)

1: present (Shin 2015, fig. 24)

[Character 45] **Number of antennomeres with antennal notch on posterior side:** species without antennal notches were coded as inapplicable (see Ch# 44 in this study).

0: 7 (between antennomeres V and XI) (Shin 2015, fig. 24)

1: 5 or 6 (between antennomeres VI or VII and XI: often notch on VI faint)

[Character 46] **Antennal notches on ventral surface of antennomeres on anterior side:** species without antennal notches were coded as inapplicable (see Ch# 44 in this study).

0: absent

1: present (only between antennomeres V and XI)

[Character 47] **Number of funicular antennomeres in male between antennomeres III–X:** this character was created to define the detailed shape of antennae. The number was counted from the antennomere III. Chaboo (2007, Ch.#61) used a similar character with two states (distal

antennomeres broader than long, longer than broad). In this study, the character states were more defined. State #2 (4 or 5 antennomeres) and #4 (7 or 8 antennomeres) included two discrete numbers because intraspecific variation was observed in several species.

0: 2 (Chaboo 2007, fig. 46G)

1: 3 (Chaboo 2007, fig. 46A)

2: 4 or 5 (Shin 2015, fig. 24)

3: 6

4: 7 or 8 (Fig. 20)

5: 0 (all antennomeres long than broad) (Simões & Monné 2014, fig. 98)

[Character 48] **Antennae, number of funicular antennomeres in female between antennomeres III–X:** the difference in antennae shape between males and females was observed in four species. This sexual dimorphism of the antennal shape was independent of to other sexual dimorphic characters such as size of abdomen and body shape (see Ch.#47 in this study).

0: 2

1: 3

2: 4 or 5

3: 6

4: 7 or 8

5: 0 (all antennomeres longer than broad)

[Character 49] **Number of basal glabrous antennomeres:** this character was used to distinguish among genera and species primarily of physonotines (Boheman 1954, 1956, 1962, Borowiec & Świętojańska 2014).

0: 3 (Chaboo 2007, fig. 46G)

1: 4 (Chaboo 2007, fig. 47K)

2: 5 (Shin 2013, fig. 16)

3: 6 (Chaboo 2015, fig. 46F)

[Character 50] **Shape of antero-medial emargination in labrum:** Chaboo (2007, Ch.#78) used the same character with two states. In this study, state 2 (bisinuate) was added.

0: narrow (Fig. 21)

1: broad (Shin 2015, fig. 16)

2: bisinuate

[Character 51] **Shape of antero-lateral line of labrum:** basal half of labrum is withdrawn into the head capsule in Cassidinae. The lateral line examined in this study was observed on the exposed anterior portion of labrum.

0: round (Shin 2015, fig. 16)

1: straight (Fig. 21)

2: concave

[Character 52] **Mandibular shape:** This character was adopted from Chaboo (2007, Ch.#79).

0: triangular (Shin & Chaboo 2012, fig. 100)

1: fist-shaped (Fig. 22)

[Character 53**] Mandibular horizontal ridge:** the horizontal ridge was observed in the basal half of each mandible and it is located next to the mandibular tooth II. The horizontal ridge was observed in most species with fist-shaped mandibles.

0: present (Fig. 22,)

1: absent

[Character 54] **Mandibular tooth I:** Chaboo (2007, Ch.#82) used the number of the mandibular teeth with 2 states (unidendate, bidentate or multiple). In this study, each mandibular tooth was considered as an independent character (Chs.#55–59). The location of each mandibular tooth was based on mandibular tooth II because its location was always next to the mandibular horizontal ridge on the base (Ch.#53). The width (as measured between top and bottom in frontal view) of each mandibular tooth between the mandibular teeth I–IV was subequal, which allowed missing teeth to be recognized. Mandibular teeth V and VI were often slightly narrower than the others.

0: present

1: absent

[Character 55] **Mandibular tooth II** (see Chs.#53 and 54 in this study).

0: present

1: absent

[Character 56] **Mandibular tooth III** (see Chs.#53 and 54 in this study).

0: present

1: absent

[Character 57] **Mandibular tooth IV** (see Chs.#53 and 54 in this study).

0: present

1: absent

[Character 58] **Mandibular tooth V** (see Chs.#53 and 54 in this study).

0: present

1: absent

[Character 59] **Mandibular tooth VI** (see Chs.#53 and 54 in this study).

0: present

1: absent

[Character 60] **Largest mandibular tooth (most prominent tooth medially in frontal view).**

0: mandibular tooth I

1: mandibular tooth II (Shin & Chaboo, fig. 59)

2: mandibular tooth III (Fig. 22)

3: mandibular tooth IV

[Character 61] **Maxillary galea:** often the basal half of maxillary galea exhibited brown coloration. Brown coloration should be distinguished from dividing line between segments.

0: undivided (Fig. 23)

1: divided (Shin 2015, fig. 18)

[Character 62] **Shape of maxillary galea:** the flattening and the shape were corresponded.

0: unflattened and oval (Fig. 23)

1: flattened and square

[Character 63] **Shape of labial ligula:** the lateral tangent lines of the ligula formed over 90˚ was considered as broad; less than 90˚ considered narrower.

0: broad and round (Shin & Chaboo 2012, fig. 62)

1: broad and pointed (Chaboo 2007, fig 24F)

2: narrow and pointed (Fig. 24)

3: narrow and rounded (Shin 2015, fig 19)

[Character 64] **Shape of labial palpomere I:** the labial palpomeres II and III were always long than broad in the examined species.

0: triangular (medial line longer than lateral line) (Shin & Chaboo, fig. 62)

1: oval or circle (as long as or slightly longer than broad) (Shin 2015, fig. 19)

2: rectangular (distinctly longer than broad) (Fig. 24)

[Character 65] **Broadest region of pronotum in dorsal view:** Chaboo (2007, Chs#84 and 85) used the shape of the lateral line of pronotum as characters, which might indicate the broadest points of the pronotum In this study, the character was separated from the shape of the lateral

line of the pronotum. The shape of the lateral line was divided into two different portions (anterior and posterior, Chs#75 and 76).

0: in anterior 1/3 region (Chaboo 2007, fig. 27)

1: in middle 1/3 region (Fig. 7)

2: in posterior 1/3 region (Fig. 6)

[Character 66] **Pronotal surface:** several species of *Physonota* and *Cistudinella* were characterized based on their pronotal surface (Hincks 1956, Borowiec 1995b).

0: smooth (Fig. 11)

1: irregularly depressed (Chaboo 2007, fig. 11C)

2: with transverse lines

3: punctate (Chaboo 2007, fig. 11I)

[Character 67] **Setae on pronotal disc:** this character was adopted from Chaboo (2007, Ch.#25) only for the surface of the pronotal disc.

0: absent (Fig. 11)

1: present (Simões & Monné 2014, fig. 99)

[Character 68] **Medial dark spot on pronotum:** Boheman (1854, 1856, 1862) used the medial dark spot to distinguish among subgroups within *Physonota*. Species with completely dark brown or black pronotum were coded as inapplicable.

0: absent

1: present (Fig. 11)

[Character 69] **Lateral dark spots on pronotum:** Boheman (1854, 1856, 1862) used the lateral dark spots to distinguish among subgroups within *Physonota*. Species with completely dark brown or black pronotum were coded as non-applicable.

0: absent

1: present (Fig. 11)

[Character 70] **Relative length to width of pronotal disc:** length was measure at the middle line and width was measure at the base. The anterior and lateral lamellae were not measured.

0: as long as or shorter than half width of pronotal disc (Fig. 3)

1: longer than half width of pronotal disc (Fig. 7)

[Character 71] **Pronotal anterior lamella:** the anterior lamella was distinguished by the differentiated surface between the disc and lamella or the projected dorsal head cavity line on the ventral surface of pronotum. Most species with the pronotum partially covering the head in dorsal view (Ch.#74(1)) still possessed the anterior lamella of the pronotum.

0: absent (Shin & Chaboo 2012, fig. 81)

1: present (Figs. 1–7)

[Character 72] C**olor of pronotal anterior lamella:** species without pronotal anterior lamella was coded as inapplicable (see Ch.#71 this study).

0: translucent (Fig. 5)

1: mostly translucent with white pigmented region (opaque) medially

2: opaque (Shin 2013, fig. 1)

[Character 73] **Shape of pronotal anterior lamella in lateral view:** species without pronotal anterior lamella was coded as inapplicable (see Ch.#71 this study).

0: evenly declined or flat (Fig. 15)

1: slight lifted (Shin 2015, figs. 7, 10)

[Character 74] **Shape of pronotal anterior region (line):** the anterior region was defined by the extended lines of the head cavity on the pronotum (Fig. 25). This character has been heavily emphasized in the previous phylogenetic studies. Borowiec (1995, Ch.#1) used this character with two states (compound eyes hidden or exposed). Chaboo (2007, Chs.#26 and 91) applied two characters based on the visibility of the compound eyes in dorsal view and the shape of anterolateral line.

0: concave (compound eyes completely exposed in dorsal view) (Shin & Chaboo 2007, fig. 81)

1: flat or slightly concave (compound eyes partially exposed in dorsal view) (Shin & Chaboo 2007, fig. 84)

2: convex (head completely covered by pronotum in dorsal view) (Figs. 1–7)

[Character 75] **Shape of pronotal anterior half on lateral line:** Chaboo (2007, Chs.#84, 85) used two characters based on the shape of the lateral lines on the pronotum. In this study, the lateral line of the pronotum was divided into anterior and posterior portions because each portion showed different variation in shape.

0: round (Figs. 1–7)

1: transverse and distinctly broader posteriorly (Shin & Chaboo 2012, figs. 88–90)

2: straight (parallel) or slightly broader posteriorly (Shin & Chaboo 2012, fig. 84)

[Character 76] **Shape of pronotal posterior half on lateral line** (see Ch.#75 in this study).

0: straight (parallel) (Shin & Chaboo 2012, figs. 90)

1: mostly rounded with straight posterior margin (Fig. 1)

2: straight and broadening posteriorly (Chaboo 2007, fig. 5A)

3: straight and narrowing posteriorly (Fig. 7)

4: round and broadening posteriorly (Fig. 6)

[Character 77] **Extension of pronotal postero-lateral angle comparing to postero-medial region:** most of tortoise beetles exhibited the pronotum with the postero-medial region more extended than the postero-lateral regions. However, some species possessed the angled postero-lateral regions as extended as the postero-medial region of the pronotum.

0: as extended as postero-medial region of pronotum (Shin & Chaboo, fig. 86)

1: not extended (Figs. 1–7)

[Character 78**] Shape of line between pronotal disc and pronotal lamella at postero-lateral region of pronotum:** this character was adopted from Chaboo (2007, Chs.#95) with modified character states. The basal line of the pronotal disc was defined by the black line.

0: pointed (less 90˚) (Figs. 1–2)

1: angled (over 90˚) (Simões & Monné 2014, fig. 99)

2: rounded or straight (around 180˚) (Figs. 3–7)

[Character 79] **Shape of half basal line (on side) of pronotal disc:** this character was adapted from Chaboo (2007, Ch.#94) with modified character states.

0: concave (Fig. 2)

1: flat (horizontal) (Shin 2013, fig. 7)

2: (weakly or broadly) sinuate (Figs. 3–7)

3: bisinuate (Chaboo 2007, fig. 10G)

[Character 80] S**hape of postero-medial expanded portion of pronotum on mesoscutellum**.

0: broadly expanded on mesoscutellum with expanded portion slightly angled (Fig. 1)

1: broadly expended on mesoscutellum with expanded portion rounded (Figs. 5–7)

2: bifid (Chaboo 2007, fig. 8E)

[Character 81**] Width of pronotal lamella at base:** all tortoise beetles possessed the pronotal lamella. Some tortoise beetles exhibited more expanded pronotal lamellae, which were broader than the half width of the pronotal disc.

0: narrower than half width of pronotal disc (Fig. 6)

1: as broad as or broader than half width of pronotal disc (Fig. 7)

[Character 82] **Continuity of lateral lamella on pronotum:** this character was used in Chaboo (2007, Ch.#87).

0: continuous to base (Figs. 1–7)

1: discontinuous to base (Simões 2014, fig. 57)

[Character 83] **Shape of dorsal head cavity line on ventral surface of pronotum (= plectrum).**

0: a projected line (Fig. 62)

1: two projected lines or band-like flattened structure (Fig. 63)

[Character 84] **Prosternal collar:** the prosternal collar is the anterior expanded portion of the prosternum. Generally, it is well-distinguished by the sulcus or depression.

0: absent (Chaboo 2007, fig. 28A)

1: present (Fig. 16)

[Character 85] **Antennal grove on prosternum:** the antennal groves were found between the prosternum and head cavity.

0: absent or indistinct (Fig. 25)

1: present

[Character 86] **Prosternal antero-lateral projections:** the prosternal antero-lateral projections might appear as having arisen from the ventral surface of the pronotum but those were expanded portions of prosternum (Shin 2015).

0: absent (Fig. 25)

1: present (Shin 2015, fig. 29)

[Character 87**] Continuity of prosternal collar:** two species of *Hemisphaerota* were coded as inapplicable because they do not possess the prosternal collar.

0: continuous from one side of ventral surface of pronotum to other side (Fig. 62)

1: mostly continuous but both sides not connected to ventral surface of pronotum

2: pronotal collar continuous only around mouth fossa (Fig. 62)

[Character 88] **Relative length between precoxal area and postcoxal area on prosternum.**

0: precoxal area longer (Fig. 25)

1: postcoxal area longer

2: length of precoxal area as long as postcoxal area

[Character 89] **Width of prosternal process between procoxal cavities:** this character was used in Chaboo (2007, Ch.#108) with two states (slender or broad). The width of the prosternal process was also used as a diagnostic feature at the genus level (Borowiec & Świętojańska 2014).

0: narrower than width of coxal cavity (Fig. 25)

1: as broad as width of procoxal cavity or broader than width of procoxal cavity

[Character 90] **Width between postero-lateral lobes of prosternal process.**

0: narrower than procoxal cavity (Fig. 63)

1: as broad as procoxal cavity

2: broader than procoxal cavity (Fig. 62)

[Character 91] **Connection between postero-lateral lobe and prosternal process.**

0: smoothly connected to medial lobe of prosternal process (Fig. 62)

1: postero-lateral lobes connected to prosternal process with posterior depressions

2: postero-lateral lobes connected to prosternal process with anterior depressions (Fig. 63)

3: postero-lateral lobe absent (Shin 2013, fig. 23)

[Character 92] **Shape of posterior edge of prosternal process:** Chaboo (2007, Ch.# 111) used with three characters states (rounded, angular, broad).

0: truncate (Chaboo 2007, fig. 64C)

1: round (Chaboo 2007, fig. 64E)

2: angular (over 90˚) (fig. 62)

[Character 93] **Surface of posterior half of prosternal process:** Chaboo (2007) created three characters (Chs.#109, 112, and113) describing the surface or prosternal process. In this study, only the surface was observed and coded.

0: flat (Fig. 62)

1: swollen (Fig. 63)

2: concave (Shin 2013, fig. 23)

[Character 94] **Shape of posterior line of pronotal hypomeron.**

0: concave (Fig. 25)

1: flat

2: convex

[Character 95] **Length of anterior mesonotal process:** the size of the mesoscutum in tortoise beetles was consistent. The length of the anterior mesonotal process was compared to the length of the lateral line of the mesoscutum.

0: shorter than length of lateral line of mesoscutum (Fig. 26)

1: as long as or longer than length of lateral line of mesoscutum (Shin 2015, fig. 31)

[Character 96] **Length of mesoscutellum.**

0: as broad as or broader than long (Fig. 11)

1: longer than broad (Chaboo 2007, fig. 27)

[Character 97] **Shape of mesoscutellum:** this character was also used in Chaboo (2007, Ch.#116).

0: triangular (Figs. 1–7)

1: square (Simões 2014, fig. 35)

[Character 98] **Antero-medial projection on mesoventrite:** this projection is generally covered by the posterior region of the prosternal process.

0: absent (Fig. 28)

1: present

[Character 99] **Shape of postero-medial ridge of mesoventrite**

0: V-shaped (Shin 2015, fig. 32)

1: U-shaped (Chaboo 2007, fig. 27B)

2: flat

[Character 100] **Shape of lateral surface of metaventrite:** this character was used in Sanderson (1948) as a diagnostic feature among the species of *Physonota*.

0: broadly convex (Shin 2015, fig. 32)

1: flattened, flattened surface forming triangular surface

2: distinctly flattened with angular projection laterally (Fig. 28)

[Character 101] **Black coloration on abdominal ventrites:** this character focused on the abdominal coloration of species of the physonotines. Four distinct patterns were observed. The abdomen with overall black or dark coloration was coded as inapplicable.

0: absent

1: present on medial and lateral edge areas (Fig. 16)

2: present only anterior region of each abdominal ventrite with posterior region brown

3: present only in later depressed areas with other region brown

4: present only in middle as one big black spot

[Character 102] **Suture between abdominal ventrites I and II:** a similar character was used in Chaboo (2007, Ch.#190) with two states (separate or fused).

0: absent (flat surface)

1: present (Fig. 16)

[Character 103] **Sexual dimorphism in abdominal shape.**

0: present (male rounded, female more elongate) (Shin et al. 2012, figs. 7–8)

1: absent

[Character 104] **Sexual dimorphism in abdominal ventrite V.**

0: absent (ventrite V as long as ventrite IV)

1: present (ventrite V 2 times longer than abdominal ventrite IV in female)

[Character 105] **Length of protibia:** the relative length of the tibia was measured. Some tortoise beetles exhibited shorter protibia and mesotibia than the length of each profemur and mesofemur. The measurement was made when the leg was folded.

0: as long as or slightly shorter (0.95 times) than profemur (Fig. 62)

1: distinctly shorter (0.75 times) than profemur (0.75 times)

[Character 106] **Length of mesotibia comparing to mesofemur** (see Ch.#105 in this study)

0: as long as or slightly shorter (0.95 times) than mesofemurr

1: distinctly shorter (0.75 times) than mesofemur

[Character 107] **Legs, dorsal flattening on tibiae:** if a species exhibited dorsal flattening on the tibia, the flattening was also found on other legs.

0: absent or indistinct

1: present

[Character 108] **Legs, black coloration on dorsal surface of tibiae:** this character was created for physonotines (most of them with brown legs). If species exhibited black coloration on the dorsal surface of the tibia, it was also found on other legs. Species with black tibiae were coded as inapplicable.

0: absent (brown, no black coloration)

1: present (on brown tibia) (Fig. 32)

[Character 109] **Legs, spine on dorso-anterior apex of tibiae:** this character was used in Boheman (1862) to define one of the subgroups in *Physonota*. This character was also used in Chaboo (2007, Ch.#168).

0: absent

1: present

[Character 110] **Length of tarsomere III in all legs:** Chaboo (2007, Ch.#181) used a similar character focusing on the length of tarsomere V instead of the length of tarsomere V.

0: elongate, extending to anterior tangent line of pretarsal claws (Simões 2014, fig. 37)

1: not extending, pretarsal claws exposed from lobes of tarsomere III (Fig. 33)

[Character 111] **Legs, paired projections on tarsomere V:** this character was a diagnostic character for species of *Enagria* (Borowiec & Świętojańska 2014).

0: absent

1: present

[Character 112] **Modification of pretarsal claw:** this character was used in Borowiec (1995a, Ch.#12) and Chaboo (2007, Ch.#187).

0: absent (Fig. 32)

1: present (one tooth on each pretarsal claw) (Shin 2013, figs. 17–19)

2: micropectinate (several small teeth on each pretarsal claw) (Riley 1986, fig. 14)

[Character 113] **Angle between pretarsal claws:** this character was used in Borowiec (1995a, Ch.#13) and in Chaboo (2007, Ch.#186). In both previous studies, this character was used only with two character states (divergent and parallel (=adjacent)). In this study, the character states were modified to be defined by angles.

0: up to 90˚

1: between 90˚ and 150˚ (Shin 2013, figs. 17–19)

2: almost 180˚ (Fig. 62)

3: adjacent (Simões 2014, fig. 38)

[Character 114] **Lateral extension of elytral discal base.**

0: absent (Figs. 1–7)

1: present (Chaboo 2007, fig. 12A)

[Character 115] **Anterior extension of elytra lamellae:** Chaboo (2007, Ch.# 132) used the same character with the same character states.

0: absent (Fig. 6)

1: present (distinctly extended near middle line of pronotum) (Simões 2014, fig. 69)

[Character 116] **Width between elytral base in female:** Chaboo (2007, Ch.#136) also used this character. In this study, the width was measured only on female specimens because males in some species with sexual dimorphism of elytral shape might possess wider elytra (Shin et al. 2012, Ch.# 124 in this study).

0: elytral base as broad as or slightly broader than pronotal base (Fig. 1)

1: elytral base distinctly broader than pronotal base (Fig. 5)

[Character 117] **Elytral height in lateral view:** Chaboo (2007, Ch.#22) used a similar character based on the dorsal line in lateral view with two character states (continuous or discontinuous). In this study, it was modified as height of elytra relative to pronotal height.

0: elytral height as tall as or slight taller than pronotal height (Chaboo 2007, fig. 14I)

1: elytral height 1.1–1.5 times length of pronotal height (Chaboo 2007, fig. 14K)

2: elytral height taller than pronotal height (over 1.5 times) (Chaboo 2007, fig. 14H)

[Character 118] **Convexity in profile (height: length ratio of elytral disc):** Boheman (1862) distinguished the subgroups based on convexity (convex or less convex). Chaboo (2007, Ch.#23) used a similar character with two states (flattened or convex (acute)). In this study, height and length were measured from the discal area because the lamella often expanded ventrally.

0: slight convex (less than 0.3) (Chaboo 2007, fig. 14I)

1: moderately convex (between 0.3 and 0.5) (Chaboo 2007, fig. 13B)

2: distinctly convex (over 0.5) (Chaboo 2007, fig. 13M)

[Character 119] **Dorsal line of elytra in profile:** Boheman (1862) distinguished the subgroups based on angulate dorsal line in lateral view. Chaboo (2007, Chs.#23 and 151) used each acute (= angulate) elytra and spinose elytra in different characters.

0: rounded (Fig. 14)

1: angulate (over 60˚) (Fig. 15, Simões & Monné 2014, fig. 100)

2: profoundly acute, forming a spine (less than 60˚) (Simões 2014, fig. 70)

[Character 120] **Broadest point of elytra in dorsal view**

0: at base (when lateral sides parallel apply 0) (Fig. 2)

1: between the base and posterior tangent line of elytral umbones (Fig. 5)

2: between posterior tangent line of elytral umbones and middle of elytra (Fig. 1)

[Character 121] **Elytral umbo(nes):** this character was also used in Chaboo (2007, Chs.#89) with the same character states.

0: present (distinct) (Fig. 6)

1: absent (indistinct) (Shin 2013, fig. 1)

[Character 122] **Bulging structure on each mid-lateral region of elytron:** This structure was described in all species of *Asteriza* (Shin et al. 2012), *C. punctipennis*, *Ph. convexa*, *Ph. pacifica*, *Cassida nebulosa*, *Cheridotis miniata*, *Omotenia humeralis*, and *Paranota enifera* in this study.

0: present (distinct) (Fig. 3)

1: absent (indistinct) (Fig. 6)

[Character 123] **Shape of outline between base and posterior tangent line of elytral umbones in dorsal view:** this character was also used in Chaboo (2007, Ch.#129) with two character states (subparallel or rounded wider at posterior). In tortoise beetles, the posterior half of the elytral lateral line is always narrower posteriorly. In this study, the measured region was delimited by the base and the posterior tangent line of the umbones to clarify the variation.

0: parallel (Fig. 2)

1: broader posteriad (Fig. 1)

2: narrower posteriad (Chaboo 2007, fig. 5A)

[Character 124] **Sexual dimorphism in elytral lamella in umbo area** (Shin et al. 2012).

0: present (broader in male than in female) (Shin et al. 2012, figs. 7–8)

1: absent

[Character 125] **Medial margin interval line of elytra:** commonly the medial margin was defined by stria or punctures. In this study, only the stria structure was considered as the interval line.

0: absent (Fig. 3)

1: present (Fig. 2)

[Character 126] **Setae on elytral surface:** this character was also used in Chaboo (2007, Ch.#25).

0: absent

1: present (Simões & Monné 2014, Fig. 102)

[Character 127] **Punctures on elytral surface.**

0: absent (Fig. 7)

1: present (Figs. 1–3)

[Character 128] **Shape of punctuation on elytra:** Chaboo (2007, Ch.#144) used the punctuation on the elytra with three character states (striae, random or in round clusters). In this study, only two states were considered because no species were found with punctures in round clusters.

0: regular, forming column (= striae) (Fig. 2)

1: irregularly punctate (Fig. 3)

[Character 129] **Size of punctures on elytra:** the state coarse was chosen when the middle of the puncture was clearly defined at a lower level than the elytral surface

0: fine (Fig. 2)

1: coarse (Fig. 1)

[Character 130] **Space between punctures on elytra:** this character and its character states were used to characterize the density of the punctation on the elytra.

0: broader than 5 times of diameter of punctures (Fig. 3)

1: narrower than 5 times of diameter of punctures (Shin 2013, fig. 6)

2: mixed (irregular) (Fig. 1)

[Character 131] **Reticulation among punctures on elytra.**

0: absent

1: present (Shin 2013, Fig. 10)

[Character 132] **Width of elytra lamella at posterior tangent line of umbones in female:** the width of the elytral lamella has been considered an important character for identification of tortoise beetles. Borowiec (1955a, Ch#11) used the width of the elytral lamella to distinguish tortoise beetles from leaf-mining beetles. Chaboo (2007, Ch.#134) compared the widths between the elytral disc and the elytra lamella. In this study, the states were more defined and measured only at the posterior tangent line of the elytra umbones in females (see Ch#124 in this study).

0: as broad as or narrower than width of mesoscutellum (Fig. 2)

1: broader than width and narrower 1/4 width of elytral disc (Fig. 3)

2: broader than 1/4 width and narrower than 1/2 width of elytral disc (Fig. 5)

3: as broad as 1/2 width or broader than 1/2 width of elytral disc (Fig. 7)

[Character 133] **Transparency of elytral lamellae.**

0: translucent (Fig. 5)

1: opaque (Simões & Monné 2014, fig. 102)

[Character 134] **Punctures on elytral lamellae:** this character was used to distinguish among the species of *Cistudinella* (Hincks 1956).

0: smooth

1: punctate

[Character 135] **Marginal thickening on elytral lamella:** this is a diagnostic character for species of *Asteriza* (Shin et al. 2012, Borowiec & Świętojańska 2014).

0: absent (Fig. 6)

1: present (Fig. 3)

[Character 136] **Shape of postero-medial region of elytral disc (elytra meeting point):** a similar character was used with the postero-medial region of elytral lamellae in Boheman (1854, 1856, 1862) (see Ch.#138 in this study). In this study, the shape of the elytral disc and shape of the elytral lamella were used as two separate characters.

0: round (Fig. 6)

1: pointed (Fig. 7)

[Character 137] **Continuity of elytral lamellae at rear end.**

0: continuous (Fig. 7)

1: discontinuous (vague) (Fig. 5)

[Character 138] **Shape of posterior end of elytral lamellae (elytra meeting point):** This character was used in Boheman (1854, 1856, 1862) to distinguish among the subgroups of *Physonota*. Chaboo (2007, Ch.#140) also used a similar character with two states (truncate or round) for coding of some leaf-mining beetles and other cassidines.

0: rounded (Fig. 6)

1: pointed (Fig. 4)

[Character 139] **Shape of elytral hypomeron next to metathoracic pleuron.**

0: linear or round (Fig. 16)

1: angled

[Character 140] **Length of epipleural ridge on elytra in ventral view:** this character was one of the diagnostic characters for the species in Eugenysini (Hincks 1952).

0: short (ending before middle of elytra) (Fig. 16)

1: long (extending over middle of elytra) (Shin 2013, fig. 12)

[Character 141] **Longitudinal carina on ventral surface of elytra:** this character was used in Chaboo (2007, Ch.#154) with the same character states.

0: present (Fig. 30)

1: absent

[Character 142] **Connection between longitudinal carina and brace on ventral surface of elytron:** this character was used in Chaboo (2007, Ch.#155) with the same character states. The species without the longitudinal carina (i.e. two species of *Enagria*) were coded as inapplicable (see Ch.#141 in this study).

0: separate

1: connected (Fig. 30)

[Character 143] **Angle between longitudinal carina and brace on ventral surface of elytron:** the character state was determined by the direction of the elytral brace because the direction of the longitudinal carina was consistent. The species without the longitudinal carina (i.e. two species of *Enagria*) were coded as inapplicable (see Ch.#141 in this study).

0: angled (Fig. 30)

1: parallel, or smoothly connected

[Character 144] **Width of elytral lamella on posterior end:** the comparative width of elytral lamella was measured based on the length of mesoscutellum because the length of the mesoscutellum was consistent among tortoise beetles.

0: as broad as or narrower than length of mesoscutellum (Fig. 2)

1: longer than mesoscutellum and shorter than 2 times length of mesoscutellum (Fig. 1)

2: longer than 2 times but shorter than 3 times length of mesoscutellum (Chaboo 2007, fig. 7L)

[Character 145] **Size of median lobe in aedeagus:** variation was found in the proportion of the length of the phallobase to the length of the median lobe. However, the length of phallobase was thought to be consistent among tortoise beetles. In this study, the length of the median lobe was measured as compared to the length of the phallobase.

0: shorter than 2 times length of phallobase (Shin 2015, fig. 35)

1: longer than 2 times length of phallobase (Fig. 34)

[Character 146] **Shape of gastral spiculum in aedeagus:** gastral spiculum was located in the posterior region of the median lobe. The variation in shape was previously described in Shin & Chaboo (2012), Shin et al. (2012), and Shin (2015).

0: anterior tip with paired arms (Y-shaped)

1: anterior tip reduced (V-shaped) and paired arms connected (Fig. 34)

2: anterior tip absent and paired arms separate as two segments (Shin et al. 2012, fig. 64)

3: absent

[Character 147] **Shape of paired arms of gastral spiculum in aedeagus:** The species without the gastral spiculum (i.e. *Basiprionota octopunctata*) were coded as inapplicable (see Ch.#146 in this study).

0: straight (Shin & Chaboo, fig. 68)

1: rounded (Fig. 34)

2: sinuate or slightly curved (Shin et al. 2012, fig. 64)

[Character 148] **Size of seminal vesicle of male genitalia:** the variation in thickness was previously described in Shin & Chaboo (2012), Shin et al. (2012), and Shin (2015).

0: thick (2 times as thick as or thicker than ejaculatory duct) (Shin et al. 2012, fig. 59)

1: thin (slightly thicker than ejaculatory duct) (Fig. 34)

[Character 149] **Angle between paired arms of gastral spiculum in aedeagus:** the angle between the separate arms was measured from the extended lines. Gastral spiculum was fixed on the membranous structure surrounding the median lobe. Therefore, the angle between the arms

was fixed. The species without the gastral spiculum (i.e. *Basiprionota octopunctata*) were coded as inapplicable (see Ch.#146 in this study).

0: less than 90˚ (Shin & Chaboo 2012, fig. 68)

1: more than 90˚ (Shin 2015, fig. 35)

[Character 150] **Shape of spermathecal vasculum in female genitalia:** the shape of the spermatheca showed great variation among the examined specimens. The character states were defined based on the distance between the apex and the opening of the vasculum.

0: loop (distance between apex and opening of vasculum as broad as or narrower than 1.5 times width of vasculum at broadest point) (Shin 2015, fig. 40)

1: falcate (distance between apex and opening of vasculum as broad as between 1.5 times and 3 times width of vasculum at broadest point) (Fig. 35)

2: C-shaped (distance between apex and opening of vasculum broader than 3 times width of vasculum at broadest point) (Shin & Chaboo 2012, fig. 78)

[Character 151] **Relative width of spermathecal ampulla with width of vasculum in female genitalia:** the spermathecal ampulla is a small chamber adjacent to the opening of the vasculum. The width and length of the spermathecal ampulla varied whereas the width of the vasculum was non-variable. In this study, the relative width was measured for the ampulla relative to the width of the vasculum.

0: narrower than vasculum at broadest point (Fig. 35)

1: as broad as or broader than vasculum at broadest point (Shin & Chaboo, 2012, fig. 78)

2: distinctly broader than vasculum at broadest point

[Character 152] **Relative length of spermathecal ampulla with length of vasculum in female genitalia.**

0: shorter than1/4 length of vasculum or absent (Shin 2015, fig. 39)

1: as long as 1/4 length of vasculum or longer than 1/4 length of vasculum (Fig. 35)

[Character 153] **Direction of vasculum apex in female genitalia.**

0: toward to opening (Shin et al. 2012, figs. 67–70)

1: toward same direction with posterior region of vasculum (Shin 2015, fig. 39)

2: toward to opposite direction of vasculum opening (Shin & Chaboo, 2012, fig. 72)

[Character 154] **Shape of spermathecal duct in female genitalia:** Chaboo (2007, Chs.#206, 207, 208) used three characters based on length, shape, and number of coils. In this study, only four patterns were observed from the morphology of the spermathecal ducts.

0: tightly coiled long duct (Chaboo 2007, fig. 76J)

1: loosely tangled (short duct) (Fig. 35)

2: tangled (long duct) (Shin et al. 2012, fig. 67)

3: not coiled or tangled (irregularly curved long duct) (Chaboo 2007, fig. 75J)

[Character 155] **Extra chamber near opening of vasculum in female genitalia:** This character was used in Chaboo (2007, Ch.#200) based on the number of the chamber(s) with two states (one

or more than one). In this study, only one extra chamber was found in some species and most of species lacked an extra chamber.

0: absent (Fig. 35)

1: present (Chaboo 2007, fig. 75C)

Appendix 3. Data Matrix for Cladistic Analysis

All multiple character states were indicated in the data matrix. Inapplicable character state was coded with "-" and treated as a separate character state.

	1	2	3	4	5	6	7	8	9	10	11	12	13	14	15	16	17	18	19	20	21	22	23	24	25	26	27	28	29	30	31
Hemisphaerota cyanea	1	0	1	1	1	0	1	0	0	1	1	1	0	0	2	0	1	0	0	0	1	0	1	-	0	-	0	-	-	-	-
Hemisphaerota sp.	1	0	1	1	1	0	1	0	0	1	1	1	0	0	2	0	0	0	1	0	1	0	1	-	0	-	0	-	-	-	-
Basiprionota octopunctata	1	0	0	1	1	0	1	0	0	1	1	1	0	0	0	1	0	0	0	0	1	0	1	1	0	-	0	-	-	-	-
Asteriza blakeae	1	0	0	0	1	1	0	1	0	1	1	0	1	0	0	0	1	0	0	1	0	1	1	1	1	0	1	0	0	0	0
Asteriza darlingtoni	1	0	0	0	1	1	0	1	0	1	1	0	1	0	0	0	1	0	0	1	0	1	1	1	1	0	1	0	0	0	0
Asteriza flavicornis	1	0	0	1	1	1	0	1	0	1	1	0	1	0	0	0	1	0	1	1	0	1	1	1	1	1	1	0	0	0	0
Asteriza tainosa	1	0	0	1	1	1	0	1	0	1	1	0	1	0	0	0	1	0	1	1	0	1	1	1	1	1	1	0	0	0	0
Cistudinella apiata	1	1	1	1	0	1	1	0	0	0	1	1	1	1	012	0	1	0	1	1	0	0	1	0	0	-	1	0	1	1	1
Cistudinella foveolata	0	1	1	1	0	1	1	0	0	0	1	1	1	1	0	0	0	0	0	1	0	0	1	0	0	-	1	0	2	1	0
Cistudinella inanis	1	1	1	1	0	1	1	0	0	0	1	1	1	1	1	0	1	1	1	1	0	0	1	0	0	-	1	0	2	1	0
Cistudinella lata	1	1	1	0	0	0	1	0	0	0	1	1	1	1	0	0	1	0	1	1	0	0	1	0	0	-	1	1	2	1	0
Cistudinella lateripunctata	1	1	1	1	0	1	1	0	1	0	1	1	1	1	0	0	0	1	0	1	0	0	1	0	0	-	1	0	1	1	0
Cistudinella notata	1	1	1	1	1	1	0	0	0	0	1	1	2	1	0	0	1	1	1	1	0	0	1	0	0	-	1	0	2	1	0
Cistudinella obducta	1	1	1	1	0	1	1	0	1	0	1	1	1	1	0	0	0	0	1	1	0	0	1	0	0	-	1	0	2	1	0
Cistudinella parva	1	1	1	1	0	1	1	0	0	0	1	1	1	1	0	0	1	0	1	1	0	0	1	0	0	-	1	?	2	1	0
Cistudinella peruana	1	1	0	1	1	0	1	0	0	0	1	1	0	1	0	0	1	1	1	1	0	0	1	0	0	-	1	0	2	1	0
Cistudinella punctipennis	1	1	1	1	0	1	1	0	0	0	1	1	1	1	0	0	0	0	1	1	0	0	1	0	0	-	1	0	2	1	0
Eurypedus nigrosignatus	1	1	1	1	1	0	1	1	1	0	0	1	2	1	0	0	1	0	1	1	0	1	1	0	0	-	1	0	1	1	1
Eurypedus peltoides	1	1	1	1	0	1	1	1	0	0	1	2	1	0	0	0	1	0	1	1	0	1	1	0	0	-	1	0	1	1	1
Enagria angulifera	1	0	0	0	1	1	1	0	1	0	1	0	0	0	0	0	0	1	1	0	0	1	1	1	1	0	1	0	1	1	0
Enagria ovata	1	0	0	0	1	1	1	0	1	0	1	0	0	0	0	0	0	1	1	0	0	1	1	1	1	0	1	0	1	1	0
Eurypepla calochroma	1	0	0	1	0	0	1	0	0	1	1	0	01	0	0	0	1	1	0	1	0	1	1	0	1	0	1	0	0	0	0
Physonota alutacea	1	0	0	1	1	01	0	1	2	1	1	1	1	0	1	0	0	0	1	0	0	1	1	1	1	1	1	0	0	0	0
Physonota arizonae	1	0	0	0	1	1	1	1	1	0	1	1	1	0	2	0	0	0	1	0	0	1	1	1	1	0	1	0	0	1	0
Physonota attenuata	1	0	0	0	1	1	0	1	2	1	1	1	1	0	2	0	0	1	1	0	0	1	1	1	1	0	1	0	0	0	0
Physonota calcarata	1	0	0	1	0	2	1	1	0	0	1	1	1	?	2	0	0	0	1	0	0	1	1	0	1	0	1	0	2	0	0
Physonota caudata	0	0	0	0	0	1	0	1	2	1	1	1	0	0	2	0	0	0	1	0	0	1	1	1	1	0	1	0	2	0	0
Physonota cerea	0	0	0	0	0	0	0	0	1	0	1	0	0	0	0	0	1	0	1	1	0	1	1	1	1	0	1	0	0	1	0
Physonota citrina	0	0	0	0	0	1	0	0	1	0	1	1	0	0	0	0	01	0	1	1	0	1	1	1	1	0	1	0	0	1	0
Physonota convexa	1	0	0	0	1	1	1	1	1	1	1	1	2	0	2	0	0	1	1	1	0	1	1	1	1	0	1	0	0	0	0
Physonota disjuncta	1	0	0	0	0	1	0	0	1	0	0	0	0	0	0	0	0	0	1	0	0	1	1	1	1	0	1	0	0	1	0
Physonota eucalypta	1	0	0	0	1	1	0	0	1	0	1	1	2	0	2	0	0	0	1	0	0	1	1	1	1	0	1	0	0	1	0
Physonota gigantea	1	0	0	0	1	1	0	1	1	1	1	1	0	0	0	0	1	0	1	0	0	1	1	1	1	0	1	0	1	0	0
Physonota helianthi	1	0	0	0	0	12	0	2	2	0	1	1	1	0	2	0	0	1	1	0	0	1	1	0	1	0	1	0	1	0	0
Physonota humilis	0	0	0	0	0	1	0	0	1	0	1	0	1	0	0	0	0	0	1	0	0	1	1	0	1	0	1	0	1	1	0
Physonota incrustata	1	0	0	0	1	1	0	0	1	1	1	1	2	0	2	0	0	0	1	0	0	1	1	1	1	0	1	0	0	0	0
Physonota limoniata	1	0	0	0	1	1	0	0	1	0	1	1	2	0	2	0	0	0	1	0	0	1	1	1	1	0	1	0	0	1	0
Physonota lutarella	1	0	0	1	1	1	0	1	2	1	1	1	1	0	2	0	1	0	1	0	0	1	1	1	1	1	1	0	1	1	0
Physonota maculiventris	1	0	0	1	1	1	1	2	2	0	1	1	1	1	2	0	0	1	1	0	0	1	1	0	1	1	1	0	0	0	1
Physonota mexicana	0	0	0	0	0	1	0	0	0	0	1	0	0	0	0	0	0	1	1	0	0	1	1	1	1	0	1	0	2	1	1
Physonota nitidicollis	0	0	0	0	1	1	0	0	2	0	1	1	0	0	0	0	1	0	1	1	0	1	1	1	1	0	1	0	1	1	0
Physonota ovalis	0	0	0	0	0	1	0	0	1	0	1	1	1	0	2	0	0	0	1	0	0	1	1	1	1	0	1	0	1	1	1
Physonota pacifica	?	0	?	?	?	?	?	2	2	1	1	1	1	0	2	0	1	0	1	0	0	1	1	1	?	?	?	?	?	?	?
Physonota picticollis	1	0	0	1	1	1	0	0	1	0	1	1	1	0	2	0	0	0	1	0	0	1	1	0	1	0	1	0	1	1	0
Physonota puncticollis	1	0	0	1	1	1	0	0	1	0	1	1	1	0	0	0	0	0	1	0	0	1	1	0	1	1	1	0	0	1	0
Physonota separata	1	0	0	0	0	12	0	0	2	0	1	1	1	0	2	0	0	0	1	0	0	1	1	1	1	1	1	0	1	1	0
Physonota sp.	?	0	?	?	?	?	?	1	2	0	0	1	2	0	2	0	0	1	1	0	0	1	1	1	?	?	?	?	?	?	?
Physonota stigmatillis	1	0	0	0	0	1	1	2	2	0	0	1	1	0	2	0	0	0	0	0	0	1	1	1	1	0	1	0	1	0	0
Physonota sublaevigata	0	0	0	0	0	0	0	0	0	0	1	1	0	0	0	0	0	1	1	1	0	1	1	0	1	0	1	0	1	1	1
Physonota translucida	0	0	0	1	1	1	1	0	0	0	1	1	1	0	0	0	0	0	1	1	0	1	1	1	1	1	1	0	2	1	1
Physonota turgida	1	0	0	0	0	1	0	0	1	0	1	1	1	0	0	0	0	0	1	0	0	1	1	1	1	0	1	0	0	0	0
Physonota unipunctata	1	0	0	0	1	1	0	0	1	0	1	1	0	0	0	0	1	0	1	0	0	1	1	1	1	0	1	0	1	0	0
Physonota vitticollis	1	0	0	0	1	12	0	0	0	0	1	1	1	0	2	0	0	0	1	1	0	1	1	1	1	0	1	0	2	0	0
Physonota vittifera	1	0	0	0	0	1	0	1	1	0	1	1	1	0	2	0	0	0	1	0	0	1	1	0	1	0	1	0	1	0	0
Platycycla deruta	1	0	0	1	1	2	1	0	1	0	1	1	1	0	02	0	1	0	1	1	0	1	1	0	1	0	1	0	0	0	0
Aspidimorpha dissentanea	0	1	1	0	0	1	1	0	0	1	0	0	2	0	0	1	0	0	1	0	0	1	1	1	1	0	-	1	0	0	1	1
Lacooptera murrayi	0	1	1	0	1	0	1	0	0	1	0	1	0	0	0	1	0	0	1	0	0	1	1	1	1	0	1	0	0	1	1
Aspidimorpha sp.	1	1	1	1	1	1	1	0	0	1	0	0	0	0	0	1	0	0	1	0	0	1	1	1	1	0	-	1	0	1	0	1
Aspidimorpha miliaris	1	0	1	1	1	0	1	0	0	1	0	1	1	0	0	1	0	1	0	0	0	1	1	1	1	-	1	0	1	1	0
Cassida nebulosa	1	0	1	1	1	1	0	0	0	1	1	0	0	0	1	1	0	0	0	0	0	1	1	1	1	0	1	0	1	1	0
Cheridotis miniata	1	0	1	1	1	0	1	0	0	1	1	1	0	0	0	1	0	1	1	0	0	1	1	1	1	1	0	-	-	-	-
Coptocycla undecimpunctata	1	1	1	1	1	0	1	0	0	1	1	1	1	0	0	1	0	1	1	0	0	1	1	1	1	0	0	-	-	-	-
Dorynota bidens	1	1	0	0	1	0	1	0	2	1	1	1	2	0	0	0	0	0	1	0	0	0	2	0	0	-	0	-	-	-	-
Omotenia humeralis	0	0	0	1	1	0	1	0	0	1	0	0	0	0	0	0	0	1	0	0	0	0	1	0	0	-	0	-	-	-	-
Paranota enifera	1	0	0	0	1	0	1	0	0	1	1	1	1	0	0	0	0	0	1	0	0	0	2	0	0	-	0	-	-	-	-
Paratriona turrifera	1	0	0	0	1	0	1	0	0	1	1	0	1	0	0	0	0	1	1	0	0	0	2	0	0	-	0	-	-	-	-
Chlamydocassis bicornuta	1	1	0	0	0	0	1	0	1	0	1	1	1	1	1	0	0	0	0	1	0	0	1	0	0	-	0	-	-	-	-
Chlamydocassis cribripennis	1	1	1	0	0	0	1	0	2	0	1	1	1	1	0	0	0	0	0	0	0	0	1	0	0	-	0	-	-	-	-
Chlamydocassis metallica	1	1	1	0	0	0	1	0	1	0	1	1	0	1	0	0	0	0	0	0	0	0	1	0	0	-	0	-	-	-	-
Goniochenia quadraticollis	1	0	0	0	0	1	1	0	1	0	1	1	1	0	1	0	1	0	0	1	0	0	2	0	1	0	1	0	1	1	0
Herissa pantherina	1	0	0	0	1	0	1	1	1	1	1	1	1	0	1	1	1	0	1	1	1	0	0	-	0	-	1	0	1	0	0
Polychalma multicava	1	1	0	0	0	0	1	1	0	0	1	1	1	1	0	0	1	0	0	1	0	0	1	0	0	-	0	-	-	-	-
Zeugonota quadrinodosa	1	1	1	0	0	0	1	0	1	1	1	1	1	1	1	0	1	0	1	1	0	0	1	0	0	-	0	-	-	-	-
Carlobruchia tricostata	1	1	0	0	1	3	0	1	1	1	0	1	1	0	1	1	0	0	1	1	1	1	2	0	0	-	1	1	2	1	1
Canistra osculatii	1	0	0	?	1	?	?	0	0	0	1	1	0	0	0	1	1	0	0	0	1	1	2	0	0	-	?	?	?	?	?
Cassidinoma denticulata	1	0	0	0	0	3	0	1	1	1	0	1	1	0	1	1	1	0	1	1	1	1	0	0	0	-	1	1	2	1	1
Cyclosoma palliata	1	1	1	0	0	3	1	0	0	0	1	1	1	0	0	0	1	0	1	1	0	1	2	0	1	-	1	1	2	1	0
Discomorpha variegata	1	1	0	1	1	0	1	0	0	0	1	1	1	0	0	0	1	1	1	1	0	1	2	0	1	1	1	0	2	1	0
Omocerus bicornis	1	0	0	0	0	3	1	0	1	1	1	1	1	0	0	0	1	0	1	1	0	1	2	0	0	-	1	0	1	1	0
Polychalca punctatissima	1	0	0	0	1	3	1	0	1	0	1	1	1	0	0	0	1	0	1	1	0	1	1	0	0	-	1	1	2	1	0
Agenysa caedemadens	0	0	0	0	0	1	1	0	1	0	1	1	0	0	0	0	1	0	0	0	1	?	1	0	0	-	0	-	-	-	-
Chelymorpha cassidea	0	0	0	0	0	1	1	0	1	0	1	1	1	0	1	0	0	0	1	0	1	1	1	0	0	-	0	-	-	-	-
Mesomphalia gibbosa	0	0	0	0	0	1	1	0	1	0	0	1	1	0	1	0	1	0	1	1	1	0	2	0	0	-	0	-	-	-	-
Stolas sp.	0	0	0	0	0	?	1	0	1	0	0	1	0	0	0	0	1	0	0	0	1	0	1	0	0	-	0	-	-	-	-

	32	33	34	35	36	37	38	39	40	41	42	43	44	45	46	47	48	49	50	51	52	53	54	55	56	57	58	59	60	61	62
Hemisphaerota cyanea	-	-	-	-	0	0	0	1	0	2	0	-	0	-	0	1	1	3	1	1	0	1	1	0	1	1	1	1	1	1	0
Hemisphaerota sp.	-	-	-	-	0	0	0	0	0	2	0	-	0	-	0	1	1	3	1	1	0	1	1	0	1	1	1	1	1	1	0
Basiprionota octopunctata	-	-	-	-	1	0	0	0	0	0	0	-	0	-	0	5	5	2	?	1	1	0	1	0	0	0	0	0	1	1	0
Asteriza blakeae	0	0	2	0	0	0	0	0	1	0	0	-	0	-	0	3	3	0	0	1	1	0	0	0	0	0	0	1	2	0	0
Asteriza darlingtoni	0	0	2	0	0	0	0	0	1	0	0	-	0	-	0	3	3	0	0	1	1	0	0	0	0	0	0	1	2	0	0
Asteriza flavicornis	0	0	2	0	0	0	0	0	1	0	0	-	0	-	0	3	3	0	0	1	1	0	0	0	0	0	0	1	2	0	0
Asteriza tainosa	0	0	2	0	0	0	0	0	1	0	0	-	0	-	0	3	3	0	0	1	1	0	0	0	0	0	0	1	2	0	0
Cistudinella apiata	0	0	1	0	0	1	1	0	1	0	1	4	1	0	0	3	3	0	0	1	1	0	1	0	0	0	1	1	3	1	0
Cistudinella foveolata	0	0	2	0	0	1	1	0	1	0	1	3	1	0	0	3	3	0	0	1	1	0	1	0	0	0	1	1	2	1	0
Cistudinella inanis	0	0	1	0	0	1	1	0	1	0	1	5	1	0	0	3	3	0	0	1	1	0	0	0	1	1	1	0	3	1	0
Cistudinella lata	1	0	1	?	0	0	1	1	1	1	1	3	1	0	0	5	5	0	0	1	1	0	1	0	0	0	0	1	2	1	0
Cistudinella lateripunctata	0	0	2	0	0	1	1	0	1	1	1	3	1	0	1	3	3	0	0	1	1	0	1	1	0	0	0	1	2	1	0
Cistudinella notata	0	01	2	1	0	1	1	0	1	0	1	3	1	0	0	2	2	0	0	1	1	0	1	0	0	0	0	0	1	2	1	0
Cistudinella obducta	0	01	2	0	0	1	1	0	1	0	1	3	1	0	0	3	3	0	0	1	1	0	1	0	0	0	1	1	1	1	0
Cistudinella parva	1	0	1	?	0	0	1	0	1	1	1	4	1	0	0	5	5	0	0	1	1	0	1	0	0	0	0	1	2	0	0
Cistudinella peruana	0	0	2	0	0	1	1	0	0	0	1	3	1	0	0	3	3	0	0	1	1	0	1	1	0	0	0	1	1	1	0
Cistudinella punctipennis	0	0	1	?	0	0	1	0	1	0	1	4	1	0	0	5	5	0	0	1	1	0	1	0	1	0	0	0	3	1	0
Eurypedus nigrosignatus	0	1	0	1	0	1	1	-	1	0	2	4	1	0	0	1	1	1	1	1	1	0	0	0	0	0	1	1	1	1	0
Eurypedus peltoides	0	1	0	1	0	1	1	-	1	0	2	5	1	0	0	1	1	1	1	1	1	0	0	0	0	0	1	1	1	1	0
Enagria angulifera	0	0	2	0	0	0	1	1	1	0	1	3	0	-	0	?	1	1	0	0	1	0	0	0	0	0	0	0	2	0	0
Enagria ovata	0	0	2	0	0	0	1	1	1	0	1	3	0	-	0	0	1	1	0	0	1	0	0	0	0	0	0	0	2	0	0
Eurypepla calochroma	0	0	2	0	0	0	1	0	0	0	0	-	0	-	0	5	5	0	0	0	1	0	0	0	0	0	0	0	1	0	0
Physonota alutacea	0	0	2	0	0	0	1	1	2	0	1	2	0	-	0	3	3	0	0	1	1	0	1	0	0	0	0	0	2	0	0
Physonota arizonae	0	0	2	0	0	0	1	0	2	0	1	3	0	-	0	0	0	1	0	0	1	0	0	0	0	0	0	1	2	0	0
Physonota attenuata	0	0	2	0	0	0	1	1	2	0	1	3	0	-	0	3	3	1	0	0	1	0	1	0	0	0	0	1	2	0	1
Physonota calcarata	0	0	2	0	0	0	1	1	2	0	1	4	0	-	0	1	1	1	0	0	1	0	0	0	0	0	0	0	2	0	1
Physonota caudata	0	0	2	0	0	1	1	1	2	0	1	5	0	-	0	3	3	1	0	0	1	0	1	0	0	0	0	0	2	0	1
Physonota cerea	0	0	2	?	0	0	1	0	1	0	1	4	0	-	0	3	?	0	0	0	1	0	0	0	0	0	0	1	2	0	0
Physonota citrina	0	0	2	0	0	0	1	0	1	0	1	3	0	-	0	3	3	0	0	0	1	0	0	0	0	0	0	1	1	0	0
Physonota convexa	0	0	2	0	0	0	1	0	1	0	0	-	0	-	0	1	1	0	0	1	1	0	0	0	0	0	0	0	2	0	0
Physonota disjuncta	0	0	2	0	0	0	1	1	2	0	1	5	0	-	0	0	0	0	0	0	1	0	0	0	0	0	0	1	1	0	0
Physonota eucalypta	0	0	2	0	0	1	1	1	1	0	1	5	0	-	0	3	3	1	0	0	1	0	1	0	0	0	0	0	2	0	0
Physonota gigantea	0	0	2	0	0	0	1	1	2	1	0	-	0	-	0	3	3	0	1	0	1	0	0	0	0	0	0	1	2	0	0
Physonota helianthi	0	0	2	0	0	0	1	1	1	0	1	3	0	-	0	0	0	1	0	0	1	0	0	0	0	0	0	1	2	0	0
Physonota humilis	0	0	2	0	0	0	1	1	1	0	1	4	0	-	0	3	3	1	0	0	1	0	0	0	0	0	0	0	2	0	0
Physonota incrustata	0	0	2	0	0	1	1	1	1	0	2	3	0	-	0	3	3	1	0	1	1	0	0	0	0	0	0	1	2	0	1
Physonota limoniata	0	0	2	0	0	1	1	1	1	0	1	5	0	-	0	3	3	1	0	0	1	0	1	0	0	0	0	0	2	0	0
Physonota lutarella	0	0	2	0	0	0	1	0	1	0	1	4	0	-	0	3	3	1	0	0	1	0	1	0	0	0	0	0	2	0	1
Physonota maculiventris	0	0	2	0	0	0	1	1	1	0	1	4	0	-	0	3	0	0	1	0	1	0	0	0	0	0	0	1	1	0	0
Physonota mexicana	0	0	2	0	0	0	1	1	1	0	1	4	0	-	0	0	3	1	0	0	1	0	0	0	0	0	0	1	1	0	0
Physonota nitidicollis	0	0	2	0	0	0	1	0	2	0	1	23	0	-	0	3	3	0	0	0	1	0	0	0	0	0	0	1	2	0	0
Physonota ovalis	0	0	2	0	0	0	1	0	1	0	1	4	0	-	0	0	1	0	0	0	1	0	0	0	0	0	0	1	1	0	0
Physonota pacifica	?	?	?	?	0	0	1	1	1	0	1	4	0	-	0	0	0	0	0	1	1	0	?	0	0	0	0	?	2	0	0
Physonota picticollis	0	0	2	0	0	0	1	0	2	1	1	3	0	-	0	0	0	1	0	0	1	0	0	0	0	0	0	0	2	0	0
Physonota punctcollis	0	0	2	0	0	0	1	0	1	0	1	3	0	-	0	?	3	1	0	0	1	0	1	0	0	0	0	0	2	0	0
Physonota separata	0	0	2	0	0	0	1	1	1	0	1	3	0	-	0	0	0	1	0	0	1	0	0	0	0	0	0	0	2	0	0
Physonota sp.	?	?	?	?	0	0	1	1	2	0	1	3	0	-	0	3	3	1	0	0	1	0	?	0	0	0	?	?	?	0	0
Physonota stigmatillis	0	0	3	0	0	1	1	1	2	1	0	-	0	-	0	3	3	0	0	1	1	0	1	0	0	1	1	1	2	0	0
Physonota sublaevigata	0	0	2	0	0	0	1	0	2	0	1	45	0	-	0	3	3	0	0	0	1	1	0	0	0	0	0	0	2	0	0
Physonota translucida	0	0	2	0	0	0	1	1	2	0	1	4	0	-	0	3	3	1	0	0	1	0	0	0	0	0	0	0	2	0	0
Physonota turgida	0	0	2	0	0	0	1	0	1	0	1	34	0	-	0	0	0	1	0	0	1	0	0	0	0	0	0	1	2	0	0
Physonota unipunctata	0	0	2	0	0	0	1	0	1	0	1	3	0	-	0	0	0	0	0	0	1	0	0	0	0	0	0	1	2	0	0
Physonota vitticollis	0	0	3	0	0	0	1	1	1	0	1	3	0	-	0	3	3	1	0	0	1	0	0	0	0	0	0	0	2	0	0
Physonota vittifera	0	0	2	?	0	0	1	1	1	0	1	3	0	-	0	0	?	1	0	0	1	0	0	0	0	0	0	0	2	0	0
Platycycla deruta	0	0	2	0	0	0	1	0	1	0	1	2	0	-	0	5	5	0	0	0	1	0	1	0	0	1	1	1	2	0	0
Aspidimorpha dissentanea	0	0	1	0	0	0	1	0	2	0	1	0	1	0	0	5	5	3	0	0	1	0	0	0	0	0	0	1	2	1	0
Lacooptera murrayi	0	0	1	?	0	0	1	0	2	0	0	-	1	1	0	5	5	3	0	0	1	0	0	0	0	0	0	1	1	1	0
Aspidimorpha sp.	0	0	1	1	0	0	1	0	2	1	1	012	1	1	0	5	5	3	0	1	1	0	0	0	0	0	0	1	1	1	0
Aspidimorpha miliaris	0	0	1	0	0	0	1	0	2	0	1	1	1	1	0	5	5	3	0	0	1	0	0	0	0	0	0	0	2	1	0
Cassida nebulosa	0	0	2	2	0	0	1	0	1	0	1	-	1	1	1	3	3	3	0	0	1	0	0	0	0	0	0	1	1	1	0
Cheridotis miniata	-	-	-	-	0	0	1	0	0	0	1	-	0	-	0	3	3	2	0	0	1	0	0	0	0	1	1	1	2	1	0
Coptocycla undecimpunctata	-	-	-	-	0	0	1	0	2	1	1	-	1	1	0	5	5	2	0	0	1	0	0	0	0	0	0	0	2	1	0
Dorynota bidens	-	-	-	-	0	0	0	0	0	0	1	-	0	-	0	5	5	2	0	0	0	0	0	0	0	0	0	0	2	0	0
Omotenia humeralis	-	-	-	-	1	0	0	0	0	0	2	-	0	-	0	5	5	2	0	0	1	0	0	0	0	0	0	1	1	1	0
Paranota enifera	-	-	-	-	0	0	0	0	0	2	0	-	1	1	0	5	5	2	0	0	0	0	0	0	0	0	0	0	2	1	0
Paratriona turrifera	-	-	-	-	1	0	0	0	0	0	0	-	0	-	0	5	5	2	0	0	1	0	0	0	0	0	0	1	1	1	0
Chlamydocassis bicornuta	-	-	-	-	0	1	1	-	1	0	2	-	1	0	0	1	1	1	0	0	1	0	1	0	0	1	1	1	2	1	1
Chlamydocassis cribripennis	-	-	-	-	0	1	1	-	1	0	2	-	1	0	0	3	3	1	0	0	1	0	1	0	0	1	1	1	2	1	1
Chlamydocassis metallica	-	-	-	-	0	1	1	-	1	0	2	-	1	0	0	5	5	1	0	0	1	0	0	0	0	1	1	1	2	1	1
Goniochenia quadraticollis	0	0	2	0	1	0	1	-	1	1	2	-	1	0	0	5	5	0	0	1	1	0	1	1	1	1	1	1	-	1	1
Herissa pantherina	0	0	2	0	0	0	1	-	1	0	2	-	1	0	0	5	5	0	0	0	1	0	1	0	0	0	0	1	2	1	0
Polychalma multicava	-	-	-	-	1	0	1	-	1	1	2	-	1	0	1	3	3	0	0	1	0	0	0	0	0	0	0	0	2	1	0
Zeugonota quadrinodosa	-	-	-	-	?	0	?	-	1	0	2	-	1	0	0	0	0	0	0	0	1	0	0	0	0	0	0	0	2	1	0
Carlobruchia tricostata	0	0	1	0	1	0	0	-	1	0	2	-	1	1	0	5	5	2	2	2	1	0	0	0	0	0	0	0	2	1	1
Canistra osculatii	?	?	?	?	1	0	0	0	1	1	0	-	1	0	0	5	5	2	2	2	1	0	?	1	1	?	?	0	?	1	?
Cassidinoma denticulata	0	0	1	0	1	0	0	-	1	0	2	-	1	1	0	5	5	2	2	1	1	0	1	1	0	0	0	0	2	1	1
Cyclosoma palliata	0	0	1	0	1	0	0	-	1	0	2	-	0	-	0	5	5	3	?	0	1	0	0	1	0	0	0	0	2	1	1
Discomorpha variegata	0	0	1	2	1	0	0	-	1	0	2	-	0	-	0	5	5	3	?	1	1	0	0	0	0	0	0	1	1	1	0
Omocerus bicornis	0	0	0	1	1	0	0	-	1	0	2	-	0	-	0	5	5	3	0	1	1	0	1	1	0	1	1	1	2	1	1
Polychalca punctatissima	0	0	1	2	1	0	0	-	1	1	2	-	0	-	0	4	4	3	0	1	1	1	1	0	0	0	0	0	2	1	1
Agenysa caedemadens	-	-	-	-	1	0	0	-	2	1	2	-	0	-	0	4	4	1	0	0	0	0	0	0	0	0	0	0	1	1	0
Chelymorpha cassidea	-	-	-	-	0	0	1	-	1	0	1	5	0	-	0	2	2	1	0	0	0	0	0	0	0	0	0	0	1	1	0
Mesomphalia gibbosa	-	-	-	-	1	0	1	-	2	1	2	-	0	-	0	5	5	1	0	0	1	0	0	0	0	0	0	1	1	1	0
Stolas sp.	-	-	-	-	1	0	0	-	2	1	2	-	0	-	0	5	?	1	0	0	0	0	0	0	0	0	0	0	1	1	0

	63	64	65	66	67	68	69	70	71	72	73	74	75	76	77	78	79	80	81	82	83	84	85	86	87	88	89	90	91	92	93
Hemisphaerota cyanea	0	1	0	3	0	-	-	0	0	-	-	0	1	0	1	2	2	0	0	0	1	0	0	0	-	1	1	2	0	2	2
Hemisphaerota sp.	0	1	0	3	0	-	-	0	0	-	-	0	1	0	1	2	2	0	0	0	1	0	0	0	-	1	1	2	0	2	2
Basiprionota octopunctata	3	0	2	0	0	0	1	0	1	0	-	0	0	1	1	0	3	1	0	0	1	1	0	0	0	0	0	1	0	2	0
Asteriza blakeae	2	2	2	0	0	1	1	0	1	0	0	2	0	4	1	2	2	1	0	0	0	1	0	0	0	1	0	1	0	2	0
Asteriza darlingtoni	2	2	2	0	0	1	1	0	1	0	0	2	0	4	1	2	2	1	0	0	0	1	0	0	0	1	0	1	0	2	0
Asteriza flavicornis	2	2	2	0	0	1	1	0	1	0	0	2	0	4	1	2	2	1	0	0	0	1	0	0	0	1	0	1	01	2	0
Asteriza tainosa	2	2	2	0	0	1	1	0	1	0	0	2	0	4	1	2	2	1	0	0	0	1	0	0	0	1	0	1	0	2	0
Cistudinella apiata	3	0	2	0	0	0	0	0	1	0	0	1	0	1	0	0	0	1	0	0	1	1	0	0	1	1	0	2	1	2	0
Cistudinella foveolata	3	0	2	3	0	0	0	0	1	0	0	1	0	1	0	0	0	1	0	0	1	1	0	0	1	1	0	2	1	2	0
Cistudinella inanis	3	0	2	3	0	0	0	0	1	0	0	1	0	1	1	0	0	1	0	0	1	1	0	0	1	1	0	2	1	2	0
Cistudinella lata	0	0	2	3	0	0	1	0	1	0	-	1	0	1	1	0	0	1	0	0	1	1	0	0	1	1	0	1	1	2	0
Cistudinella lateripunctata	3	0	2	3	0	0	0	0	1	0	0	1	0	1	0	0	0	1	0	0	1	1	0	0	1	1	0	1	1	2	0
Cistudinella notata	3	0	2	3	0	0	1	0	1	0	0	1	0	1	1	0	0	1	0	0	1	1	0	0	1	1	1	2	1	2	0
Cistudinella obducta	0	0	2	3	0	0	0	0	1	0	0	1	0	1	0	0	0	1	0	0	1	1	0	0	1	1	0	1	1	2	0
Cistudinella parva	?	0	2	3	0	0	1	0	1	0	0	1	0	1	1	0	0	1	0	0	1	1	0	0	1	1	0	1	1	2	0
Cistudinella peruana	3	1	2	3	0	0	0	0	1	0	0	1	0	1	0	0	0	1	0	0	1	1	0	0	1	1	0	2	1	2	0
Cistudinella punctipennis	3	0	2	3	0	0	0	0	1	0	0	1	0	1	0	0	0	1	0	0	1	1	0	0	1	1	0	1	1	2	0
Eurypedus nigrosignatus	3	0	2	3	0	1	1	1	1	0	1	2	0	01	1	0	0	0	0	0	1	1	0	1	1	0	0	2	1	2	0
Eurypedus peltoides	3	0	2	3	0	1	1	0	1	0	1	2	0	01	1	0	0	0	0	0	1	1	0	1	1	0	0	2	1	2	0
Enagria angulifera	2	0	2	0	0	0	0	1	1	0	0	2	0	4	1	2	2	0	0	0	0	1	0	0	0	0	0	0	0	2	0
Enagria ovata	2	0	2	0	0	0	0	1	1	0	0	2	0	4	1	2	2	0	0	0	0	1	0	0	0	0	0	0	0	2	0
Eurypepla calochroma	2	0	2	0	0	1	0	1	1	0	0	2	0	4	1	2	2	0	0	0	0	1	0	0	0	0	0	2	1	2	0
Physonota alutacea	0	2	2	0	0	1	1	1	1	0	0	2	0	4	1	2	2	1	0	0	0	1	01	0	0	0	0	2	0	2	0
Physonota arizonae	1	1	2	0	0	1	1	1	1	0	0	2	0	4	1	2	2	0	0	0	0	1	0	0	0	0	0	0	0	0	0
Physonota attenuata	0	1	2	0	0	1	1	1	1	1	0	2	0	3	1	2	2	1	1	0	0	1	0	0	0	0	0	1	0	1	0
Physonota calcarata	1	2	2	0	0	1	1	0	1	0	1	2	0	4	1	2	2	0	0	0	0	1	0	0	0	2	0	1	0	2	1
Physonota caudata	0	1	2	0	0	1	1	1	1	1	0	2	0	3	1	2	2	0	1	0	0	1	0	0	0	0	0	0	0	2	0
Physonota cerea	3	1	2	2	0	0	0	1	1	0	0	2	0	4	1	2	2	0	0	0	0	1	1	0	2	0	0	1	0	2	0
Physonota citrina	3	1	2	0	0	0	0	1	1	0	0	2	0	4	1	2	2	0	0	0	0	1	1	0	2	0	0	1	0	2	0
Physonota convexa	0	0	2	0	0	1	1	1	1	0	0	2	0	4	1	2	2	0	0	0	0	1	1	0	0	0	0	2	0	2	2
Physonota disjuncta	1	0	2	0	0	1	1	1	1	0	0	2	0	4	1	2	2	0	0	0	0	1	0	0	0	0	0	0	0	2	0
Physonota eucalypta	0	?	1	0	0	0	1	1	1	01	0	2	0	3	1	2	2	0	1	0	0	1	0	0	0	0	0	2	0	2	0
Physonota gigantea	0	1	2	0	0	1	1	1	1	1	0	2	0	4	1	2	2	1	0	0	0	1	0	0	0	0	0	1	0	2	0
Physonota helianthi	1	2	2	0	0	1	1	1	1	0	0	2	0	4	1	2	2	1	0	0	0	1	0	0	0	0	0	1	0	2	0
Physonota humilis	2	1	2	0	0	1	0	1	1	1	0	2	0	3	1	2	2	0	0	0	0	1	0	0	0	0	0	2	0	1	0
Physonota incrustata	0	1	1	0	0	1	1	1	1	1	0	2	0	3	1	2	2	1	1	0	0	1	0	0	0	0	0	2	0	2	0
Physonota limoniata	0	1	1	0	0	0	1	1	1	01	0	2	0	3	1	12	2	0	1	0	0	1	0	0	0	0	0	2	0	2	0
Physonota lutarella	2	1	2	0	0	1	1	1	1	0	0	2	0	4	1	2	2	1	0	0	0	1	0	0	0	0	0	2	3	2	2
Physonota maculiventris	2	1	2	0	0	1	1	1	1	0	0	2	0	4	1	2	2	1	0	0	0	1	0	0	0	2	0	2	1	2	0
Physonota mexicana	0	0	2	0	0	1	1	1	1	01	0	2	0	3	1	1	2	0	0	0	0	1	0	0	0	0	0	1	0	0	0
Physonota nitidicollis	3	2	2	0	0	1	0	1	1	0	0	2	0	4	1	2	2	0	0	0	0	1	1	0	2	0	0	0	0	2	1
Physonota ovalis	1	1	2	0	0	1	1	1	1	0	1	2	0	4	1	2	2	1	0	0	0	1	0	0	0	0	0	1	0	2	0
Physonota pacifica	?	?	2	0	0	1	1	1	1	0	0	2	0	4	1	2	2	1	0	0	0	1	0	0	0	2	0	2	0	2	0
Physonota picticollis	0	1	2	0	0	1	1	1	1	0	0	2	0	4	1	2	2	0	0	0	0	1	0	0	0	0	0	0	0	2	0
Physonota puncticollis	1	1	2	3	0	1	1	1	1	0	1	2	0	3	1	1	2	0	0	0	0	1	0	0	0	0	0	2	0	0	0
Physonota separata	2	1	2	0	0	1	1	1	1	0	0	2	0	4	1	2	2	1	0	0	0	1	0	0	0	0	0	2	0	2	0
Physonota sp.	0	1	2	0	0	1	1	1	1	0	0	2	0	4	1	2	2	1	1	0	0	1	0	0	0	0	0	2	0	1	0
Physonota stigmatillis	0	1	2	0	0	1	1	1	1	0	0	2	0	4	1	2	2	0	0	0	0	1	0	0	0	0	0	0	0	2	0
Physonota sublaevigata	2	1	2	0	0	1	0	1	1	0	0	2	0	4	1	2	2	0	0	0	0	1	1	0	2	0	0	0	0	2	0
Physonota translucida	1	0	1	0	0	0	0	1	1	1	0	2	0	3	1	2	2	0	0	0	0	1	0	0	0	0	0	1	0	1	0
Physonota turgida	2	1	2	0	0	1	0	1	1	0	0	2	0	4	1	2	2	1	0	0	0	1	0	0	0	0	0	0	0	2	0
Physonota unipunctata	0	1	2	0	0	1	0	1	1	0	0	2	0	4	1	2	2	1	0	0	0	1	0	0	0	0	0	0	0	2	1
Physonota vitticollis	3	2	2	0	0	1	1	1	0	0	0	2	0	4	1	2	2	0	0	0	0	1	0	0	0	0	0	2	0	2	0
Physonota vittifera	0	0	2	0	0	1	1	1	1	0	1	2	0	4	1	2	2	0	0	0	0	1	0	0	2	0	0	2	0	2	0
Platycycla deruta	0	1	1	0	0	0	0	1	1	0	0	2	0	3	1	2	2	0	0	0	0	1	0	0	0	0	0	2	0	0	0
Aspidimorpha dissentanea	0	0	2	0	0	0	0	0	1	0	0	2	0	4	1	2	2	0	0	0	1	1	0	0	0	0	0	1	3	2	0
Lacooptera murrayi	0	0	0	0	0	-	-	0	1	0	1	1	2	3	1	2	2	0	0	0	1	1	0	0	0	0	0	1	3	2	0
Aspidimorpha sp.	1	1	1	2	0	0	0	0	1	0	0	2	0	4	1	2	2	0	0	0	1	1	0	0	0	0	0	2	3	2	0
Aspidimorpha miliaris	1	2	2	0	0	0	0	0	1	0	1	2	0	4	1	1	2	1	0	0	1	1	0	0	1	0	1	2	0	2	2
Cassida nebulosa	1	1	2	13	0	0	0	0	1	0	1	2	0	4	1	2	2	0	0	0	1	1	1	0	0	0	0	2	3	2	0
Cheridotis miniata	3	2	2	0	0	0	0	0	1	0	0	2	0	4	1	2	2	1	0	0	1	1	0	0	1	1	0	0	0	1	2
Coptocycla undecimpunctata	0	0	1	0	0	0	0	0	1	2	1	2	0	3	1	2	2	0	0	0	1	1	0	0	1	1	0	0	0	1	0
Dorynota bidens	2	1	1	0	1	-	-	1	1	2	0	2	0	3	1	2	2	3	0	1	1	1	0	0	2	0	1	2	0	?	2
Omotenia humeralis	2	1	1	0	0	0	0	0	0	-	-	1	0	3	1	1	2	0	0	1	1	1	0	0	1	0	0	0	0	2	0
Paranota enifera	2	1	1	13	0	0	0	0	1	0	0	2	0	3	1	1	2	3	0	1	1	1	1	0	2	1	0	2	0	2	0
Paratriona turrifera	2	1	1	1	0	0	0	0	1	0	1	2	0	3	1	1	2	0	0	1	1	1	0	0	1	2	0	1	0	1	2
Chlamydocassis bicornuta	0	2	2	12	0	-	-	0	0	-	-	1	0	1	0	0	2	0	0	0	1	1	0	0	1	2	0	2	1	2	2
Chlamydocassis cribripennis	0	2	2	1	0	-	-	0	0	-	-	1	0	1	0	1	0	0	0	0	1	1	0	0	1	0	1	2	1	2	0
Chlamydocassis metallica	0	0	2	12	0	-	-	0	0	-	-	1	0	1	0	0	0	0	0	0	1	1	0	0	1	1	0	2	1	2	0
Goniochenia quadraticollis	0	0	2	0	1	-	-	0	0	-	-	1	12	01	1	1	2	0	0	0	1	1	0	0	1	0	0	1	1	?	0
Herissa pantherina	2	0	2	0	0	-	-	0	0	-	-	1	0	1	0	0	0	1	0	0	1	1	0	0	1	0	0	0	1	2	1
Polychalma multicava	2	0	2	0	0	-	-	0	0	-	-	1	0	1	1	0	0	0	0	0	1	1	0	0	1	0	0	1	1	?	0
Zeugonota quadrinodosa	0	0	2	1	0	-	-	1	0	-	-	1	0	1	1	0	3	0	0	0	1	1	0	0	1	0	0	2	1	2	0
Carlobruchia tricostata	2	0	2	13	0	-	-	1	0	-	-	1	0	1	1	0	3	1	0	0	1	1	0	0	1	0	1	2	1	2	2
Canistra osculatii	?	?	2	0	0	-	-	0	0	-	-	1	0	1	1	0	2	1	0	0	1	1	0	0	1	0	1	2	1	2	2
Cassidinoma denticulata	2	0	2	1	0	-	-	1	0	-	-	1	0	1	1	0	3	1	0	0	1	1	0	0	1	0	1	2	1	2	2
Cyclosoma palliata	2	0	2	1	0	-	-	1	0	-	-	0	2	2	1	0	3	0	0	0	1	1	0	0	1	0	1	2	0	2	2
Discomorpha variegata	1	0	2	0	0	-	-	0	0	-	-	0	0	2	1	0	3	0	0	0	1	1	0	0	1	1	1	2	1	2	0
Omocerus bicornis	1	0	2	13	0	-	-	1	0	-	-	0	0	1	1	0	2	0	0	0	1	1	0	0	1	0	1	2	0	1	2
Polychalca punctatissima	1	0	2	3	0	-	-	0	0	-	-	0	0	2	1	0	2	0	0	0	1	1	1	0	1	0	1	2	0	2	2
Agenysa caedemadens	0	0	2	1	0	-	-	1	0	-	-	1	2	1	1	1	2	1	1	0	1	1	0	0	0	0	0	0	2	2	2
Chelymorpha cassidea	0	0	2	3	0	-	-	1	0	-	-	1	0	1	1	0	2	1	0	0	1	1	1	0	1	0	0	0	0	2	2
Mesomphalia gibbosa	0	0	2	0	0	-	-	1	0	-	-	1	2	1	1	1	2	1	0	0	1	1	0	0	1	0	0	0	2	2	2
Stolas sp.	0	0	2	0	0	-	-	1	0	-	-	1	2	1	1	1	1	1	1	0	1	1	0	0	1	0	0	0	2	2	2

	94	95	96	97	98	99	100	101	102	103	104	105	106	107	108	109	110	111	112	113	114	115	116	117	118	119	120	121	122	123	124
Hemisphaerota cyanea	2	1	1	0	0	1	1	-	1	1	0	0	1	0	-	0	0	0	0	2	0	0	0	1	1	0	2	0	0	1	1
Hemisphaerota sp.	2	1	1	0	0	1	1	0	1	1	0	0	1	0	-	0	0	0	0	2	0	0	0	1	1	0	2	0	0	1	1
Basiprionota octopunctata	1	1	0	0	1	0	0	0	1	1	0	0	0	0	0	0	1	0	0	1	0	0	1	2	2	0	2	0	0	1	1
Asteriza blakeae	0	0	1	0	0	0	2	2	1	0	0	1	0	1	0	0	1	0	0	1	0	0	0	2	1	0	1	0	1	1	0
Asteriza darlingtoni	0	0	1	0	0	0	2	2	1	0	0	1	0	1	0	0	1	0	0	1	0	0	0	2	1	0	1	0	1	1	0
Asteriza flavicornis	0	0	1	0	0	0	2	2	1	0	0	1	0	1	0	0	1	0	0	1	0	0	0	2	1	0	1	0	1	1	0
Asteriza tainosa	0	0	1	0	0	0	2	2	1	0	0	1	0	1	0	0	1	0	0	1	0	0	0	2	1	0	1	0	1	1	0
Cistudinella apiata	1	0	0	0	0	1	0	3	1	0	0	0	0	1	0	0	1	0	0	1	0	0	0	2	1	01	2	0	0	1	1
Cistudinella foveolata	1	0	0	0	0	0	1	2	1	0	0	0	0	1	0	0	1	0	0	0	0	0	0	2	1	0	2	0	0	1	0
Cistudinella inanis	1	0	0	0	0	0	1	0	1	0	0	0	0	1	0	0	1	0	0	2	0	0	0	2	1	0	2	0	0	1	1
Cistudinella lata	1	0	0	0	0	0	1	2	1	0	0	0	0	1	0	0	1	0	0	1	0	0	0	2	1	0	2	0	0	1	?
Cistudinella lateripunctata	1	0	0	0	0	0	0	3	1	0	0	0	0	1	0	0	1	0	0	0	0	0	0	2	1	0	12	0	0	1	1
Cistudinella notata	1	0	0	0	0	0	0	3	1	0	0	0	0	1	1	0	1	0	0	0	0	0	0	2	1	0	2	0	0	1	0
Cistudinella obducta	1	1	0	0	0	0	1	0	1	0	0	0	0	1	0	0	1	0	0	0	0	0	0	2	1	0	2	0	0	1	1
Cistudinella parva	1	0	0	0	0	0	1	-	1	0	0	0	0	1	1	0	1	0	0	1	0	0	0	2	1	0	2	0	0	1	0
Cistudinella peruana	1	0	0	0	0	0	0	2	1	0	0	0	0	1	0	0	1	0	0	2	0	0	0	2	1	1	2	0	0	1	0
Cistudinella punctipennis	1	0	0	0	0	0	0	0	1	1	0	0	0	0	0	0	1	0	0	0	0	0	0	2	1	0	2	0	1	1	1
Eurypedus nigrosignatus	0	1	1	0	0	0	0	2	1	1	0	0	1	1	-	0	1	0	0	1	0	0	0	0	0	0	0	0	0	0	1
Eurypedus peltoides	0	1	1	0	0	0	0	2	1	1	0	0	1	1	-	0	1	0	0	1	0	0	0	0	0	0	0	0	0	0	1
Enagria angulifera	0	0	0	0	0	0	0	4	1	1	1	0	0	0	01	0	1	1	0	0	0	0	0	0	0	0	2	0	0	1	1
Enagria ovata	0	0	0	0	0	0	0	4	1	1	1	0	0	0	01	0	1	1	0	0	0	0	0	0	0	0	2	0	0	1	1
Eurypepla calochroma	1	0	0	0	0	0	0	3	1	0	0	0	1	0	0	0	1	0	0	1	0	0	1	1	1	0	1	0	0	1	0
Physonota alutacea	0	0	1	0	0	1	2	1	1	01	0	0	0	1	1	0	1	0	0	1	0	0	0	2	2	01	2	0	0	1	1
Physonota arizonae	1	0	0	0	0	0	1	3	1	1	0	0	0	0	1	0	1	0	0	1	0	0	0	1	1	0	2	0	0	1	1
Physonota attenuata	1	0	1	0	0	1	0	3	1	1	0	0	0	1	1	0	1	0	0	1	0	0	0	0	0	0	2	0	0	1	1
Physonota calcarata	0	0	1	0	0	0	0	2	1	1	0	0	0	1	1	1	1	0	0	2	0	0	1	1	1	0	2	0	0	1	0
Physonota caudata	2	0	0	0	0	1	0	1	1	0	0	0	0	1	1	0	1	0	0	2	1	0	0	1	0	0	1	0	0	1	1
Physonota cerea	1	0	0	0	0	0	2	2	1	0	0	0	0	0	0	0	1	0	0	1	0	0	0	2	2	1	2	0	0	1	0
Physonota citrina	1	0	0	0	0	0	2	2	1	0	0	0	0	0	0	0	1	0	0	1	0	0	0	2	2	1	2	0	0	1	1
Physonota convexa	0	0	1	0	0	1	2	1	1	0	0	0	0	1	1	0	1	0	0	2	0	0	1	2	2	0	2	0	1	1	0
Physonota disjuncta	0	0	0	0	0	1	0	2	1	1	0	0	0	1	0	0	1	0	0	1	0	0	0	1	1	0	2	0	0	1	1
Physonota eucalypta	0	0	1	0	0	0	0	1	1	1	0	0	0	0	1	0	1	0	0	2	0	0	0	0	0	0	2	0	0	1	1
Physonota gigantea	0	0	0	0	0	-	0	3	1	1	0	0	0	1	1	0	1	0	0	2	0	0	0	1	0	0	2	0	0	1	1
Physonota helianthi	1	0	0	0	0	1	0	2	1	0	0	0	0	1	1	0	1	0	0	0	0	0	0	1	1	0	2	0	0	1	1
Physonota humilis	1	0	0	0	0	1	1	3	1	1	0	0	0	1	1	0	1	0	0	0	1	0	1	1	1	0	2	0	0	1	1
Physonota incrustata	0	0	1	0	0	0	1	1	1	1	0	0	0	1	1	0	1	0	0	2	0	0	0	1	0	0	2	0	0	1	1
Physonota limoniata	0	0	1	0	0	0	0	1	1	1	0	0	0	0	1	0	1	0	0	2	0	0	0	0	0	0	2	0	0	1	1
Physonota lutarella	0	0	1	0	0	0	2	1	1	0	0	0	0	1	1	0	1	0	0	2	0	0	0	2	2	01	2	0	0	1	1
Physonota maculiventris	0	0	1	0	0	0	0	4	1	0	0	0	0	1	1	1	1	0	0	2	0	0	0	1	1	0	2	0	0	1	1
Physonota mexicana	1	0	0	0	0	2	0	23	1	1	0	0	1	1	1	0	1	0	0	1	1	0	0	0	0	0	12	0	0	0	1
Physonota nitidicollis	0	0	1	0	0	0	2	2	1	0	0	0	0	0	0	0	1	0	0	1	0	0	0	2	2	1	2	0	0	1	1
Physonota ovalis	0	0	1	0	0	0	1	3	1	1	0	0	0	0	0	0	1	0	0	1	0	0	0	1	1	0	2	0	0	1	1
Physonota pacifica	0	0	1	0	0	0	1	3	1	?	0	0	0	1	1	0	1	0	0	2	0	0	0	1	1	0	2	0	1	1	1
Physonota picticollis	1	0	0	0	0	0	1	3	1	0	0	0	0	1	1	0	1	0	0	0	0	0	0	1	1	0	2	0	0	1	1
Physonota puncticollis	0	0	0	0	0	2	0	3	0	?	0	0	1	1	1	0	1	0	0	1	1	0	0	0	0	0	12	0	0	0	1
Physonota separata	1	0	1	0	0	0	0	03	1	0	0	0	0	1	1	1	1	0	0	0	0	0	0	1	0	0	2	0	0	1	1
Physonota sp.	0	?	1	0	?	0	1	3	1	0	0	0	0	1	1	0	1	0	0	2	0	0	0	1	1	0	2	0	0	1	0
Physonota stigmatillis	0	0	1	0	0	0	2	2	1	?	0	0	0	1	1	0	1	0	0	2	0	0	0	1	0	0	2	0	0	1	0
Physonota sublaevigata	1	0	1	0	0	0	2	02	1	0	0	0	0	0	0	0	1	0	0	1	0	0	0	2	2	1	2	0	0	1	0
Physonota translucida	1	0	0	0	0	1	1	3	1	1	0	0	1	1	1	0	1	0	0	2	1	0	0	1	1	0	2	0	0	1	1
Physonota turgida	1	0	0	0	0	0	0	3	1	1	0	0	0	0	0	0	1	0	0	1	0	0	0	1	1	0	2	0	0	1	1
Physonota unipunctata	0	0	0	0	0	0	0	2	1	1	0	0	0	0	0	0	1	0	0	1	1	0	0	1	1	0	2	0	0	1	1
Physonota vitticollis	0	0	1	0	0	0	0	2	1	1	0	0	0	1	1	1	1	0	0	1	0	0	0	1	0	0	2	0	0	1	1
Physonota vittifera	0	0	0	0	0	0	0	2	1	?	0	0	0	1	1	0	1	0	0	1	1	0	0	1	0	0	2	0	0	1	?
Platycycla deruta	2	0	0	0	0	0	1	2	1	1	0	0	1	1	1	0	1	0	0	2	0	0	0	0	0	0	2	0	0	1	1
Aspidimorpha dissentanea	0	0	0	0	1	0	0	4	1	0	0	0	0	1	0	0	1	0	2	1	1	0	0	2	1	1	2	0	0	1	1
Lacooptera murrayi	0	0	0	0	1	0	0	0	1	0	0	0	1	1	0	0	1	0	2	1	0	1	0	2	1	2	1	0	0	1	1
Aspidimorpha sp.	0	0	0	0	1	1	0	0	1	1	0	0	1	0	0	0	0	0	2	1	0	0	0	1	1	0	1	0	0	1	1
Aspidimorpha miliaris	1	0	0	0	0	0	1	02	1	0	0	0	1	1	0	0	1	0	2	1	1	0	1	1	0	0	2	0	0	1	1
Cassida nebulosa	1	0	0	0	1	0	0	4	1	1	0	0	0	0	0	0	0	0	0	1	1	0	0	2	0	0	2	0	1	0	1
Cheridotis miniata	0	0	0	0	1	1	0	0	1	1	0	0	1	1	0	0	0	0	0	1	0	0	0	2	1	0	2	0	1	1	1
Coptocycla undecimpunctata	1	0	0	0	1	0	0	0	1	1	0	0	1	0	0	0	0	0	0	1	0	1	0	2	1	0	2	0	0	1	1
Dorynota bidens	1	0	0	1	0	?	0	?	1	1	0	0	0	0	-	0	0	0	0	0	1	1	1	2	2	2	0	1	0	2	1
Omotenia humeralis	0	0	0	0	0	1	0	3	0	1	0	0	1	0	0	0	1	0	0	0	0	1	1	2	2	1	2	0	1	1	1
Paranota enifera	1	0	0	1	0	0	1	0	1	1	0	0	0	1	1	0	1	0	0	0	3	0	1	1	2	2	2	0	0	1	2
Paratriona turrifera	1	0	0	0	0	0	1	0	1	1	0	0	1	0	0	0	0	0	0	3	0	1	1	2	2	1	1	0	1	1	1
Chlamydocassis bicornuta	0	0	0	0	0	1	1	-	1	1	0	0	1	1	-	0	1	0	0	0	1	0	0	1	1	0	0	0	0	0	1
Chlamydocassis cribripennis	0	0	0	0	0	1	2	-	1	1	0	0	0	1	-	0	1	0	0	0	1	0	0	2	2	0	0	0	0	0	1
Chlamydocassis metallica	0	0	0	0	0	1	1	-	1	1	0	0	0	1	-	0	1	0	0	0	1	0	0	2	1	0	0	0	0	0	1
Goniochenia quadraticollis	0	1	0	0	0	0	0	-	1	1	0	0	0	1	-	0	1	0	0	0	1	0	1	2	2	1	2	0	0	1	1
Herissa pantherina	1	0	1	0	0	0	0	-	1	0	0	0	0	0	-	0	1	0	0	0	0	0	0	1	2	0	2	0	0	1	1
Polychalma multicava	1	?	0	0	?	?	1	-	1	0	0	0	1	1	-	0	1	0	0	0	1	0	0	2	2	1	2	0	0	1	1
Zeugonota quadrinodosa	?	0	0	0	0	1	1	-	1	1	0	0	0	1	-	0	1	0	0	0	0	0	0	1	1	0	2	0	0	0	1
Carlobruchia tricostata	1	1	1	0	1	0	1	-	1	0	0	0	0	0	-	0	1	0	0	0	0	0	0	1	1	0	2	0	0	1	1
Canistra osculatii	1	?	0	0	?	0	1	-	1	1	0	0	0	0	-	0	1	0	0	1	1	0	1	2	1	0	2	0	0	1	1
Cassidinoma denticulata	1	1	1	0	1	0	1	-	1	1	0	0	0	0	-	0	1	0	0	1	0	0	1	2	2	0	1	0	0	1	1
Cyclosoma palliata	2	1	0	0	1	1	1	-	1	1	0	0	0	1	-	0	1	0	0	1	0	0	0	1	1	1	2	0	0	1	1
Discomorpha variegata	1	1	0	0	1	1	1	-	1	1	0	0	0	1	-	0	1	0	0	1	0	0	1	2	2	1	1	0	0	1	1
Omocerus bicornis	2	1	0	0	1	1	0	-	1	1	0	0	0	0	-	0	1	0	0	2	1	0	1	2	1	0	0	0	0	2	1
Polychalca punctatissima	2	1	1	0	1	1	2	-	1	1	0	0	0	0	-	0	1	0	0	2	0	0	1	2	2	0	1	0	0	1	1
Agenysa caedemadens	1	0	0	0	0	0	1	-	1	0	0	0	0	1	-	0	1	0	1	1	1	0	1	2	1	1	2	1	0	1	1
Chelymorpha cassidea	2	0	1	0	0	0	1	-	1	1	0	0	0	1	-	0	1	0	1	2	0	0	0	2	1	0	2	0	0	1	0
Mesomphalia gibbosa	1	1	0	0	0	0	1	-	1	1	0	0	0	1	-	0	1	0	1	1	1	0	1	2	2	1	2	0	0	1	1
Stolas sp.	1	0	0	0	0	0	0	-	1	0	0	0	0	1	-	0	1	0	1	0	1	0	1	2	1	0	2	1	0	1	1

	125	126	127	128	129	130	131	132	133	134	135	136	137	138	139	140	141	142	143	144	145	146	147	148	149	150	151	152	153	154	155
Hemisphaerota cyanea	0	0	1	0	1	1	0	1	1	1	0	0	0	0	0	0	0	0	0	0	0	0	0	1	0	0	2	1	2	0	0
Hemisphaerota sp.	0	0	1	0	1	1	0	1	1	1	0	0	0	0	0	0	0	0	0	0	0	0	0	1	0	0	2	1	2	0	0
Basiprionota octopunctata	0	0	1	1	0	0	0	1	1	1	0	0	0	0	0	0	1	-	-	0	0	3	-	0	-	?	?	?	?	?	?
Asteriza blakeae	0	0	1	1	0	0	0	1	0	1	1	0	1	0	0	0	0	0	1	0	0	2	1	0	0	0	0	1	0	1	0
Asteriza darlingtoni	0	0	1	1	0	0	0	1	0	1	1	0	1	0	0	0	0	0	1	0	0	2	1	0	0	0	0	1	0	1	0
Asteriza flavicornis	0	0	1	1	0	0	0	1	1	1	1	0	1	0	0	0	0	0	1	0	0	2	1	0	0	0	0	1	0	1	0
Asteriza tainosa	0	0	1	1	0	0	0	1	1	1	1	0	1	0	0	0	0	0	1	0	0	2	1	0	0	0	0	1	0	1	0
Cistudinella apiata	1	0	1	0	1	01	0	1	0	1	0	0	0	1	0	0	0	1	0	0	1	0	0	0	0	0	2	0	0	2	0
Cistudinella foveolata	0	0	1	1	1	01	0	1	0	0	0	0	0	1	0	0	0	0	0	0	0	0	1	0	0	2	2	1	0	3	0
Cistudinella inanis	1	0	0	0	0	0	0	1	1	0	0	0	1	0	0	0	0	0	0	0	1	0	1	0	0	0	1	1	0	2	0
Cistudinella lata	1	0	0	0	0	0	0	1	0	0	0	0	0	0	0	0	0	0	0	0	?	?	?	?	?	0	1	1	0	3	0
Cistudinella lateripunctata	1	0	1	1	1	01	0	1	0	1	0	0	0	01	0	0	0	0	0	0	1	1	1	0	0	0	2	0	0	2	0
Cistudinella notata	0	0	0	0	0	0	0	1	0	1	0	0	0	0	0	0	0	1	0	0	0	0	1	0	0	0	1	1	1	1	0
Cistudinella obducta	1	0	1	1	1	01	0	1	0	0	0	0	0	0	0	0	0	0	0	0	1	1	1	0	0	0	1	0	0	2	0
Cistudinella parva	0	0	1	0	1	1	0	1	0	1	0	0	0	0	0	0	0	1	0	0	?	?	?	?	?	0	1	1	1	1	0
Cistudinella peruana	0	0	1	0	1	0	0	1	0	0	0	0	0	0	0	0	0	1	0	0	0	1	0	0	0	0	2	1	0	2	0
Cistudinella punctipennis	0	0	1	1	1	01	0	1	0	0	0	0	0	1	0	0	0	1	0	0	?	?	?	?	0	0	1	1	1	2	0
Eurypedus nigrosignatus	1	0	1	0	0	0	0	0	1	0	0	0	0	0	0	0	0	1	0	0	1	1	1	1	0	0	1	0	0	2	0
Eurypedus peltoides	1	0	1	0	0	0	0	0	1	0	0	0	0	0	0	0	0	1	0	0	0	1	1	1	0	0	1	0	0	2	0
Enagria angulifera	0	0	0	0	0	0	0	1	0	1	0	0	0	1	0	0	1	-	-	0	?	?	?	?	?	0	0	1	0	0	0
Enagria ovata	0	0	0	1	0	0	0	1	0	1	0	0	0	1	0	0	1	-	-	0	1	1	0	1	0	0	0	1	0	0	0
Eurypepla calochroma	0	0	1	1	0	1	0	2	0	0	0	0	1	0	0	0	0	1	1	0	1	2	0	0	0	0	0	1	0	0	0
Physonota alutacea	0	0	1	1	0	0	0	1	0	1	0	0	1	0	0	0	0	1	1	0	1	1	1	1	0	1	2	1	0	2	0
Physonota arizonae	1	0	1	1	0	1	0	1	0	1	0	0	0	0	0	0	1	-	-	0	1	1	2	1	0	1	1	0	0	2	0
Physonota attenuata	1	0	1	1	0	0	1	2	0	0	0	1	0	1	0	0	1	-	-	0	1	1	0	1	0	0	0	1	0	2	0
Physonota calcarata	0	0	1	1	0	01	0	2	0	1	0	0	0	0	0	0	0	1	0	1	0	0	0	1	0	1	2	1	2	1	0
Physonota caudata	0	0	1	1	0	01	0	2	0	1	0	1	0	1	0	0	0	1	0	2	1	2	0	1	0	0	1	1	0	1	0
Physonota cerea	0	0	1	1	0	1	0	2	1	1	0	0	0	0	0	0	0	1	0	0	0	2	0	1	0	?	?	?	?	?	0
Physonota citrina	0	0	1	1	0	1	0	1	0	1	0	0	0	0	0	0	0	1	0	0	0	2	0	0	0	1	1	1	1	3	0
Physonota convexa	0	0	1	1	0	01	0	1	0	1	0	0	1	0	0	0	0	1	0	0	1	1	0	1	0	0	1	1	0	1	0
Physonota disjuncta	0	0	1	1	0	0	0	12	0	1	0	0	0	0	0	0	0	1	0	0	1	2	1	1	0	0	2	0	0	1	0
Physonota eucalypta	0	0	1	1	0	01	0	2	0	1	0	0	0	1	0	0	0	1	1	1	1	1	0	0	0	0	2	1	0	1	0
Physonota gigantea	0	0	1	1	0	0	0	2	0	0	0	0	0	0	0	0	0	1	0	0	1	1	1	0	0	0	1	1	0	1	0
Physonota helianthi	0	0	1	01	0	1	0	1	0	1	0	0	0	0	0	0	0	1	0	0	0	1	0	1	0	1	1	0	0	2	0
Physonota humilis	0	0	1	0	0	1	0	2	0	1	0	1	0	1	0	0	1	-	-	1	0	1	1	1	0	0	1	0	0	0	0
Physonota incrustata	0	0	1	1	0	1	0	2	0	1	0	1	0	1	0	0	0	1	0	1	1	1	1	1	0	0	1	0	0	1	0
Physonota limoniata	0	0	1	1	0	01	0	2	0	1	0	0	0	1	0	0	0	1	1	1	1	1	0	0	0	0	2	1	0	1	0
Physonota lutarella	0	0	1	1	0	01	0	1	0	1	0	0	0	0	0	0	0	1	0	1	1	1	0	0	0	0	1	1	0	1	0
Physonota maculiventris	0	0	1	1	0	01	0	2	0	1	0	0	0	0	0	0	0	1	0	0	1	1	1	1	0	1	1	1	0	1	0
Physonota mexicana	0	0	1	0	1	01	0	2	0	1	0	1	0	1	0	0	1	-	-	0	1	2	0	0	0	0	0	0	0	0	0
Physonota nitidicollis	0	0	1	1	1	1	0	1	1	1	0	0	0	0	0	0	0	1	1	0	0	2	0	1	0	1	2	0	0	3	0
Physonota ovalis	1	0	1	01	0	1	0	1	0	1	0	0	0	0	0	0	0	1	0	0	0	2	0	1	0	1	2	1	0	1	0
Physonota pacifica	0	0	1	1	1	1	0	1	0	1	0	0	1	0	0	0	0	1	0	0	?	?	?	?	?	?	?	?	?	?	?
Physonota picticollis	1	0	1	1	0	1	0	1	0	1	0	0	0	0	0	0	1	-	-	0	1	1	0	1	0	0	1	0	0	2	0
Physonota puncticollis	0	0	1	0	1	01	0	2	0	1	0	1	0	1	0	0	1	-	-	1	?	?	?	?	0	0	0	1	1	0	0
Physonota separata	0	0	1	0	0	0	0	2	0	1	0	0	0	0	0	0	0	1	0	0	1	1	0	0	0	0	1	1	0	0	0
Physonota sp.	0	0	1	1	0	1	1	1	0	0	0	0	0	0	0	0	?	?	?	1	?	?	?	?	?	?	?	?	?	?	?
Physonota stigmatillis	0	0	1	1	0	0	0	1	0	1	0	0	0	0	0	0	0	1	1	0	1	1	1	1	0	0	1	0	0	3	0
Physonota sublaevigata	0	0	1	1	1	1	0	1	0	1	0	0	0	0	0	0	0	1	0	0	?	?	?	?	0	1	1	1	1	3	0
Physonota translucida	0	0	1	1	0	01	0	2	0	1	0	1	0	1	0	0	1	-	-	1	1	2	1	1	0	0	0	0	0	0	0
Physonota turgida	0	0	1	01	0	1	0	1	0	1	0	0	0	0	0	0	0	1	0	0	0	1	1	1	0	1	1	1	1	3	0
Physonota unipunctata	1	0	1	1	0	1	0	1	0	1	0	0	0	0	0	0	0	1	0	0	0	1	1	1	0	2	2	0	0	3	0
Physonota vitticollis	0	0	1	0	0	1	0	2	0	1	0	0	0	0	0	0	0	1	1	0	1	2	0	1	0	0	1	0	0	0	0
Physonota vittifera	0	0	1	1	0	0	0	2	0	1	0	0	0	0	0	0	0	1	1	0	0	1	1	1	0	?	?	?	?	?	0
Platycycla deruta	0	0	1	1	0	0	0	3	0	1	0	1	0	0	0	0	0	1	0	2	1	1	0	1	0	1	2	1	0	2	0
Aspidimorpha dissentanea	0	0	1	0	0	2	0	2	0	0	0	1	0	0	1	0	1	-	-	1	0	3	-	0	-	0	2	0	0	2	0
Lacooptera murrayi	1	0	1	1	1	2	1	2	0	1	0	1	0	1	1	0	1	-	-	1	1	3	-	0	-	?	?	?	?	?	?
Aspidimorpha sp.	0	0	1	1	1	1	0	2	0	1	0	0	0	0	1	0	1	-	-	0	0	3	-	0	-	0	1	0	0	2	0
Aspidimorpha miliaris	0	0	1	0	0	01	0	2	0	0	0	0	0	0	1	0	1	-	-	1	0	3	-	1	-	1	2	0	0	1	0
Cassida nebulosa	1	0	1	0	1	1	0	1	0	1	0	0	0	0	0	0	0	0	0	0	0	3	-	1	-	1	1	0	0	0	0
Cheridotis miniata	0	0	1	0	0	0	0	1	0	0	0	0	0	0	0	0	0	0	0	0	?	?	?	?	?	1	2	0	0	0	0
Coptocycla undecimpunctata	0	0	1	1	0	01	0	2	1	1	0	0	0	0	0	0	0	1	0	0	?	?	?	?	?	0	1	0	0	0	0
Dorynota bidens	0	1	1	0	1	1	0	1	1	1	0	0	0	0	1	0	0	1	0	0	?	?	?	?	?	?	?	?	?	?	?
Omotenia humeralis	0	0	1	0	1	1	0	1	0	1	0	0	1	0	0	0	0	1	0	0	0	3	-	1	-	1	1	0	0	0	0
Paranota enifera	0	0	1	1	1	1	1	1	0	1	0	0	0	0	1	0	0	1	0	0	0	3	-	0	-	0	1	0	0	1	0
Paratriona turrifera	0	0	1	1	1	1	0	1	0	1	0	0	0	0	1	0	0	1	1	0	0	3	-	0	-	1	1	1	0	1	0
Chlamydocassis bicornuta	0	0	1	1	1	1	0	0	1	1	0	0	0	0	0	0	0	1	0	0	?	?	?	?	?	?	?	?	?	?	?
Chlamydocassis cribripennis	0	0	1	1	1	0	0	1	1	1	0	0	1	0	0	0	0	1	0	0	?	?	?	?	?	?	?	?	?	?	?
Chlamydocassis metallica	0	0	1	1	1	1	0	0	1	1	0	0	1	0	0	0	0	1	0	0	0	0	1	0	0	1	2	1	0	1	0
Goniochenia quadraticollis	0	1	1	1	0	1	1	1	1	1	0	0	0	1	0	0	0	1	0	1	0	0	0	0	0	1	2	1	1	02	0
Herissa pantherina	0	0	1	1	0	1	1	1	1	1	0	0	0	0	0	0	0	1	0	0	0	1	2	1	0	1	1	1	0	2	0
Polychalma multicava	0	0	1	1	1	01	0	1	1	1	0	0	0	-	0	0	?	?	?	1	?	?	?	?	-	?	?	?	?	?	-
Zeugonota quadrinodosa	0	0	1	1	1	1	1	0	1	1	0	0	0	0	0	0	0	1	0	0	0	1	1	1	0	1	1	1	0	1	0
Carlobruchia tricostata	0	0	1	1	1	1	1	1	1	1	0	0	0	0	0	0	0	1	0	1	0	1	1	1	0	0	0	0	0	0	0
Canistra osculatii	0	0	1	1	1	1	1	0	2	1	1	0	0	0	0	0	0	1	0	0	?	?	?	?	?	?	?	?	?	?	?
Cassidinoma denticulata	0	0	1	1	0	0	0	1	1	1	0	0	0	0	0	0	0	1	0	0	0	1	1	0	1	1	1	1	0	1	0
Cyclosoma palliata	0	0	1	1	0	01	0	1	1	1	0	0	0	-	0	0	0	1	0	0	?	?	?	?	?	1	1	0	0	0	0
Discomorpha variegata	0	0	1	1	1	1	0	2	1	1	0	0	0	0	0	0	0	1	0	0	0	1	1	1	1	1	2	1	0	0	0
Omocerus bicornis	0	0	1	1	1	1	0	0	1	1	0	0	1	0	0	0	0	1	0	0	0	0	1	0	1	2	1	0	0	0	1
Polychalca punctatissima	0	0	1	1	1	1	0	1	1	1	0	0	0	0	0	0	0	1	0	0	1	0	0	0	1	0	0	1	1	0	1
Agenysa caedemadens	0	0	1	1	0	1	1	3	1	1	0	0	0	1	0	1	0	0	0	2	?	?	?	?	?	?	?	?	?	?	?
Chelymorpha cassidea	0	0	1	1	0	1	0	0	1	1	0	0	1	0	0	1	0	0	0	0	0	1	1	1	1	0	1	1	0	1	0
Mesomphalia gibbosa	0	1	1	1	0	0	1	2	1	1	0	0	0	1	0	1	0	0	0	1	1	1	0	1	0	1	1	1	0	1	0
Stolas sp.	0	0	1	1	0	0	0	3	1	1	0	0	0	0	0	1	0	0	0	1	0	1	1	1	1	?	?	?	?	?	?

CHAPTER 4
A histological comparison of the two color morphotypes of the Geiger tortoise beetle with a brief natural history (Coleoptera: Chrysomelidae)

***** Formatted for submission to the journal *Coleopterists Bulletin* with the following co-author:
Steven R. Davis, Division of Invertebrate Zoology, American Museum of Natural History, Central Park West at 79th St., New York, NY 10024-5192 U.S.A. sdavis@amnh.org

ABSTRACT

The life cycle of *Eurypepla calochroma* Blake was reviewed. Eggs and two color morphotypes, brown and green, were illustrated for the first time. The internal structures of elytra between brown and green individuals were compared by histological sectioning and scanning electron microscopy. The basic cuticular layers (epi-, exo-, and endocuticle) were found in both morphotypes. Three differences of the internal structures of elytra between brown and green morphotypes were reported: 1) the endocuticle is thicker with more layers in green individuals than those in brown individuals with only one layer; 2) the thickness of the endocuticle in brown elytra was equal across the elytron, while the thickness of the endocuticle in green elytra was thicker near the columns than those between the columns; and 3) an endocuticular multilayer reflector (EMLR) was found only in the dorsal cuticular layer of the green elytron. The presence of green coloration in the elytron was hypothesized when the EMLR was present in the elytron and the interspace between the layers of the EMLR was filled with hemolymph.

KEY WORDS

Multilayer reflector, Tortoise beetle, elytra, histology, Florida, Geiger tree

INTRODUCTION

The family Chrysomelidae (leaf beetles) is one of the largest groups of beetles, with possibly over 50,000 species (Jolivet *et al.* 2008). This species diversity makes it the second largest family among the phytophagans following Curculionidae (weevils) (Riley *et al*. 2002). Leaf beetles are extremely diverse in size and shape (Jolivet and Hawkeswood 1995; Jolivet and

Cox 1996; Jolivet 1997). The tortoise beetles (members of the subfamily Cassidinae) are distributed worldwide and exhibit fascinating morphological diversity (Chaboo 2007; Borowiec and Swiętojańska 2014). One of the most interesting aspects is their body coloration, often showing remarkable variation within a species and even among individuals within a population (Chaboo 2007; Borowiec and Swiętojańska 2014).

The genus *Eurypepla* Boheman currently comprises of four species (*Eurypepla brevilineata* Boheman, *E. calochroma* Blake, *E. jamaicensis* Linnaeus, *E. vitrea* Boheman) and is distributed in the Yucatan Peninsula (Mexico), Cuba, Jamaica, the Bahamas, and southern Florida (USA), including the Florida Keys (Borowiec and Swiętojańska 2014). Exclusively, all species of *Eurypepla* feed on *Cordia sebestena* Linnaeus (Fig. 1, Geiger tree, Boraginaceae) (Fabricius 1801, Barber 1916, Blake 1966). In southern Florida, the Geiger tree is commonly used for landscaping; *E. calochroma* is readily found on these trees. Woodruff (1976) described the natural history of *E. calochroma* including descriptions of the prepupa (as larva), the pupa, and the adult with illustrations. Chaboo (2004, 2007, listed larval behaviors such as feeding on the lobes of flowers, gregariousness, and the abdominal movement against disturbances. Interestingly, the larvae of *E. calochroma* lack urogomphi; instead, their dorsum is covered by wet fecal material (Woodruff 1976, Chaboo 2007). During field observation in 2013, two different color morphotypes were observed in both sex of *E. calochroma*: brown and green individuals (Figs. 2–3). In addition, brown individuals often exhibited some yellow regions and black spot on postero-lateral region of each elytron (Fig. 2). Previously different color morphotypes have been observed in other tortoise beetles species (e.g., *Charidotella sexpunctata* (Fabricius)) and it has been assumed that the brown morphotype represents a teneral form

(Barrow 1979). However, preliminary observations indicate that live individuals of this brown morphotype remained brown for longer than 10 days in nature and in lab conditions.

Herein, the brief life history of *E. calochroma* is reviewed with images of all life stages from live specimens on the Geiger tree. Eggs and two color morphotypes are introduced for the first time. The internal structure of the elytra for both green and brown individuals are characterized through histological sections and scanning electron microscopy.

MATERIALS AND MATHODS

Field Collection:

Specimens were observed and collected daily in Fort Lauderdale and Davie, Florida from four different sites (April 25–28, 2013).

SITE 1: 26° 6' 1.77"N, 80° 7' 14.42"W (Fort Lauderdale, under SE 17th Street Causeway)

SITE 2: 26° 2' 50.96"N, 80° 15' 0.72"W (Davie, Target parking area)

SITE 3: 26° 5' 3.20"N, 80° 14' 20.15"W (Davie, University of Florida, Davie campus)

SITE 4: 26° 4' 29.40"N, 80°19' 5.10"W (Davie, SW 36th Court)

Specimens collected (more than 200 specimens from each site) were directly placed in 70% ethanol as voucher specimens. In addition, five male and five female specimens of each brown and green individuals were collected at Site 3 for histological sectioning and scanning electron microscopy (SEM) and fixed in 4% paraformaldehyde (transferred into 70% ethanol after three days).

Histological sectioning:

For histology, cross sections were cut in the range of the postero-lateral dark spot region on each elytron (when elytron was separated from the body, the dark spot became conspicuous). The posterior half of each elytron of two green individuals (four pieces) and two brown individuals (four pieces) were cut and transferred to 100% ethanol for dehydration overnight. Each piece of elytron passed through a 100% ethanol/ LR White® solution (1:1) two times for 12~ hours each time before being placed in 100% LR White® resin in gelatin capsules in an oven for 24 hours at 60˚C for thermal curing. After polymerization, embedded specimens were removed from the gelatin capsules and sectioned using a Leica EM UC6 ultratome with diamond knife, producing semi-thin sections of 5µm thickness. Sections were transferred to glass slides with water drops, left on a slide warmer for one hour at 60°C, stained with toluidine blue for 15 minutes, and rinsed with tap water. Sections were subsequently air dried and mounted in Permount™. Stained sections were digitally photographed with a Leica DFC230 camera mounted on a Zeiss Axioskop 2 plus compound microscope using the Leica Firecam software. Measurements were made with Image J. Adobe Photoshop CS5 was used for enhancing images.

Electron microscopy:

To prepare elytron sections for SEM, cross sections were cut in the range of the postero-lateral dark spot region of each elytron. Each elytron of two green (four pieces) and two brown individuals (four pieces) were cut. The pieces were transferred to 100% N-butyl-ethanol for 6~ hours for dehydration and softening of the cuticle; this step was repeated two times at room temperature. The pieces in 100% N-butyl-ethanol were directly transferred to liquid paraffin, left to incubate in the oven for 6 hours at 59˚C, and transferred to fresh liquid paraffin to incubate overnight at 59˚C. Paraffin-embedded specimens were mounted and preserved in

refrigerator at 4˚C until paraffin coagulated. Mounted specimens were sectioned with an Olympus Cut 4060 rotary microtome, producing semi-thin sections at a thickness of 20μm and placed on small glass dishes. The sections were deparaffinized in xylene several times until no paraffin residue was left when the xylene left to evaporate. The deparaffinized sections were washed in 100% ethanol for 2 hours (3 times) and allowed to dry. Sections were mounted on aluminum stubs using adhesive Pelco tabs and isopropanol-based colloidal graphite. Specimens were coated with 30nm of gold. SEM images of the sections were captured using a LEO 1550 FESEM.

Terminology:

The terminology for the internal structure of the dorsal cuticular layers followed van de Kamp & Greven (2010). The term “endocuticular multi-layer reflector” (EMLR) was derived from a multi-layer reflector of the exocuticle in Vigneron *et al*. (2007) because the multi-layer reflector in *E. calochroma* was believed to be endocuticular, rather than exocuticle in origin.

RESUTS

Field observation of *E. calochroma* (Figs. 1–7):

The life cycle of *E. calochroma* (Figs. 1–7) is that of a typical tortoise beetle life cycle with four instar stages and a prepupal stage (= 5th larval stage in Chaboo 2007). Adults of *E. calochroma* (Figs. 2–3) spend most of their lives on the host plant (Geiger tree, Fig. 1). Females lay their eggs on the upper or lower side of a leaf (Fig. 4): number of eggs in each clutch varies between 27 and 80 (n=23 clutches). Eggs are covered by fine fibrous webs. The four instar stages (prepupal stage excluded) (Figs. 5–6) spend most of their time feeding on leaves or occasionally

petals (Chaboo 2004). The 1st and 2nd instars generally show gregarious behavior without distinct movement, while the 3rd and the 4th instars are both solitary and gregarious with distinct movement. The larvae react to physical or visual disturbance by raising their abdomen and moving towards the disturbance. Pupation (Fig. 7) occurs on the leaves, branches, and sometimes trunk of the host plant. Adults of both brown and green individuals often were observed together at each collecting site; however, the proportions of the two morphotypes differed. We found mostly green individuals at Sites 1 (12 trees) and 3 (16 trees), mostly brown at Site 2 (five trees), and roughly equally proportions at Site 4 (22 trees).

Comparison between brown and green elytra (Figs. 8–12):

The basic distinctions of epi-, exo-, and endocuticle are clear in each color morphotype (Figs. 8–10). These layers are similar to those in other beetles (Krzelj 1969, Parker *et al*. 1998, Van de Kamp and Greven 2010). Based on our observations of elytral sections from green and brown individuals, we found that the thickness of the elytra varies slightly among individual. No difference in the internal structure was found between the medial region and the lateral region (postero-lateral dark spot region) within each brown and green elytron. The layers of exocuticle and endocuticle are of a pseudo-orthogonal type (Figs. 11–12). In both morphotypes, dorsal cuticular layers are thicker than ventral cuticular layers. The epicuticle is a thin layer on the dorsal-most surface. The thickness of epicuticle is between 4μm and 5μm in both brown and green elytra. The exocuticle is located below the epicuticle and the thickness of exocuticle is between 12μm and 15μm in both brown and green elytra. The exocuticle is comprised of several thin layers and each layer of the exocuticle is similar in thickness in both brown and green elytra.

The endocuticle is as thick as the epicuticle in brown elytra and it is the thickest layer in green elytra.

Three distinct differences of the internal structure in the dorsal cuticular layer were found between the elytra of green and brown morphotypes (Figs. 8–12). **(1)** The dorsal endocuticle was thicker with more layers in green elytra than in brown elytra: we observed at least seven distinct layers in endocuticle of green elytra (Fig. 9) and only one layer in endocuticle of brown elytra (Fig. 10). More and thicker layers of endocuticle consequently resulted in a thinner sponge layer in green elytra; in brown elytra, only one thin layer of endocuticle was observed and the sponge layer was thicker than that in green elytra (Figs. 8–12). **(2)** The thickness of endocuticle in brown elytra did not vary across the elytron; it was between 4μm and 5μm (Fig. 8), while the thickness of the layers in the endocuticle was thicker near the columns (about 50μm) than at middle between columns (about 22μm) in green elytra (Fig. 9). **(3)** The endocuticular multi-layer reflector (EMLR) was observed below the endocuticle only in the dorsal cuticular layer of green elytra (Figs. 9, 10, 12). The thickness of the EMLR was consistent (about 10μm) comprising about 20 thin layers and continuous across the elytral disc. The EMLR was only present in the discal region of the elytron in whicht green coloration was present. The EMLR was absent or present as a thinner version at the lateral explanate region (lamellae) in which the dorsal coloration was transparent (Fig. 13).

DISCUSSION

The phenomenon of two color morphotypes existing within a species was reported as teneral stage in other tortoise beetle species (Barrow 1979). However, the teneral form of adults with bright yellow cuticle was observed in several individuals after eclosion in *E. calochroma*,

which suggested that the brown individuals of *E. calochroma* were not the teneral form of the adults.

Among the three differences in the internal structures between green and brown elytra, the EMLR was known to be the core structure that provides a golden or metallic color (green in *E. calochroma*) in dorsal view due to light reflection among tortoise beetles (Mason 1929, Hinton 1973, Neville 1977, Parker *et al*. 1998, Vigneron *et al*. 2007). Based on observations in the present study, we hypothesize that the elytron was green when the EMLR was present and the interspace between the layers of the EMLR was filled with hemolymph. These conditions for presence of the green coloration in the elytron were tested with a small piece of the elytron. When an elytron was cut in half, the green coloration of around the damaged area dissipated and became brown (Fig. 14). This brown region is either filled with hemolymph, causing the structure of the EMLR to change, or it is filled with air (Fig. 14A).

Both green and brown morphotypes become a pale brown and beige when the specimens desiccate. This has been reported in other tortoise beetles with metallic colors, including those in Aspidimorphini, Cassidini, and Mesomphaliini (Mason 1929, Blake 1965; Chaboo 2007; Shin *et al*. 2012; Borowiec and Świętojańska 2014). This color change or loss of color is believed to be caused by dehydration of the cuticular layers, epidermis, and sponge layer in the elytra.

In *E. calochroma*, the dorsal coloration of live brown individuals (brown with black spots and pale yellow regions (Fig. 2) is thought to originate from the pigments near the epidermis in the elytra (Vigneron *et al*. 2007). Green individuals, indeed, have the same coloration and pattern as brown individuals, which can also be observed when the specimens of green individuals are desiccated or when elytra are disarticulated. However, this basic coloration derived from the pigments is obscured by the green coloration produced by the EMLR in the dorsal view. When

the dried specimens of green individuals are rehydrated by any kind of liquid (such as ethanol, water, saline, or glycerin), most of the time, the green coloration is partially or fully recovered.

ACKNOWLEDGMENTS

The authors are grateful to K. Jensen (University of Kansas) for providing training on general histological sectioning skills to CS and general guidance for this study; M. S. Engel (University of Kansas) for his general comments and assistance; Paul Badunias (University of Florida, Davie) for help during the field work; Heather Shinogle and Prem Thapa (University of Kansas, Microscopy Lab) for allowing use of the sectioning facilities. We also thank two anonymous reviewers for valuable comments. This research was partially supported by the Program of Entomology, Department of Ecology & Evolutionary Biology, University of Kansas, and is a contribution of the Division of Entomology, University of Kansas.

CITATIONS

Barber, H. S. 1916. A review of North American tortoise beetles (Chrysomelidae; Cassidinae). Proceedings Entomological Society of Washington 18: 113–127.

Barrows, E. M. 1979. Life cycles, mating, and color change in Tortoise beetles (Coleoptera: Chrysomelidae: Cassidinae), The Coleopterists Bulletin 33(1): 9–15.

Blake, D. H. 1965. **Twelve new species of chrysomelid beetles from the West Indies (Coleoptera, Chrysomelidae). American Museum Novitates 2217: 1–13.**

Blake, D. H. 1966. Ten new chrysomelid beetles from the West Indies. Proceedings of the Entomological Society of Washington 68: 213–222.

Borowiec, L., and J. Świętojańska. 2014. Cassidinae of the world – an interactive manual (Coleoptera:Chrysomelidae). Available from: http://www.biol.uni.wroc.pl/cassidae/katalog%20internetowy/index.htm (Accessed: July 1, 2015).

Chaboo, C. S. 2004. Natural history observations in *Eurypepla calochroma* Blake (Chrysomelidae: Cassidinae: Physonotini). The Coleopterists Bulletin 58(1):142–143.

Chaboo, C. S. 2007. Biology and phylogeny of Cassidinae Gyllenhal (tortoise and leaf-mining beetles) (Coleoptera: Chrysomelidae). Bulletin of the American Museum of Natural History 305: 1–250.

Fabricius, J. C. 1801. Systema Eleutheratorum secundum ordines, genera, species adiectis synonymis, locis, observationibus, descriptionibus.Tomus I. Bibliopolii Academici Novi, Kiliae.

Hinton, H. E. 1973. 3 Natural Deception [pp. 97–159]. *In*: Illusion in Nature and Art (R. L. Gregory and Sir E. Gombrich, editors). Duckworth, London.

Jolivet, P. 1997. Biologie des coléoptères chrysomélides. Société novelles desédition boubée: Paris.

Jolivet, P. H. A., and M. L. Cox. 1996. Chrysomelidae biology: classification, phylogeny and genetics, Volume 2. SPB Academic Publishers, Amsterdam, Netherlands.

Jolivet, P., and T. J. Hawkeswood. 1995. Host plants of Chrysomelidae of the world. Leiden: Backhuys.

Jolivet, P., J. Santiago-Blay and S. Schmitt. 2008. Foreword [pp. 15–16]. *In*: Research on Chrysomelidae. Volume I (Jolivet, P., J. Santiago-Blay and S. Schmitt, editors). Leiden, Boston, MA.

Krzelj, S. 1969. Structure anatomique comparée des élytres des coléoptères. Annales de la Société Royale Zoologique de Belgique 99: 85–109.

Mason, C. W. 1929. Transient color changes in the tortoise beetles (Coleoptera: Chrysomelidae). Entomological News 40: 52–56.

Neville, A. C. 1977. Metallic gold and silver colours in some inset cuticles. Journal of Insect Physiology 23(10): 1267–1274.

Parker, A. R., D. R. McKenzie, and M. C. J. Large. 1998. Multilayer reflectors in animals using green and gold beetles as contrasting examples. The Journal of Experimental Biology 201, 1307–1313.

Riley, E. G., S. M. Clark, R. W. Flowers, and A. J. Gilbert. 2002. 124. Chrysomelidae Latreille 1802 [pp. 617–691]. *In*: American beetles. Polyphaga: Scarabaeioidea through Curcurlionoidea Volume 2 (R. H. Arnett, M. C. Thomas, P. E. Skelley, and J. H. Frank, editors). CRC Press, Baton Rouge, LA.

Shin, C., Chaboo, C. S. and S. M. Clark. 2012. Revision of the endemic Hispaniolan genus *Asteriza* Chevrolat, 1836, with description of two new species **(Coleoptera: Chrysomelidae: Cassidinae: Ischyrosonychini). Zootaxa 3227: 34–53.**

Van de Kamp, T., and H. Greven. 2010. On the architecture of beetle elytra. Entomologie heute 22: 191–204.

Vigneron, J. P., J. M. Pasteels, D. M. Windsor, Z. Vértesy, M. Rassart, T. Seldrum, J. Dumont, O. Deparis, V. Lousse, L. P. Biró, D. Ertz, and V. Welch. 2007. Switchable reflector in the Panamanian tortoise beetle *Charidotella egregia* (Chrysomelidae: Cassidinae). Physical Review 76: 1–10.

Woodruff, R. E. 1976. The tortoise beetles of Florida III, *Eurypepla calochroma floridensis* Blake (Coleoptera: Chrysomelidae). Entomology Circular, Florida Department of Agriculture & Consumer service 163: 1–2.

LIST OF FIGURES

Figs. 1–7. Biology of *Eurypepla calochroma*. 1. Host plant (Geiger tree); 2. Adult of brown morphotype; 3. Adult of green morphotype; 4. Eggs on host plant; 5. 1st (small) and 4th (large) instar larvae; 6. 2nd (small) and 3rd (large) instar larvae; 7. Pupa.

Figs. 8–10. Cross sections of elytra. 8. Brown individual; 9. Green individual; 10. Comparison of the elytral cross sections between brown and green individuals (EMLR = Endocuticular Multilayer Reflector).

Figs. 11–12. SEM images of elytral cross sections. 11. Brown individual; 12. Green individual; A) Magnified view of the EMLR; 13. Cross section of elytral lamella (explanate region) of green morphotype.

Fig. 14. Apical part of elytron immediately after being severed. A. Magnified area near severed edge, showing loss of metallic green coloration due to reduction in hemolymph pressure and infiltration of air bubbles; B. Magnified area distal to severed edge (near elytral apex) still filled with hemolymph, nearly lacking any air bubbles, and showing retention of metallic green coloration.


1

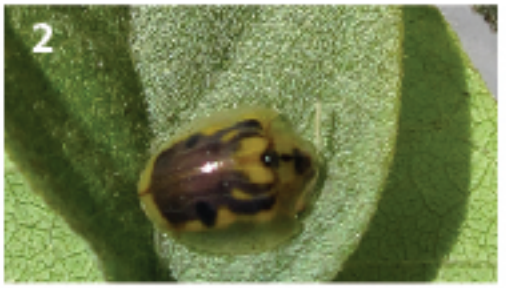
2


3


4


5


6


7


8
0.1 mm

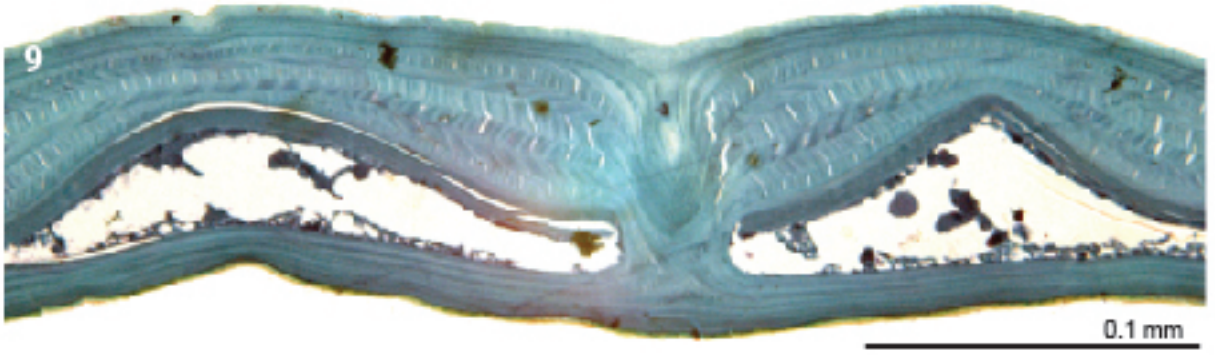
9
0.1 mm

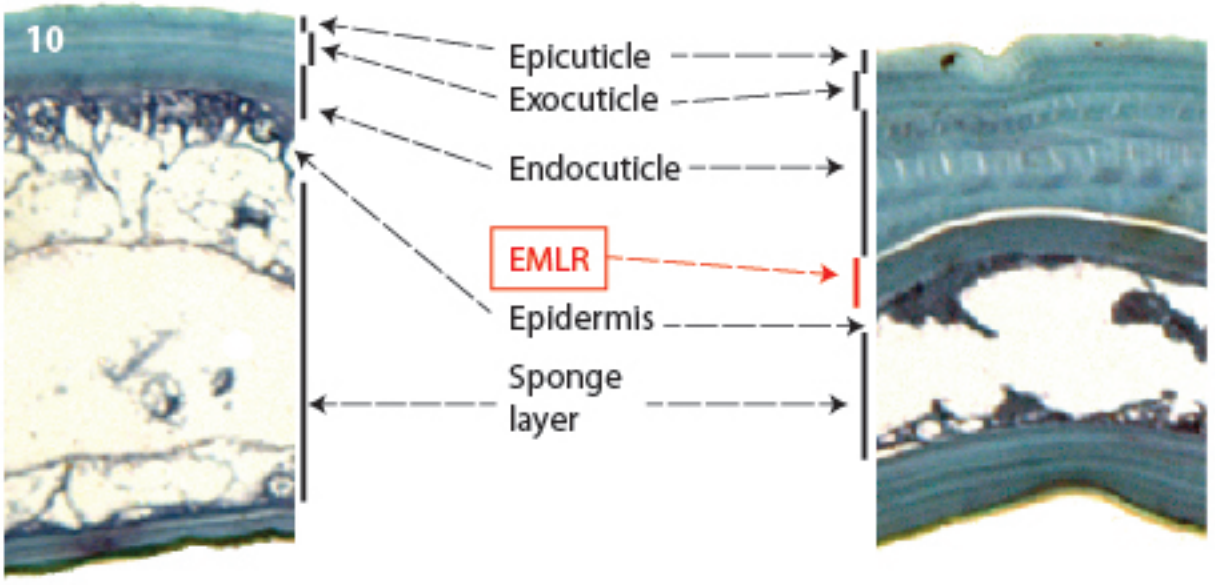
10
Epicuticle
Exocuticle
Endocuticle
EMLR
Epidermis
Sponge
layer

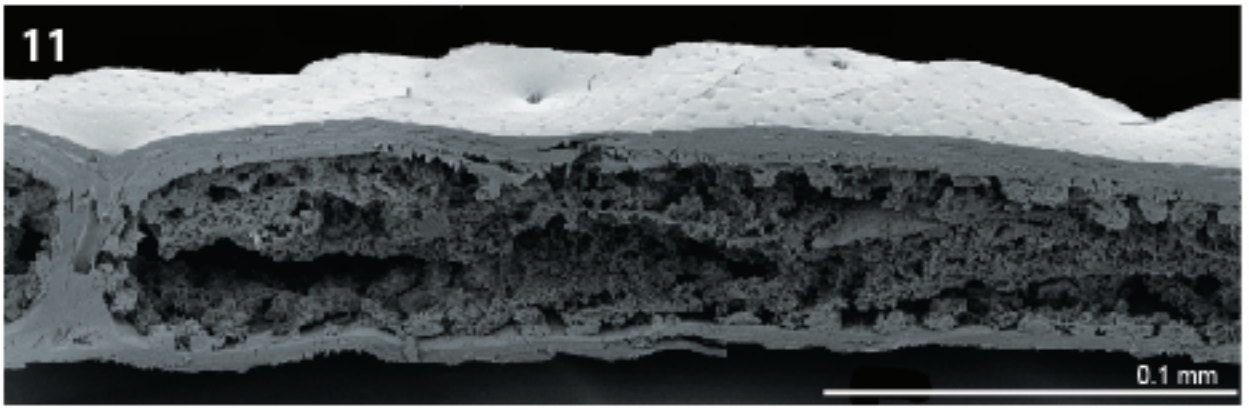
11
0.1 mm

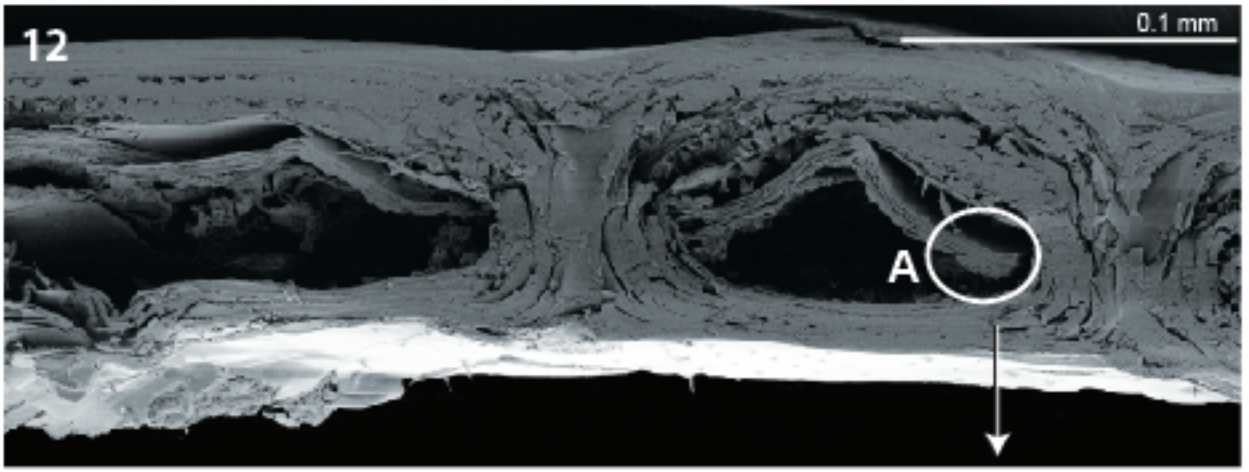
12
0.1 mm
A

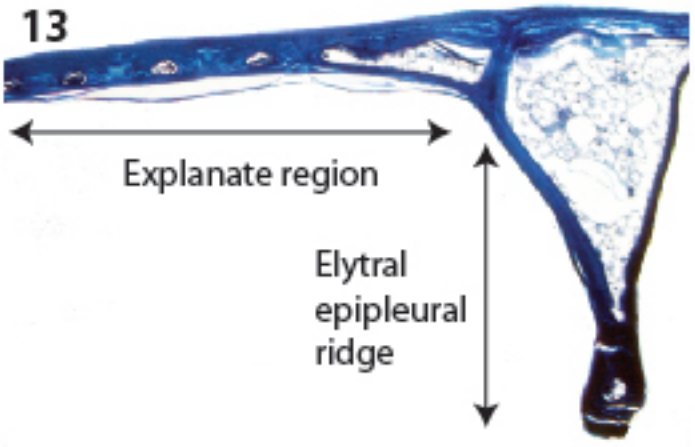
13
Explanate region
Elytral
epipleural
ridge

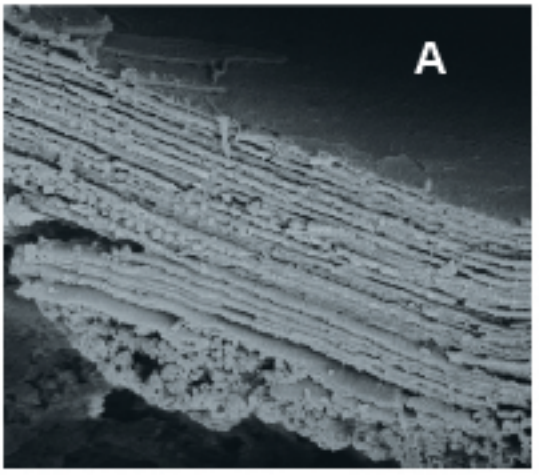
A

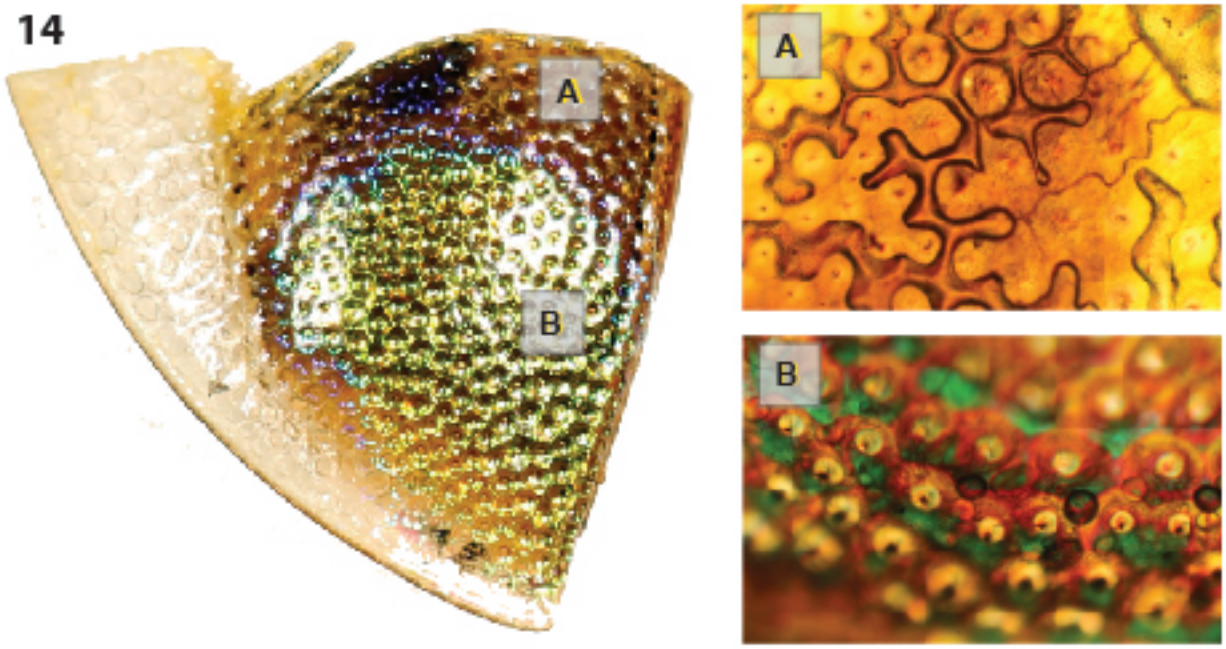
14
A
B
A
B

CHAPTER 5

Observation and histological study on color change in the Geiger tortoise beetle (Coleoptera: Chrysomelidae)

***** Formatted for submission to the journal *Coleopterists Bulletin* with the following co-author: Steven R. Davis, Division of Invertebrate Zoology, American Museum of Natural History, Central Park West at 79th St., New York, NY 10024-5192 U.S.A. sdavis@amnh.org

ABSTRACT

A pattern of color change from green to blue in the Geiger tortoise beetle (*Eurypepla calochroma* Blake) was observed. The internal staining of the elytra indicated that the endocuticular multilayer reflector (EMLR) was in contact with hemolymph. The EMLR is comprised of over 40 thin layers, and each layer nearly subequal in thickness, in which the dorsal layers were slightly thicker than the ventral ones, and the distance between the layers also appeared greater between the dorsal layers than the ventral ones. Sagittal sectioning of the pronotum confirmed that the color changing regions of the pronotum were composed of two cuticular layers, similar in structure to those regions of the elytra. The mechanism of color change in *E. calochroma* is hypothesized as a structural change caused by a reduction in the amount of hemolymph within the elytron: when hemolymph volume is reduced it decreases the distance between the thin layers in the EMLR and consequently causes reflection of shorter wavelength light. The hypothesized mechanism of the dorsal color change in *E. calochroma* was compared to the color change of another tortoise beetle species, *Charidotella egregia*. Unlike the red dorsal color in *C. egregia*, which originates from red pigments in the epidermis, the blue coloration of *E. calochroma* originates from the EMLR. Thin-film theory (= hydraulic theory) was invoked to explain the proposed hypothesis. Alterations of pH and temperature did not affect the color change in *E. calochroma*.

KEY WORDS

Multilayer reflector, tortoise beetle, elytra, color change, Geiger tree

INTRODUCTION

The phenomenon of reversible color change has been reported across several insect orders (see Vigneron et al. 2007). In Coleoptera, reversible color change has been observed in the elytra of the Hercules beetle (*Dynastes hercules* Linnaeus, Scarabaeidae) (Hinton & Jarman 1972) and several tortoise beetles (Chrysomelidae: Cassidinae) (Mason 1929, Barrows 1979, Jolivet 1994, Vigneron et al. 2007). These color changes have been hypothesized to be responses to external stimulation. For example, the dorsal color of the Hercules beetle changes passively from yellow to black in response to high humidity at night (Hinton & Jarman 1972). In contrast, the dorsal color change observed in some tortoise beetles is much more dramatic and appears to be an active response to external disturbance (Mason 1929, Jolivet 1994, Vigneron 2009). The mechanism of this dorsal color change has been hypothesized as a structural change, pigment content change, or both structure and pigment change in the cuticle (Mason 1926, 1929, Neville 1977, Jolivet 1994, Vigneron 2009). Mason (1929) introduced thin-film theory (= hydraulic theory) to explain a mechanism of color change by which turgor pressure is regulated through the cuticular multilayer reflector inside the elytron, thereby altering the thickness of the hydrated cuticular film and producing a wide variety of colors.

Vigneron et al. (2007) studied the switchable color change in *Charidoella egregia* Boheman, which exhibits a change in dorsal coloration from metallic gold to dull red in response to disturbance. Their study included detailed images of the cuticular multilayer reflector in the elytra and discussed the pattern of color change, and optical properties of light reflection and wavelengths. As the color change mechanism they introduced the “switchable mirror theory,” positing that the golden coloration originated when the cuticular multilayer in the elytra was hydrated by hemolymph, and the red color appeared when the cuticular multilayer desiccated. In addition, the red color apparently originated through pigments in the epidermal cell layer, and a

difference between the red coloration in both living and dried specimens was reported. Switchable mirror theory basically demonstrated the decomposition of the mirror (and a subsequent loss of light-reflecting ability) when the cuticular multilayer reflector was not moisturized.

Shin & Davis (2015) reported two color morphotypes of the Geiger tortoise beetle (*Eurypepla calochroma* (Blake)): one consisting of a pale yellow and brown dorsal coloration (brown individuals) and the other of individuals with a metallic green dorsal coloration (green individuals). The differences in internal structure of the elytra in brown and green individuals were as follows: **(1)** The dorsal endocuticle was thicker with more layers in green elytron than in brown elytron, **(2)** The thickness of endocuticle in brown elytron was equal across the elytron, while the thickness of the layers in the endocuticle was thicker near the columns, **(3)** The EMLR was found below the endocuticle only in the dorsal cuticular layer of green elytra (Shin & Davis 2015). In addition to the two color morphotypes, a different kind of reversible dorsal color change was observed in the Geiger tortoise beetle in southern Florida. Dorsal color change from green to blue was observed only in green individuals in response to external disturbance (Fig. 1); no color change was observed in brown individuals. Color change specifically was observed only in the anterior and posterior regions of the pronotum and in the elytral disc (excluding the lateral explanate region). The duration of the color change varied between 2–20 minutes after physical or subsequent visual disturbances, the longer durations perhaps due to increased desensitization caused by frequent disturbance during the filed observation. However, unlike *C. egregia,* blue pigments were not reported in the epidermal cell layer in *E. calochroma* (Shin & Davis 2015).

In this study, the pattern of color change in *E. calochroma* was illustrated and documented; experiments were performed to confirm the hydration of the EMLR layers with

hemolymph; previously known mechanisms of color change such as pH alteration, temperature change, and physiological change were tested with *E. calochroma*. Scanning transmission electron microscope (STEM) images were taken of the elytron; and sagittal semi-thin sections were acquired to explain the limitation in color change to only the anterior and posterior regions of the pronotum. Based on the observed structures and performed experiments, the mechanism of color change in *E. calochroma* was hypothesized; comparison of the color change mechanism between *E. calochroma* and *C. egregia* was summarized; and the function of color change in tortoise beetles was further discussed.

MATERIALS AND METHODS

Specimens Examined

Specimens were collected in Davie Florida, U.S.A. (26° 5' 3.20"N, 80° 14' 20.15"W, 25–28 IV 2013). The collected specimens (5♂, 5♀) were preserved in 70% ethanol. The voucher specimens and sectioning slides were deposited in Natural History Museum, University of Kansas.

Terminology

The terms for the internal structure of the dorsal cuticular layers follow van de Kamp & Greven (2010) and Shin & Davis (2015).

Histology

To test whether hemolymph actually moisturized the EMLR in the elytra, an elytron was removed from a specimen and punctured by a mounting pin (four punctures: middle, medial

middle, lateral middle, and near the apex of elytral disc) to facilitate staining and embedding. The punctured elytron was soaked in 70% ethanol based toluidine blue solution (50ml:0.1g) until the internal structure were stained. After staining in toluidine blue solution, the external surface of the stained elytron was quickly rinsed by dipping in tap water and dried at room temperature. The dried specimen was transferred to liquid paraffin, left to incubate in the oven for 50~hours at 59˚C. The specimen in liquid paraffin was swirled several times during incubation. The specimen was embedded in paraffin, sectioned with an Olympus Cut 4060 microtome, producing semi-thin sections at a thickness of 10µm. Sections were deparaffined in xylene (30s), and mounted in Canada balsam.

For examining the pronotum, sagittal sectioning was performed in the medial area. The pronotum was disarticulated from the specimen in 70% ethanol, transferred to 100% ethanol for dehydration for 6~hours, then transferred to fresh 100% ethanol overnight. The dehydrated pronotum was transferred to xylene for 6~hours 2 times, transferred to xylene/liquid paraffin (1:1) solution, and left to incubate in the oven 12~hours 2 times in a fresh xylene/liquid paraffin (1:1) mix. The pronotum in xylene/liquid paraffin (1:1) solution was transferred to liquid paraffin, left to incubate in the oven 12~hours at 59˚C 2 times with fresh paraffin, and embedded in paraffin. The paraffin embedded pronotum was sectioned at a thickness of 10µm with an Olympus CUT4060 retracting rotary microtome. The sections were cleared in xylene, stained with Gill's hematoxylin, counterstained with eosin, and mounted under coverslips in Canada balsam.

Stained sections of the elytron and pronotum were digitally photographed with a Leica DFC230 camera mounted on a Zeiss Axioskop 2 plus compound microscope using the Leica Firecam software. Measurements were made with Imag J. Adobe Photoshop CS5 was used for enhancing the images.

Scanning Transmission Electron Microscopy (STEM)

A piece of an elytron (posterior half) was dehydrated in 100% ethanol. Infiltration consisted of approximately twelve hour incubation periods through a series of 1:1 then 1:2 100% ethanol to LR White® of resin mixtures. Elytra were placed in gelatin capsules and embedded in pure LR White®. Following thermal curing in an oven for 24 hours at 60°C, embedded elytra were removed from the capsules and sectioned using a Leica EM UC6 ultratome with diamond knife, producing thin sections at a thickness of ~150–200 nm. Sections were transferred to #300 copper mesh grids, stained with 2% uranyl acetate for 25 minutes, and imaged in a STEM holder using a LEO 1550 FESEM (Field Emission Scanning Electron Microscope) at 30 kV.

Experimental Determination of Color Change in Response to pH Alteration, Damage on Elytra, and Temperature

To test the previously known mechanisms of color change such as pH alteration (Neville 1977), physiological change (Barrow 1979), and temperature alteration (Vigneron et al. 2007), we created or repeated the experiments from those previous studies with *E. calochroma.*

To confirm the color change of elytra by pH alternation, a non-dissected specimen (preserved in 70% ethanol) was soaked in each vinegar (about pH 2.2) and ammonia (about pH 11) for a week. The coloration on the elytron was checked daily.

To determine if the dorsal color change was caused by physiological changes such as endocrine and exocrine systems, two live individuals were examined by damaging an elytron: **(1)** the postero-lateral, humeral, and upper medial areas of an elytron was damaged by a mounting

pin; **(2)** postero-medial spot that the dorsal color change started was severed. While observing the color change after damaging the elytron, the physical disturbances were continued.

We also tested if temperature caused the dorsal color change. We removed two pairs of elytra from two specimens preserved in 70% ethanol. Each elytron from each individual was kept in boiling water for ten minutes and iced water for 10 minutes. Elytra soaked in iced water were reused for freezing.

RESULTS

We observed a consistent pattern in the dorsal color change on the discs of the elytra and pronotum. The pattern of color change on the elytra was documented with images from live specimens during field work.

Pattern of the Dorsal Color Change

Step one (Fig. 2). The first blue spot appeared posterior to the middle of each elytron (primary blue spot).

Step two (Fig. 3). A second blue spot appeared on the humeral (umbo) area of each elytron (anterior blue spot).

Step three (Fig. 4). The anterior blue spot expands postero-medially and the primary blue spot expands laterally and posteriorly.

Step four (Fig. 5). The primary and anterior blue spots expand; the expanded anterior blue spot (region) connected to the primary blue spot on each elytron.

Step five (Fig. 6). Most regions of the elytron exhibited blue or greenish blue except for the regions surrounding the mesoscutellum and lateral portions of the elytral humeri.

Step six (Fig. 7). The color change is completed as blue coloration became distinct in all discal areas of the elytron.

The dorsal color change pattern in *E. calochroma* was consistent among most individuals. However, at any step the color change stopped and green coloration returned (or often stayed at step one longer than 10 minutes) if any disturbances ceased.

Internal Staining of Elytron

In previous studies (Mason 1926, 1929, Neville 1977, Jolivet 1994, Vigneron 2009), the color change in tortoise beetles was speculated to be a change in the interval layers of the multilayer reflector by hemolymph. However, none of those studies actually demonstrated whether hemolymph actually infiltrated between the layers of the EMLR. The semi-thin sections of the internally-stained elytron by toluidine blue (Fig. 8) showed that, **(1)** the dorsal cuticular layers (epi-, exo- and endocuticle) were transparent (unstained), and **(2)** the EMLR was stained by toluidine blue. These indicate that the dorsal cuticular layers did not contact any fluid, while the EMLR was fully immersed in fluid and likely responsible for the structural change caused by saturation with hemolymph.

Scanning Transmission Electron Micrograph (Fig. 9)

STEM images of the elytron revealed thin layers of exocuticle. The thickness among the exocuticular layers did not vary. In endocuticle, at least 10 layers were observed. The layers of the endocuticle form a lattice-structure. The middle layers were thicker than the upper or lower layers: the thickest layer was about 5 times thicker than uppermost and lowermost layers of endocuticle. The cuticular multilayer reflector was observed between the endocuticle and

epidermis in the dorsal cuticular layer of the elytron. The EMLR was thinner than the endocuticle (less than the half thickness of endocuticle). STEM imaging of the elytron showed that the structure of the EMLR with over 40 layers: each layer nearly subequal in thickness, though the dorsal layers were slightly thicker than the ventral ones, and the distance between the layers also appeared greater in the dorsal layers.

Sagittal Thin Section of Pronotum (Fig. 10)

An EMLR was found across the dorsal cuticle of the pronotum while it was absent in the prosternum. The anterior (Fig. 10A) and posterior regions (Fig. 10B) of the pronotum were formed by two cuticular layers as in the elytra: both regions having extended areas of folded cuticle to form dorsal and ventral cuticles. These double-layered regions of the pronotum correspond to those which are able to undergo a color change. Between anterior and posterior double-layered regions, single-layered regions were observed with muscle attachment. No color change was observed in the single-layered middle region.

pH Alternation, Damaging Elytra, and Temperature Alteration

Each elytron in vinegar or ammonia remained green over 7 days: pH alternation did not induce color change in *E. calochroma.* Normal color change on the damaged elytra was still observed: this indicated that the primary spot did not contain any glands or cells responsible for the color change (Figs. 11–12). The elytra in boiling water and iced water remained green. When the elytra were frozen, the green coloration disappeared and brown coloration appeared (Fig.17). However, the green coloration started reappearing when the ice started melting.

DISCUSSION

Both green and blue colorations due to epidermal or cuticular pigments are rare or absent among beetles (Mason 1926, Crowson 1981). The origins of green and blue colors in beetles have been reported as caused by multilayer reflectors in the cuticle (Parker et al. 1998, Seago et al. 2009). Unfortunately, we were unable to observe sections representing time periods during actual color and physical change of the EMLR. Due to the preparation time required in histological sectioning, such as during embedding and staining, as well as structural changes which may be introduced through cryo-sectioning, it is difficult to directly observe the changes which occur within the cuticle during color change.

The color change in *E. calochroma* was first hypothesized to be caused by reactions of physiological changes such as endocrine and exocrine systems because the color change was relatively quick and the pattern of the dorsal color change among individuals of *E. calochroma* was consistent (Hinton 1960). The location of the primary spot on each elytron was identical to the mid-lateral black spot in brown individuals, which originates from pigments in the epidermis (Shin & Davis 2015). We therefore hypothesized that the color change could be caused by chemical reactions, such as in the release of chemical compounds or enzymes from glands or specialized cells. We assumed putative glands or specialized cells were located in the primary spot area because color change always began at that location. However, no differences were found in cell types or in general cuticular structure between the primary spot and other surrounding areas in histological sections (Shin & Davis 2015). In this study, two simple experiments with live individuals were performed focusing on the primary spot. We tested if the color change still occurred when the primary spot was damaged. We damaged the primary spot, elytral humeral area, and upper median area on the elytron by penetrating the elytron with an

insect mounting pin (arrow marked, Fig. 11), resulting in no effect; color change still occurred on the damaged elytron (Fig. 11). We also severed the elytron just anterior to the primary spot and were still able to observe color change in the basal half of the elytron (Fig. 12). We concluded that the pattern of color change in *E. calochroma* might be due to a structural change in the elytron (analogous to a pocket filled with liquid), in which areas of less volume changed color first, or perhaps the black spots and brown areas actually facilitated the change to a blue coloration due to certain compositions of their cuticles. Parker et al. (1998) found a layer with black pigments underlying the cuticular reflector in *Calloodes grayanus* (White) (Scarabaeidae), which assisted the formation of a green color by absorbing the transmitted portion of the incident light and altered the color of the green reflection. It is possible that these black or brown pigmented areas in the cuticle might amplify the blue coloration or cause it to be more conspicuous, or they may be areas consisting of slightly thinner EMLR layers and therefore are the first to reflect blue wavelengths during changes in hemolymph pressure.

Hypothesized Color Change Mechanism

In the EMLR with each layer nearly subequal in thickness, different wavelengths of light are reflected depending on the layer by which the light was reflected (Fig. 13, “chirped structure” in Parker et al. 1998). Between green and blue, blue light is reflected at a deeper cuticular layer in a multilayer reflector than is green light. Given that the EMLR was stained by toluidine blue in this study, the intervals between the layers of the EMLR might change depending on the volume of hemolymph introduced into the elytron. The same hypothesis also has been described and supported in previous studies (Mason 1929, Hinton 1973, Neville 1977, Vigneron et al. 2007).

Based on the findings in the present study (hemolymph in the EMLR (Fig. 8) and the structure of the chirped multilayer reflector (Fig. 9)), and considering the light-reflecting properties of a chirped multilayer reflector (Fig. 13), the mechanism of the dorsal color change in *E. calochroma* was hypothesized to be a change in the distance between the EMLR layers by variable hemolymph amount. When the elytron loses hemolymph, the internal structures including the EMLR were thought to have condensed, and as a result the distance between the layers of the EMLR became narrower due to the folded structure of the elytron and confined reservoirs of hemolymph between the dorsal and ventral cuticular layers. This condensing mechanism by losing hemolymph within the EMLR due to the folded structure of the elytra also explained why only the anterior and posterior regions of the pronotum changed color but not the middle areas (despite also having the EMLR). With the assumption that the incident light was reflected at a certain depth in the EMLR, the condensed EMLR with narrower distance caused reflection of the shorter blue wavelengths (Fig. 14).

Dorsal color changes in both *E. calochroma* and *C. egregia* could be explained by the structural change of the chirped multilayer reflector (= EMLR). However, in some instances Vigneron et al. (2007) described endocuticular layers as exocuticular layers: endocuticle generally exists as multilayered structures (lattice structure: piles or balkens and laminae) among beetles (van de Kamp & Geven 2010). In this study, the endocuticle was not stained by toluidine blue which indicated that endocuticular layers were not infilled by hemolymph. It is still unclear if Vigneron et al. (2007) actually observed an EMLR between the endocuticle and epidermis, but based on their TEM and some SEM images it is assumed that their reference was to the endocuticle. The exocuticle and endocuticle were transparent or slightly yellowish in this study (Fig. 8). The transparent endocuticle and exocuticle were also illustrated in Vigneron et al.

(2007). We also found pores and channels in the endocuticular and exocuticular layers, but those did not penetrate the EMLR, which implied that evaporation of hemolymph and gas exchange between the EMLR and the external space might not occur as hypothesized in Vigneron et al. (2007). However, the hypothesized color change mechanism in this study still agrees with the switchable mirror theory. The main differences between the color changes between *E. calochroma* and *C. egregia* are **(1)** the EMLR of *E. calochroma* retained the ability to reflect colored light following dehydration; the multilayer reflector in *C. egregia* lost this ability and allowed incident light to reach the epidermis upon dehydration, and **(2)** *E. calochroma* reflected blue light from the EMLR under low hemolymph amount; *C. egregia* showed a red color upon elytron dehydration, which was a result of the decomposition of the hydrated multilayer reflector acting as a mirror and allowing the incident light to reflect off of the red pigments in the epidermis (Fig. 15). If the cuticle of *E. calochroma* were identical to that of *C. egregia*, the dorsal coloration would change to brown upon a decrease in hemolymph amount, revealing the underlying color of the pigments in the epidermis.

Thin-Film Theory, pH Alteration, and Temperature Alteration

Mason (1929) introduced thin-film theory (= hydraulic theory) and explained the color change mechanism based on an alteration in cuticle thickness and turgor pressure in the EMLR with a severed piece of elytron. He demonstrated that the loss of hemolymph in the elytron allowed a shorter wavelength color to be reflected. The proposed mechanism in this study agrees with Mason's mechanism by the alternation of the distance between the layers of the EMLR, although it was uncertain whether hemolymph turgor could actually be involved in the color change. Therefore, a similar experiment to that of Mason's (1929) severing of the elytra was

performed in this study and in Shin & Davis (2015). The severed apical piece of elytron lost its green color and turned brown due to loss of hemolymph around the cut area (Shin & Davis 2015). The inner area (far from the severed margin), however, still exhibited a green coloration (Fig. 12). Upon closer inspection, a fine blue line between the brown and green areas was observed. This thin blue line demonstrated that the loss of hemolymph in the elytron caused the distance between the layers in the EMLR to condense and narrow. When the base of an elytron was cut from live or ethanol-preserved green individuals, green coloration immediately disappeared and a blue or purple coloration appeared (Fig. 16). This also demonstrated that losing hemolymph narrowed the distance between the layers in the EMLR.

Alteration in pH by the epidermal cells was suggested by Neville (1977) as a cause of the color change in *Aspidimorpha tecta* Boheman (= *A. quadriremis* (Gylllenhal)). When entire specimens of green *E. calochroma* from 70% ethanol were transferred to vinegar (about pH 2.2) and ammonia (about pH 11), the green coloration remained. When elytra were soaked in boiling water and ice water (before the water frozen), they exhibited their typical green color at both temperatures. However, when an elytron was frozen in water, the green coloration disappeared and it exhibited a dull brown color as with *C. egregia* in Vigneron et al. (2007). During thawing of the ice, the brown elytron first exhibited a purple to bluish color (while the water temperature and pressure were still low) and transitioned to green (Fig. 17).

Function of Color Change in Tortoise Beetles

Different functions of the metallic (golden or green) colorations and the color changes in tortoise beetles have been suggested in previous studies. Regarding functions of the metallic colorations, mimicry (Hinton 1973, Neville 1977, Barrows 1979, Jolivet 1994), camouflage

(Mason 1929, Barrows 1979, Jolivet 1994), and mating and maturity signals (Barrows 1979, Jolivet 1994) have been suggested. In regards to color change, aposematism (Hinton 1973) and a simple reaction mechanism to external disturbances for protective purposes (Jolivet 1994) have been proposed. Dorsal colorations in the normal/resting state and coloration following color change differs depending on the species of tortoise beetles. This indicates that the purpose or the benefit of dorsal coloration might be different depending on the species. For *E. calochroma*, the green coloration might function as camouflage or as a maturity signal given that the leaves of the host plant (Geiger tree, *Cordia sebestena* Linneaus, Boraginaceae) are green and mating was only observed in green individuals; no mating behaviors were observed in brown individuals. The color change of *E. calochroma* may also be a simple reaction to external disturbances as proposed by Jolivet (1994). However, protective functions of color change need to be tested more thoroughly. Aposematism as a function of color change in *E. calochroma* seems implausible since color change occurred after external disturbance and took between 2 and 20 minutes.

Future Directions

Several questions still remain regarding metallic colorations and the seemingly sporadic ability of color change among the tortoise beetles. Metallic green coloration has been observed among several different lineages of tortoise beetles (Borowiec & Świętojańska. 2014). Its origins and distribution across the tortoise beetle phylogeny remain unclear. It might be interesting to test whether the presence of such metallic colorations and cuticular multilayer reflectors are homologous or could be used as characters of phylogenetic utility.

When one elytron was cut in *E. calochroma*, the other elytron still changed color and a pumping action was observed in the organ near the base of the severed elytron responsible for cycling hemolymph through the elytra. This pumping behavior was assumed to be reducing the volume of hemolymph in the elytron, though the exact volume and physiological process is unknown, as is the operation of this mechanism in the prothorax.

ACKNOWLEDGMENTS

The authors are grateful to K. Jensen (University of Kansas) for providing training on general histological sectioning to CS and general guidance for this study; M. S. Engel (University of Kansas) for his comments and assistance; Paul Bardunias (University of Florida, Davie) for help during field work; Heather Shinogle and Prem Thapa (University of Kansas, Microscopy Lab) for allowing use of the sectioning facilities. This research was partially supported by the Program of Entomology, Department of Ecology & Evolutionary Biology, University of Kansas, and is a contribution of the Division of Entomology, University of Kansas Natural History Museum. Partial support was also provided by NSF DEB-1110590 (to M.S. Engel, P. Cartwright, and S.R. Davis) through the University of Kansas, and to SRD by the Gerstner and Kalbfleisch postdoctoral fellowships through the American Museum of Natural History and Richard Gilder Graduate School.

REFERENCES

Barrows, E. M. 1979. Life cycles, mating, and color change in Tortoise beetles (Coleoptera: Chrysomelidae: Cassidinae), The Coleopterists Bulletin 33(1): 9–15.

Borowiec, L. and J. Świętojańska. 2014. Cassidinae of the world – an interactive manual (Coleoptera:Chrysomelidae). Available from: http://www.biol.uni.wroc.pl/cassidae/katalog%20internetowy/index.htm (Accessed: July 1, 2015).

Crowson, R. A. 1981. The biology of the Coleoptera. Academic Press, Harcourt Brace Jovanovich Publishers.

Hinton, H. E. and G. M. Jarman. G. M. 1972. Physiological colour change in the Hercules beetle. Nature 238: 160–161.

Hinton, H. E. 1973. Natural deception [pp. 97–159]. *In*: Illusion in nature and art (Gregory, R. L. and E. H. Gombrich, editors). Duckworth, London, U.K..

Jolivet, P. 1994. Physiological colour changes in tortoise beetles [pp. 319–325]. *In*: Novel aspects of the biology of Chrysomelidae (Jolivet, P. H., M. L. Cox, and E. Petitpierre, editors). Kluwer Academic Publisher, Netherlands.

Mason, C. W. 1926. Structural colors in insects. I, The Journal of Physical Chemistry 30(3): 383–395.

Mason, C.W. 1929. Transient color changes in the tortoise beetles (Coleoptera: Chrysomelidae), Entomological News 40: 52–56.

Neville, A.C. 1977. Metallic gold and silver colors in some insect cuticles, Journal of Insect physiology 23: 1267–1274.

Parker, A. R., D. R. McKenzie and M. C. Large. 1998. Multilayer reflectors in animals using green and gold beetles as contrasting examples, Journal of Experimental Biology 201: 1307–1313.

Seago, A. E., P. Brady, J. P. Vigneron and T. D, Schulltz. 2009. Gold bugs and beyond: a review of iridescence and structural colour mechanisms in beetles (Coleoptera), The Journal of the Royal Society 165–184.

Shin, C. and S. R. Davis. 2015. A histological comparison of the two color morphotypes of the Geiger tortoise beetle with a brief natural history (Coleoptera: Chrysomelidae) (Chapter 5 of the Ph.D. thesis, unpublished).

van de Kamp, T. and H. Greven. 2010. On the architecture of beetle elytra, Entomologie Heute 22: 191– 204.

Vigneron, J. P., J. M. Pasteels, D. M. Windsor, Z. Vértesy, M. Rassart, T. Seldrum, J. Dumont, O. Deparis, V. Lousse, L. P. Biró, D. Ertz and V. Welch. 2007. Switchable reflector in the Panamanian tortoise beetle *Charidotella egregia* (Chrysomelidae: Cassidinae), Physical Review 76(31907): 1–10.

LIST OF FIGURES

Fig. 1. *Eurypepla calochroma*, left: green coloration in resting state; right: blue coloration after external disturbances.

Figs. 2–7. Pattern of the dorsal color change in *E. calochroma*.

Fig. 8. Thin section of elytron, stained internally with toluidine blue; black arrows indicate endocuticular multilayer reflector (blue stained) between epidermis and endocuticle.

Fig. 9. Scanning transmission electron micrograph of thin section of elytron: ep (epicuticle), ex (exocuticle), en (endocuticle), EMLR (endocuticular multilayer reflector), ed (epidermis).

Fig. 10. Sagittal thin section of prothorax: A. anterior fold, B. posterior fold.

Figs. 11–12. Damaged elytra. 11. Right elytron with three punctures produced by insect pin (pink arrows), 12. Damage produced by severing the right elytron just above the primary spot area.

Fig. 13. Generalized diagram of chirped cuticular multilayer reflector from Parker et al. (1998), redrawn.

Figs. 14 –15. Hypothesized dorsal color change in this study as shown through modification of the EMLR. 14. *E. calochroma*: left, at resting (green) state; right, after disturbance (blue);

incident light traveling through cuticle with blue wavelengths reflected after disturbance; 15. *C. egregia*: left, at resting (gold or yellow) state; right, after disturbance (red); multilayer reflector dehydrated leading to decomposition of chirped mirror and reflection of red light due to underlying pigment in the epidermis; grey lines (layers in multilayer reflector), yellow (hemolymph), colored arrows (reflected colors), brown color in Fig. 14 (brown pigment in epidermis), red color in Fig. 15 (red pigment in epidermis).

Figs. 16–17. Color change in elytra. 16. Severed elytron from live specimen; 17. Elytra frozen in ice, thawing proceeding from left to right; left (mainly brown with some blue coloration); right (purple, blue, and green coloration).


1


2


3

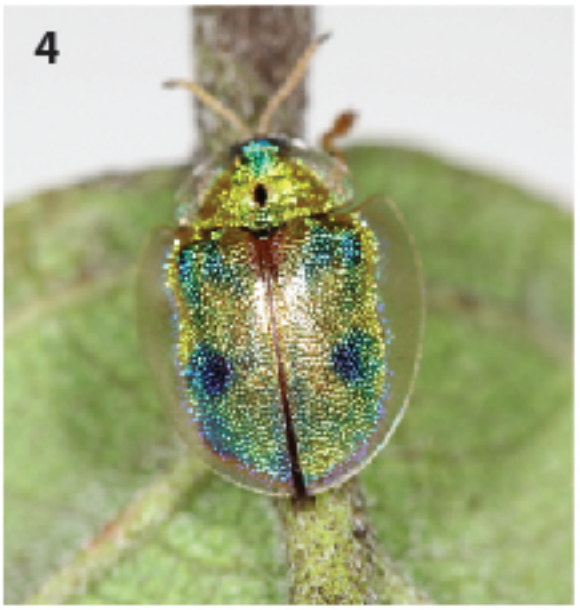
4

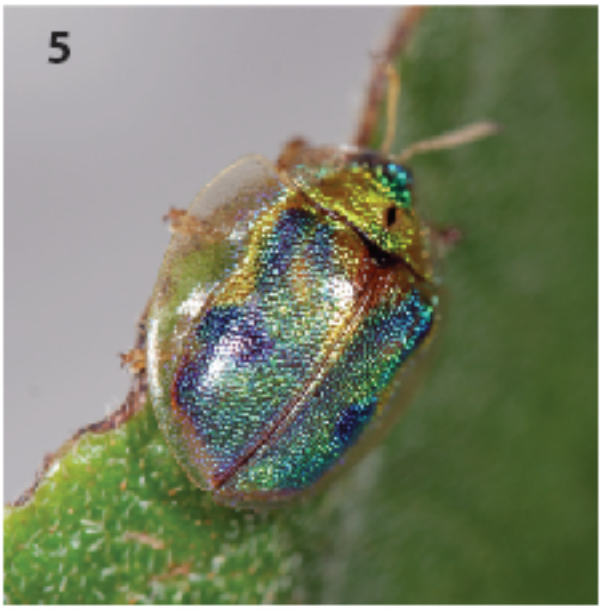
5


6

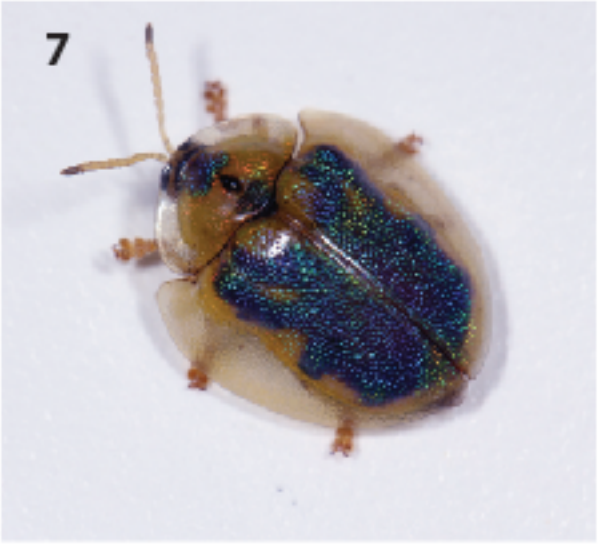
7

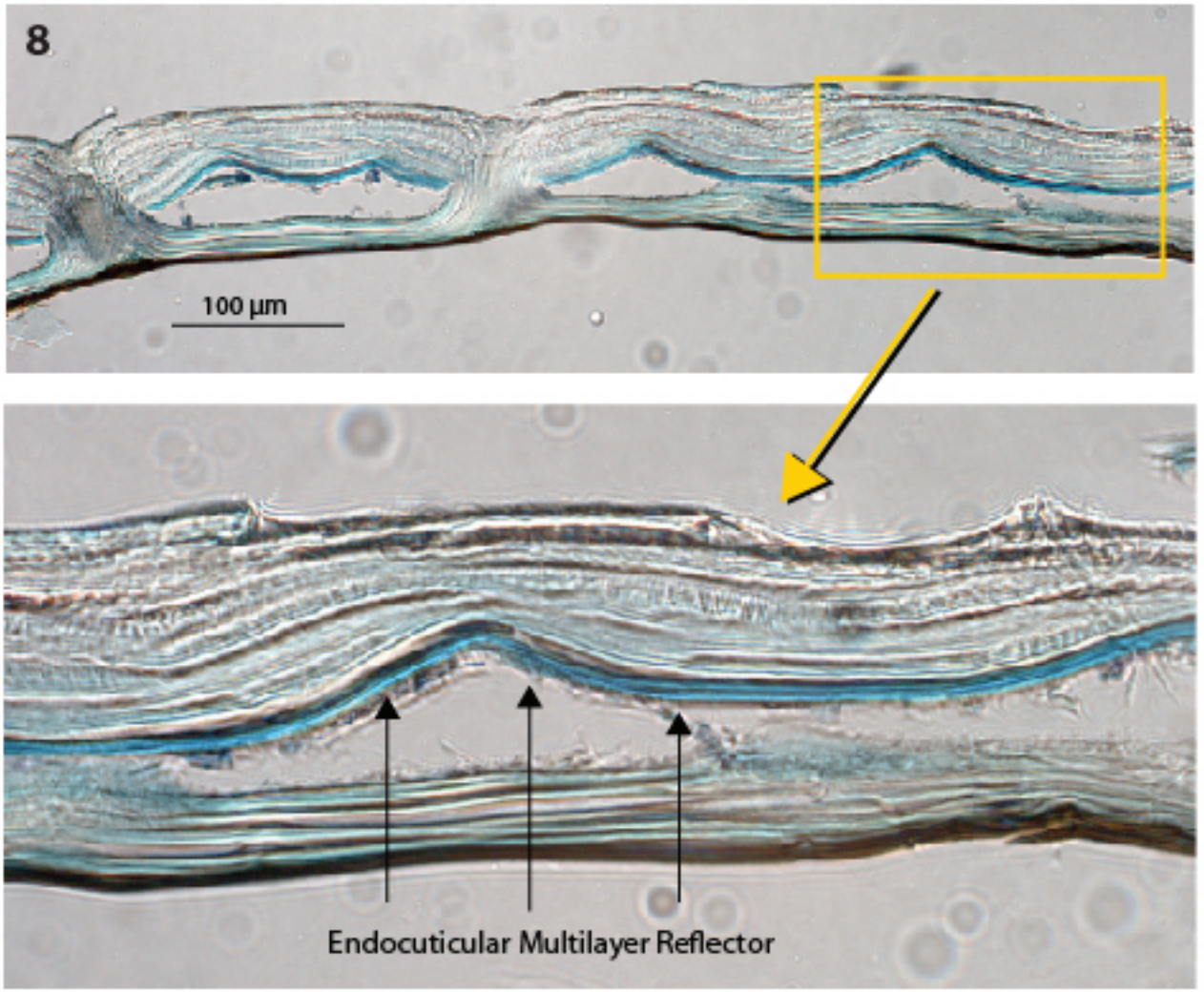
8
100 µm
Endocuticular Multilayer Reflector

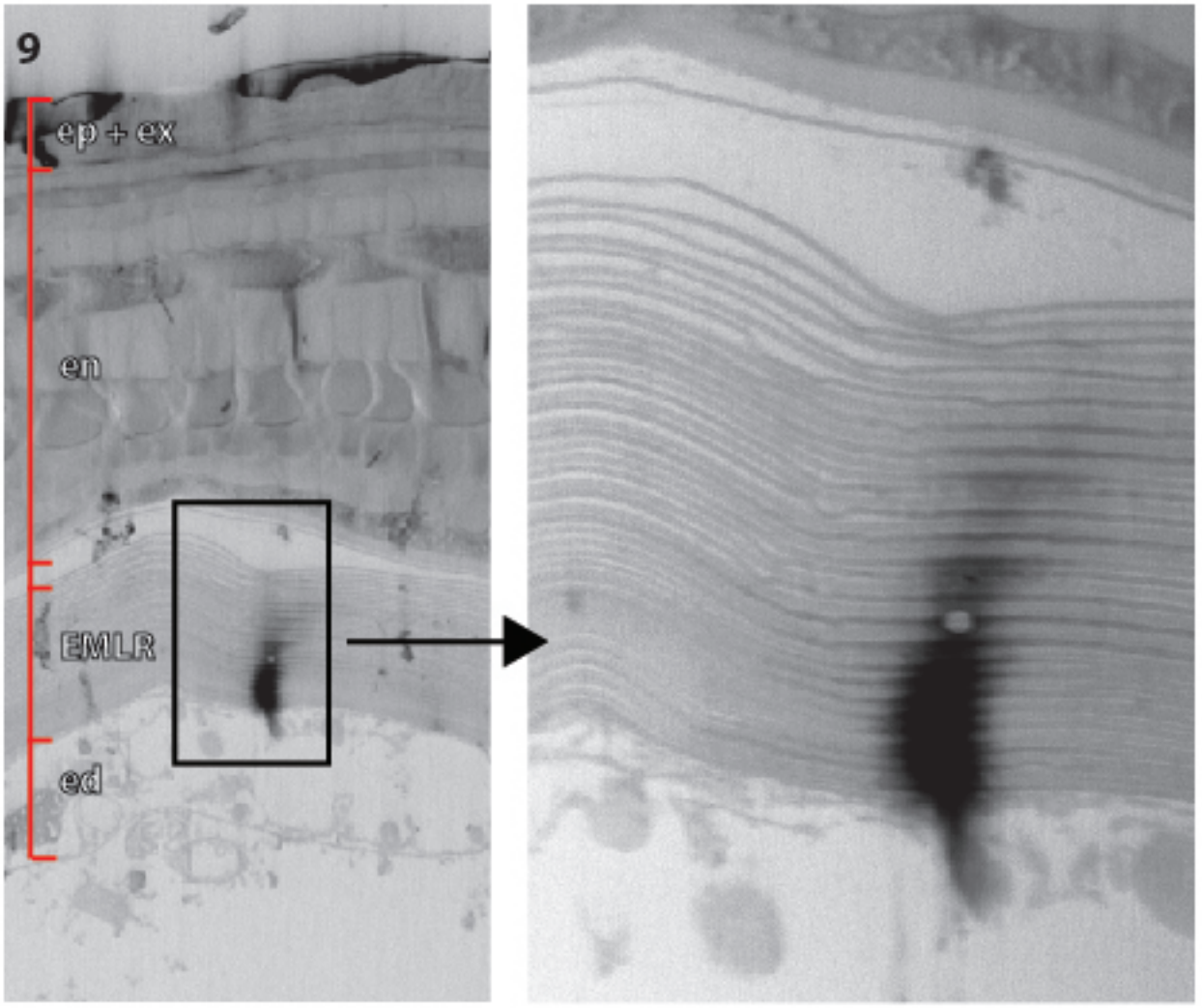
9
ep + ex
en
EMLR
ed

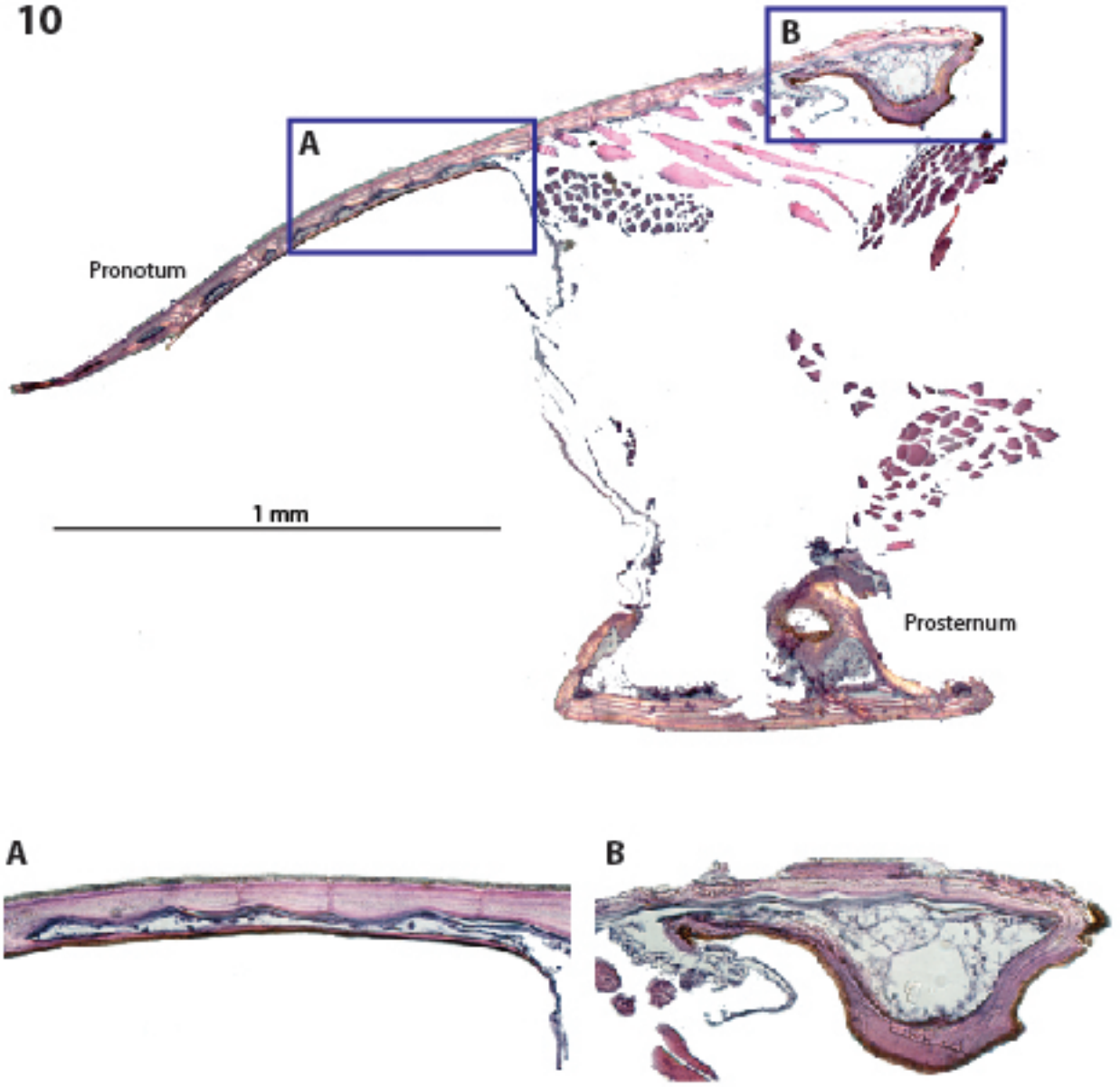
10
B
A
Pronotum
1 mm
Prosternum
A
B


11


12

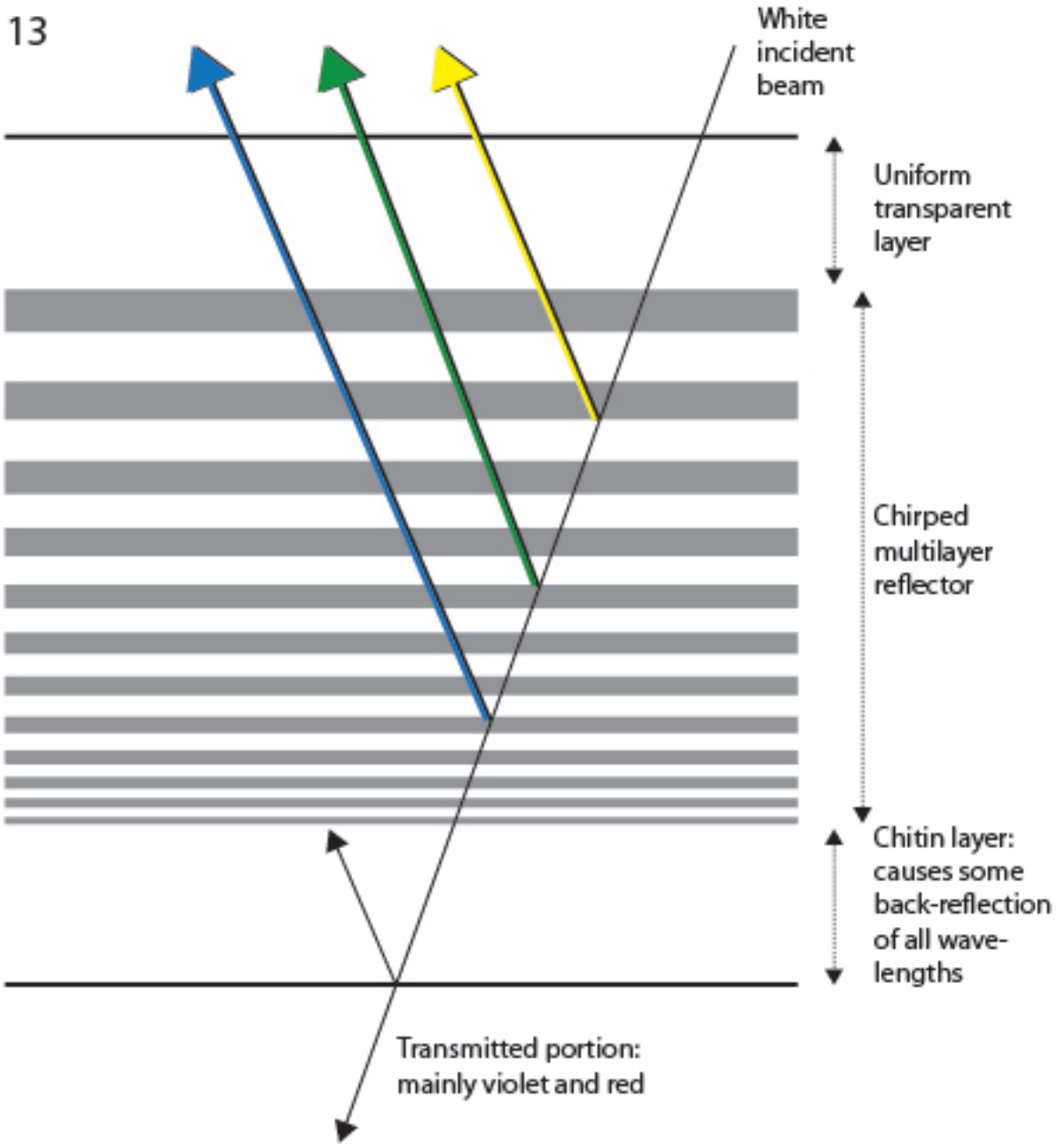
13
White incident beam
Uniform transparent layer
Chirped multilayer reflector
Chitin layer: causes some back-reflection of all wave-lengths
Transmitted portion: mainly violet and red

14

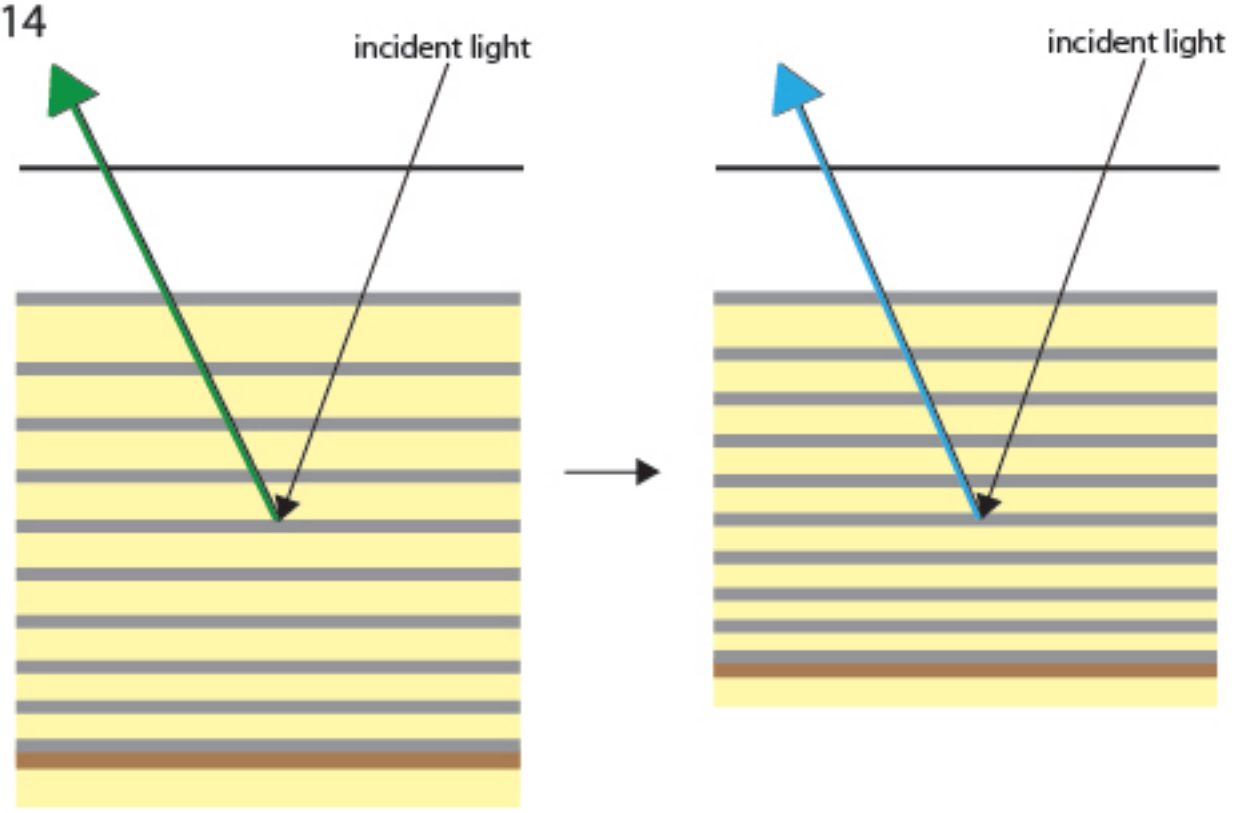
incident light
incident light

15

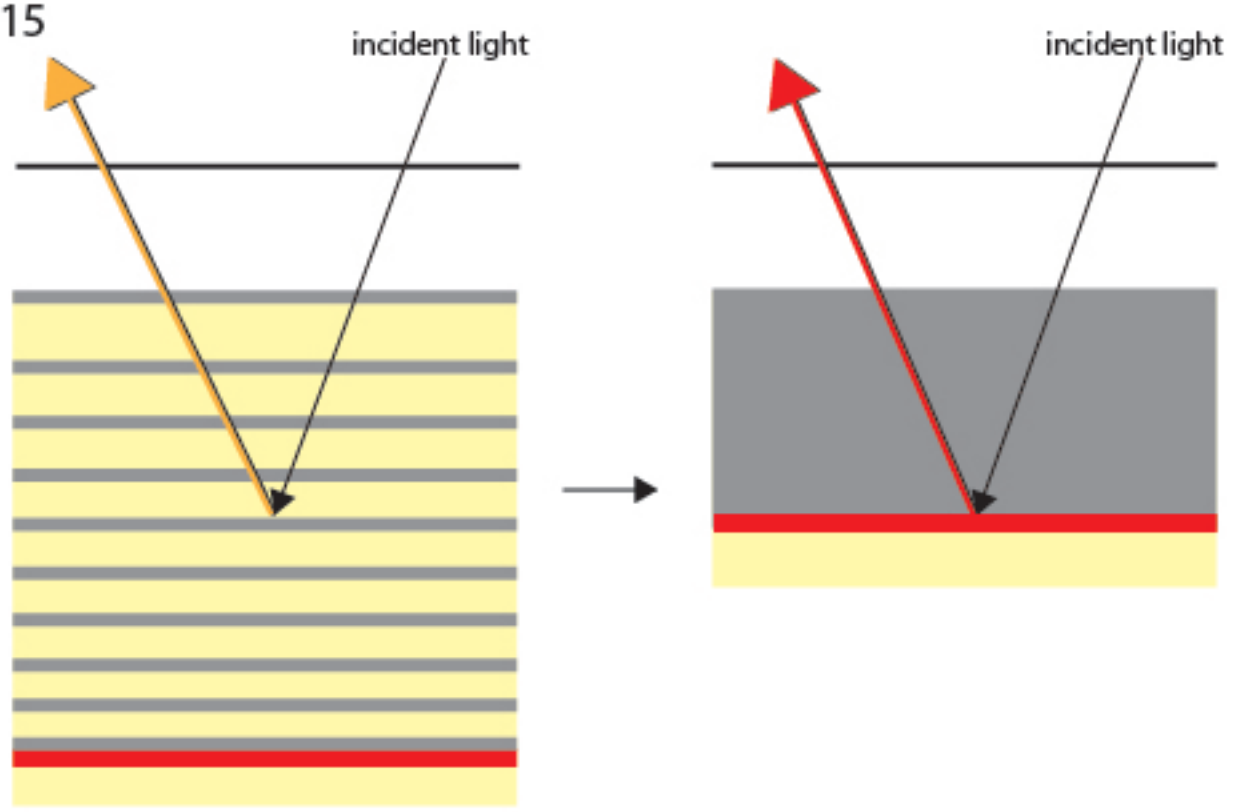
incident light
incident light

16

17

Time

DISCUSSION AND FURTURE DIRECTIONS

The contributions of this study can be summarized as follows: **(1)** the morphology and systematics of members of the historically recognized tribe Ischyrosonychini in the broadest sense was explored through revisionary studies and a phylogenetic analysis based on morphology; **(2)** morphological characters used in previous phylogenetic studies (Borowiec 1995, Chaboo 2007) were reevaluated and modified as necessary; **(3**) novel external morphological characters were presented and their phylogenetic utility tested; **(4)** based on the resulting hypothesis of phylogenetic relationships, the traditional Ischyrosonychini were found to comprise two independent linages; **(5)** the tribe Asterizini was resurrected for one of these lineages, Ischyrosonychini retained for the other, and the diagnosis and membership revised for both; **(6)** the biology of *Eurypepla calochroma* (Blake) was described and illustrated along with a detailed comparison between brown and green color morphotypes using histological and microscopical techniques; and **(7)** the reversible color change (green to blue) observed in *E. calochroma* was studied using histological and microscopical techniques and a potential mechanism proposed.

Most studies on the tortoise beetles have been in the form of faunal and collection lists, species descriptions, and revisions at the generic level (see Borowiec & Świętojańska 2014). The more recently published studies on tortoise beetle included more detailed morphological work and provided more insights into phylogenetic aspects of the group (Borowiec & Świętojańska 2011, 2013, Shin et al. 2012, Simões 2014, Simões & Monné 2014, Shin 2015a, 2015b). This study, concentrated on documenting the morphological and color variations in this group and resolves several taxonomic issues by synonymizing several species and suggesting reclassifications. Considering the previous taxonomic studies and recent taxonomic actions, the

diversity at generic and species levels of the tortoise beetles might have been overestimated. This emphasizes the importance on the basic taxonomic studies at generic and species levels with proper taxonomic actions, based on robust phylogenetic hypotheses of interrelationships.

The most unexpected result in this study was the resurrection of Asterizini, which, in addition to *Asteriza (*syn. *Enagria* and *Physonota*), includes *Eurypepla* and *Platycycla*. Interestingly, the four species of *Asteriza* (see Shin et al. 2012) are the only species in this group reported from Hispaniola. The genus *Asteriza* was described earlier than any of the physonotines due to its distinct morphology (the coloration and thickened edge of elytral lamella). The monotypic genus *Platycycla* and the genus *Eurypepla* (also possibly monotypic) might need to be considered to be included in *Asteriza* as subgenus of *Physonota* as proposed in Hincks (1952).

In this study, the Ischyrosonychini was revised to include only the two original genera, *Cistudinella* and *Eurypedus* Gistel. The monophyly of both of these genera was confirmed. The additional morphological characters, such as antennal notches and the head stridulatory file were added to the generic diagnoses (Shin 2015b). However, a revisionary study is required for *Cistudinella* to confirm the actual species diversity and to understand the morphological circumscription of the genus. It is worth considering the studies on biogeography and niche modeling of each genus in Ischyrosonychini because most species in *Cistudinella* and *Eurypedus* were distributed in the areas around the Amazon Basin but have no records from within the Amazon Basin. A biogeographic study may provide an interesting insight into the evolutionary patterns in Ischyrosonychini as a whole or for each genus separately in connection to the formation of the Amazon Basin.

Understanding the evolutionary pattern in the tortoise beetle is far from complete. As indicated in the phylogeny section in this study (Shin 2015b), monophyly of most tortoise beetle

tribes is either suspect or requires confirmation. There are three main issues concerning the phylogeny of the tortoise beetles at the tribal level: (1) Monophyly of Cassidini and elucidating the evolutionary relationships among the genera in Cassidini: the test for monophyly in this group should be made a priority. Cassidini is currently the largest tribe with about 1,300 described species in 87 genera, and it is the only tribe in which the species are distributed in both Old and New Worlds (Borowiec & Świętojańska 2014). Members of Cassidini exhibit external morphology as disparate as its diversity but its monophyly has always been assumed (Riley 1986, Chaboo 2007, Borowiec & Świętojańska 2014) rather than tested. (2) Monophyly of Aspidimorphini and relationship with the Cassidini: the monophyly of the Aspidimorphini was suggested by Świętojańska (2001) using morphological data, geographical distributions, and feeding preference, but it has never been tested. In addition, its phylogenetic relationship to Cassidini is still questionable (Borowiec 1995, Shin 2015b). (3) Monophyly of the unresolved New World tribes (Eugenysini, Goniocheniini, and Mesomphaliini) and the phylogenetic relationship among these tribes: the close relationship among these three tribes has been proposed or partially resolved in the previous and present phylogenetic studies (Borowiec 1995, Chaboo 2007, Shin 2015b). However, none of studies included a proper taxon sampling to confirm the monophyly of each and relationship among the three tribes.

Various aspects of the biology of tortoise beetles have been studied (see Chaboo 2007). In this study (Shin 2015a, 2015b), the morphology, sexual dimorphism, and variation of head stridulatory files were introduced and used in the phylogenetic analysis. The function of stridulation has rarely been investigated in this group. Previous studies suggested putative functions of stridulation as a defense mechanism and inter-sexual or intraspecific communication (Schmitt 1994, Wessel 2006, Chaboo 2007). In contrast, Dumortier (1963) simply speculated

that stridulation in Chrysomelidae was a simple reaction to disturbance. However, the function could be different depending on the groups. For example, the females of *Eurypedus* lack stridulatory files (Shin 2015a) altogether this sexual dimorphism might imply inter-sexual communication for mating in *Eurypepla*. Depending on the shape, the number of file ridges, and plectral structure, stridulation might produce different sounds. These questions on the stridulation should also be further investigated.

The coloration and color change of the Geiger tortoise beetle were studied together with a brief life history (Shin & Davis 2015a, 2015b). The histological methods expanded the knowledge of detailed morphology of the dorsal cuticular layer in the elytra in this species. In the study of the comparison between the two color morphotypes (green and brown, Shin & Davis 2015a), differences were observed mainly in endocuticle, including the endocuticular multilayer (EMLR). As a future task, it might be interesting to investigate the differential survival between the two color morphotypes. For example, the brown individuals may have a shorter duration of pupation than that of green individuals; it would also be interesting to determine whether any ecological or environmental factors may affect the dorsal coloration. The number of thin layers in EMLR differed between the images by scanning electron microscopy (around 26 layers by SEM in chapter 4) and scanning transmission electron microscopy (over 40 layers by STEM in chapter 5). The different numbers might indicate individual variation or technical issues, which also need to be confirmed by examining more specimens.

The distinct coloration, generally described metallic coloration in tortoise beetles (green in *E. calochroma*), were observed several different lineages of the tortoise beetles. Based on the conditions documented in Shin & Davis (2015a), it should be tested with other tortoise beetles exhibiting the metallic coloration along with detailed morphological study using histological

techniques. This may demonstrate the evolutionary trend of dorsal coloration of the tortoise beetles. The function of the color change in *E. calochroma* was speculated as a simple reaction responding to the external disturbances by Shin & Davis (2015b). However, it would be an interesting question to investigate if additional physiological or additional physical differences between the two color states can be demonstrated.

CITATIONS

Borowiec, L. 1995. Tribal classification of the cassidoid Hispinae (Coleoptera: Chrysomelidae). In: Biology, Phylogeny, and Classification of Coleoptera. (eds.) Pakaluk, J. & Ślipiński, S.A., Warszawa, 541–558.

Borowiec, L. & Świętojańska, J. 2011. The tortoise beetles of Madagascar (Coleoptera: Chrysomelidae: Cassidinae), Part 1: Basiprionotini, Aspidimorphini, and Cassidini (except the genus *Cassida*). Polish Taxonomical Monographs, Polish Taxonomical Society, 18: 1–246.

Borowiec, L. & Świętojańska, J. 2013. The tortoise beetles of Madagascar (Coleoptera: Chrysomelidae: Cassidinae), Part 2: Cassidini, the genus *Cassida* Linnaeus. Polish taxonomical monographs, Polish Taxonomical Society, 20: 1–293.

Borowiec, L. & Świętojańska, J. 2014. Cassidinae of the World – an interactive manual (Coleoptera: Chrysomelidae). Available from http://www.biol.uni.wroc.pl/cassidae/katalog%20internetowy/index.htm (Accessed: July 1 2015).

Chaboo, C.S. 2007. Biology and phylogeny of Cassidinae Gyllenhal (tortoise and leaf-mining beetles) (Coleoptera: Chrysomelidae). Bulletin of the American Museum of Natural History, 305: 1–250.

Dumortier, B. 1963. Morphology of sound emission apparatus in Arthropoda. In: Acoustic Behaviour of Animals. (ed.) Brusenl, R.G., Elsevier Publishing Company, New York, 277–345.

Hincks, W.D. 1952. The genera of the Cassidinae (Coleoptera: Chrysomelidae). Transactions of the Royal Entomological Society of London, 103: 327–358.

Hsiao, T.H. & Windsor, D.M. 1999. Historical and biological relationships among Hispinae inferred from 12S mtDNA sequence data. In: Advances in Chrysomelidae Biology 1. (ed.) Cox, M.L., Backhuys Publishers, Leiden, 39–50.

Riley, E.G. 1986. Review of the tortoise beetle genera of the tribe Cassidini occurring in America, North of Mexico (Coleoptera: Chrysomelidae: Cassidinae). Journal of the New York Entomological Society, 94(1): 98–144.

Schmitt, M. 1994. Stridulation in leaf beetles (Coleoptera, Chrysomelidae). In: Novel aspects of the biology of Chrysomelidae. (eds.) Joliver, P.H., Cox, M.L. & Petitpierre, E., Kluwer Academic Publisher, Netherlands, 319–325.

Shin, C. 2013. A new genus of mesomphaliine tortoise beetle (Coleoptera: Chrysomelidae), with description of a new flightless species from Haiti. The Coleopterists Bulletin, 67(4): 521–531.

Shin, C. 2015a. A revision of the Neotropical tortoise beetle genus *Eurypedus* (Coleoptera: Chrysomelidae). (Chapter 2 of the Ph.D. thesis, unpublished).

Shin, C. 2015b. A phylogenetic study of the tortoise beetle tribe Ischyrosonychini based on morphological data (Coleoptera: Chrysomelidae). (Chapter 3 of the Ph.D. thesis, unpublished).

Shin, C. & Chaboo, C.S. 2012. A revision and phylogenetic analysis of *Stoiba* Spaeth 1909 (Coleoptera: Chrysomelidae). Zookeys, 224: 1–36.

Shin, C., Chaboo, C.S. & Clark, S.M. 2012. Phylogenetic revision of the Hispaniolan endemic genus *Asteriza* Chevrolat, 1836 (Coleoptera: Chrysomelidae: Cassidinae: Ischyrosonychini). Zootaxa, 3227: 34–53.

Shin, C. & Davis, S.R. 2015a. A histological comparison on the two morphotypes of *Eurypepla calochroma* with a brief natural history (Coleoptera: Chrysomelidae) (Chapter 4 of the Ph.D. thesis, unpublished).

Shin, C. & Davis, S.R. 2015b. Observation and histological study on color change in Geiger Tortoise beetles (Coleoptera: Chrysomelidae) (Chapter 5 of the Ph.D. thesis, unpublished).

Simões, M.V.P. 2014. Taxonomic revision of the genus *Paranota* Monrós and Viana, 1949 (Coleoptera: Chrysomelidae: Cassidinae: Dorynotini). The Coleopterists Bulletin, 68(4): 631–655.

Simões, M.V.P. & Monné, M.L. 2014. Taxonomic revision of the genus *Mesomphalia* Hope, 1839 (Insecta, Coleoptera, Chrysomelidae). Zootaxa, 3835(2): 151–197.

Wessel, A. 2006. Stridulation in the Coleoptera — An overview. In: Insect sound and communication (Physiology, Behaviour, Ecology and Evolution). (eds.) Drosopoulos, S. & Claridge, M.F., Taylor & Francis Group, Boca Raton, FL, 397–404.